112

ARIZONA
DEPARTMENT OF WATER RESOURCES

# DESIGN MANUAL FOR ENGINEERING ANALYSIS OF FLUVIAL SYSTEMS

1985

# DESIGN MANUAL FOR ENGINEERING ANALYSIS OF FLUVIAL SYSTEMS

Prepared for

Arizona Department of Water Resources
99 East Virginia Avenue
Phoenix, Arizona 85004

By

Simons, Li & Associates, Inc.

120 West Broadway, Suite 170
P.O. Box 2712
Tucson, Arizona 85702

3555 Stanford Road
P.O. Box 1816
Fort Collins, CO 80522

Project Number AZ-DWR-05
RDF162, 166, 232/R522

March 1985

## ACKNOWLEDGEMENTS

This manual was prepared for the State of Arizona, Department of Water Resources, by Simons, Li & Associates, Inc. (SLA). The contract was under the supervision of Mr. Robert L. Ward, P.E., Chief of the Flood Control Section, Department of Water Resources. Under his guidance and direction, a truly useful, practical design manual was developed. The Project Manager at SLA was Mr. Michael E. Zeller, P.E., and the primary author was Dr. James D. Schall, P.E. Input data and calculations for the comprehensive design example presented in Chapter VII were provided by Ms. Pat Deschamps, P.E., Project Engineer, Department of Water Resources. Technical review was provided by Dr. Ruh-Ming Li, P.E. The Department of Water Resources also wishes to acknowledge the financial contribution and review comments provided by the Flood Control District of Maricopa County. The District's participation in this project was greatly appreciated.

## CONDITIONS OF USE

This manual was developed by Simons, Li & Associates, Inc. under contract to the State of Arizona, Department of Water Resources. The use of this manual by any individual or group entity is with the express understanding that Simons, Li & Associates, Inc. and the State of Arizona make no warranties, express or implied, concerning the accuracy, completeness, reliability, usability, or suitability for any particular purpose of the information contained herein. Furthermore, neither Simons, Li & Associates, Inc. nor the State of Arizona shall be under any liability whatsoever to any such individual or group entity by any reason of use made thereof.

TABLE OF CONTENTS


Page

Acknowledgments . . . . . ii
Conditions of Use . . . . . iii
List of Figures . . . . . viii
List of Tables . . . . . xi
Definition of Symbols . . . . . xiii

I. INTRODUCTION . . . . . 1.1

II. GENERAL DESIGN CONSIDERATIONS

2.1 Channel and Watershed Response . . . . . 2.1
2.2 Sand-Bed Channels . . . . . 2.3
2.3 Cobble-Bed Channels . . . . . 2.4
2.4 General Solution Approach . . . . . 2.5

2.4.1 Three-Level Analysis . . . . . 2.5
2.4.2 Level I - Qualitative Geomorphic Analysis . . . . . 2.5
2.4.3 Level II - Quantitative Geomorphic and Basic Engineering Analysis . . . . . 2.6
2.4.4 Level III - Quantitative Analysis Using Mathematical Models . . . . . 2.6

2.5 Data Requirements . . . . . 2.7

2.5.1 General . . . . . 2.7
2.5.2 Level I Data Requirements . . . . . 2.7
2.5.3 Level II Data Requirements . . . . . 2.8
2.5.4 Level III Data Requirements . . . . . 2.12
2.5.5 Data Generation Concepts . . . . . 2.12

III. HYDROLOGIC ANALYSIS

3.1 Relation of Hydrology to Other Analyses . . . . . 3.1
3.2 Establishing Return Period Discharges and Durations . . . . . 3.2

3.2.1 General . . . . . 3.2
3.2.2 Rational Method . . . . . 3.4
3.2.3 SCS TR-55 Methods . . . . . 3.6
3.2.4 USGS Flood-Frequency Analysis . . . . . 3.6
3.2.5 Other Regionalized Methods . . . . . 3.7
3.2.6 Channel Geometry Techniques . . . . . 3.7

3.3 Development of Flood Hydrographs . . . . . 3.8

3.3.1 General . . . . . 3.8
3.3.2 Characterization of Design Storm . . . . . 3.8

TABLE OF CONTENTS (continued)

Page

3.3.3 Determination of Runoff Volume . . . . . 3.11
3.3.4 Hydrograph Development . . . . . 3.13

3.4 Selection of Design Event for Fluvial Systems Analysis . . . . 3.13
3.5 Discretizing Flood Hydrographs . . . . . 3.17

IV. HYDRAULIC ANALYSIS OF ALLUVIAL CHANNELS

4.1 General . . . . . 4.1
4.2 Resistance to Flow . . . . . .4.1

4.2.1 Common Resistance Parameters and Their Relationships . . . . . 4.1
4.2.2 Resistance to Flow in Fine-Grained Alluvial Channels . . . . . 4.4
4.2.3 Resistance to Flow in Cobble/Boulder-Bed Alluvial Channels . . . . . 4.8

4.3 Boundary Shear Stress Calculations . . . . . 4.15
4.4 Normal Depth Calculations . . . . . 4.18

4.4.1 Definition . . . . . 4.18
4.4.2 Normal Depth Calculation for Trapezoidal Channels . . . 4.21
4.4.3 Normal Depth Calculation for Natural Channels . . . . . 4.22

4.5 Water-Surface Profiles . . . . . 4.22
4.6 Additional Effects on Flow Depth in Alluvial Channels . . . . 4.23

4.6.1 Importance . . . . . 4.23
4.6.2 Antidune and Dune Height . . . . . 4.24
4.6.3 Superelevation . . . . . 4.24
4.6.4 Debris Accumulation . . . . . 4.29
4.6.5 Total Freeboard Requirement . . . . . 4.29

4.7 Examples . . . . . 4.31

4.7.1 Analysis of Resistance to Flow in Sand-Bed Channels . . 4.31
4.7.2 Analysis of Flow in Rough Channels . . . . . 4.34

V. SEDIMENT TRANSPORT ANALYSIS

5.1 General Concepts . . . . . 5.1

5.1.1 Basic Sediment Transport Theory . . . . . 5.1
5.1.2 Basic Terminology . . . . . 5.3

TABLE OF CONTENTS (continued)

Page

5.2 Level I Analysis . . . . . 5.4

5.2.1 Plan Form Characteristics . . . . . 5.4
5.2.2 Lane Relation and Other Geomorphic Relationships . . . 5.11
5.2.3 Aerial Photograph Interpretation . . . . . 5.16
5.2.4 Bed- and Bank-Material Analysis . . . . . 5.20
5.2.5 Land-Use Changes . . . . . 5.22
5.2.6 Flood History and Rainfall-Runoff Relations . . . . . 5.24

5.3 Level II Analysis . . . . . 5.25

5.3.1 Watershed Sediment Yield . . . . . 5.25
5.3.2 Detailed Analysis of Bed and Bank Material . . . . . 5.31
5.3.3 Profile Analysis . . . . . 5.38
5.3.4 Incipient Motion Analysis . . . . . 5.42
5.3.5 Armoring Potential . . . . . 5.45
5.3.6 Sediment Transport Capacity . . . . . 5.50
5.3.7 Equilibrium Slope . . . . . 5.73
5.3.8 Sediment Continuity Analysis . . . . . 5.82
5.3.9 Quantification of Vertical and Horizontal Channel Response . . . . . 5.87
5.3.10 Local Scour Concepts . . . . . 5.92
5.3.11 Contraction Scour . . . . . 5.102
5.3.12 Bend Scour . . . . . 5.105
5.3.13 Evaluation of Low-Flow Channel Incisements . . . . . 5.110
5.3.14 Evaluation of Gravel Mining Impacts . . . . . 5.111
5.3.15 Cumulative Channel Adjustment . . . . . 5.116

5.4 Level III Analysis . . . . . 5.119

5.4.1 General . . . . . 5.119
5.4.2 Application of Level III Analysis . . . . . 5.119

VI. CHANNEL DESIGN CRITERIA

6.1 General . . . . . 6.1
6.2 Bank/Levee Height . . . . . 6.1
6.3 Bank/Levee Toedown . . . . . 6.2
6.4 Lateral Migration . . . . . 6.2
6.5 Grade-Control Structures . . . . . 6.5
6.6 Common Bank Protection Methods . . . . . 6.6

VII. COMPREHENSIVE DESIGN EXAMPLE

7.1 Project Description . . . . . 7.1
7.2 Level I . . . . . 7.1
7.3 Level II . . . . . 7.8

TABLE OF CONTENTS (continued)

Page

7.3.1 Levee Embankment Height . . . . . 7.8
7.3.2 Levee Embankment Stabilization . . . . . 7.11

7.3.2.1 Erosion of Embankment Material . . . . . 7.11
7.3.2.2 Toe-Down Requirement For Stabilization System . . . . 7.12

7.3.2.2.1 Armor Potential . . . . . 7.12
7.3.2.2.2 Long-Term Aggradation/Degradation . . . . . 7.14
7.3.2.2.3 Low Flow Incisement . . . . . 7.22
7.3.2.2.4 Local Scour . . . . . 7.23
7.3.2.2.5 General Scour . . . . . 7.25
7.3.2.2.6 Sand Wave Troughs . . . . . 7.32

7.3.3 Lateral Migration . . . . . 7.33

7.4 Summary and Conclusions . . . . . 7.37

VIII. REFERENCES . . . . . 8.1

APPENDIX A - PACIFIC SOUTHWEST INTER-AGENCY COMMITTEE (PSIAC) METHOD FOR PREDICTING WATERSHED SOIL LOSS

APPENDIX B - MODIFIED UNIVERSAL SOIL LOSS EQUATION (MUSLE) FOR PREDICTING WATERSHED SOIL LOSS

LIST OF FIGURES


| | | Page |
|---|---|---|
| Figure 1.1 | October 1983 flood, Pantano Wash, Tucson, Arizona | 1.2 |
| Figure 1.2 | October 1983 flood, Rillito River, Tucson, Arizona | 1.3 |
| Figure 1.3 | October 1983 flood, Santa Cruz River, Tucson, Arizona | 1.4 |
| Figure 1.4 | October 1983 flood, Rillito River, Tucson, Arizona | 1.5 |
| Figure 2.1 | Watershed-river system | 2.2 |
| Figure 2.2 | Definition sketch illustrating typical measured sediment discharges vs. water discharge relation | 2.10 |
| Figure 3.1 | Typical sediment yield frequency curve | 3.15 |
| Figure 3.2 | Definition sketch of the hydrograph discretization process | 3.18 |
| Figure 3.3 | Hydrograph discretization | 3.19 |
| Figure 4.1 | Forms of bed roughness in sand-bed channels | 4.9 |
| Figure 4.2 | Relation of bed form to stream power and median fall diameter of bed sediment | 4.11 |
| Figure 4.3 | Variation of boundary shear stress in a trapezoidal cross section | 4.16 |
| Figure 4.4 | Maximum unit tractive force versus aspect ratio (b/d) | 4.17 |
| Figure 4.5 | Effect of bend on boundary shear stress | 4.19 |
| Figure 4.6 | Definition sketch of the energy and hydraulic grade lines in open-channel flow | 4.20 |
| Figure 4.7 | Definition sketch of antidune height | 4.25 |
| Figure 4.8a | Definition sketch of superelevation in a channel bend | 4.26 |
| Figure 4.8b | Definition sketch of superelevation and flow separation conditions in a short radius bend | 4.26 |
| Figure 5.1 | Definition of sediment load components | 5.2 |
| Figure 5.2 | River channel patterns | 5.5 |

LIST OF FIGURES (continued)


Page

Figure 5.3 Classification of river channels . . . . . 5.8

Figure 5.4 Schematic of the Lane relationship for qualitative analysis . . . . . 5.12

Figure 5.5 Slope-discharge relations . . . . . 5.14

Figure 5.6 Channel pattern versus slope and sinuosity . . . . . 5.15

Figure 5.7 Example illustrating qualitative information derived from time sequence analysis of aerial photographs . . . . . 5.21

Figure 5.8 Annual rainfall for Santa Margarita watershed . . . . . 5.26

Figure 5.9 Maximum annual mean daily discharge for Santa Margarita River . . . . . 5.27

Figure 5.10 Annual runoff-rainfall ratio for Santa Margarita watershed . . . . . 5.28

Figure 5.11a Selected particle size gradations . . . . . 5.39

Figure 5.11b Representative gradation curve . . . . . 5.40

Figure 5.12 Shields' relation for beginning of motion . . . . . 5.43

Figure 5.13 Frequency of motion for various particle sizes . . . . . 5.46

Figure 5.14 Armored bed of Salt River upstream of Gilbert Road near Mesa, Arizona, and excavation through armor layer of the Salt River near Mesa Arizona . . . . . 5.48

Figure 5.15 Relationship of discharge of sands to mean velocity for six median sizes of bed sands, four depths of flow, and a water temperature of 60°F . . . . . 5.59

Figure 5.16 Colby's correction curves for temperature, fine sediment, and median particle size . . . . . 5.60

Figure 5.17 Bed material gradation curve for example using Colby Method . . . . . 5.64

Figure 5.18 Log - log plot of uncorrected sediment discharge ($q_{s_i}$) vs. hydraulic depth ($Y_h$) . . . . . 5.65

Figure 5.19 Relationship between equilibrium slope and channel bed controls . . . . . 5.78

LIST OF FIGURES (continued)


| | | Page |
|---|---|---|
| Figure 5.20 | Existing and Equilibrium Slope Profiles for Example Problem | 5.83 |
| Figure 5.21 | Temporal change of scour hole depth during a storm . . . . . | 5.93 |
| Figure 5.22 | Common pier shapes . . . . . | 5.95 |
| Figure 5.23 | Scour increase factor $K_{aL}$, for piers not aligned with flow . . . . . | 5.98 |
| Figure 5.24 | Definition sketch of embankment length "a" . . . . . | 5.100 |
| Figure 5.25 | Illustration of terminology for bend scour calculations . . | 5.107 |
| Figure 5.26 | Relative time for filling a gravel pit and reaching equilibrium for a low and high flow event . . . . . | 5.113 |
| Figure 5.27. | Critical time for erosion of a flood-plain gravel pit . . . | 5.115 |
| Figure 5.28. | Definition sketch of the temporal changes at the upstream edge of a gravel pit . . . . . | 5.117 |
| Figure 6.1. | Calculated risk diagram . . . . . | 6.3 |
| Figure 7.1. | Project plan view, Pinto Creek at Sportsman's Haven . . . . | 7.2 |
| Figure 7.2. | Time sequence analysis of historical aerial photographs . . | 7.4 |
| Figure 7.3. | Comparison of historical bed profiles . . . . . | 7.6 |
| Figure 7.4. | Block diagram of Level II analysis . . . . . | 7.9 |
| Figure 7.5. | Average gradation curve, Pinto Creek at Sportsman's Haven . | 7.15 |
| Figure 7.6. | Cross-section geometry for upstream sediment supply section . . . . . | 7.18 |
| Figure 7.7. | Plan view of levee alignment analyzed in local scour evaluation . . . . . | 7.24 |
| Figure 7.8. | Discretized 100-year flood hydrograph . . . . . | 7.27 |
| Figure 7.9 | Sediment transport rating curve - Reach 2, Pinto Creek at Sportsman's Haven . . . . . | 7.28 |

LIST OF TABLES


| | | Page |
|---|---|---|
| Table 2.1 | Partial Listing of Data Requirements for a Level I Analysis | 2.9 |
| Table 2.2 | Partial Listing of Data Requirements for a Level II Analysis | 2.11 |
| Table 3.1 | USGS Offices with WATSTORE Information | 3.3 |
| Table 3.2 | USGS Offices with NAWDEX Information | 3.5 |
| Table 3.3 | Water and Sediment Discharge Data for Hydrograph Discretization Example | 3.20 |
| Table 4.1 | Manning Roughness Coefficients, n | 4.5 |
| Table 4.2 | Values of Manning's Coefficient n for Design of Channels with Fine to Medium Sand Beds | 4.10 |
| Table 4.3 | Superelevation Formula Coefficients | 4.28 |
| Table 5.1 | Agencies with Information on Aerial Photographs | 5.19 |
| Table 5.2 | Recommended Size Range, Analysis Concentration, and Quantity of Sediment for Commonly Used Methods of Particle Size Analysis | 5.34 |
| Table 5.3 | Minimum Recommended Sample Weights for Sieve Analysis | 5.35 |
| Table 5.4 | Incipient Motion Characteristics | 5.47 |
| Table 5.5 | Sediment Transport Calculation Procedures | 5.52 |
| Table 5.6a | Results of Regression Analysis, $0.001 \leq S_0 \leq 0.01$ | 5.55 |
| Table 5.6b | Results of Regression Analysis, $0.01 < S_0 \leq 0.04$ | 5.56 |
| Table 5.7 | Range of Parameters Examined for Power Relationships | 5.57 |
| Table 5.8 | Geometric Mean Calculations for Colby Example | 5.68 |
| Table 5.9 | Uncorrected Sediment Transport Rate for Colby Example | 5.68 |
| Table 5.10 | Total Sediment Transport Rate for Colby Example | 5.71 |
| Table 5.11 | Bed Material Discharge Calculations for Colby Method Example Using Sediment Size Fractions | 5.72 |

LIST OF TABLES (continued)


| | | Page |
|---|---|---|
| Table 5.12 | Short-Term General Scour/Deposition Response | 5.88 |
| Table 5.13 | Sediment Continuity Results (100-Year Flood) | 5.91 |
| Table 5.14 | Reduction Factors When Applying Formulas for Square Nose Piers to Other Shapes | 5.97 |
| Table 7.1 | Equilibrium Slope Calculations for Reach 2 | 7.21 |
| Table 7.2 | General Scour Analysis Using Sediment Continuity 100-year Event | 7.29 |
| Table 7.3 | Pinto Creek 100-year Sediment Continuity Analysis | 7.31 |
| Table 7.4 | Calculation of Antidune Trough Depths | 7.34 |
| Table 7.5 | Summary of Soil Cement Toe-down Dimensions | 7.39 |

## DEFINITION OF SYMBOLS

| | |
|---|---|
| $A$ | Area |
| $A_w$ | Total wetted roughness cross-sectional area |
| $b$ | Bottom width |
| $b_p$ | Pier width |
| $b_{rg}$ | Roughness geometry parameter in Bathurst's procedure (1978) |
| $C$ | Chezy resistance factor |
| $c$ | Sediment concentration (ppm by weight) |
| $d$ | Depth of flow measured normal to direction of flow |
| $D$ | Diameter of pipe |
| $D_a$ | Sediment particle size of the armor layer |
| $D_c$ | Sediment particle size at incipient motion |
| $D_i$ | Percent finer particle size (i.e. $D_{50}$, $D_{90}$, etc.) |
| $f$ | Darcy-Weisbach friction factor |
| F.B. | Freeboard distance |
| $Fr$ | Froude number |
| $Fr_p$ | Pier Froude number |
| $G$ | Gradation coefficient |
| $G_s$ | Specific gravity |
| $g$ | Acceleration of gravity |
| $h_a$ | Antidune height from crest to trough |
| $h_f$ | Friction loss |
| $L$ | Length |
| $n$ | Manning's roughness coefficient |
| $p$ | Probability |
| $P$ | Wetted perimeter |
| $P_c$ | Percent of material coarser than armor size |
| $q$ | Water discharge per unit width |
| $Q$ | Water discharge |
| $q_b$ | Bed-load transport per unit width |
| $q_p$ | Peak water discharge per unit width |
| $q_s$ | Bed-material sediment discharge per unit width |
| $R$ | Hydraulic radius |
| $r_c$ | Radius of curvature |
| $R_p$ | Pier Reynolds number |

| | |
|---|---|
| $S$ | Slope |
| $S_e$ | Slope of energy gradient |
| $S_o$ | Slope of channel bed |
| $S_{50}$ | Median size of short axis of particle in Bathurst's procedure (1978) |
| $T$ | Top width |
| $t_c$ | Time of concentration |
| $V$ | Mean velocity |
| $V_*$ | Shear velocity |
| $VOL_{inc}$ | Water volume from probability weighting |
| $VOL_{meas}$ | Water volume from gaging station data |
| $VOL_s$ | Sediment volume |
| $W$ | Width of flow |
| $X$ | Distance downstream of a channel bend at which secondary flow becomes negligible |
| $Y$ | Depth of flow measured vertically |
| $y_c$ | Critical flow depth |
| $Y_h$ | Hydraulic depth |
| $y_o$ | Normal depth |
| $Y_{50}$ | Median size cross-stream axis of particle in Bathurst's procedure (1978) |
| $z$ | Side slope angle (horizontal:1) |
| $\Delta y_{agg}$ | Additional flow depth due to long-term aggradation |
| $\Delta y_d$ | Additional flow depth from debris accumulation |
| $\Delta y_s$ | Additional flow depth from separation in short-radius bends |
| $\Delta y_{se}$ | Superelevation |
| $\Delta Z_a$ | Depth to formation of armor layer |
| $\Delta Z_{bs}$ | Bend scour depth |
| $\Delta Z_{deg}$ | Change in bed elevation from long-term degradation |
| $\Delta Z_{gs}$ | General scour depth |
| $\Delta Z_i$ | Low-flow channel incisement depth |
| $\Delta Z_{\ell s}$ | Local scour depth |
| $\Delta Z_{tot}$ | Total vertical adjustment in bed elevation |
| $\gamma$ | Specific weight of water |
| $\gamma_s$ | Specific weight of sediment |
| $\rho$ | Density |
| $\tau_c$ | Critical tractive force |

| | |
|---|---|
| $\tau_0$ | Boundary shear stress (tractive force) |
| $\sigma$ | Standard deviation |
| $\upsilon$ | Kinematic viscosity |
| $\pi$ | Pi (3.14) |

# I. INTRODUCTION

The rigid boundary conditions upon which most flood control studies are currently based do not acknowledge the potential for river systems to move both laterally and vertically. Failure to address this problem in the design and construction of flood control projects, bridges or other structures located within a flood plain can lead to their premature destruction or obsolescence. Recognizing this deficiency in typical design procedures, the Arizona Department of Water Resources initiated development of this design manual.

The purpose of this design manual is to present techniques and procedures that may be used to make a thorough engineering analysis of major fluvial systems in order that the natural processes associated with such systems can be accounted for in the design of flood control projects. The importance of this is vividly illustrated by the photographs in Figures 1.1 to 1.4.

Figures 1.1 (Pantano Wash - Tucson, Arizona) and 1.2 (Rillito River - Tucson, Arizona) illustrate the lateral migration that can occur during a flood. In particular, the power line poles of Figure 1.1 illustrate the extent of lateral migration possible during a single flood. Figures 1.3 (Santa Cruz River - Tucson, Arizona) and 1.4 (Rillito River - Tucson, Arizona) illustrate the potential for both loss of life and property during a single event. In Figure 1.3, the Cortaro Farms Road bridge was completely destroyed, and in Figure 1.4 a townhome is on the verge of falling into the river. The situations illustrated all developed during the October 1983 flooding in southeastern Arizona. The need for an engineering analysis in order to predict fluvial system response, and to design adequate mitigating measures that will prevent or limit the dangers illustrated in Figures 1.1 to 1.4, is self-evident.

Information in this manual addresses the dynamics of watershed and channel systems considering hydrologic, hydraulic, geomorphic, erosion and sedimentation aspects. The emphasis is placed upon practical implementation of state-of-the-art technology in identifying, evaluating and designing for the natural processes associated with major fluvial systems. Depending upon engineering judgment and project economics, the principles discussed herein can also be applied to the design of small conveyance drainage systems. Only that information considered absolutely essential to understanding the basic theory of the application procedures has been presented, while other relevant, but

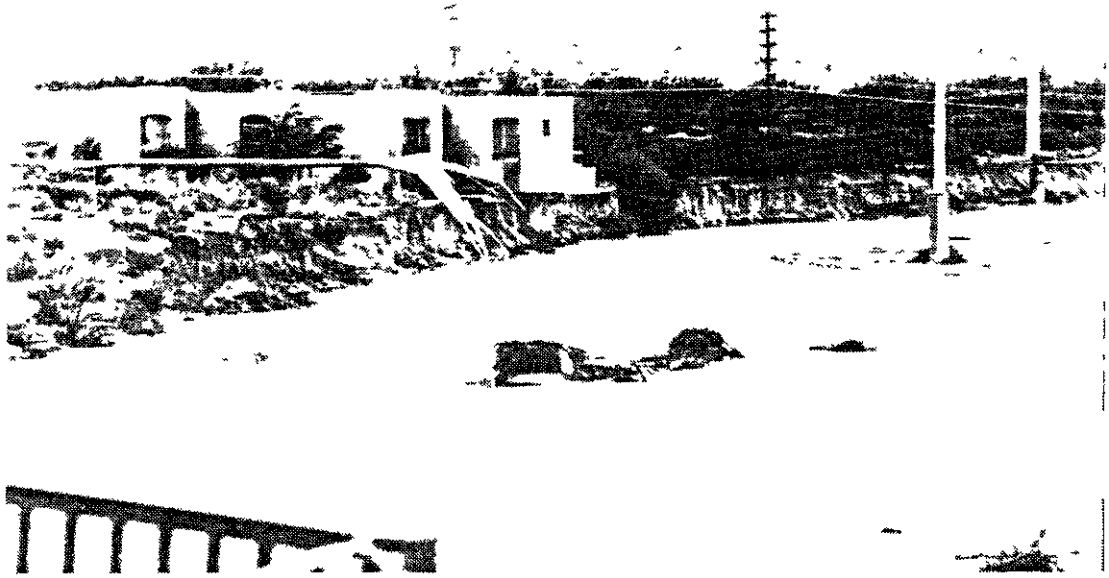

Figure 1.1. View from the Speedway Blvd. bridge looking upstream along the east bank of the Pantano Wash, Tucson, Arizona (Photo date: October,1983).

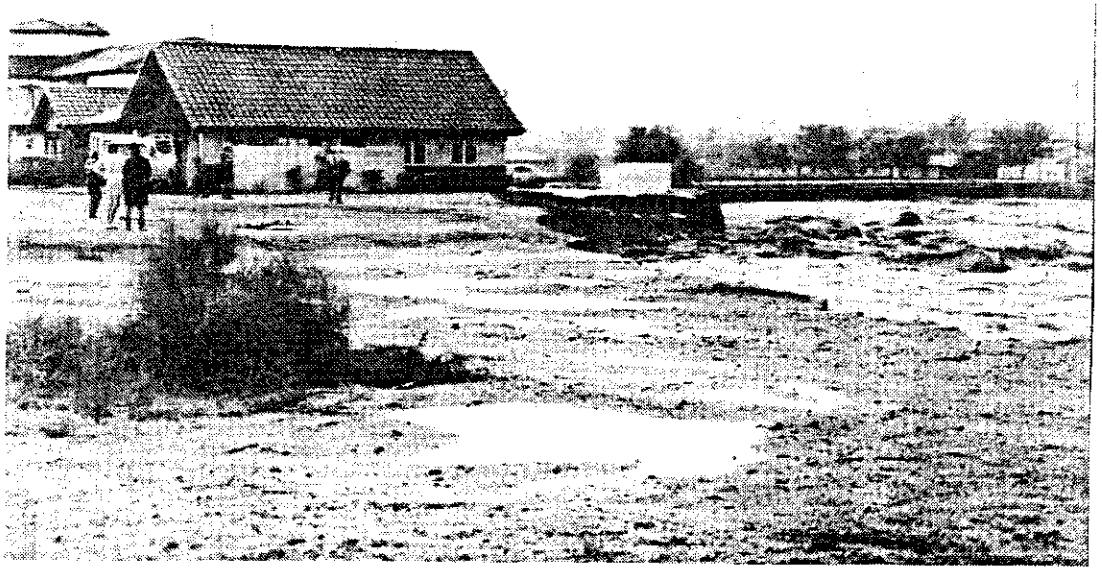

Figure 1.2. View from south bank looking northwest toward the First Avenue bridge over the Rillito River, Tucson, Arizona (Photo date: October, 1983).

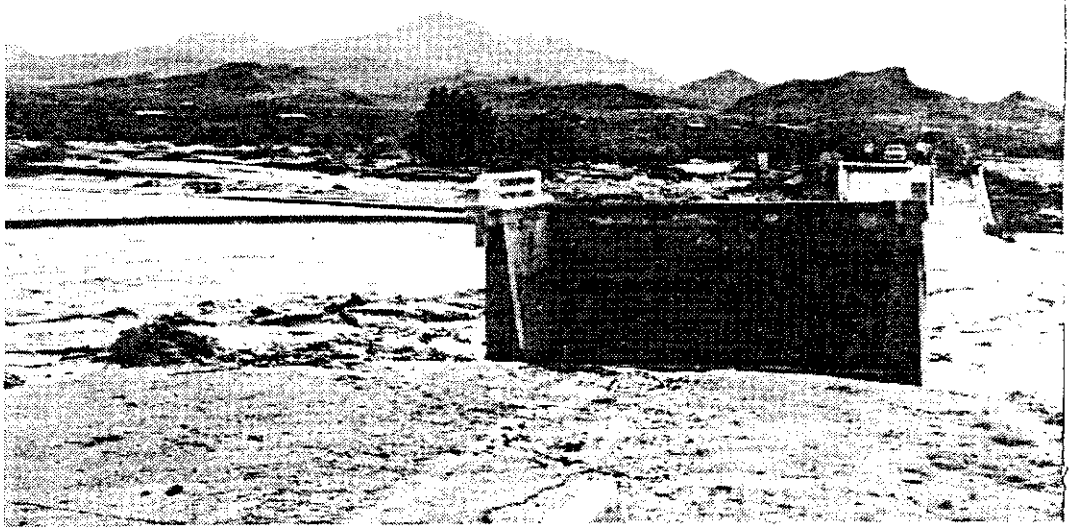

Figure 1.3. View from east bank looking west across the Cortaro Road bridge at the Santa Cruz River, Tucson, Arizona
(Photo date: October, 1983).

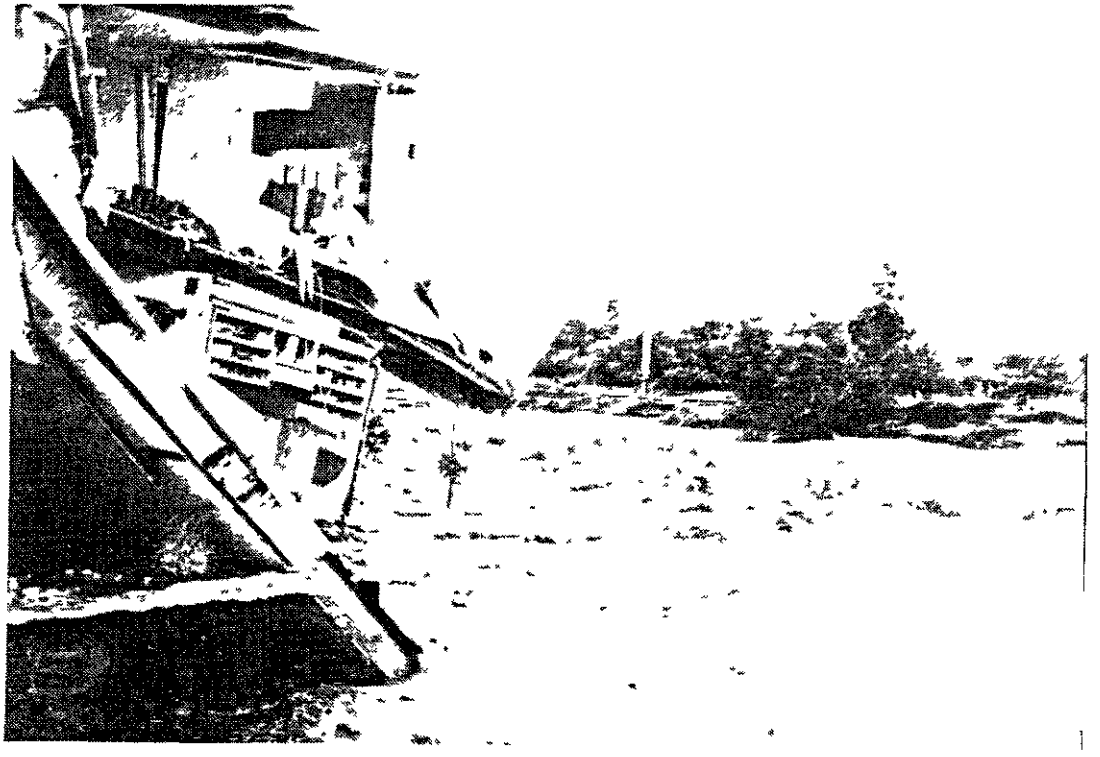

Figure 1.4. View from the west bank looking northeast across the Rillito River, Tucson, Arizona (Photo date: October, 1983).

non-essential, information has been cited by reference only. This approach allows the user who might be interested in details to locate the desired information, while allowing those who are not so interested in details to efficiently proceed through the design process.

Design manual organization provides a logical sequence of steps to guide the user from start to finish, both through individual elements of a single design and the overall integration of many elements of a comprehensive fluvial system analysis and design effort. Hydrologic Analysis (Chapter III) is the first major analysis after General Design Considerations (Chapter II). After completing the hydrologic analysis, information required as input for Hydraulic Analysis of Fluvial Channels (Chapter IV) is available. Similarly, results of this analysis are required prior to Sediment Transport Analysis (Chapter V). Chapter V completes the analysis component, providing the baseline data and knowledge necessary for application of various channel design techniques discussed in Chapter VI. To illustrate the integration of information resulting from each chapter, a comprehensive design example is given in Chapter VII.

The design manual is targeted for use by practicing engineers in the water resources field, or other individuals with equivalent knowledge or training. Consequently, an understanding of the basic concepts of hydrology and hydraulics has been assumed. Only that information necessary or essential to analysis of sediment transport is reviewed and/or provided in Chapters III and IV, resulting in a brief, highly-specialized treatment of the subject. Should additional information be required on general concepts, the user is referred to any hydrology and/or hydraulics textbook.

In contrast, subject material in Chapter V on Sediment Transport Analysis is presented in more detail. Beginning with Subsection 5.2, each subsection consists of three elements: DISCUSSION, APPLICATION, and EXAMPLE. The discussion material briefly describes the usefulness of the methodology and presents relevant theory and equations. The applications material presents information necessary to apply the methodology including rules of thumb and reasonable parameter values. Finally, an example is presented. Typically, it represents a simplistic case only intended to illustrate key points; however, when practical, these examples are based on case histories.

## II. GENERAL DESIGN CONSIDERATIONS

### 2.1 Channel and Watershed Response

A generalized definition of the idealized fluvial system is the three-zone description provided by Schumm (1977). In this description, Zone 1 is the drainage basin, watershed, or sediment source area; Zone 2 is the transfer zone; and Zone 3 is the sediment sink, or region of deposition. The three subdivisions are based on the predominant processes occurring in each, since sediments are stored, eroded, and transported in all zones. Zone 1 involves primarily the upper watershed and various tributary watersheds that contribute to the channel network of Zone 2. Zone 3 concerns primarily the coastal region, since this is considered the ultimate deposition zone. Consequently, in the analysis of inland watersheds, such as those of Arizona, Zone 3 is not of immediate importance and the fluvial system is often redefined as the interaction of the watershed and the alluvial channel network. Figure 2.1 provides a conceptual drawing of the fluvial system as defined.

Limiting our scope to this definition of the fluvial system still defines a highly complex system involving the interaction of many natural processes. These natural processes, often referred to as physical processes, govern the response of the fluvial system to various inputs and/or disturbances. The two primary inputs are climatic factors and man's activities. The most important climatic factor for erosion/sedimentation analyses is precipitation, in the form of either rain or snow. Man's activities include water resources development, watershed conversion, resource acquisition (energy, sand/gravel, etc.), development and operation of transportation systems, etc.

The response of the fluvial system to these inputs and/or disturbances is governed by the relevant physical processes. For example, the physical process describing soil detachment from raindrop impact is important in evaluating system response to precipitation. The physical process of overland flow, described by the interaction of such factors as slope, roughness, and precipitation excess, defines watershed response by establishing sediment transport supply available during a given precipitation event. Similarly, within the channels of the fluvial system, the physical processes describing sediment transport capacity establish whether or not the channel will aggrade or degrade in response to the precipitation-generated water and sediment runoff.

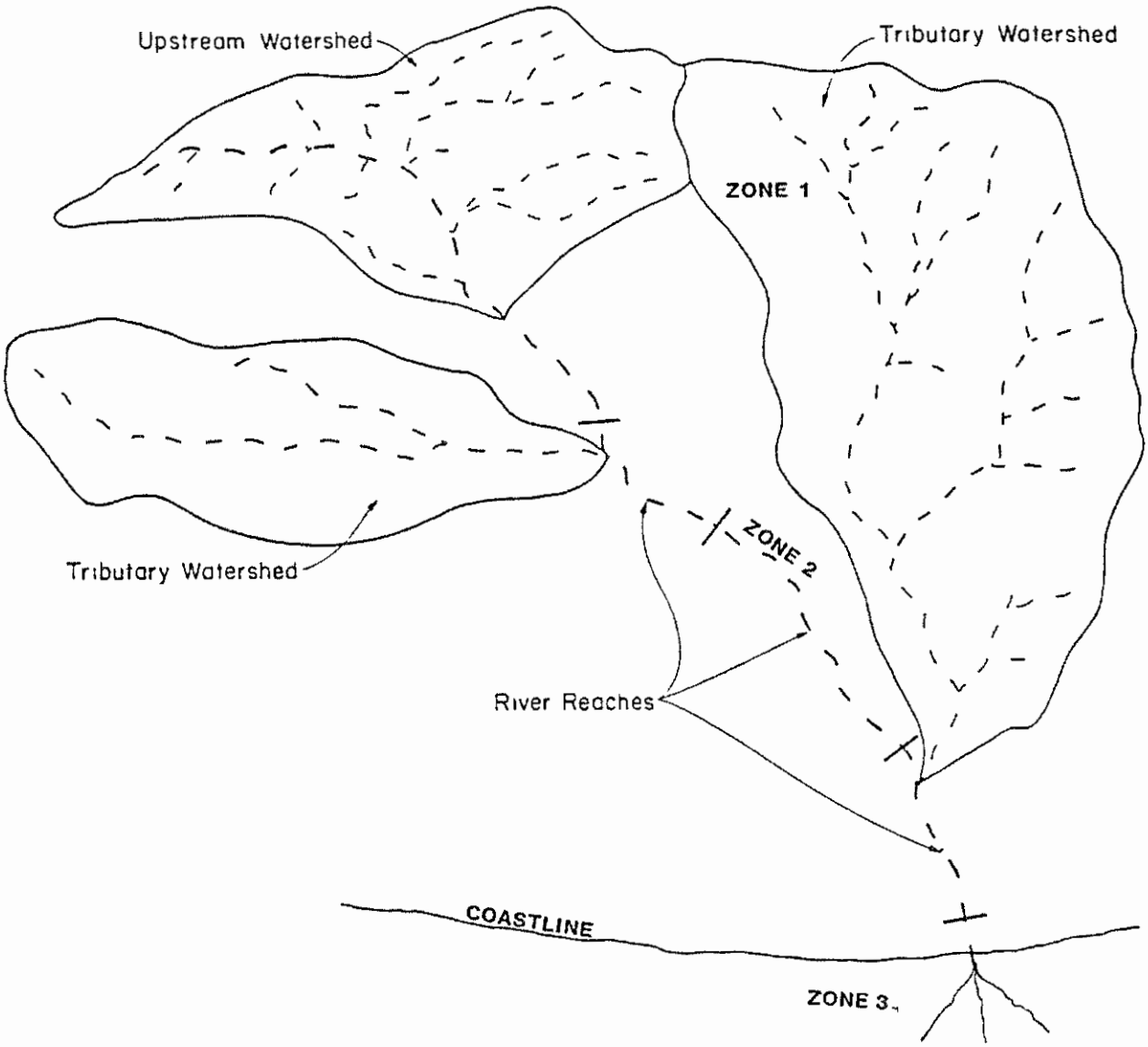


Figure 2.1. Watershed-river system.

Throughout all these events man's activities will modify fluvial system response by influencing the governing physical processes. Perhaps the most important concept to realize about fluvial systems is that they are dynamic systems attempting to achieve a state of balance or equilibrium. Consequently, the fluvial system is either adjusting to altered conditions or is in a state of dynamic equilibrium with present conditions. In either case, natural and man-induced changes can initiate responses that may be propagated through long periods of time or large areas. This dynamic nature requires that the analysis of problems (even on a small, localized scale) and development of solutions be considered in terms of the entire system. A classic example illustrating the dynamic nature of the fluvial system is the implementation of flood control reservoirs or debris basins. These structures can induce downstream degradation by limiting the delivery of upstream sediments. The dynamic action-response mechanisms of fluvial systems must be acknowledged and incorporated into any analysis or design effort, small or large.

## 2.2 Sand-Bed Channels

The analysis and design of fluvial systems in sandy-soil regions presents unique problems not encountered with more well-developed soils. In this context, "sandy" is used in the engineering sense to describe loose, cohesionless soils. Sandy soils are most predominant in the semi-arid and arid regions of the country. In comparison, the higher precipitation of a more humid environment produces vegetation and soils that are well developed and stabilized. Under these natural conditions, streams carry low suspended sediment loads reflecting the stability in upland watersheds. Additionally, high precipitation produces a dilution effect on the sediments that are eroded.

Vegetation and land forms in arid and semi-arid regions reflect the lack of water. Compared with more humid regions, topography is more abrupt, hillslopes are usually steeper and shorter, and soils are thinner with little organic content. Dryland conveyances are usually incised, intermittent or ephermeral channels. When the channels do flow, it is usually in response to small storm cells of limited areal extent producing high-intensity, short-duration storms. This type of storm creates "flashy" runoff, producing both excessive erosion in upland watersheds and a pronounced capacity for sediment transport in the channel system. Due to high drainage density (number of channels per unit area), water and sediment runoff occurs very efficiently. Peak discharge is high, and time to peak and flow duration are short.

The combination of large sediment yield, large transport capacity and "flashy" runoff can cause rapid changes in the configuration of sandy-soil channels. These changes include lateral migration, scour, degradation and aggradation, and can cause changes in stream form, bedform, flow resistance and other geometric and hydraulic characteristics. Designing either a stable alluvial channel (one without a channel lining) or a stable, lined channel under such dynamic conditions requires a detailed understanding of sediment transport and stream channel response. For example, unlined channels must be designed to minimize excessive scour, while lined channels must be designed to prevent deposition of sediments. Channel linings in dryland areas are typically composed of some type of artificial stabilization due to the difficulties in growing the required type of vegetation. Unlined channels are most successful when designed under the concept of dynamic equilibrium, which simply allows for sediment transport conditions without scour. These topics and others are presented in detail in the following chapters.

## 2.3 Cobble-Bed Channels

The erodibility or stability of any channel largely depends on the size and gradation of particles in the bed. As water flows through a channel located in a well-graded alluvium (i.e. consisting of clay, silt, sand, gravel or boulders) smaller particles that are more easily transported are carried away while the larger particles remain. This process, referred to as armoring, results in what will be defined as a cobble-bed channel, although the particles remaining on the bed can be as small as gravels. Compared to the more uniformly graded sand-bed channel, cobble-bed channels are relatively stable; however, they are still moveable boundary channels that can experience significant change during floods. Therefore, one of the important factors in cobble-bed analysis or design is evaluation of the stability of the armor layer and the maximum discharge it can sustain without being disrupted.

Another category of cobble-bed channels, in addition to those developed through the armoring process, are the boulder-lined channels of steep mountainous regions. Except in very large floods, these channels are very stable, with water cascading through sections of rapids connected by pools. This characteristic of flow and the large size of the roughness elements inhibits analysis by the more common and familiar techniques applicable to relatively

flat channels. When appropriate, brief discussions of analysis and design techniques for these very specialized conditions are presented.

## 2.4 General Solution Approach

### 2.4.1 Three-Level Analysis

The recommended solution procedure for sediment transport analysis generally involves three levels of analysis. The levels are defined as (I) qualitative, involving geomorphic concepts; (II) quantitative, involving geomorphic concepts and basic engineering relationships; and (III) quantitative, involving sophisticated mathematical modeling concepts. A qualitative Level I analysis provides insight into complicated fluvial system response mechanisms. The general knowledge obtained at this level provides understanding and direction to the Level II or III quantitative analysis. Additionally, the governing physical processes are usually identified in the general solutions of Levels I and II, allowing proper selection (or development) of a model for Level III that is efficient to use and applicable to the problems being analyzed. For long-term analysis where data are continually collected and/or updated, an iterative procedure of refinement becomes an important aspect of Levels II and III. As the data base becomes more complete and accurate, the type and level of analysis can become more sophisticated.

The three-level approach has been used extensively in the Southwest, and has been found to provide the most efficient analysis approach with the greatest accuracy for a given problem. The risk is minimized, since all results and conclusions are cross-checked to the other levels of analysis. The following paragraphs discuss some of the important concepts in each level of analysis.

### 2.4.2 Level I - Qualitative Geomorphic Analysis

The qualitative geomorphic analysis employed in Level I relies strongly on expertise and practical experience. Geomorphology is the study of surficial features of the earth and the physical and chemical processes of changing land forms, while fluvial geomorphology is the geomorphology (and mechanics) of watershed and river systems. Qualitative geomorphic techniques are primarily based on a well-founded understanding of the physical processes governing watershed and river response. Therefore, an important first step is to assemble and review previous work and data applicable to the study area,

and for key project participants to become familiar with the study area. A site visit by key personnel ensures identification of important characteristics of the study area. Additionally, being in the study area and contacting the local interest groups concerned provides excellent insight and perspective for the study. Site visits are an essential element of a successful study.

After completing the necessary site visits there are a number of simplified concepts and procedures that contribute to a qualitative analysis. These include aerial photograph analysis, historical land-use patterns, and relatively simple relationships describing basic geomorphic concepts. The Level I analysis is discussed in detail in Section 5.2.

### 2.4.3 Level II - Quantitative Geomorphic and Basic Engineering Analysis

In Level I, geomorphic principles are applied to predict watershed and stream response and do not require detailed data, only a general understanding of the direction of change of the stream conditions. Geomorphic principles can also be applied to available data to more accurately evaluate watershed or channel responses. This analysis, when coupled with traditional analyses involving basic engineering relationships, allows an initial quantitative evaluation of response. Analysis techniques used in Level II involve evaluation of trends in the historical thalweg elevation, quantitative evaluation of bed and bank sediments, application of the Shields relation and other geomorphic/engineering relations, application of sediment transport equations and the sediment continuity principle, frequency analysis of water and sediment transport data, etc. Level II analyses can be completed by hand calculator; however, use of a computer can expedite some calculations. For example, the analysis of sediment continuity using appropriate sediment transport relations is also often completed with the aid of computer programs. A detailed discussion of the Level II analysis is presented in Section 5.3.

### 2.4.4 Level III - Quantitative Analysis Using Mathematical Models

The Level III analysis is the most accurate method of analysis and involves computer application of various physical-process mathematical models. A mathematical model is simply a quantitative expression of the relevant physical processes. Various types of mathematical models for sediment routing are available, depending on the application (watershed or channel analysis) and the level of analysis necessary. For example, channel models range from

application of quasi-dynamic models (such as HEC-6 or HEC-2SR) to complicated dynamic sediment routing methods. In general, available models can be directly applied, or applied with minor modifications, to meet any project requirements. Criteria for electing to proceed with a Level III analysis are presented in Section 5.4.

## 2.5 Data Requirements

### 2.5.1 General

The quality and accuracy of any analysis are dependent on the data base available to the study. The type and number of data necessary depend greatly upon the sophistication of the analysis techniques (i.e., whether Level I, II, or III); however, for any analysis the level of effort required to establish the data base can represent a significant portion of the entire level of effort. The data base is developed from available data and any data collected during the project. Below is a brief discussion of the data requirements for each of the three levels of analysis.

### 2.5.2 Level I Data Requirements

The data required for a Level I geomorphic type analysis involves information on general trends and conditions describing the fluvial system characteristics, rather than specific, quantitative values. Some of the geomorphic relations used to qualitatively describe system action-response (the Lane relation or the slope-discharge relation) rely on estimates of dominant slope and/or discharge; however, due to the nature of the formulas and their intended applications, these numbers do not need to be accurate, refined values.

Other data required in a geomorphic analysis involve information describing historical trends or patterns. This information is generally interpreted on a qualitative basis, relying largely on personal experience and expertise. A typical example is the analysis of aerial photographs covering a span of several years. The amount of information extracted depends in part on the years covered. Similarly, insight derived from analysis of the flood history of a given drainage depends on the length of record available.

Table 2.1 summarizes some of the major data requirements of a Level I analysis.

### 2.5.3 Level II Data Requirements

Level II data requirements involve specific estimates of various parameters necessary to apply a range of quantitative geomorphic and basic engineering formulas. The data required might include specific, detailed numerical information on the watershed geometry (area, slope, length, drainage density, channel characteristics), sediment produced and delivered by the watershed (water discharge, sediment discharge, soil types, geology, representative particle sizes transported, gradation), man's influence (dams, sand and gravel extraction), and so forth. For many larger watersheds, data on these processes have been collected by various governmental agencies. The quality of the data and the length of record often vary so that careful evaluation is required to insure the data are useful for the purposes of the study. For example, most sediment discharge data have been collected only during low-flow periods; however, it is commonly accepted that the majority of sediment transport occurs during relatively short periods of high flow. Plotting low-flow sediment discharge data against water discharge for a given watershed generally produces poor results with no apparent trend. Consequently, data extrapolation or establishment of a descriptive equation for the watershed would appear impossible. However, if several additional high-flow data points were available, a distinguishable trend might be established (see Figure 2.2).

This situation can develop even when data have been collected over many years if no major storms occurred during the period of record. Therefore, the available data must be carefully interpreted and used to avoid erroneous conclusions. Additionally, the available data base is typically much smaller that that required to conduct the study. Consequently, the necessary additional data must be established by field measurement or by data generation techniques. A brief overview of several basic concepts in data generation is given in Section 2.5.5.

Some of the specific data requirements necessary to conduct a Level II analysis are presented in Table 2.2.

Table 2.1. Partial Listing of Data Requirements for a Level I Analysis.

| |
|---|
| General Channel Slope & Cross Section Characteristics |
| Representative (Dominant) Discharge |
| Bed and Bank Material Characteristics |
| Land-Use Changes |
| Major Structures and History |
| Aerial Photographs |
| Flood History |
| Fire History |
| Tectonic Activity |

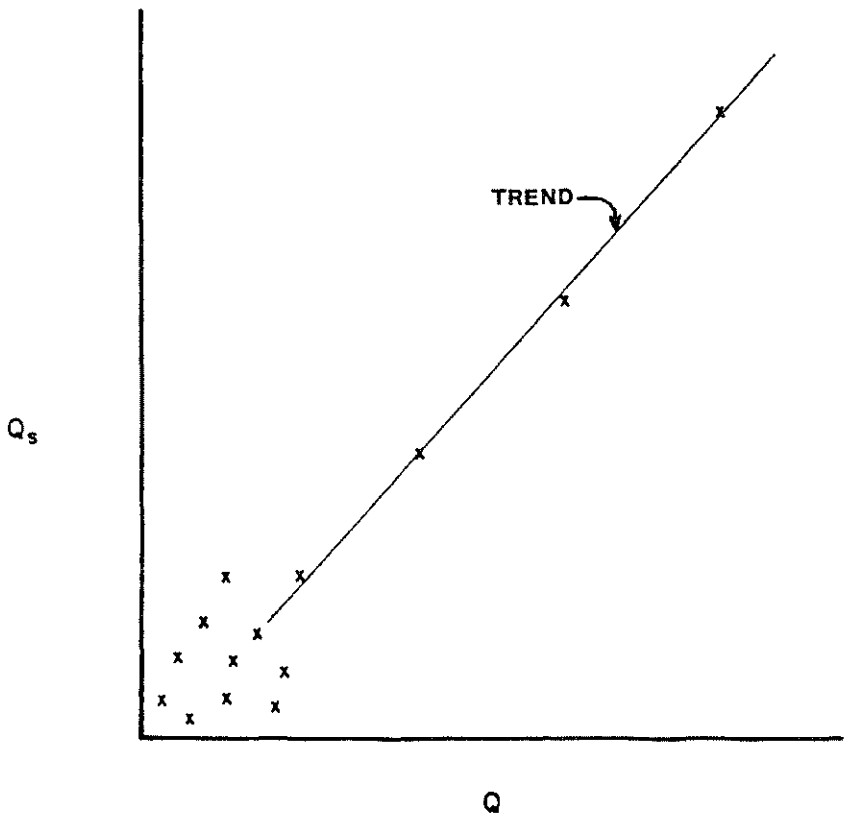


Figure 2.2. Definition sketch illustrating typical measured sediment discharges vs. water discharge relation.

Table 2.2. Partial Listing of Data Requirements for a Level II Analysis.

| |
|---|
| Watershed Geometry (Area, Slope, Length, Drainage Density) |
| Channel Geometry (Profile, Cross Sections, Sinuosity) |
| Hydraulic Data (Flow Depth, Velocity) |
| Water Discharge Records |
| Sediment Discharge Data |
| Discharge-Frequency Relations |
| Flood Hydrographs |
| Particle Size Gradations |
| Sand and Gravel Extraction Data |
| Reservoir Operating Procedure |
| HEC-2 Data/Runs |
| Reservoir Deposition Data |

### 2.5.4 Level III Data Requirements

For any study involving physical-process mathematical modeling (Level III), it is necessary to define a spatial and temporal description that provides a realistic representation of the system for simulation purposes. This is particularly true for large-scale modeling where it is not practical to account for every possible inflow and outflow. Consequently, knowledge of the critical areas or areas of importance is necessary to develop the spatial representation. The actual data required to do this are not significantly different from those necessary for a Level II analysis, although more detail is often required for the mathematical modeling of Level III.

### 2.5.5 Data Generation Concepts

Data generation techniques can involve direct extrapolation and transposition of the available information, or indirect extrapolation through application of engineering relations based on the governing physical processes. The method of establishing the necessary additional information is determined by the priority or importance of the given area and the potential accuracy of the data generation methods available.

Data generation by direct extrapolation within a given watershed, or the transposition of data between watersheds, must be done properly to achieve accurate results. For example, transposition of sediment discharge data between watersheds cannot be accomplished accurately by assuming that a simple relation exists between water and sediment discharge rates (i.e., $Q_s \propto Q^b$), although this is generally an adequate relation for describing sediment transport rates within a given watershed without anticipated land-use changes. By considering the governing physical processes, one realizes that sediment transport is more directly related to individual hydraulic parameters, for example velocity and depth, which for a given discharge can vary significantly between various channels. Therefore, a better relation for describing sediment discharge for purposes of transposition of data is $Q_s \propto V^b d^c$. Consequently, watersheds that are similar in various erosion-related characteristics may allow adequate transposition of data by this type of relation.

Indirect extrapolation of data involves the application of a physically based engineering equation or relation. For example, one method to generate additional sediment transport data for a given watershed would be to use the available data to calibrate an applicable sediment transport equation or model, and then use the calibrated equation or model to generate new data.

The importance of understanding the governing physical processes in data generation is necessary for any variable, not just sediment discharge. Properly conducted data generation can provide accurate results that maximize the utility of available information.

# III. HYDROLOGIC ANALYSIS

## 3.1 Relation of Hydrology to Other Analyses

Hydrologic analysis is a necessary first step to most water resource-related design projects. For example, the design of a spillway or flood-control channel is based on a design flood, where the characteristics of the flood depend on watershed and climatic variables. Similarly, hydrologic analysis is an important first step in fluvial systems analysis, since water is the driving mechanism for erosion and sediment transport. Knowledge of the runoff hydrograph provides the necessary information for determining runoff hydraulics at points of interest in the watershed or channel network.

Determination of runoff hydrology relies on evaluation of measured streamflow data or, in the absence of measured data, estimation of the runoff hydrograph through evaluation of the important physical processes. The latter is quite often the situation that the water resource engineer must deal with and the procedure involves a logical sequence of steps, beginning with the estimation of rainfall magnitudes corresponding to a specified return period and duration. After determining the relevant rainfall magnitudes, runoff volume is calculated by estimating losses, largely those due to infiltration. The volume of runoff is then used in conjunction with watershed characteristics to estimate a runoff hydrograph. The runoff hydrograph provides information on important variables such as peak discharge, flow duration, and time to peak. Methodologies also exist for direct estimation of these parameters, particularly peak discharge, without requiring the development of the runoff hydrograph.

It is not the objective of this chapter to provide a detailed discussion of the various methodologies or procedures available for a hydrologic analysis. Numerous textbooks and government publications are available with this information and it is not necessary to duplicate it here. Therefore, only a brief review of available and/or applicable techniques is provided. Adequate references are cited to allow the user to locate detailed discussions, as needed, of the various techniques.

The primary objective of this chapter is to illustrate some of the specialized applications of this hydrologic information when conducting fluvial systems analysis or design. These applications center on temporal considerations, both during a single flood (short term) and over many floods and/or years (long term). The more familiar application of hydrologic infor-

mation in hydraulic structures design relies primarily on a single large flood event, the logic being that if the structure will withstand this flood, it will certainly withstand the smaller flows occurring between large events. However, with fluvial systems analysis and design, the cumulative effect of erosion/sedimentation occurring throughout all flows is important. While this cumulative effect is seldom as significant as a single large flood (it is often said that 90 percent of all river channel changes occur during ten percent of the flows), it can be an important component in some applications.

## 3.2 Establishing Return Period Discharges and Durations

### 3.2.1 General

The peak rate of runoff or peak discharge is a natural by-product of the determination of the runoff hydrograph. However, many hydraulic designs are based on direct estimates of peak discharge without requiring other hydrograph information. In general, computation of the hydrograph is the more satisfactory procedure; however, since many analyses use a peak-discharge approach, a few of the common approaches are included here and could be utilized when budget or other constraints necessitate a low level of effort.

Estimation of peak discharge is simpler than the procedures for development of the entire hydrograph. Determining the method to use depends on the available data and the applicability of a given relationship to the design conditions. For a gaged watershed the estimate is made by a hydrologic analysis of the drainage and stream, characteristics of the climate and the accumulated streamflow data. An efficient method to access data and conduct analysis on gaged watersheds is the U.S. Geological Survey (USGS) WATSTORE system. The WATSTORE system is a computerized data processing, storage, retrieval and analysis package for thousands of USGS-maintained stream gaging stations, water quality stations, sediment stations, water level observation wells and lake and reservoir monitoring stations. Typical analyses available through WATSTORE include frequency analysis and flow duration curves. Information on the availability of specific types of data, acquisition of data or products, and user charges can be obtained locally from USGS Water Resource Division district offices. Table 3.1 lists the district offices in the southwest geographical area, and also provides an address for general inquiries about WATSTORE.

To obtain information on gaged watersheds not maintained by the USGS, the NAWDEX program may be of value. The NAWDEX program, administered by the USGS,

Table 3.1. USGS Offices with WATSTORE Information.

| Water Resource Division District Offices in Southwest Geographic Area |
| --- |
| Tucson, Arizona |
| Menlo Park, California |
| Albuquerque, New Mexico |

| General Inquiries |
| --- |
| Chief Hydrologist<br>U.S. Geological Survey<br>437 National Center<br>Reston, Virginia 22092 |

is a national confederation of water-oriented organizations working together to improve access to water data. Organizations involved with NAWDEX range from governmental (Federal, state and local) to academic and private. NAWDEX does not maintain the available data bases, but rather provides a variety of services to assist users in identifying, locating and obtaining the required data. The locations of local assistance centers in the Southwest for NAWDEX and for general inquiries about the system are provided in Table 3.2.

Development of hydrologic information from gaged watersheds is relatively straightforward; however, most smaller drainages are ungaged and an estimate of the design flow must be made on limited topographic and climatic data. Bibliographies by Chow (1962) and Reich (1960) identify and review many of the possible methods of estimating peak flows from ungaged watersheds. Some of the more common methods applicable to the Southwest are reviewed in the following paragraphs.

### 3.2.2 Rational Method

The Rational Method is a common method for peak flow estimation; however, it has many limitations that must be considered. These limitations are discussed by McPherson (1969) and others. Basically the equation $Q = CiA$ tends to oversimplify a complicated runoff process. However, because of the simplicity of the Rational Method, it remains widely used.

The assumptions used in developing the Rational Method are:

1. The rainfall occurs at a uniform intensity over the entire watershed.
2. The rainfall occurs at a uniform intensity for a duration equal to or greater than the time of concentration.
3. The frequency of the runoff equals that of the rainfall used in the equation.

The time of concentration $t_c$ is defined as the time required for water to flow from the most remote (in time of flow) point of the watershed to the outlet, once the soil has become saturated and minor depressions are filled (Schwab, et al., 1966). Accurately evaluating the time of concentration is one of the major problems in using the Rational formula.

Reich (1971) cites references that indicate the potential of the Rational formula and that its prediction on the average was close to observed peaks,

Table 3.2. USGS Offices with NAWDEX Information.

| Local Assistance Centers in the Southwest Geographical Area |
| --- |
| Tucson, Arizona |
| Menlo Park, California |
| Albuquerque, New Mexico |

| General Inquiries |
| --- |
| National Water Data Exchange (NAWDEX)<br>U.S. Geological Survey<br>421 National Center<br>Reston, Virginia 22092 |

although there is usually considerable scatter. The formula has generally been limited to watersheds of less than three square miles (2,000 acres).

### 3.2.3 SCS TR-55 Methods

The SCS has developed several methods that are commonly used for predicting runoff, ranging from peak flow estimation to complete hydrograph development. The method presented in SCS TR-55 (1975) is a graphical procedure for estimating peak discharges using the time of concentration and the travel time. This method is an approximation of the detailed hydrograph analysis produced by the computer program presented in SCS TR-20.

The graphical approach is applicable to a watershed where runoff characteristics are uniform and valley routing is not required. The relationship was developed by computing hydrographs for a one-square-mile drainage area, along with a range of times of concentration, and routing them through stream reaches with a range of travel times. A constant runoff curve number of 75 and a Type II (late peaking) rainfall sufficient to yield three inches of runoff were assumed.

The result of these computations is a curve relating the time of concentration $t_c$ to the peak discharge in cubic feet per second per square mile per inch of runoff, $q_p$. The curve is applicable for watersheds where the runoff can be represented by one curve number, CN, which implies the land use, soils and cover are similar and uniformly distributed throughout the watershed. As in the Rational method, accurate evaluation of the time of concentration is a major problem in application. The method is applicable for watersheds up to approximately 20 square miles in size. The runoff volume is obtained from a table and peak discharge is calculated from an equation.

A second graphical approach is presented in the SCS TR-55 publication for agricultural drainage areas up to 2,000 acres (three square miles). The method is reported to provide a quick and reliable estimate of peak discharge for most agricultural areas of the United States.

### 3.2.4 USGS Flood-Frequency Analysis

The U.S. Geological Survey (USGS) has developed graphical methods for determining the probable magnitude and frequency of floods of varying recurrence intervals for most of the United States. The graphs were developed on the basis of a comprehensive study of all flood data available in each region by flood-frequency analysis. The relations are generally developed for rural

watersheds and are based on gaging station records having ten or more years of record not materially affected by storage or diversion. Therefore, results obtained from this empirical, graphical procedure will represent the magnitude and frequency of natural floods within the range and recurrence intervals defined by the base data. The publication for the State of Arizona (Roeske, 1978) was developed as a joint effort between the Arizona Department of Transportation and the USGS.

### 3.2.5 Other Regionalized Methods

The literature contains many articles on experimental models for flood flow frequency estimation at ungaged locations. However, a literature evaluation by McCuen, et al. (1977) indicates that the literature does not adequately reflect what is currently being used. Instead, the literature contains many articles on experimental models that have been designed for a specific region or a specific problem. Thus, the volume of the literature on the techniques that are currently being extensively used (e.g., the Rational formula and the SCS technique) is not in proportion to the frequency of use of these techniques.

The use of a regionalized technique can often produce more reliable results than the more commonly used generalized techniques. However, care must be exercised in applying a regionalized method to ensure its validity to the given problem.

### 3.2.6 Channel Geometry Techniques

Several studies of alluvial stream channels of the western U.S. (Leopold, et al., 1964; Osterkamp and Hedman, 1981) have shown relationships between channel size and discharge characteristics. In perennial streams the active-channel level is nearly coincident with the stage corresponding to mean annual discharge. For ephemeral streams the active-channel capacity is usually more indicative of higher return flows, such as the 10-year flood. In general, fewer channel geometry relationships have been proposed for ephemeral streams, since there are few streamflow records of adequate length for analysis.

Greater accuracy can be achieved by considering sediment properties. Osterkamp and Hedman (1981) have presented groups of channel geometry equations according to channel type as characterized by the channel-sediment variables. They also demonstrate that consideration of channel gradient and discharge variability can improve discharge estimates.

This method can be a highly useful tool because (1) estimates are easily made, and (2) the channel size is a direct result of the water passing a given site, and thus a reliable index. However, care must be taken in selecting the site and the datum for the field channel measurements. As in all regression techniques, the accuracy of the mathematical relationships is dependent on the accuracy of the data base.

## 3.3 Development of Flood Hydrographs

### 3.3.1 General

Development of accurate flood hydrographs follows the logical sequence of steps reviewed in Section 3.2 (establishment of rainfall volume for design storm, determination of corresponding runoff volume and development of hydrograph considering watershed characteristics). This procedure accounts for the governing physical processes and is generally more accurate for peak discharge estimation than the methods reviewed in Section 3.2. Furthermore, any analysis involving routing of floods requires that the discharge hydrograph be known.

It is possible to approximate a hydrograph using a re-scaled or transformed record, i.e., re-scaling the recorded streamflow of an upstream gage by a ratio of drainage areas or by regression equations. This technique can provide acceptable results, particularly when a low level of effort is required, but when possible, hydrographs should be based on the governing physical processes. One of the most commonly used methods of hydrograph development is the Soil Conservation Service (SCS) unit hydrograph approach. This approach derives hydrographs from runoff calculations involving evaluation of precipitation amounts, interception, infiltration, surface detention, time of travel, etc. A brief review of the basic analyses for development of hydrographs is provided in the following sections, along with applicable methodologies.

### 3.3.2 Characterization of Design Storm

The first step in developing runoff hydrographs for an ungaged drainage is characterization of the design storm. The existence and length of record of rain gages and the size and location of the watershed determine the methods and considerations necessary in determining the character and magnitude of the storm. Since many designs are formulated in terms of return period, the volume of rainfall corresponding to a specified return period and duration

must be determined by frequency analysis. In preparing a design the engineer is likely to choose one of two courses in calculating the volume of rainfall: (1) use data from an on-site gage, data suitably transferred from nearby gages with long records, or a combination of on-site and transferred data used to perform a frequency analysis, or (2) use one of the National Weather Service (NWS) publications that present the results of frequency analysis performed on their rain gage network in the form of isopluvial maps. Most statistical hydrology textbooks (e.g. Haan, 1977; Kite, 1977, Yevjevich, 1972) discuss methodologies for frequency analysis. Since most sites will not have on-site records of sufficient length, and due to the amount of work involved in synthesizing a record of sufficient length by transferring data, the second course (NWS Publications) is most likely to be used.

Currently there are three publications by NWS that are in regular use. In chronological order, they are: (1) Technical Paper No. 40 (TP40) by Herschfield (1961); (2) Precipitation-Frequency Atlas of the Western United States (11 volumes, 1973); and (3) "Five to 60-Minute Precipitation Frequency for the Eastern and Central United States (1977). TP40 presents the results of depth-duration frequency analysis investigations for the contiguous United States performed by NWS and its precursor agency, the United States Weather Bureau. In addition, new studies for the high plains states appeared in this paper for the first time. The maps presented in TP-40 are considered most reliable for relatively flat regions. However, in the western United States, the mountainous terrain often causes large variations in precipitation. To correct this problem, the Precipitation-Frequency Atlas of the western United States was introduced in several volumes. This publication contains much larger-scale rainfall-duration-frequency maps than TP-40, and it corrects for such factors as slope, elevation, distance to moisture, location, normal annual precipitation, barriers to airflow and surface roughness, not included in TP-40. For Alaska, the publication used is TP-47, Probable Maximum Precipitation and Rainfall-Frequency Data for Alaska. Storms in the eastern United States are still characterized by TP-40; however, a more recent publication for storms of 5 to 60 minutes duration has recently been published by NWS (1977), under the title "Five to 60-Minute Precipitation Frequency for the Eastern and Central United States (HYDRO-55)." However, for 24-hour duration events, the rainfall atlas for the western United States and TP-40 and 47 are the most commonly used documents.

The procedure for using the NWS atlases to obtain point rainfall volumes is quite straightforward. Studies can utilize 24-hour or 6-hour duration storms for varying return periods (e.g. 2, 10, 25 or 100 years). In western states, isopluvial maps are printed for each of these storms. Determining the appropriate storm volume is a matter of reading the map at the watershed location.

The determination of rainfall volume is only the first step in characterizing the design storm. Obviously, if there is no water left after infiltration there will be no runoff and therefore no further need for concern regarding surface water hydrology. In small watersheds the character of the runoff hydrograph is largely determined by the character of the hyetograph and the infiltration properties of the drainage. Therefore, estimates of the peak runoff are quite sensitive to the temporal distribution of rainfall. The methods for distributing intensities over time are in common use and are standardized to some degree. However, they are somewhat subjective, requiring judgment on the part of the user.

To further compound matters, there are three distinct types of rainfall/runoff events which can occur in Arizona. They are:

1. Convective Thunderstorms. Normally occurring in July and August, these storms are created by moisture that moves into the state from the Gulf of Mexico and combines with air movement from the heated mountainous terrain to produce intense, short-lived rainstorms. Often these storms are accompanied by thunder, lightning and strong, gusty winds. Generally their durations do not exceed one hour. However, upon occasion they have been known to continue for as long as six hours. Maximum areal coverage of individual storm cells is on the order of 90 to 100 square miles, but maximum rainfall amounts and intensities (sometimes exceeding 10 inches per hour) are usually confined to less than a two mile-square central core of rainfall. Historically, these types of storms generally have had their major impacts upon drainage catchments which are less than 25 square miles in areal extent.

2. General Summer Storms. Normally occurring in August and September, these storms originate off the west coast of Mexico as tropical storms or hurricanes and bring damaging winds and flood-producing rainfall into the state. Generally their durations range from one to four days, although they have been known to last as little as six hours and as long as ten days. Maximum areal coverage of general summer storms can easily exceed many thousands of square miles; however, maximum rainfall amounts and intensities are often concentrated within multiple isolated cells of less than 100 square miles in area. Historically, major impacts from these storms have generally occurred upon drainage catchments which range in size from 100 to 5,000 square miles.

3. General Winter Storms. Normally originating over the Pacific Ocean, these storms move rapidly eastward through the state. Precipitation from winter storms is usually of light or moderate intensity. At times, however, these winter storms have been the source of precipitation for the wettest years of record and have produced some of the most damaging floods. This has been especially true when warm rainfall has occurred over well-developed snowpacks in the higher elevations of the state, producing rapid runoff over large areas. Durations for winter rains range from a few hours to several days. Maximum areal coverage can exceed tens of thousands of square miles. The major drainage catchments in the state usually exhibit the most significant impacts from these winter storms, primarily because major catchments are fed by numerous tributaries, which cumulatively may constitute many thousands of square miles in watershed area.

There are basically two kinds of methods for constructing hyetographs from designated storm volumes. The first type is the construction of a synthetic storm through the use of depth-duration-frequency (DDF) curves or standard SCS or other regionalized rainfall distributions. When using the DDF curves, time intervals are selected and the rainfall intensity for each selected interval is computed by dividing the total amount of rainfall for that interval by the time of the interval. The result is the creation of several different rainfall intensities representative of finite time intervals during the storm. These intensities are then appropriately arranged by the user based on knowledge of local conditions. The ordering is the main source of subjectivity in these methods. Such synthetic methods have the advantage of at least providing a consistent set of rainfall intensities.

The second method is to use a storm record of many years from a nearby recording rain gage as the pattern for distributing rainfall. The difficulty in this approach is that the resulting intensities may be of differing return periods. Therefore, despite the intuitive advantage of having been recorded on site, the historical event does not provide a consistent approach to the formulation of a design storm.

### 3.3.3 Determination of Runoff Volume

Once the design storm has been specified, the next step in obtaining a runoff hydrograph is the determination of runoff volume. This calculation requires estimation of the effects of interception, infiltration and surface detention. With respect to rainfall on watersheds, especially in the western U.S., the most important of these processes is usually infiltration. The most commonly used method for determination of runoff volume is the SCS curve

number approach. This method was developed for use with nonrecording rain gages; that is, the method is used to predict total volume of runoff from total volume of rainfall. In its publication, Design of Small Dams [U.S. Bureau of Reclamation (USBR), 1977], the USBR summarized and modified the SCS method for use with temporally arranged rainfall. This modification of the SCS method is suggested for the determination of runoff volume.

While the SCS method has gained wide acceptance and is in common use, serious errors can result in its application. In many cases methods that are based on field measurements are preferred. One of the most common of these methods is the Horton infiltration equation. Both the Horton and the SCS methods model the soil response independently of storm characteristics. This attribute, and the fact that the effects of watershed modification are difficult to reflect in either method, is leading many hydrologists to utilize more physically sound approaches, i.e., Green and Ampt (1911). Many of these approaches have been ignored in the past due to the necessity of laborious calculations. However, with the advent of extremely powerful small calculating devices, this objection is becoming obsolete (for example, see numerical solutions of Green-Ampt infiltration equation discussed by Li, et al., 1976). In the future it is likely that more physically based methods will be adopted.

Alternative infiltration approaches include methods based to a greater degree on infiltration methods at the site and that incorporate a mathematical description of the infiltration process. At this point it should be remembered that the SCS method is not entirely equivalent to calculation of infiltration. The SCS method strives to determine the retention characteristics of the drainage. Retention includes interception as well as infiltration. If one abandons the SCS method, some attempt must be made to determine losses to interception; however, infiltration is usually the most significant of these processes. In many western watersheds vegetation is so sparse that essentially all rainfall reaches the ground. Even where vegetative cover is relatively dense, infiltration is usually more significant as a hydrologic process than interception.

### 3.3.4 Hydrograph Development

A discussion of design flood analysis for small dams is presented in the USBR's (1977) "Design of Small Dams." This discussion includes development of unit hydrographs resulting from the runoff calculations discussed above. The USBR approach is based on runoff calculated by the SCS method; however, any method that produces temporally distributed excess rainfall provides the necessary information for calculation of a hydrograph. The user is referred to the USBR publication, or almost any hydrology textbook, for detailed procedures for unit hydrograph and triangular hydrograph analysis.

## 3.4 Selection of Design Event for Fluvial Systems Analysis

Selection of an appropriate design event for fluvial systems analysis is generally not as straightforward as it is for other water resource projects. For example, hydraulic structures design is usually based on a single large flood that the structure must withstand. The selection of the appropriate design event is generally based on an acceptable level of risk. By comparison, the selection of the design event for fluvial systems analysis depends largely on project objectives. For example, information on long-term cumulative erosion rates resulting from numerous floods over many years may be of interest. Conversely, the short-term erosion or scour occurring during a single event, for example at a bridge crossing, may be required. Therefore, temporal considerations established by project objectives will govern the selection of the design event.

For short-term analysis the single event is often a frequency-based flood, for example the 2-, 10- or 100-year event. Another possibility is the Probable Maximum Flood, defined as the most severe combination of critical meteorologic and hydrologic conditions that is reasonably possible in the region, or the Standard Project Flood, which results from the most severe combination of meteorologic and hydrologic conditions that is considered reasonably characteristic of the region, but excluding extremely rare combinations. Generally, the standard project storm rainfall amounts to approximately 50 percent of the rainfall for the probable maximum flood (Viessmann, et al., 1972).

For long-term analysis the objective is to evaluate the cumulative effects of a broad range of flow conditions. One approach that can be used is based on the concept of dominant discharge. The dominant discharge is that value which is predominantly responsible for the geometric characteristics of the channel. Although it is difficult to precisely establish the dominant discharge, the value is typically between the 2- and 5-year events for perennial streams and between the 5- and 10-year events for intermittent and ephemeral channels. The aggradation/degradation occurring for this dominant discharge is then assumed to represent the average annual value which can be extrapolated in time to evaluate long-term conditions (i.e., if the mean annual sediment delivery is 1,000 cubic yards, the total delivery over 10 years is 10 x 1,000, or 10,000 cubic yards).

A better approach than dominant discharge for long-term analysis of erosion/sedimentation is one which accounts for the probability of occurrence of various flood events during any one year. For example, if $VOL_s$ is the sediment delivery at a specific location for a given flood and $P$ is the probability of occurrence of that flood in one year, the product $VOL_s \times P$ represents the contribution of that one flood to the long-term mean annual delivery. To account for the contribution of all possible flows the integration

$$\overline{VOL_s} = \int_0^1 VOL_s \, dP \qquad (3.1)$$

is required. This integration is best accomplished through use of frequency curve concepts. The frequency curve for sediment delivery can be estimated graphically by computing the sediment delivery expected for each of several floods of known return periods. Figure 3.1 illustrates the estimation of a sediment delivery frequency curve. The area under this curve (between the limits of 0 and 1) then represents the mean annual sediment delivery. This area can be computed graphically or numerically. The numerical procedure involves summing the incremental trapezoidal areas established by calculation of $VOL_s$ for various return periods, with approximations for $VOL_s$ at probabilities of 0 and 1 in order to satisfy the limits of integration defined by Equation 3.1. Assuming this calculation is completed for the 2-, 5-, 10-, 25-, 50- and 100-year events, the mean annual sediment delivery would be approximately

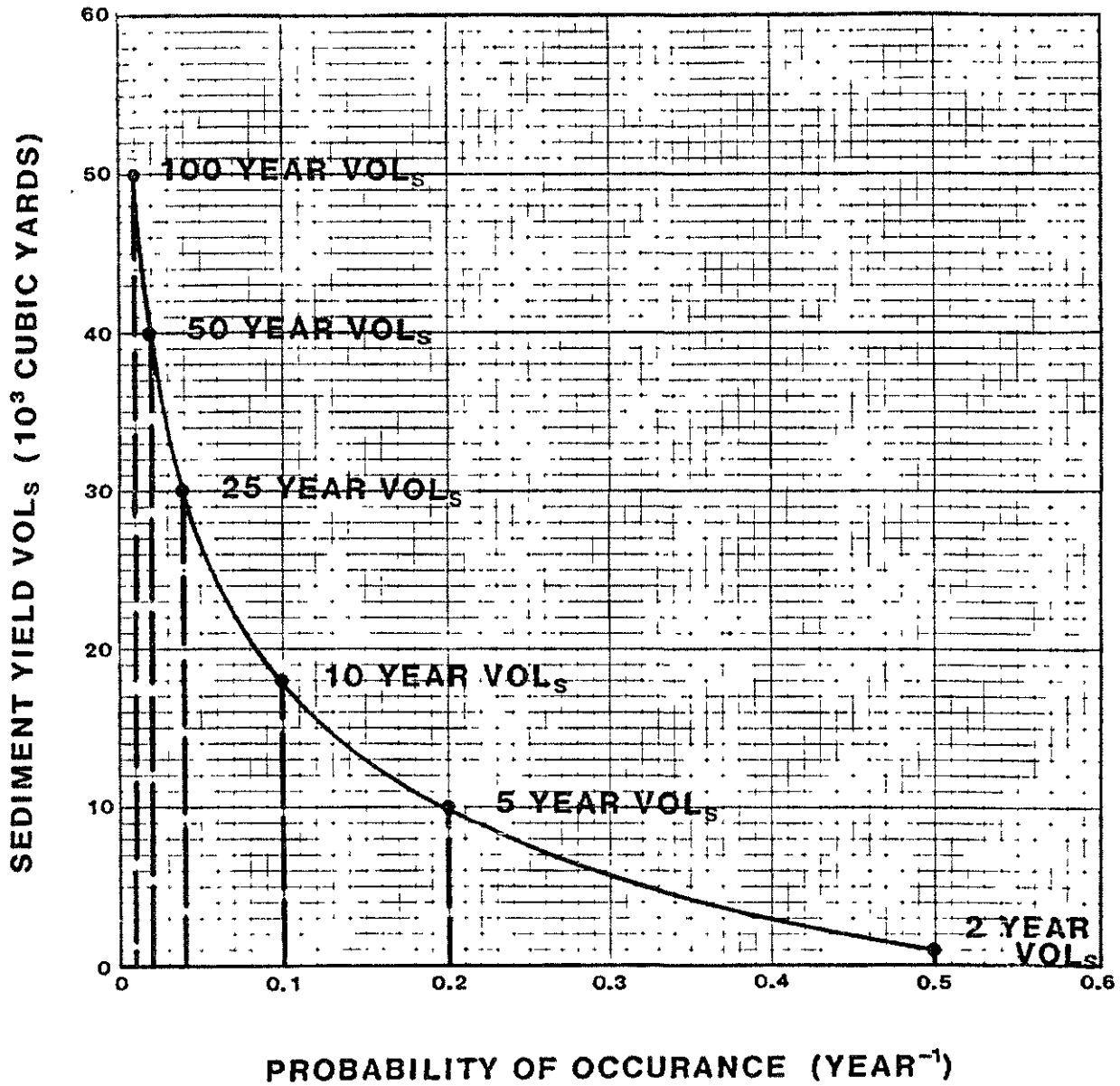


Figure 3.1. Typical sediment yield frequency curve.

$$(VOL_s)_m = 0.01\ (VOL_s)_{100} + 0.01\ \left(\frac{(VOL_s)_{100} + (VOL_s)_{50}}{2}\right) \qquad (3.2)$$

$$+ 0.02\ \left(\frac{(VOL_s)_{50} + (VOL_s)_{25}}{2}\right) + 0.06\ \left(\frac{(VOL_s)_{25} + (VOL_s)_{10}}{2}\right)$$

$$+ 0.1\ \left(\frac{(VOL_s)_{10} + (VOL_s)_5}{2}\right) + 0.3\ \left(\frac{(VOL_s)_5 + (VOL_s)_2}{2}\right)$$

$$+ 0.5\ \left(\frac{(VOL_s)_2 + 0}{2}\right)$$

As a check on this calculation, it is useful to apply the weighting relationship (Equation 3.2) with the corresponding water discharge hydrographs and compare the calculated value to the mean annual water delivery as determined from stream gaging data. In an arid or semi-arid area, differences in these two estimates of long-term mean annual water yield may reflect numerical errors resulting from the trapezoidal rule approximation. Alternatively, it may reflect an inadequate record length of measured data or inadequate hydrological analysis in developing return period hydrographs. In a more humid environment, these same factors may be responsible for differences between measured and calculated water yield. Additionally, differences could result from base flows that are not adequately accounted for in the flood-based incremental probability calculation. For arid and semi-arid application, assuming adequate record length and hydrology, a correction factor for application to the probability weighted sediment delivery can be defined as

$$K = \left(\frac{VOL_{meas}}{VOL_{inc}}\right)^2$$

where $VOL_{inc}$ is mean annual water volume calculated from Equation 3.2, and $VOL_{meas}$ is the mean annual water volume determined from gaging station data. The square of the ratio is taken since the relationship between water and sediment discharge is proportional to water discharge to the power of 1.5 to 2.0. Under the assumption of adequate record length and hydrology, the correction for numerical errors in evaluation of water yield should be relatively small, say no more than 10 to 20 percent. The maximum value for K would then be about 1.5. As a rule of thumb, this value should be assumed if

the measured record length is extremely short (i.e., 10 to 20 years) or the calculated value of K is unusually large or small.

### 3.5 Discretizing Flood Hydrographs

To evaluate the cumulative erosion/sedimentation occurring during a flood, as will be discussed in Section 5.3.8, it is usually necessary to discretize the hydrograph. The only alternative to the discretization process is when the water discharge hydrograph can be approximated by a triangular hydrograph. Under these conditions calculation of the cumulative erosion/sedimentation can be simplified. When a triangular hydrograph approximation is not possible, it is necessary to discretize the water discharge hydrograph, which provides a series of constant discharges acting over short time intervals as illustrated in Figure 3.2. The hydraulic, erosion and sedimentation analyses are completed for each discharge level and weighted according to the time interval over which they occur. The cumulative erosion/sedimentation occurring during the flood is then the sum of the weighted values. For calculation purposes it is often efficient to maintain a uniform time interval. The discharge levels are then selected so that the total volume of the discretized hydrograph is not appreciably different from the original hydrograph (in other words, so that the incremental volume of the discretized hydrograph above the original hydrograph cancels the volumes not represented below the original hydrograph). This procedure is easily accomplished graphically (visually), which also allows slight adjustments to provide for convenient discharge levels.

Figure 3.3 illustrates the discretization of a flood hydrograph. The volume of the original hydrograph, determined by planimetering, is 4,456 acre-feet (AF), while the volume of the discretized hydrograph, determined by summing the incremental rectangular areas, is 4,473 AF. Table 3.3 summarizes the calculated sediment transport rates for the given discharge rates of the discretized hydrograph, as determined by techniques discussed in Chapter V. The total sediment delivery during the storm is then computed from the discretized hydrograph as:

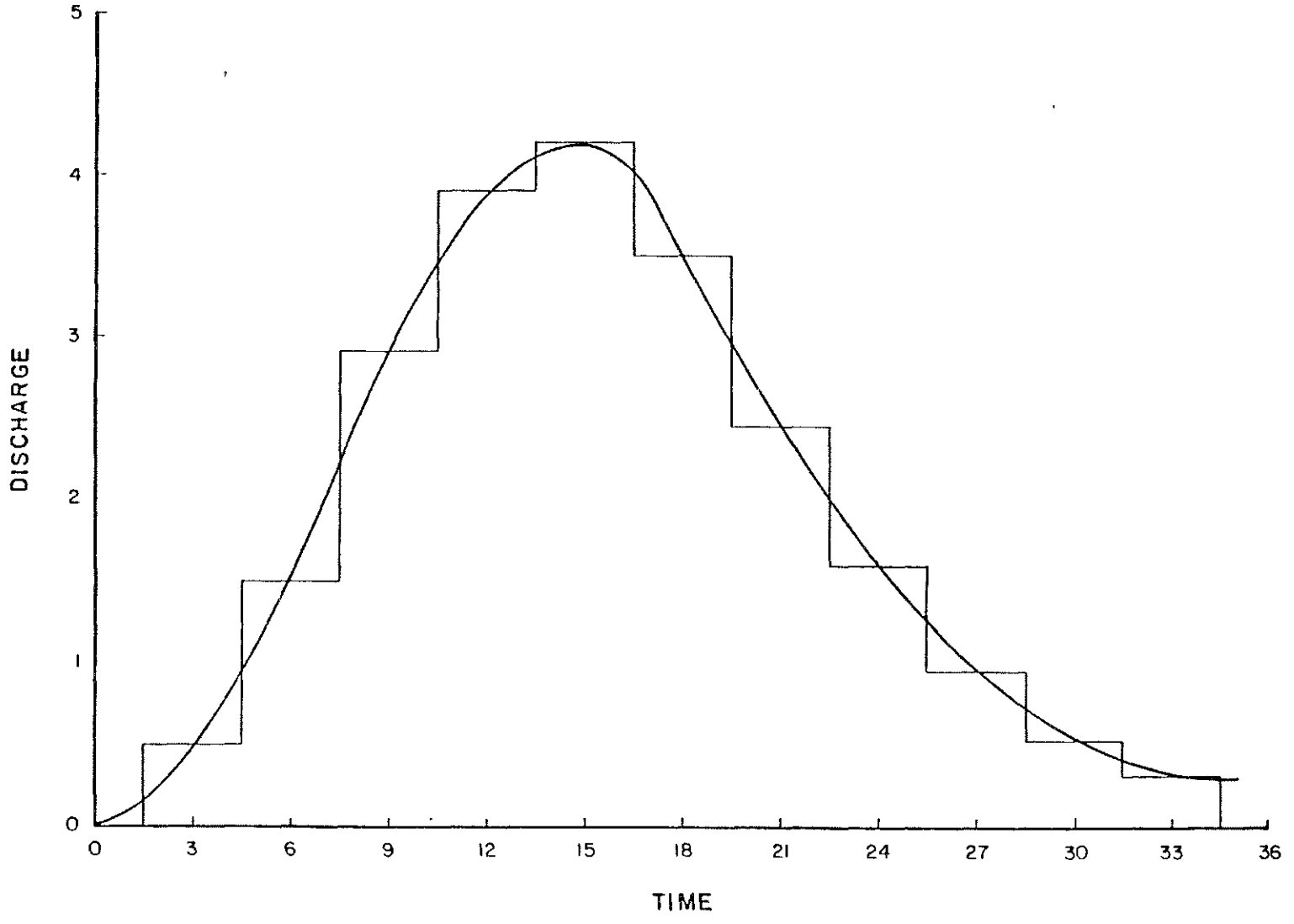


Figure 3.2. Definition sketch of the hydrograph discretization process.

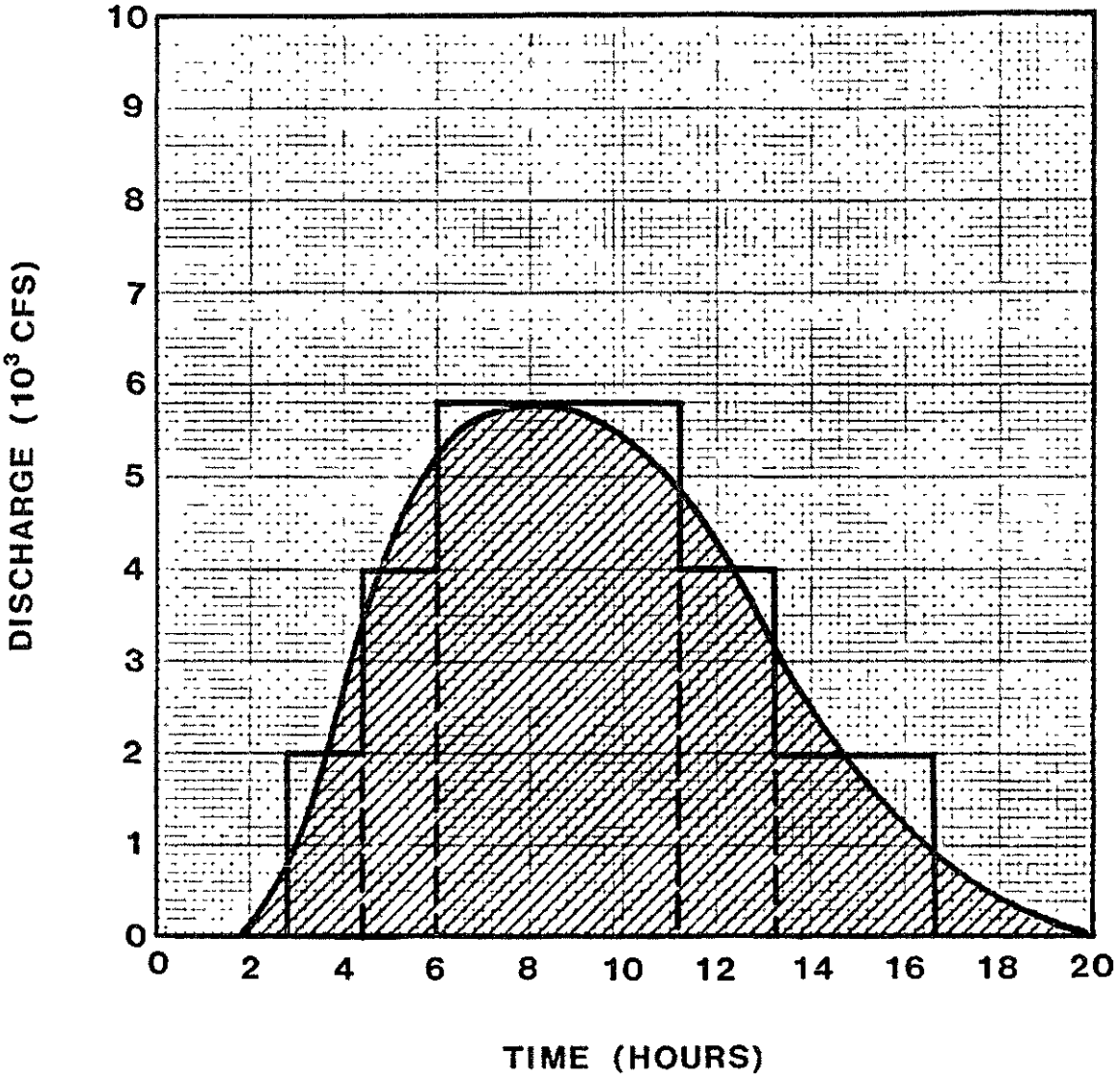


Figure 3.3. Hydrograph discretization.

Table 3.3. Water and Sediment Discharge Data for Hydrograph Discretization Example.

| Water Discharge (cfs) | Sediment Discharge (cfs) |
|---|---|
| 2,000 | 1.4 |
| 4,000 | 4.1 |
| 5,800 | 7.4 |

$$VOL_s = \sum_{\Delta t=1}^{5} Q_s \, \Delta t$$

$$= [1.4(1.4) + 4.1(1.6) + 7.4(5.4) + 4.1(2.0) + 1.4(2.8)] \frac{3,600}{43,560}$$

$$= 11 \text{ AF}$$

where

$\frac{3,600}{43,560}$ represents the conversion factor from cfs-hours to acre-feet.

# IV. HYDRAULIC ANALYSIS OF ALLUVIAL CHANNELS

## 4.1 General

In open-channel flow the water surface is not confined, therefore surface configuration, flow pattern and pressure distribution within the flow will depend on gravity. In rigid-boundary open channels no deformation or movement of the bed and banks is considered. In alluvial channels, where the channel is located in a natural alluvium of silt, clay, sand and gravel, the bed and banks are free to move, and consequently channel characteristics will depend on flow conditions. Under these circumstances the concepts of moveable-boundary hydraulics must be utilized. In using procedures presented in this manual, it is assumed the reader has a working knowledge of methods to determine the erodibility of the channel bed and banks, and has applied that knowledge to the project under evaluation. Procedures for analyzing the erodibility of earth channels are presented in Technical Release No. 25 (SCS, 1977) as well as the Corps of Engineers, "Hydraulic Design of Flood Control Channels" (COE, 1970). It is assumed the engineer has applied these or similar procedures to his project and has determined the applicability of moveable boundary hydraulic/sediment transport procedures, such as those presented in this manual.

Understanding and utilization of the concepts of rigid-boundary hydraulics are essential for analysis of alluvial channels, and it is assumed that users of this manual have this knowledge. This chapter presents some of the more specialized knowledge surrounding moveable-boundary hydraulics as required for fluvial systems analysis.

## 4.2 Resistance to Flow

### 4.2.1 Common Resistance Parameters and Their Relationships

The three most common parameters for describing resistance to steady uniform flow are:

1. The Darcy-Weisbach friction factor $f$.
2. The Chezy resistance factor $C$.
3. The Manning roughness coefficient $n$.

The Darcy-Weisbach formula, developed primarily for flows in pipes, states that

$$h_f = f \frac{L}{D} \frac{V^2}{2g} \tag{4.1}$$

where $h_f$ is the friction loss associated with the flow in pipes, $f$ is the friction factor, $L$ is the length of the pipe, $D$ is the diameter of the pipe, $V$ is the mean velocity of flow therein, and $g$ is the acceleration of gravity.

Since $D = 4R$ and the energy gradient $S_E = (h_f)/L$, Equation 4.1 may be written in terms of the friction factor as

$$f = \frac{8gRS_E}{V^2} \tag{4.2}$$

where $R$ is the hydraulic radius. Noting that $V_*^2 = gRS_E$, Equation 4.2 yields

$$\frac{V}{V_*} = \frac{8}{\sqrt{f}} \ . \tag{4.3}$$

Equation 4.3 can be applied to flow in open channels and sometimes is presented as

$$\frac{Fr}{\sqrt{S_E}} = \sqrt{\frac{8}{f}} \tag{4.4}$$

or

$$f = \frac{8S_E}{Fr^2} \tag{4.5}$$

where $Fr$ is the Froude number $(\frac{V}{\sqrt{gY_h}})$ .

The Chezy coefficient is related to Manning's $n$ by

$$C = \frac{1.49}{n} R^{1/6} \tag{4.6}$$

and by definition (i.e., $V = C\sqrt{RS}$) to the Darcy friction factor $f$, since

$$\bar{\tau}_o = \gamma RS \tag{4.7a}$$

$$= f \rho \frac{V^2}{8} \tag{4.7b}$$

giving

$$C = \sqrt{\frac{8g}{f}} \tag{4.8}$$

where $\rho$ is the density of water.

For the interested reader, it should also be noted that $f$ and $n$ are related as follows:

$$f = \frac{116.5\ n^2}{R^{1/3}} \tag{4.8a}$$

Several empirical formulas have been suggested that relate the bed-material particle size to Manning's $n$. For sand-bed channels, Meyer-Peter and Muller recommend

$$n = \frac{D_{90}^{1/6}}{26} \quad (D_{90} \text{ in meters}) \tag{4.9}$$

Lane and Carlson (1953), as a result of their San Luis Valley study, suggested the formula

$$n = \frac{D_{75}^{1/6}}{39} \quad (D_{75} \text{in inches}) \tag{4.10}$$

where the beds of the canals studied were covered with cobbles. In a Highway Research Board publication, Anderson et al. (1970) recommend

$$n = 0.0395\ D_{50}^{1/6} \quad (D_{50} \text{ in feet}) \tag{4.11}$$

Engineers have varying preferences for resistance parameters. The parameter $f$ is used for both open-channel and pressure flow. Additionally, $f$ is dimensionally consistent, while the Manning $n$ and Chezy $C$ are empirically based. Consequently, the ASCE Task Force Committee (1963) recommended the use of the Darcy $f$ for both open-channel and pressure flow.

However, the Manning n remains the most commonly used open-channel flow resistance factor. Use of Manning's n gives good results for fully rough and smooth conditions in rigid-boundary channels, but is less satisfactory for alluvial boundary flow, as its value is highly dependent on the form of bed roughness (see Section 4.2.2). Values of n for various kinds of rigid boundary surfaces have been tabulated and methods for determining the Manning's coefficient to account for a number of influencing factors such as cross section shape and channel irregularity are presented in numerous handbooks. V. T. Chow's Open Channel Hydraulics (1959) gives a detailed list of n values and methods of determining an n value in a complex channel section. A short summary of n values commonly used in alluvial conditions is given in Table 4.1.

### 4.2.2 Resistance to Flow in Fine-Grained Alluvial Channels

The equations developed in Section 4.2.1 assume flat-bed, rigid-boundary channels with no sediment transport and are strictly valid for these conditions only. A complicating factor in evaluating channel roughness in an erosion/sedimentation investigation is that the bed configuration of an alluvial channel seldom forms a smooth, regular boundary. Rather, it is characterized by shifting forms generated by the flow that vary in size, shape, and location as influenced by changes in flow, temperature, sediment load, and other variables. These bed forms constitute a major part of the resistance to flow exhibited by an alluvial channel and exert a significant influence on flow parameters such as depth, velocity and sediment transport.

Bed configurations that may form in an alluvial channel are plane bed without sediment movement, ripples, dunes, plane bed with sediment movement, antidunes, and chutes and pools. A detailed discussion of bed forms and their characteristics is provided by Simons and Senturk (1977) or Simons, Li & Associates, Inc. (1982).

The different bed forms are associated with two flow regimes, with a transition zone in between, used to classify flow in alluvial channels. The two regimes and their associated bed configurations are:

A. Lower flow regime

   1. Ripples
   2. Dunes

Table 4.1. Manning Roughness Coefficients, n.

| | Manning n Range |
|---|---|
| LINED OPEN CHANNELS: | |
| Gravel bottom, sides as indicated: | |
| Formed concrete | 0.017-0.020 |
| Random stone in mortar | 0.020-0.023 |
| Dry rubble (riprap) | 0.023-0.033 |
| UNLINED OPEN CHANNELS: | |
| Earth, uniform section: | |
| Clean, recently completed | 0.016-0.018 |
| Clean, after weathering | 0.018-0.020 |
| With short grass, few weeds | 0.022-0.027 |
| In gravely, soil, uniform section, clean | 0.022-0.025 |
| Earth, fairly uniform section: | |
| No vegetation | 0.022-0.025 |
| Grass, some weeds | 0.025-0.030 |
| Dense weeds or aquatic plants in deep channels | 0.030-0.035 |
| Sides, clean, gravel bottom | 0.025-0.030 |
| Sides, clean, cobble bottom | 0.030-0.040 |
| Dragline excavated or dredged: | |
| No vegetation | 0.028-0.033 |
| Light brush on banks | 0.035-0.050 |
| Rock: | |
| Based on design section | 0.033 |
| Based on actual mean section: | |
| a. Smooth and uniform | 0.035-0.040 |
| b. Jagged and irregular | 0.040-0.045 |
| Channels not maintained, weeds and brush uncut: | |
| Dense weeds, high as flow depth | 0.08-0.12 |
| Clean bottom, brush on sides | 0.05-0.08 |
| Clean bottom brush on sides, highest stage of flow | 0.07-0.11 |
| Dense brush, high stage | 0.10-0.14 |

Table 4.1. (continued)

| | Manning n Range |
|---|---|
| CHANNELS AND SWALES WITH MAINTAINED VEGETATION (values shown are for velocities of 2 to 6 fps): | |
| Depth of flow up to 0.7 foot: | |
| Bermuda grass, Kentucky bluegrass, buffalo grass: | |
| a. Mowed to 2 inches . . . . . | 0.045-0.07 |
| b. Length 4 to 6 inches . . . . . | 0.05-0.09 |
| Good stand, any grass: | |
| a. Length about 12 inches . . . . . | 0.09-0.18 |
| b. Length about 24 inches . . . . . | 0.15-0.30 |
| Fair stand, any grass: | |
| a. Length about 12 inches . . . . . | 0.08-0.14 |
| b. Length about 24 inches . . . . . | 0.13-0.25 |
| Depth of flow 0.7-1.5 feet: | |
| Bermuda grass, Kentucky bluegrass, buffalo grass: | |
| a. Mowed to 2 inches . . . . . | 0.035-0.05 |
| b. Length 4 to 6 inches . . . . . | 0.04-0.06 |
| Good stand, any grass: | |
| a. Length about 12 inches . . . . . | .0.07-0.12 |
| b. Length about 24 inches . . . . . | .0.10-0.20 |
| Fair stand, any grass: | |
| a. Length about 12 inches . . . . . | .0.06-0.10 |
| b. Length about 24 inches . . . . . | .0.09-0.17 |
| NATURAL STREAM CHANNELS: | |
| Minor streams (surface width at flood stage less than 100 ft): | |
| Fairly regular section: | |
| a. Some grass and weeds, little or no brush . . . . . | 0.030-0.035 |
| b. Dense growth of weeds, depth of flow materially greater than weed height . . . . | 0.035-0.05 |
| c. Some weeds, light brush on banks . . . | 0.04-0.05 |
| d. Some weeds, heavy brush on banks . . . | 0.05-0.07 |
| e. Some weeds, dense willows on banks . . . | .0.06-0.08 |
| f. For trees within channel, with branches submerged at high stage, increase all above values by . . . . . | .0.01-0.10 |

Table 4.1. (continued)

| | Manning n Range |
|---|---|
| Irregular sections, with pools, slight channel meander; increase values in 1 a-e about | 0.01-0.02 |
| Mountain streams, no vegetation in channel, banks usually steep, trees and brush along banks submerged at high stage: | |
| a. Bottom of gravel, cobbles, and few boulders | 0.04-0.05 |
| b. Bottom of cobbles, with large boulders | 0.05-0.07 |
| <u>Flood plains (adjacent to natural streams)</u>: | |
| Pasture, no brush: | |
| a. Short grass | 0.030-0.035 |
| b. High grass | 0.035-0.05 |
| Cultivated areas: | |
| a. No crop | 0.03-0.04 |
| b. Mature row crops | 0.035-0.045 |
| c. Mature field crops | 0.04-0.05 |
| Heavy weeds, scattered brush | 0.05-0.07 |
| Light brush and trees: | |
| a. Winter | 0.05-0.06 |
| b. Summer | 0.06-0.08 |
| Medium to dense brush: | |
| a. Winter | 0.07-0.11 |
| b. Summer | 0.10-0.16 |
| Dense willows, summer, not bent over by current | 0.15-0.20 |
| Cleared land with tree stumps, 100-150 per acre: | |
| a. No sprouts | 0.04-0.05 |
| b. With heavy growth of sprouts | 0.06-0.08 |
| Heavy stand of timber, a few down trees, little undergrowth: | |
| a. Flood depth below branches | 0.10-0.12 |
| b. Flood depth reaches branches | 0.12-0.16 |

B. Transition zone: bed configurations range from dunes to plane beds or to antidunes.

C. Upper flow regime

1. Plane bed with sediment movement
2. Antidunes

   a. Standing waves
   b. Breaking antidunes

3. Chutes and pools

In lower flow regime, resistance to flow is large and sediment transport is small. Conversely, in upper flow regime resistance to flow is small and sediment transport is large. Figure 4.1 illustrates the variation of resistance to flow with bed form condition. Table 4.2 provides the range of resistance coefficients typical for each bed form and the recommended value for sediment transport analysis. The different values utilized for flood control versus sediment transport studies relate to the objectives of each study. Values in the upper range are used for flood control since a conservative estimate of flow depth is desirable. Values in the lower range are used for sediment transport, bank stability and riprap/revetment analysis since a conservative estimate of velocity is required.

Therefore, in order to properly select the Manning $n$ of an alluvial channel, the bed form during the flood must be known. Figure 4.2 identifies bed form as a function of median fall diameter and stream power. Fall diameter may be approximated by the median diameter ($D_{50}$), which is known from particle size gradation analysis of a bed material sample; however, stream power, defined as the product of velocity and boundary shear stress ($\tau_0 V$) is a function of hydraulic conditions as determined by the water-surface profile calculations. Therefore, the analysis procedure requires first assuming a bed form condition in order to define Manning's $n$ and then, after calculation, verifying that the assumed bed form was correct.

### 4.2.3 Resistance to Flow in Cobble/Boulder-Bed Alluvial Channels

When the relative roughness is large, such as in steep mountain rivers with cobble/boulder beds, the resistance problem has additional complications. Large-scale roughness exists when flow depth is the same order of magnitude as bed-material height. The velocity profile under these conditions is com-

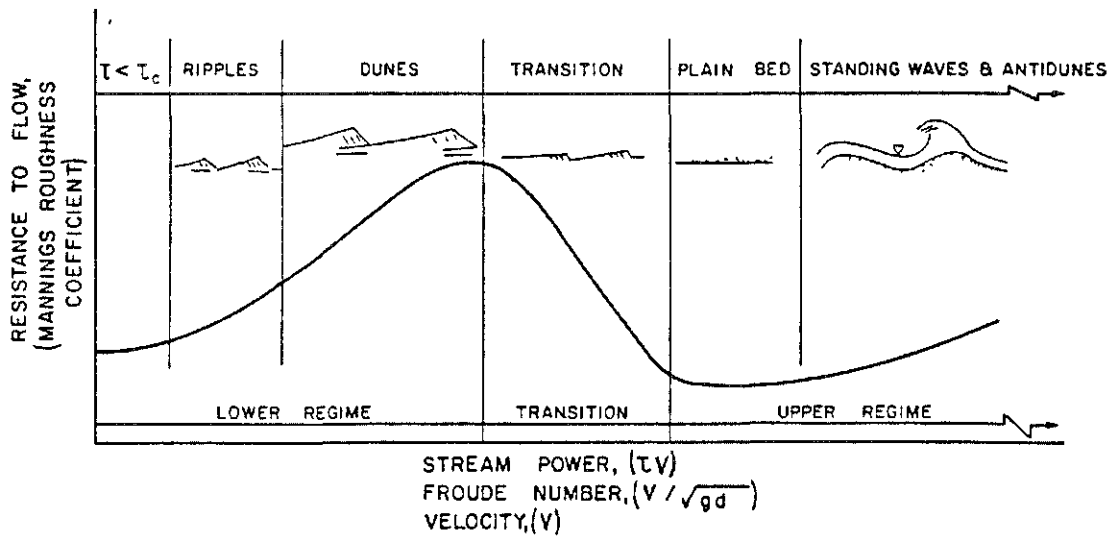


Figure 4.1. Forms of bed roughness in sand-bed channels.

Table 4.2. Values of Manning's Coefficient n for Design of Channels with Fine to Medium Sand Beds.

| Bed Roughness | Typical Range | Recommended Value for Flood Studies | Recommended Value for Sediment Transport Studies |
|---|---|---|---|
| Ripples | 0.018-0.030 | 0.030 | 0.022 |
| Dunes | 0.020-0.035 | 0.035 | 0.030 |
| Transition | 0.014-0.025 | 0.030 | 0.025 |
| Plane Bed | 0.012-0.022 | 0.030 | 0.020 |
| Standing Waves | 0.014-0.025 | 0.030 | 0.020 |
| Antidunes | 0.015-0.031 | 0.030 | 0.025 |

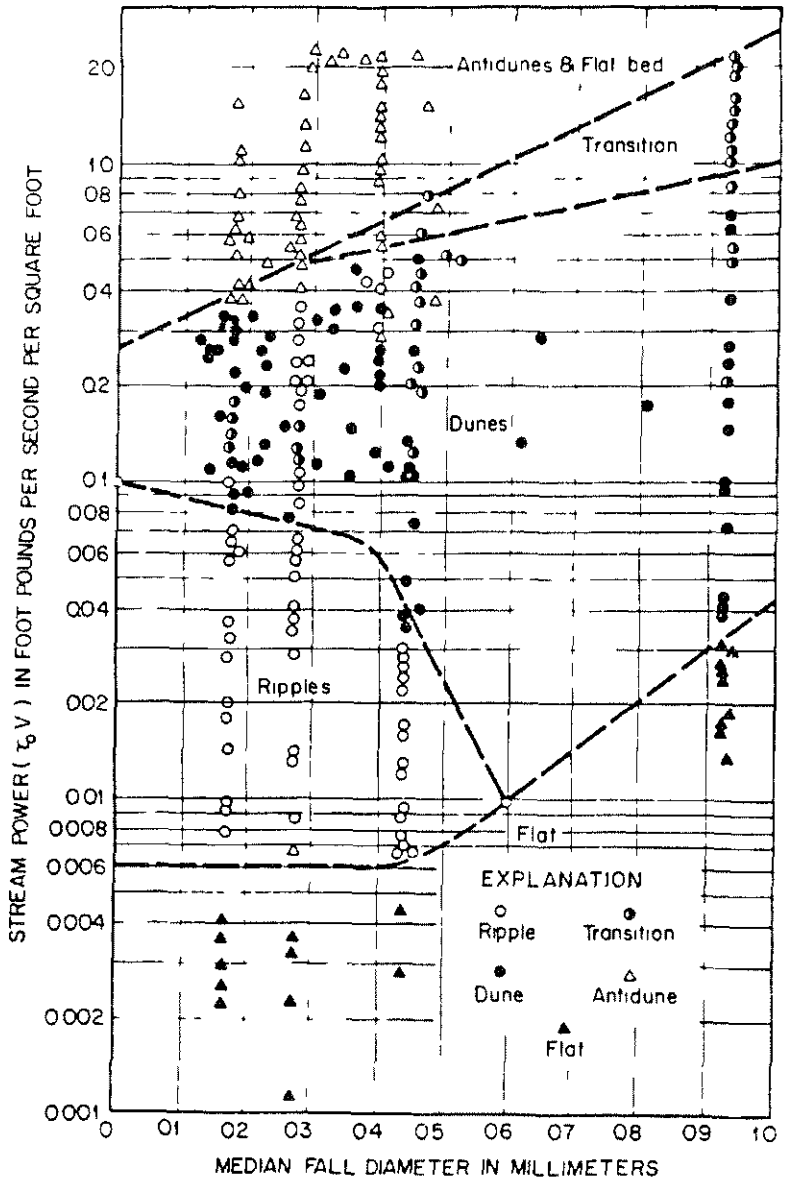


Figure 4.2. Relation of bed form to stream power and median fall diameter of bed sediment (after Simons and Richardson, 1966).

pletely disrupted and the roughness elements act individually, producing a total resistance based mainly on the sum of their form drags. Wall effects dominate the flow, so roughness geometry and distortions of the free surface around elements have the most effect on flow resistance. Channel geometry is indirectly important to the extent that it affects the flow around elements. Under these conditions the Manning equation cannot adequately describe flow conditions and a different resistance equation must be utilized. The following paragraphs describe a resistance equation for large roughness channels developed by Bathurst (1978), that should be used in place of Manning's equation for analysis of flow conditions in large roughness channels.

As discharge varies, relative roughness can change by an order of magnitude. Roughness height is represented by the length of the short axis of the bed material particles which is greater than or equal to fifty percent of the short axis of the bed material particles by count. The short axis is chosen since it more closely approximates the roughness height. A relative submergence (flow depth vs. roughness height) larger than about 15 corresponds to small-scale roughness. In this case roughness elements of the boundary act collectively as one surface, exerting a frictional shear on the flow. The shear is translated into a velocity profile, the shape of which is determined by roughness geometry, channel geometry, and any free surface distortions. Large scale roughness is considered to exist when relative submergence is less than about 4. The region between large- and small-scale roughness (relative submergence 4 to 15) is a transition region with intermediate-scale roughness. In this region flow resistance will be determined by some interaction of the two extremes.

As a result of these relative roughness relationships, different flow resistance equations may be required at the same section for different discharges. At low discharges, relative submergence will be low and cumulative form drag will be an important component to total resistance. At high discharges, relative submergence will increase and a small-scale roughness formula may become suitable. If large-scale roughness elements are removed during high flow, a sand-bed channel may be exposed. If this occurs, or if significant sediment transport occurs, the presence of bed forms should be anticipated. Such a sequence of events occurs when a cobble-bed armor layer is ruptured by high flow.

In order to provide data with which to develop a flow resistance

equation for cobble/boulder channels, measurements from flume studies were compiled by Bathurst (1978). Measurements were made of flows over different roughness beds at a variety of slopes and discharges. Most of the measurements were made with fixed beds, but a few were made using loose beds in order to study the effect of bed-material movement on flow resistance.

Theoretical analysis, supported by results of the flume study, suggests that, for the range of Reynolds numbers given by $4x10^4 < V D_{50}/\nu < 2x10^5$, resistance is likely to fall significantly as Reynolds number increases. However, if there are roughness elements protruding through the free surface, the effect is small by comparison to Froude number effects related to the appearance of hydraulic jumps and generation of free surface drag. For the bed as a whole, free surface drag decreases as Froude number and relative submergence increase. Once the elements are submerged, Froude number effects related to free surface drag are small, but Froude number effects related to standing waves may be important.

The effect of roughness geometry can largely be described by a single parameter $b_{rg}$, the function of effective roughness concentration. This accounts for the variation of the roughness geometry both with depth and with bed material, although it does not make allowance for differing element shapes. Mathematically, $b_{rg}$ is defined as follows:

$$b_{rg} = [1.175 \left(\frac{Y_{50}}{W}\right)^{0.557} \left(\frac{d}{S_{50}}\right)]^{0.648} \sigma^{-0.134} \qquad (4.12)$$

where $Y_{50}$ = size of cross-stream axis of a roughness element which, by count, is greater than or equal to 50 percent of the cross-stream axes of a sample of elements

$W$ = surface width of a section

$d$ = mean depth normal to flow (use hydraulic depth, A/W)

$S_{50}$ = size of short axis of a roughness element which, by count, is greater than or equal to 50 percent of the short axes of a sample of elements (note that the short axis is the shortest axis of the particle regardless of orientation, whereas the cross-stream axis is a function of how the particle is resting on the bed).

$\sigma$ = standard deviation of the size distribution.

When only $D_{50}$ data are available, Bathurst suggests that the median size of the short axis may be set equal to $0.57\ D_{50}$ and the cross-stream and long axes are equivalent, and equal to $D_{50}/0.57$. These values are considered most representative of bed material that is block-like in shape.

Similarly the effect of channel geometry is accounted for by the relative roughness area $A_w/Wd'$ where $A_w$ is the total wetted roughness cross-sectional area and $d'$ = depth of flow from free surface to bed datum level. This parameter indicates the proportion of a channel cross section occupied by roughness, and therefore the degree of funneling of flow. For river channels of homogeneous boundary material, relative roughness area can be expressed as

$$\frac{A_w}{Wd'} = \left(\frac{W}{d}\right)^{-b_{rg}} . \qquad (4.13)$$

Based on analysis of flume data, the resistance equation for large-scale roughness $(b_{rg} < 0.755)$ is (Bathurst, 1978):

$$\frac{\overline{V}}{(gdS)^{0.5}} = \left(\frac{8}{f}\right)^{0.5} = \left(\frac{0.28}{D_{rg}} Fr\right)^{\log (0.755/b_{rg})}$$

$$\times \left[13.434 \left(\frac{W}{Y_{50}}\right)^{0.492} D_{rg}^{1.025} (W/Y_{50})^{0.118}\right] \times \left(\frac{A_w}{Wd'}\right) \qquad (4.14)$$

This equation does not apply where Reynolds number effects (where viscous forces tend to damp out turbulence) are significant, where there is bed-material movement, or where there is a system of standing waves. However, within its range of application, the equation seems to work well as long as the various parameters, particularly the roughness sizes and the channel wetted perimeter, are derived or measured. In spite of its complex form, Equation 4.14 contains relatively few parameters and can be applied using a simple iteration procedure to evaluate flow conditions in large roughness channels, similar to the solution of the Manning equation for small roughness channels. The example at the end of the chapter illustrates application of the equation.

## 4.3 Boundary Shear Stress Calculations

Calculation of the boundary shear stress, or tractive force, is required in many alluvial channel computations. Consequently, it is important to know and understand the various methodologies that may be utilized to evaluate boundary shear stress. Equation 4.7a represents the basic theoretical equation for the mean boundary shear stress in a cross section as derived from application of the momentum principle to a control volume in uniform flow.

Equation 4.7b is derived from both Equation 4.7a and the Darcy equation as applied to open-channel flow ($D = 4R$). Consequently, the appropriate velocity to use is the mean channel velocity. Equation 4.7b is often preferred to Equation 4.7a for evaluating boundary shear stress, because it eliminates difficulties or uncertainty in defining the energy slope. Additionally, Equation 4.7b is more readily applied to evaluation of the mean boundary shear stress in overbank areas by using the mean overbank velocity.

The above equations (Equations 4.7a and b) define the mean boundary shear stress in the cross section. The variation of the boundary shear stress across the channel was first described by Lane (1955), as illustrated in Figure 4.3. This figure indicates that theoretically the boundary shear stress goes to zero at the corners of a channel; however, in reality it is more reasonable to assume that it is not zero, but rather some value less than the maximum value occurring on the channel sides or bottom. For design purposes, it is appropriate to base decisions on the maximum boundary shear stress occurring in the cross section, regardless of the specific location of interest, for example, at the toe of a riprapped channel side wall. For channels of different geometric properties, Figure 4.4 may be used to evaluate the maximum boundary shear stress on the channel sides or bottom, relative to $\gamma dS$. It is important to realize that these figures are based on the boundary shear stress defined by $\gamma ds$, not the mean boundary shear stress in the cross section as defined by $\gamma RS$ (or $1/8\ \rho\ f\ V^2$). For channels of small width/depth ratio (i.e., less than 10), $\gamma dS$ will be larger than $\gamma RS$. As the width/depth ratio becomes larger, $\gamma dS$ approaches $\gamma RS$ such that, for width/depth ratios greater than 10, they may be considered equal. Under this condition, as indicated by Figure 4.4, the maximum boundary shear stress and the mean boundary shear stress are equal on the channel bottom, while the maximum value on the side will be about 0.78 times the mean boundary shear stress. For application of Figures 4.3 and 4.4 to irregular channels, it is best to use the depth (d) defined by the hydraulic depth (A/T).

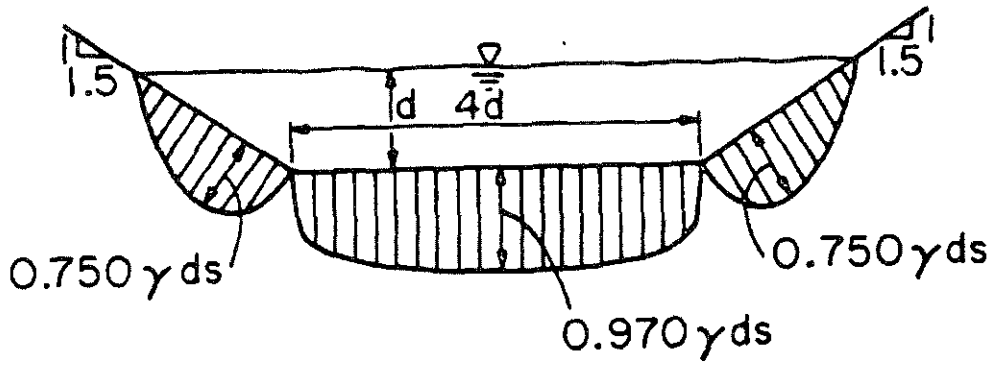


Figure 4.3. Variation of boundary shear stress in a trapezoidal cross section.

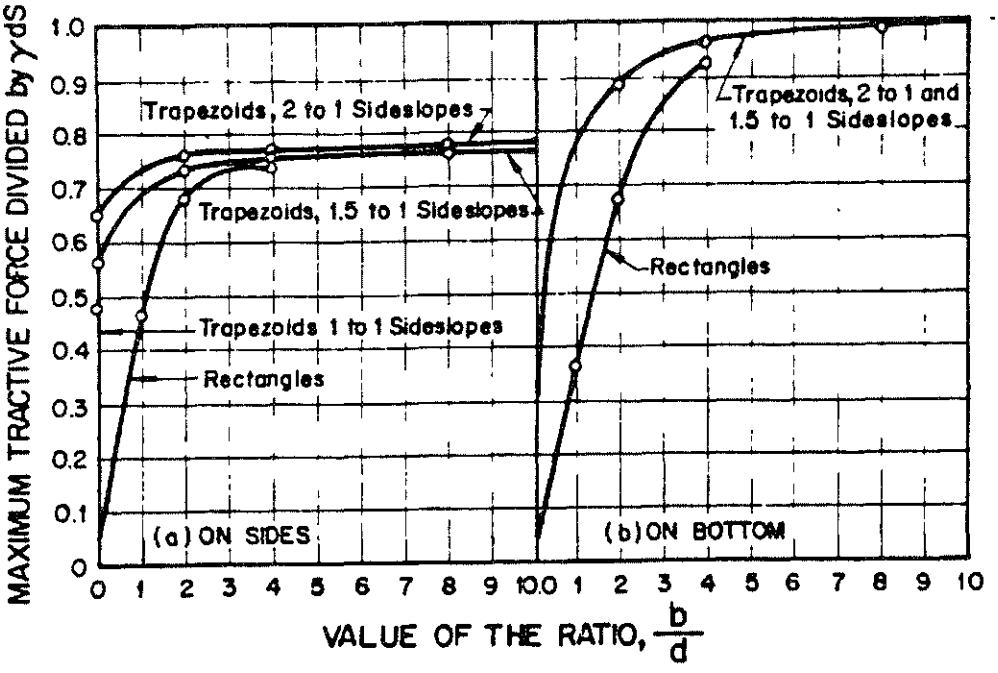


Figure 4.4. Maximum unit tractive force versus aspect ratio (b/d).

Equations 4.7a and b also define the mean boundary shear stress only for straight channels. Flow around a bend in a channel generates secondary currents that modify the velocity profile and boundary shear stress distribution; in particular, the boundary shear stress becomes greater on the outside of the bend. Figure 4.5 gives the ratio of the boundary shear stress on the outside of the bend to the mean boundary shear stress, relative to the radius of curvature of the bend.

## 4.4 Normal Depth Calculations

### 4.4.1 Definition

The hydraulic grade line, or the hydraulic gradient, in open-channel flow is the water surface, and in pipe flow it connects the elevations to which water would rise in piezometer tubes along the pipe. The energy gradient is at a distance equal to the velocity head above the hydraulic gradient. In both open-channel and pipe flow the fall of the energy gradient for a given length of channel or pipe represents the loss of energy by friction, excluding local miscellaneous losses. Figure 4.6 summarizes these definitions. When considered together, the hydraulic gradient and the energy gradient reflect not only the loss of energy by friction, but also the conversions between potential and kinetic energy.

In the majority of cases the objective of hydraulic computations relating to flow in open channels is to determine the elevation of the water surface, from which other hydraulic parameters at any desired location may be easily computed. These problems involve three general relationships between the hydraulic gradient and the energy gradient. For uniform flow the hydraulic gradient and the energy gradient are parallel and the hydraulic gradient becomes an adequate basis for the determination of friction loss, since no conversion between kinetic and potential energy is involved. In accelerated flow, the hydraulic gradient is steeper than the energy gradient; and in retarded flow the energy gradient is steeper than the hydraulic gradient. An analysis of flow under these conditions cannot be made without consideration of both the energy gradient and hydraulic gradient.

The depth of flow existing under conditions of uniform flow is defined as the normal depth. Uniform flow develops when the flow resistance is just balanced by gravitational force. Under these conditions the slope of the energy grade line $S_E$ is equal to the bed slope, $S_o$. The normal depth is

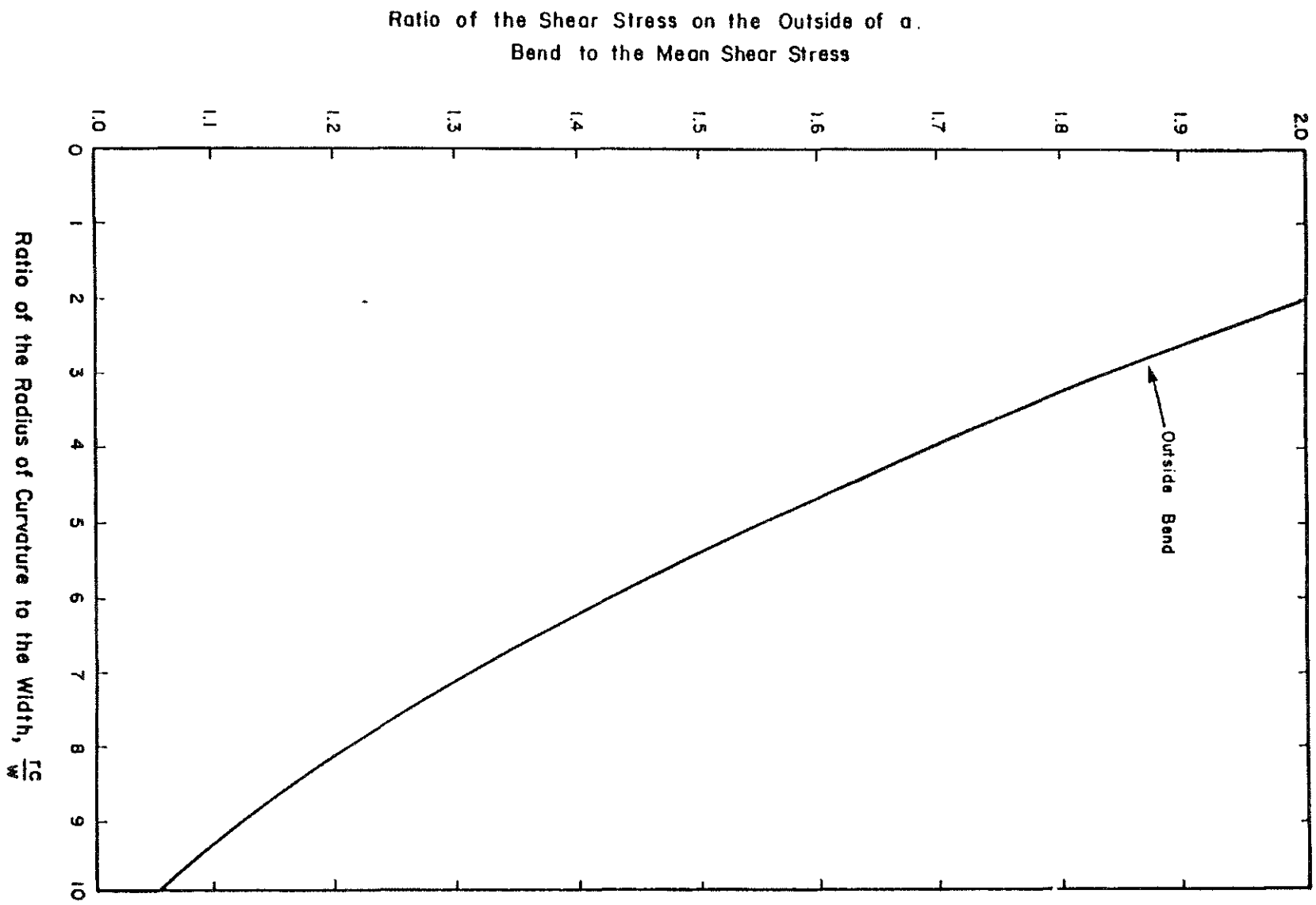


Figure 4.5. Effect of bend on boundary shear stress (after Soil Conservation Service design manual).

frequently of interest, particularly when calculations of the water-surface profile are required (water-surface profiles are discussed in the next section of this chapter). The type of water-surface profile existing in a given situation depends on the relationship existing between the normal depth, the critical depth, and the existing depth of flow for a given discharge. In this section normal depth calculations in trapezoidal and natural channels will be discussed. Uniform flow very seldom exists in natural channels; however, in practice, this assumption is frequently made.

### 4.4.2 Normal Depth Calculation for Trapezoidal Channels

Manning's equation can be written for discharge as

$$Q = \frac{1.486}{n} AR^{2/3} S^{1/2} . \tag{4.15}$$

Area and wetted perimeter for a trapezoidal channel may be expressed as a function of depth as follows:

$$A = z y^2 + by \tag{4.16}$$

where $z$ describes the side slope as the ratio of horizontal to vertical distance, $b$ is the bottom width and $y$ is the depth. Wetted perimeter is given by

$$P = b + 2y (1 + z)^{1/2} . \tag{4.17}$$

Therefore, the discharge for a given normal depth, $y_o$, is

$$Q = \frac{1.486}{n} \frac{(z y_o^2 + by_o)^{5/3} S^{1/2}}{[b + 2y_o(1+z)^{1/2}]^{2/3}} . \tag{4.18}$$

For a known discharge this equation may be solved for normal depth $y_o$ in terms of the other known parameters by use of an iterative technique such as Newton's iterative method. The equation actually solved, in this case for $y_o$, would be

$$\frac{nQ}{1.486 S^{1/2}} = \frac{[zy_o^2 + by_o]^{5/3}}{[b + 2y_o (1+z)^{1/2}]^{2/3}} . \tag{4.19}$$

### 4.4.3 Normal Depth Calculation for Natural Channels

Using data taken at a given cross section, wetted perimeter $P$ is often related to cross-sectional flow area $A$ by regression. The resulting expression is usually a power function of the form

$$P = a_1 A^{b_1} \quad . \tag{4.20}$$

Similarly, flow area may be related to flow depth as

$$A = a_2 y^{b_2} \quad . \tag{4.21}$$

Here, $a_1$, $a_2$, $b_1$, and $b_2$ are statistically fitted coefficients and exponents. By using these expressions, hydraulic radius $R$ in Equation 4.15 may be expressed as a function of $y$ as follows:

$$R = \frac{A}{P} = \frac{a_2 y^{b_2}}{a_1 \left(a_2 y^{b_2}\right)^{b_1}} = \frac{a_2}{a_1 a_2^{b_1}} y^{(b_2 - b_2 b_1)} \quad . \tag{4.22}$$

Therefore, Equation 4.15 may be rewritten in terms of depth of flow in a natural channel as

$$Q = \frac{1.486}{n} a_2 y_o^{b_2} \left[ \frac{a_2}{a_1 a_2^{b_1}} y_o^{(b_2 - b_2 b_1)} \right]^{2/3} S_o^{1/2} \quad . \tag{4.23}$$

This equation may be solved directly for $y_o$, resulting in

$$y_o = \left[ \left( \frac{Qn}{1.49\ S_o^{1/2}} \right)^{3/2} \left( \frac{a_1}{a_2^{(5/2 - b_2)}} \right) \right]^{\left(\frac{2}{5b_2 - 2b_1 b_2}\right)} \quad . \tag{4.24}$$

## 4.5 Water-Surface Profiles

Water-surface profile computations assume that changes in depth and velocity take place slowly over large distances, resistance to flow dominates and acceleration forces may be neglected. This type of flow is called gradually varied flow. Calculations under these conditions involve (1) the determination of the general characteristics of the water-surface profile, and (2) the elevation of the water surface or depth of flow.

In gradually varied flow, the actual flow depth $y$ is either larger than or smaller than the normal depth $y_0$, and either larger than or smaller than the critical depth $y_c$. The water-surface profiles, which are often called backwater curves, depend on the magnitude of the actual depth of flow $y$ in relation to the normal depth $y_0$ and the critical depth $y_c$. Normal depth $y_0$ is the depth of flow that would exist for steady uniform flow as determined using the Manning or Chezy velocity equations, and the critical depth is the depth of flow when the Froude number equals 1.0. Reasons for the depth being different than the normal depth are changes in slope of the bed, changes in cross section, obstruction to flow, and imbalances between gravitational forces accelerating the flow and shear forces retarding the flow.

In working with gradually varied flow the first step is to determine what type of backwater curve would exist. The second step is to perform the numerical computation of water-surface elevations. Open-channel flow textbooks, such as Chow's (1959) or Henderson's (1966), detail the analysis of gradually varied flow. Various computer programs have also been developed for application to gradually varied flow analysis, the most widely known of which is the U.S. Army Corps of Engineers HEC-2 program.

## 4.6 Additional Effects on Flow Depth in Alluvial Channels

### 4.6.1 Importance

Calculation of flow depth based on the assumption of gradually varied flow using a suitable roughness coefficient is not always sufficient in alluvial channels. Since the bed of the channel is not uniform and the alignment of the channel is sinuous, the flow depth will vary accordingly. Hydraulic structures whose performance depends on adequate clearance above the water surface must take into consideration additional effects. Bridges, levees, and man-made conveyance channels may suffer significant damage if they are designed on gradually varied flow depths alone. The depth of flow can be significantly affected by the formation of antidunes in upper regime flow, superelevation of the flow through a bend, and the accumulation of debris.

### 4.6.2 Antidune and Dune Height

For natural or man-made channel segments with sand beds, it is necessary to estimate the height of bed forms moving through the channel, particularly where freeboard or scour requirements are critical. This can be done by estimating antidune or dune height.

Antidunes can form in either the transition zone (between lower and upper regime) or upper flow regime (Simons and Senturk, 1977). Kennedy (1963) made a detailed study of antidune flow. He suggested that the wave length is generally given by $2\pi V^2/g$ (g is the gravitational acceleration) and two-dimensional waves break when the ratio of wave height to wave length reaches a value of approximately 0.14. This theory assumes that the depth of flow is roughly equal to the maximum height of the antidune. Thus, the antidune height $h_a$ from crest to trough (see Figure 4.7) can be estimated utilizing the relation

$$h_a = 0.14 \frac{2\pi V^2}{g} = 0.027\ V^2 \qquad (4.25)$$

for $h_a < y$; assume $h_a = y_o$ when the calculated value of $h_a > y_o$, since $h_a$ can never be greater than $y_o$.

Lower regime flow also produces bed forms which should be considered in designing levee, channel, or bridge projects. Based on data collected from flume experiments (Simons and Richardson, 1960), dune formations have been observed at Froude numbers ranging from 0.38 to 0.60. The ratio of depth of flow to dune height (d/h) ranged from 1 to 5. When this ratio is 1.0, the dune troughs could be depressed below the natural channel bed a distance equal to one-half the depth of flow. As a conservative guideline, this value (one-half the depth of flow) may be used to account for dune troughs forming adjacent to a structure.

### 4.6.3 Superelevation

There are many equations for determining superelevation, but the differences in computational results that are obtained by using the different equations are small. One equation that has proven to be applicable to a wide range of conditions was first presented by Ippen and Drinker (1962). When superelevation is defined as the water surface increase above the normal water surface (see Figure 4.8a), this equation takes the form:

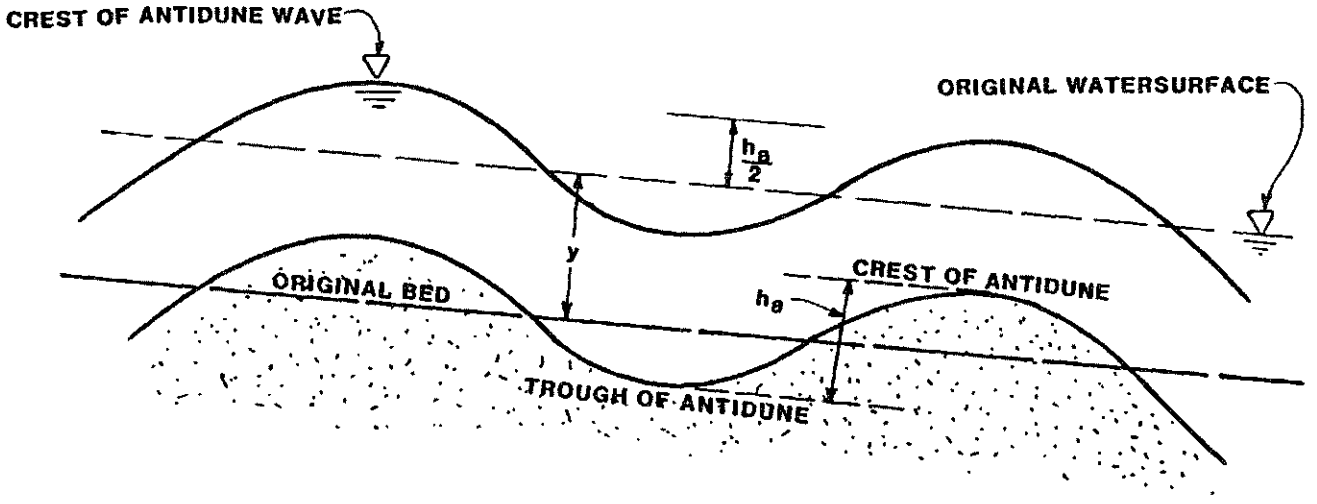


Figure 4.7 Definition sketch for antidune height.

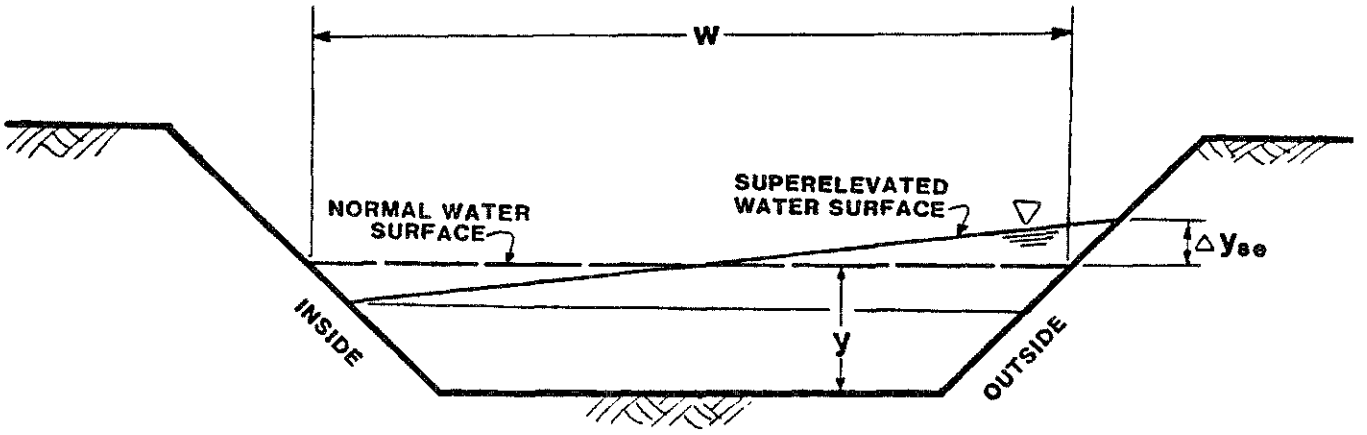


Figure 4.8a Definition sketch of superelevation in a channel bend.

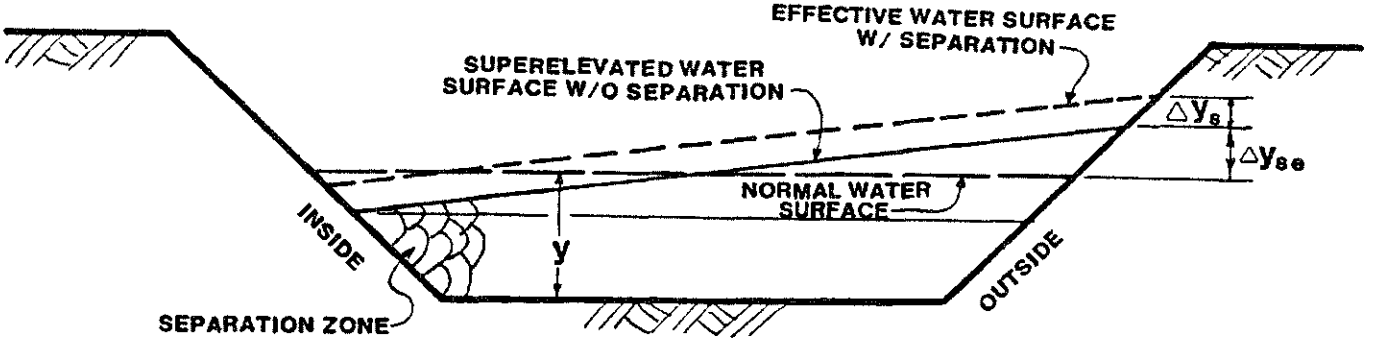


Figure 4.8b Definition sketch of superelevation and flow separation conditions in a short radius bend.

$$\Delta y_{se} = \frac{V^2}{2g} \frac{W}{r_c} \left(\frac{1}{1 - (\frac{W}{2r_c})^2}\right) \tag{4.26a}$$

where $\Delta y_{se}$ is the superelevation, $r_c$ is the radius of the channel centerline, and $W$ is the channel width at the elevation of the centerline water surface. When $W/r_c$ is small (gradual curvature), Equation 4.26a simplifies to

$$\Delta y_{se} = \frac{1}{2} \frac{V^2}{g} \frac{W}{r_c} \tag{4.26b}$$

A modified version of this equation was presented by the COE (1970) which incorporated a coefficient to account for channel and flow characteristics. The COE equation is

$$\Delta y_{se} = C \frac{V^2}{g} \frac{W}{r_c} \tag{4.26c}$$

where the values of $C$ are given in Table 4.3. It is recommended that Equation 4.26a be used for lined channels with sharp radii of curvature, and Equation 4.26c for natural, lined or unlined channels with gradual radii of curvature. It is also recommended that the values of $C$ given in Table 4.3 be applied to Equation 4.26a as well. For purposes of this calculation, a sharp radius of curvature exists when $W/r_c$ exceeds 0.33.

For sharp-radius bends subjected to high-velocity (near or greater than supercritical) flows, it may also be necessary to allow for an increase in the depth of flow as a result of flow separation in the bend. Flow separation from the inside boundary of the bend will reduce the effective cross-sectional area, induce deposition on the point bar, and locally increase the depth of flow ($\Delta y_s$). Conservatively, this can be taken as 25 percent of the velocity head, or

$$\Delta y_s = 0.25 \frac{V^2}{2g} . \tag{4.27}$$

The amount $\Delta y_s$ is an additional depth component above the superelevated water surface, as illustrated in Figure 4.8b.

Table 4.3. Superelevation Formula Coefficients (from COE, 1970).

| Flow Type | Channel Cross Section | Type of Curve | Value of C |
|---|---|---|---|
| Tranquil | Rectangular | Simple circular | 0.5 |
| Tranquil | Trapezoidal | Simple circular | 0.5* |
| Rapid | Rectangular | Simple circular | 1.0 |
| Rapid | Trapezoidal | Simple circular | 1.0* |
| Rapid | Rectangular | Spiral transitions | 0.5 |
| Rapid | Trapezoidal | Spiral transitions | 1.0* |
| Rapid | Rectangular | Spiral banked | 0.5 |

* NOTE: Equation 4.26c is based on the physics of flow in a rectangular channel. Due to the non-uniform flow distribution in a trapezoidal channel, it is recommended that these coefficients be multiplied by 1.15 if subcritical (tranquil) flow exists and 1.30 if supercritical (rapid) flow exists. This recommendation is based on information contained in the Hydraulic Design Manual published by the Los Angeles County Flood Control District.

### 4.6.4 Debris Accumulation

Natural rivers provide a good environment for the growth of trees and other phreatophytes. Channel banks, even in arid regions with intermittent stream flow, will support a significant number of large trees. The adjacent flood plain area will accumulate dead trees or debris from prior large floods. Both of these areas are capable of supplying floating debris to the main channel during large floods. Trees from the channel banks will be eroded in areas of active bank failure and dead trees in the overbank will be transported when the depth of flow becomes sufficient to float the debris. In urban areas, flood plain managers are faced with controlling a variety of floating debris.

Debris accumulation at bridge crossings can significantly influence bridge stability. The reduced conveyance resulting from partial blockage of flow area can increase flow depths and potential for overtopping. Additionally, since debris generally floats, it is the upper portion of flow that is restricted, which results in more flow of higher velocities near the bed. Therefore, debris accumulation can increase local scour and the potential for failure from undermining of piers and abutments.

There are no good rules to account for debris accumulation at bridge crossings. Quantification of the effect is largely subjective and relies on experience. In the absence of adequate data (watershed conditions, historical records, etc.), a generally accepted rule of thumb is to assume a debris accumulation equal to three times the pier width.

### 4.6.5 Total Freeboard Requirement

Freeboard is the vertical distance measured from the design water surface to the top of the channel wall or levee. In this definition, the design water surface is that resulting from uniform or gradually varied flow calculations (e.g. Manning's Equation or HEC-2 results, respectively). Freeboard is then any additional depth required to ensure overtopping does not occur in the as-built channel from factors not adequately accounted for in the design water surface calculations. These factors can include identifiable components such as long-term aggradation, superelevation, bed forms, and debris accumulation, as well as less identifiable components such as separation, excessive turbulence, variation in resistance or other coefficients used in design, and wave action. In degradational reaches it is not considered appropriate to

reduce freeboard requirements due to the uncertainties in such things as bank stability. Under these circumstances the calculated freeboard will provide an extra factor of safety to account for potential channel instability.

Freeboard is often defined as a percentage of the depth of flow, plus any other increase due to indentifiable factors (superelevation, bed forms, or debris accumulation). For example, both the Soil Conservation Service (SCS) and the Bureau of Reclamation (BR) freeboard calculations are a function of flow depth. However, as discussed by the COE (1970), "The amount of freeboard cannot be fixed by a single, widely applicable formula. It depends in large part on the size and shape of channel, type of lining, consequences of damage from overtopping and velocity and depth of flow." In this regard, it is worthwhile to mention that both the SCS and BR procedures are primarily intended for application to smaller conveyances (i.e., irrigation channels, drainage ditches). For larger channels (i.e., rivers and floodways), the COE minimum guidelines are probably more applicable. These guidelines are (COE, 1970): 2.0 feet in rectangular cross sections and 2.5 feet in trapezoidal sections for concrete-lined channels; 2.5 feet for riprapped channels; and 3.0 feet for earthen levees. However, for riprap channels or earthen channels below natural ground levels, the minimum amounts may be somewhat reduced to reflect the lower hazard under these conditions.

When calculations for superelevation, bed forms, debris accumulation, and other identifiable variances to flow are available, an initial estimate of freeboard can be calculated. For channel walls below natural ground level, which incorporate an erosion-resistant bank lining such as soil-cement or riprap, it is recommended that the freeboard for the bank lining alone be computed as:

$$F.B_{BL} = \frac{1}{2} h_a + \Delta y_{se} + \Delta y_s \qquad (4.28a)$$

The freeboard dimension for the total channel wall height (whether above ground or below ground) should include the following components:

$$F.B._{TOT\ EMB} = \frac{1}{2} h_a + \Delta y_{se} + \Delta y_s + \Delta y_d + \Delta y_{agg} \qquad (4.28b)$$

$h_a$ = antidune height defined by Equation 4.25

$\Delta y_{se}$ = superelevation defined by Equation 4.26a or 4.26c, as appropriate

$\Delta y_s$ = increase in flow depth from separation in short-radius bends (Equation 4.27)

$\Delta y_d$ = increase in depth from debris accumulation

$\Delta y_{agg}$ = increase in depth due to long-term aggradation (see Chapter V)

It is also recommended that the freeboard for bank lining (riprap, soil-cement, etc.) on above ground levee embankments be computed with Equation 4.28b. If excessive freeboard dimensions are computed with Equation 4.28b, the engineer should consider a redesign to eliminate causes of high freeboard.

If the river reach under study has a Federal Emergency Management Agency (FEMA) flood plain delineation, the minimum FEMA freeboard requirements must be complied with before channel or levee improvements will be recognized by FEMA as altering the original flood plain delineation. Under these circumstances, if the freeboard dimension calculated by Equations 4.28a or 4.28b is less than the minimum FEMA requirements, the FEMA criteria should be used. In the absence of FEMA regulation, the final decision will rely on engineering judgment and experience, particularly when the freeboard requirements vary significantly from one reach to the next.

## 4.7 Examples

### 4.7.1 Analysis of Resistance to Flow in Sand-Bed Channels

For the 2-year flood (425 cfs), a channel is observed functioning essentially as a plane bed without sediment movement. A bed-material sample is laboratory-analyzed and provides the following information:

$D_{90}$ = 0.80 mm

$D_{50}$ = 0.35 mm

$D_{10}$ = 0.15 mm

Channel geometry and flow characteristics available from gaging station measurements near the peak discharge of the 2-year event yield the following:

(flow area) A = 210 $ft^2$

(top width) T = 178 ft

(hydraulic radius) R = 1.2 ft

(bed slope) $S = 0.0005$

(channel velocity, $Q/A$) $V = 2.0$ fps

Similarly, during a 100-year event (13,000 cfs):

$A = 1{,}275\ ft^2$

$T = 350$ ft

$R = 3.6$

$V = 10.2$ fps

What is the resistance to flow during each flood?

a. For the 2-year event the channel can be analyzed by rigid-boundary equations assuming insignificant sediment transport and hence bed-form movement.

The Darcy $f$ is computed from Equation 4.5. First, evaluate the Froude number:

$$Fr = \frac{V}{\sqrt{gY_h}}$$

where $Y_h$ is the hydraulic depth $(\frac{A}{T})$

Therefore,

$$Fr = \frac{2.0}{\sqrt{32.2\ (210/178)}} = 0.32$$

Second, assuming $S_E = S_o$, then

$$f = \frac{8\ (0.0005)}{(0.32)^2} = 0.039$$

The Chezy $C$ is then computed from Equation 4.8.

$$C = \sqrt{\frac{8\ (32.2)}{0.039}} = 81$$

Manning's $n$ is computed from Equation 4.6.

$$n = \frac{1.49}{81}\ (1.2)^{1/6} = 0.019$$

For comparison, use Equation 4.9 for Manning's $n$

$$n = \frac{0.0008^{1/6}}{26} = 0.012$$

The difference of these two values reflects the difference between an analytically calculated $n$ (0.019) using various theoretical and empirical formulas that do not directly account for bed-material characteristics, and that value based on a purely empirical calculation (0.012) that incorporates primarily bed-material characteristics. If the assumption of uniform flow with insignificant sediment transport is valid, the analytically determined $n$ is a better estimate, since it represents a calibration of $n$ based on measured flow data. Furthermore, as a calibrated value, this estimate implicitly accounts for both bed-material and rigid boundary characteristics.

b. For the 100-year event the evaluation must be made under the assumption of moveable bed conditions. First, the bed form condition must be established. From Equation 4.7a, assuming $S_e = S_o$ only for purposes of bedform classification, the stream power is

$$\tau_o = \gamma RS = 62.4(3.6)(0.0005) = 0.11 \frac{lb}{ft^2}$$

$$\tau_o V = 0.11(10.2) = 1.1 \frac{lb}{ft \cdot s}$$

From Figure 4.2 with $\tau_o V = 1.1$ and $D_{50} = 0.35$ the flow condition is upper regime with antidune bed forms. From Table 4.2 the range of Manning's $n$ is 0.015 to 0.031, with a value of 0.025 recommended for sediment transport.

For comparison, apply the rigid-boundary formulas.

From Equation 4.5 with

$$Fr = \frac{10.2}{\sqrt{32.2\ (1{,}275/350)}} = 0.94$$

$$f = \frac{8\ (0.0005)}{(0.94)^2} = 0.005$$

From Equation 4.8

$$C = \sqrt{\frac{8(32.2)}{0.005}} = 227$$

From Equation 4.6

$$n = \frac{1.49}{227} (3.6)^{1/6} = 0.008$$

Unlike the above example, the analytically determined result (0.008) from rigid-boundary equations does not represent an accurate calibration because it does not properly account for the form roughness effects from the antidune bedforms. Specifically, energy dissipation in the separation zones downstream of the bedforms further complicates the nonuniform flow conditions (i.e., $S_e \neq S_o$). Additionally, the measured depth and area used in the rigid-boundary formulas may not adequately represent the actual contributing depth and area due to the ineffective flow area in the separation zones. Therefore, with movable boundary conditions the estimate of 0.025 is considered the more reliable.

### 4.7.2 Analysis of Flow in Rough Channels

The following example illustrates the iterative application of Equation 4.14 for evaluation of flow in large-roughness channels. The calculation is for conditions of field measured data by Virmani (1973) to allow evaluation of the accuracy of the computed result. The first step in application of Equation 4.14 is development of a relationship between channel width, $W$, and mean depth, $d$, for the given channel. Taking Virmani's site 10-0115 as an example, the data show that:

$$W = 64.05\ d^{0.1858}$$

Since $Wd = A$, $W = A/d$, and equating these two expressions for $W$ yields:

$$\frac{A}{d} = 64.05\ d^{0.1858}$$

or

$$A = 64.05d^{\ 1.1858}$$

The mean velocity, $\overline{V}$, is equal to $\frac{Q}{A}$, and substituting the previous expression for $A$,

$$\overline{V} = \frac{Q}{64.05\ d^{1.1858}}$$

Substituting for $W$ and $\overline{V}$ in Equation 4.14 and using Equation 4.13 to describe relative roughness area, depth is related to just discharge and the parameters of roughness geometry:

$$\frac{Q}{200.6\ d^{1.6858}\ S^{0.5}} = \left[\frac{0.001396\ Q}{b_{rg}\ d^{1.6858}}\right]^{\log(0.755/b_{rg})}$$

$$\times\ \left[104\ \left(\frac{d}{Y_{50}}\right)^{0.1858\ 0.492}\ b_{rg}^{1.675(d^{0.1858}/Y_{50})^{0.118}}\right]$$

$$\times\ \left[64.05\ d^{-0.8142}\right]^{-b_{rg}}$$

where

$$b_{rg} = \left[0.1158\ Y_{50}^{0.557}\ \frac{d^{0.8965}}{S_{50}}\right]^{0.648}\ \sigma^{-0.134}$$

Virmani's data show that:

$D_{50} = 0.144m$

$\sigma = 0.313$

$S = 0.0117$

Assuming that $S_{50} = 0.57 \times D_{50}$ and tnat the cross-stream axis $Y_{50}$ and the long axis $L_{50}$ are equivalent and equal to $D_{50}/0.57$, then

$S_{50} = 0.0821$ m

$Y_{50} = 0.253$ m

Using Equation 4.12, the calculated value of the function of effective roughness concentration, $b_{rg}$, is therefore $0.7268\ d^{0.6787}$. Substituting yields

$$\frac{Q}{21.7\ d^{1.6858}} = \left[\frac{0.000192\ Q}{d^{2.3645}}\right]^{\log(1.039/d^{0.6787})}$$

$$\times\ \left[204.5\ d^{0.0914}(0.7268\ d^{0.6787})^{1.969\ d^{0.02192}}\right]$$

$$\times\ \left[\frac{64.05}{d^{0.8142}}\right]^{-0.7267\ d^{0.6787}}$$

The only two unknowns in this equation are discharge and depth, so specifying one allows the other to be calculated. Virmani's data show that at a discharge of 0.906 $m^3s^{-1}$ the depth is 0.146 m. If, however, the depth were unknown it could have been calculated by the following iterative technique.

The known value of discharge and a guessed value of depth are substituted into the right-hand side. With depth set at, say, 1 m, the value of the right side is 4.775. Equating this with the left side of the equation, and including the known value of discharge, a calculated value of depth equal to 0.0601 m is obtained.

Using this derived value as the new guessed value of depth for the right side of the equation, the next iteration gives a depth equal to 0.11234 m. Subsequent iterations give depths of 0.1546 m, 0.1623 m and 0.1625 m. As the difference between the last two values is insignificant, the final value can be assumed to be the required value. Five iterations, therefore, seem to be sufficient for the calculation of depth, and the result is about 10 percent in error relative to the measured value.

# V. SEDIMENT TRANSPORT ANALYSIS

## 5.1 General Concepts

### 5.1.1 Basic Sediment Transport Theory

Sediment particles are transported by flowing water in one or more of the following ways: (1) surface creep, (2) saltation, and (3) suspension. Surface creep is the rolling or sliding of particles along the bed. Saltation (jumping) is the cycle of motion above the bed with resting periods on the bed. Suspension involves the sediment particle being supported by the water during its entire motion. Sediments transported by surface creep, sliding, rolling and saltation are referred to as bed load, and those transported by suspension are called suspended load. The suspended load consists of sands, silts, and clays. Total sediment load is defined as the sum of the bed load and suspended load. Generally, the amount of bed load transported by a large river is on the order of 5 to 25 percent of the suspended load. Although the amount of bed load may be small compared with total sediment load, it is important because it shapes the bed and influences channel stability, the form of bed roughness, and other factors.

The total sediment load in a channel may also be defined as the sum of bed-material load and wash load. The bed-material load is the sum of bed load and suspended bed-material load and represents that part of the total sediment discharge which is composed of grain sizes found in the bed. The wash load is that part composed of particle sizes finer than those found in appreciable quantities in the bed (Simons and Senturk, 1977). The presence of wash load can increase bank stability, reduce seepage and increase bed-material transport. Wash load can be easily transported in large quantities by the stream, but is usually limited by availability from the watershed. The bed-material load is more difficult for the stream to move and is limited in quantity by the transport capacity of the channel. Figure 5.1 summarizes the various definitions of the components of sediment load and their contribution to total sediment load.

There is no clear size distinction between wash load and bed-material load. As a rule of thumb, engineers assume that the size of bed-material particles is equal to or larger than 0.0625 mm, which is the division point between sand and silt. The sediment load consisting of grains smaller than this is considered wash load. A more reasonable criterion, although not necessarily theoretically correct, is to choose a sediment size finer than ten per-

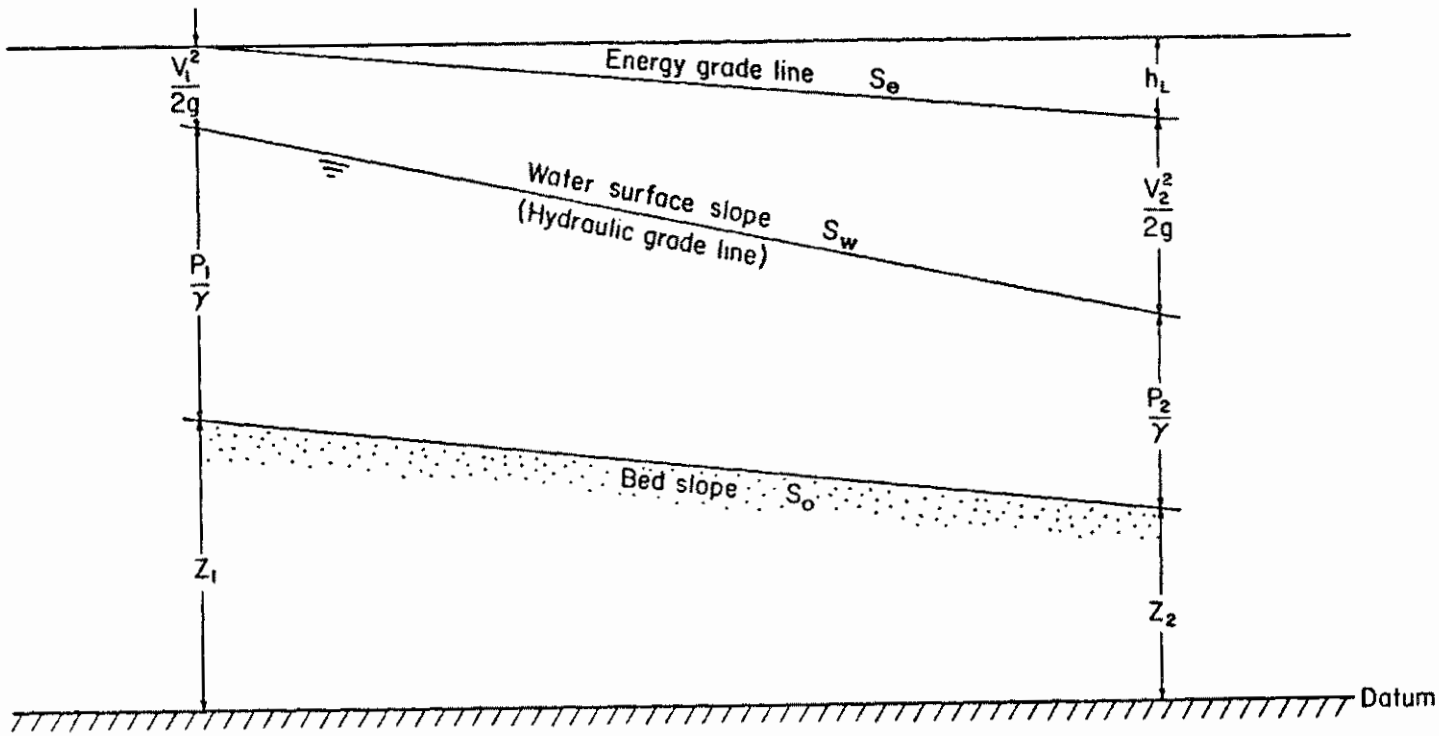


Figure 4.6. Definition sketch of the energy and hydraulic grade lines in open-channel flow.

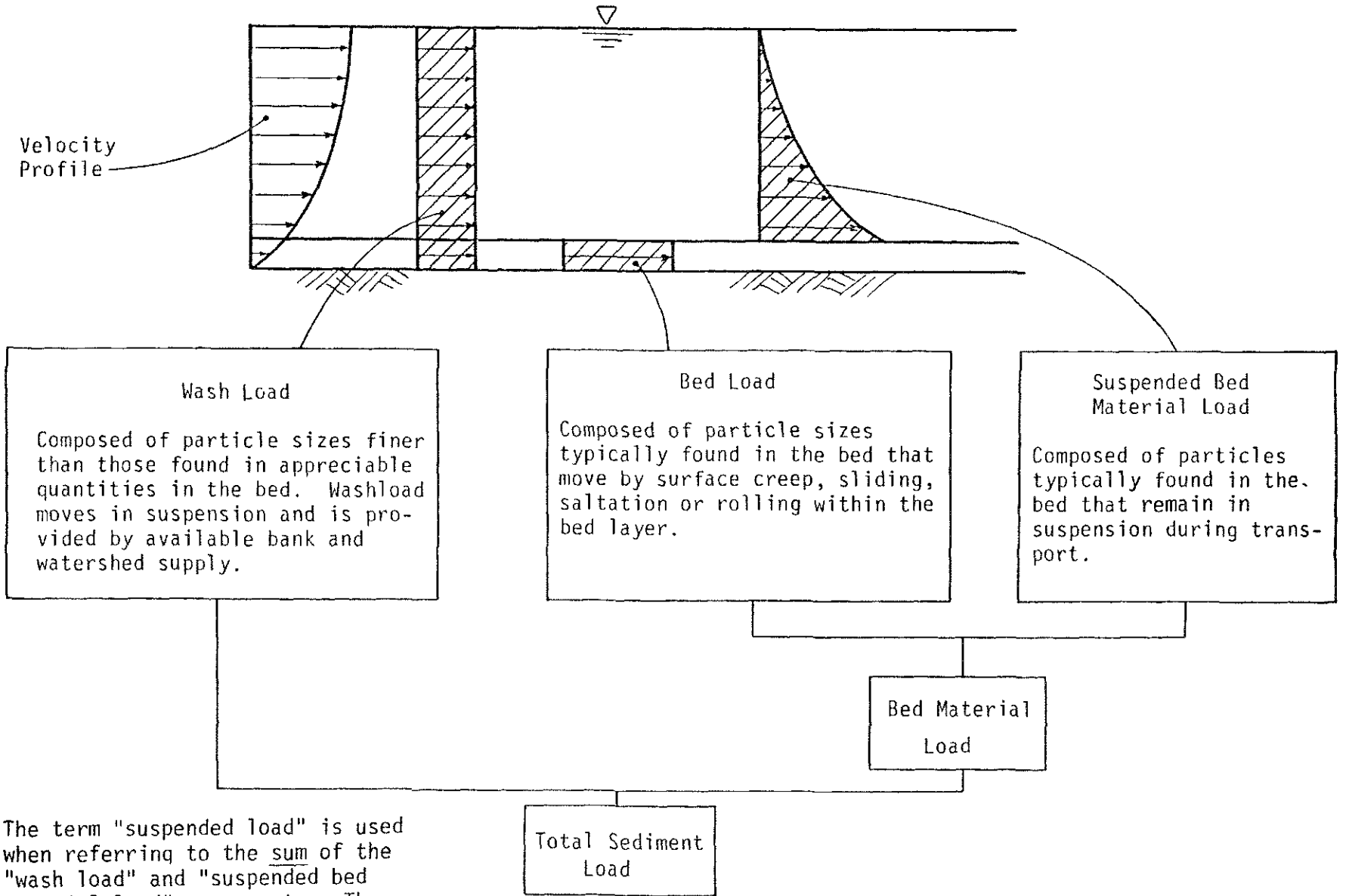


Note The term "suspended load" is used when referring to the sum of the "wash load" and "suspended bed material load" components. Therefore, an alternate definition of total sediment load is the sum of the suspended load and bed load.

Figure 5.1. Definition of sediment load components.

cent of the bed sample as the dividing size between wash load and bed-material load. It is assumed that most of the wash load is transported through the system by stream flow and little wash load is deposited on or in the stream bed. Wash load thus deposited with the coarse material is usually only a very small fraction of the total bed material.

The amount of material transported, eroded, or deposited in an alluvial channel is a function of sediment supply and channel transport capacity. Sediment supply includes the quality and quantity of sediment brought to a given reach. Transport capacity is a function of the size of bed material, flow rate, and geometric and hydraulic properties of the channel. Generally, the single most important factor determining sediment transport capacity is flow velocity. Additionally, since transport capacity is generally proportional to the third to fifth power of velocity, small changes in velocity can cause large changes in sediment transport capacity. Either supply rate or transport capacity may limit the actual sediment transport rate in a given reach.

### 5.1.2 Basic Terminology

A variety of terminology has been used to describe channel response to changing sediment transport conditions. In a very general sense, erosion and sedimentation are used in a generic fashion to describe any loss or gain of sediment. Other terminology is then used to more precisely define the erosion and sedimentation occurring under specific circumstances. For example, vertical channel response is often described by words such as aggradation, degradation, general scour and local scour, while horizontal response is typically referred to as lateral migration. The terminology describing vertical channel response has become somewhat confusing as different authors and/or publications have used the words in slightly different ways. To facilitate future discussions and to avoid confusion, the following definitions are adopted in this manual.

Aggradation and degradation are the raising or lowering of the channel bed, respectively, occurring over relatively long reaches and long time periods from changes in such things as sediment supply, controls, river geomorphology, and man-induced effects. General scour refers to a more localized vertical lowering of the channel bed over relatively short time periods, for example, the general scour in a given reach after passage of a single flood.

Special cases of general scour include contraction scour occurring in the vicinity of bridges that encroach on the flood plain and the scour that occurs downstream of a gravel pit. Unlike degradation, which has the antonym "aggradation," an accepted antonym for general scour is more difficult to define. In this manual "deposition" will be used as the counterpart to general scour. Local scour is caused by vortices resulting from local disturbances in the flow such as bridge piers and embankments. In general, the vertical changes in a channel are additive so that, for example, local scour could be occurring in a reach experiencing general scour and/or aggradation.

Lateral migration is defined as bankline shifting due to processes of bank erosion. Since aggradation/degradation, general scour/deposition, and/or any local scour along an embankment can promote bank instability, the vertical and horizontal shifting on a channel are interrelated. Degradation, general scour, local scour and lateral migration can endanger adjacent property, bridges and other hydraulic structures, while aggradation and deposition can reduce channel capacity, increase lateral erosion and increase flooding potential.

## 5.2 Level I Analysis

### 5.2.1 Plan Form Characteristics

Discussion - Rivers can be classified broadly in terms of channel pattern, that is, the configuration of the river as viewed on a map or from the air. The patterns are straight, meandering, braided, or some combination of these (Figure 5.2).

A straight channel can be defined as one that does not follow a sinuous course. Leopold and Wolman (1957) have pointed out that truly straight channels are rare in nature. Although a stream may have relatively straight banks, the thalweg, or path of greatest depth along the channel, is usually sinuous (Figure 5.2b). As a result, there is no simple distinction between straight and meandering channels.

The sinuosity of a channel, defined as the ratio between the thalweg length and the down-valley distance, is most often used to distinguish between straight and meandering channels. Sinuosity varies from a value of unity to a value of three or more. Leopold, Wolman and Miller (1964) took a sinuosity of 1.5 as the division between meandering and straight channels. It should be

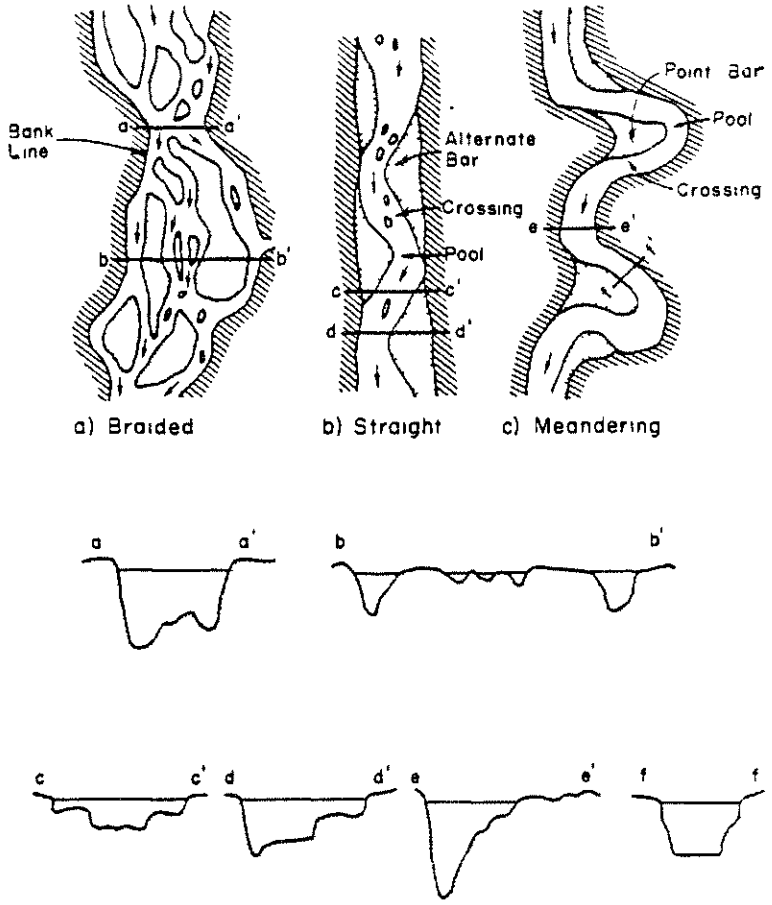


Figure 5.2. River channel patterns.

noted that in a straight reach with a sinuous thalweg developed between alternate bars (Figure 5.2b), a sequence of shallow crossings and deep pools is established along the channel.

A braided stream or river is generally wide with poorly defined and unstable banks, and is characterized by a steep, shallow course with multiple channel divisions around alluvial islands (Figure 5.2a). Braiding was studied by Leopold and Wolman (1957) in a laboratory flume. They concluded that braiding is one of many patterns which can maintain quasi-equilibrium among the variables of discharge, sediment load, and transporting ability. Lane (1957) concluded that, generally, the two primary causes that may be responsible for the braided condition are (1) overloading, that is, the stream may be supplied with more sediment than it can carry, resulting in deposition of part of the load; and (2) steep slopes, which produce a wide, shallow channel where bars and islands form readily.

A meandering channel is one that consists of alternating bends, giving an S-shape appearance to the plan view of the river (Figure 5.2c). More precisely, Lane (1957) concluded that a meandering stream is one whose channel alignment consists principally of pronounced bends, the shapes of which have <u>not</u> been determined predominantly by the varying nature of the terrain through which the channel passes. The meandering river consists of a series of deep pools in the bends and shallow crossings in the short straight reach connecting the bends. The thalweg flows from a pool through a crossing to the next pool forming the typical S curve of a single meander loop.

<u>Application</u> - Knowledge of the various channel types and their characteristics provides the engineer or designer with a basic understanding of channel behavior. Alluvial channels of all types deviate from a straight alignment. The thalweg oscillates transversely and initiates the formation of bends. In general, the engineer concerned with channel stabilization should not attempt to develop straight channels. In a straight channel the alternate bars and the thalweg (the line of greatest depth along the channel) are continually changing, thus the current is not uniformly distributed through the cross section but is deflected toward one bank and then the other. When the current is directed toward a bank, the bank is eroded in the area of impingement and the current is deflected and impinges upon the opposite bank further downstream. The angle of deflection of the thalweg is affected by the curvature formed in the eroding bank and the lateral extent of erosion.

In general, bends are formed by the process of erosion and deposition. Erosion without deposition to assist in bend formation would result only in escalloped banks. Under these conditions the channel would simply widen until it was so large that the erosion would terminate. The material eroded from the bank is normally deposited over a period of time on the point bars that are formed downstream. The point bars constrict the bend and enable erosion in the bend to continue, accounting for the lateral and longitudinal migration of the meandering stream. Erosion is greatest across the channel from the point bar. As the point bars build out from the downstream sides of the points, the bends gradually migrate down the valley. The point bars formed in the bendways clearly define the direction of flow. The bar generally is streamlined and its largest portion is oriented downstream. If there is very rapid caving in the bendways upstream, the sediment load may be sufficiently large to cause middle bars to form in the crossing.

Because of the physical characteristics of straight, braided, and meandering streams, all natural channel patterns intergrade. Although braiding and meandering patterns are strikingly different, they actually represent extremes in a continuum of channel patterns. On the assumption that the pattern of a stream is determined by the interaction of numerous variables whose range in nature is continuous, one should not be surprised at the existence of a complete range of channel patterns. A given channel, then, may exhibit both braiding and meandering, and alteration of the controlling parameters in a reach can change the character of a given stream from meandering to braided or vice versa.

Figure 5.3 summarizes the subclassifications of river channels within the major types of meandering, straight and braided channels that are of use to the geomorphologist and engineer. Information in this figure provides guidelines for qualification of channel characteristics for practical applications.

Example - From field observations and review of recent aerial photographs, the following characteristics have been determined:

- sinuosity = 1.2
- wide, braided channel

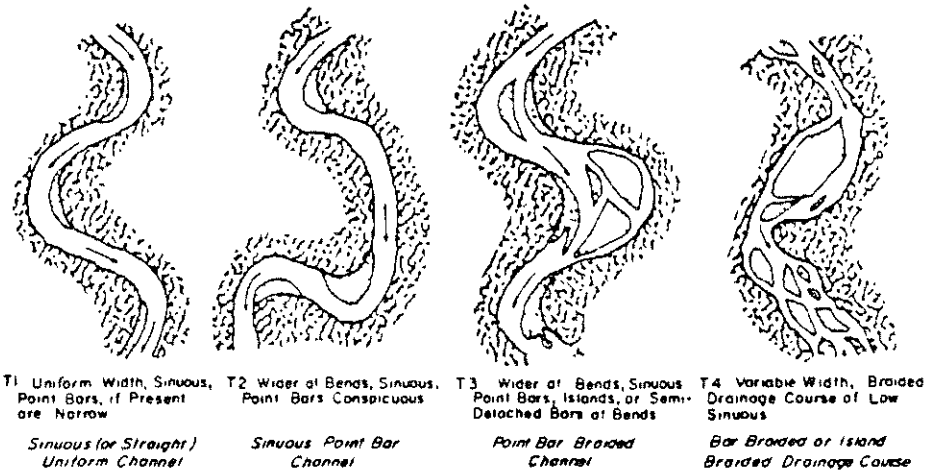


(a) Variability of unvegetated channel width: channel pattern at normal discharge

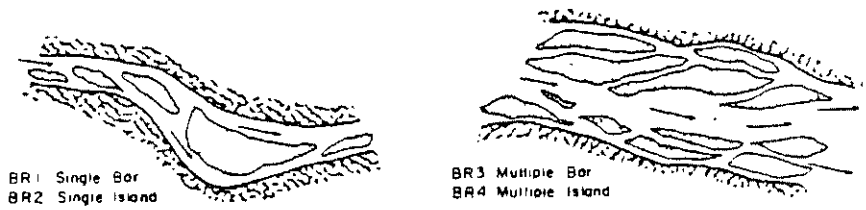


(b) Braiding patterns

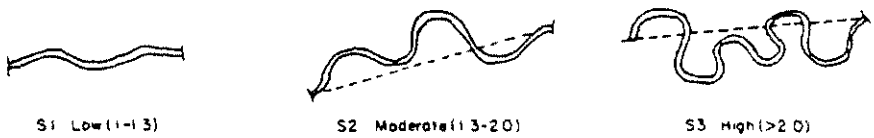


(c) Types of sinuosities

Figure 5.3. Classification of river channels (after Culbertson et al., 1967)

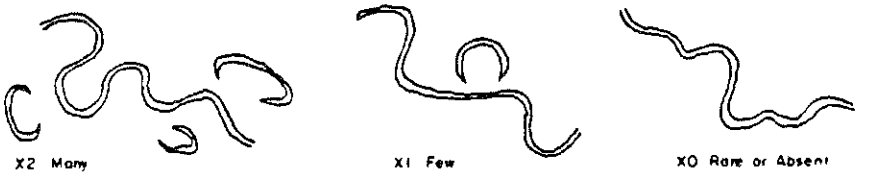


(d) Oxbow lakes on floodplain

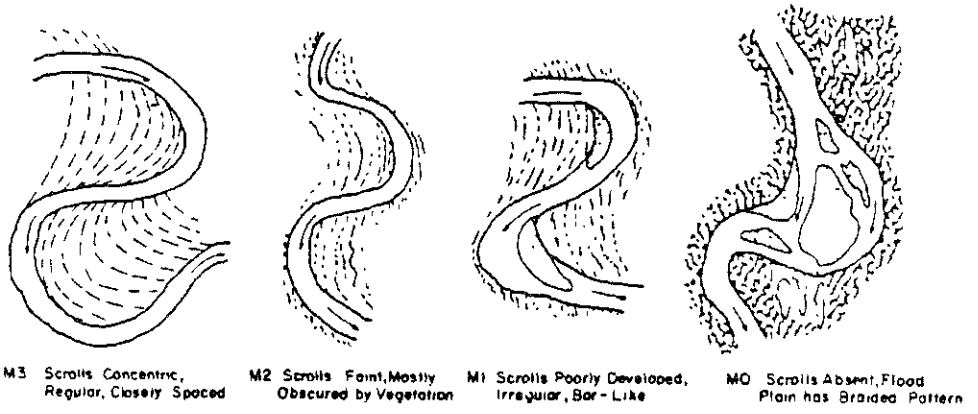


(e) Types of meander scroll formations

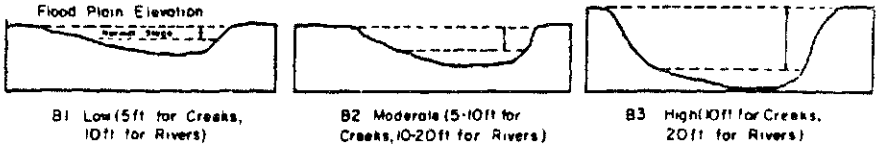


(f) Types of bank heights

Figure 5.3. (continued)

(g) Types of natural levee formations

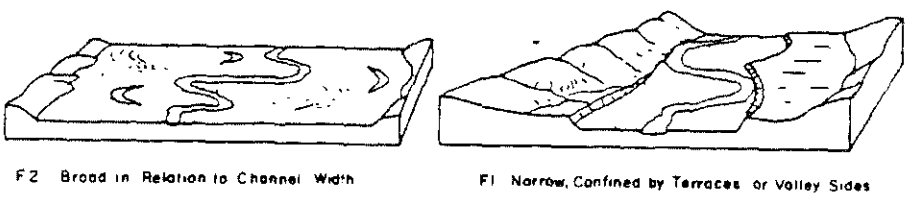


(h) Types of modern floodplains

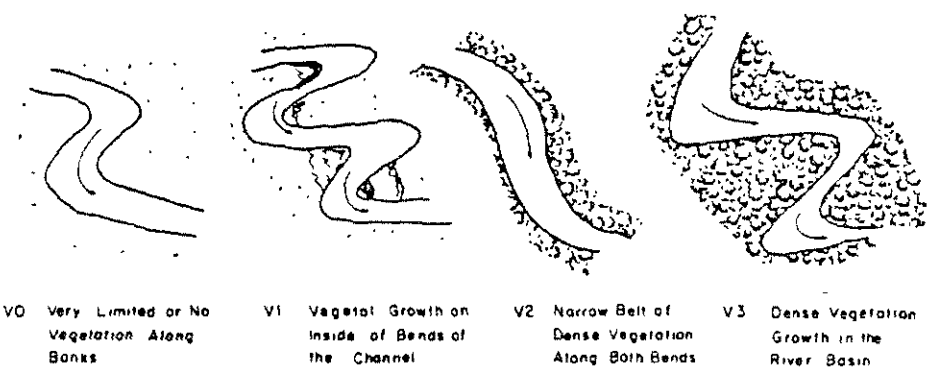


(i) Types of vegetal patterns

Figure 5.3. (continued)

- low-flow bank height, about 2 to 3 feet
- evidence of meander scars in flood plain

From these observations, it can be concluded that the channel is presently, and has been historically, unstable. The low sinuosity, braided character and low banks suggest a steep, wide water course with poorly defined, unstable banks.

### 5.2.2 Lane Relation and Other Geomorphic Relationships

Discussion - A number of geomorphic relationships are available that can provide insight on the general characteristics of a channel and its response to various impacts or changes. The usefulness of these procedures is to provide the engineer or designer with a qualitative understanding that will guide quantitative calculations and assist in formulating conclusions.

Application - A basic physical process that occurs in a channel is its tendency, in the long run, to achieve a balance (equilibrium) between the product of water flow and channel slope and the product of sediment discharge and sediment size. The most widely known geomorphic relation embodying this equilibrium concept is known as Lane's principle. The basic relation is (Lane, 1955):

$$QS \propto Q_S D_{50} \tag{5.1}$$

where $Q$ is the water discharge, $S$ is the channel slope, $Q_s$ is the sediment discharge and $D_{50}$ is the median diameter of the bed material. Figure 5.4 illustrates the equilibrium concept as proposed by Lane.

A similiar set of relationships was given by Schumm (1977):

$$Q \simeq \frac{b_1 d_1 \lambda}{S} \tag{5.2a}$$

and

$$Q_s \simeq \frac{b_1 \lambda_1 S}{d_1 P} \tag{5.2b}$$

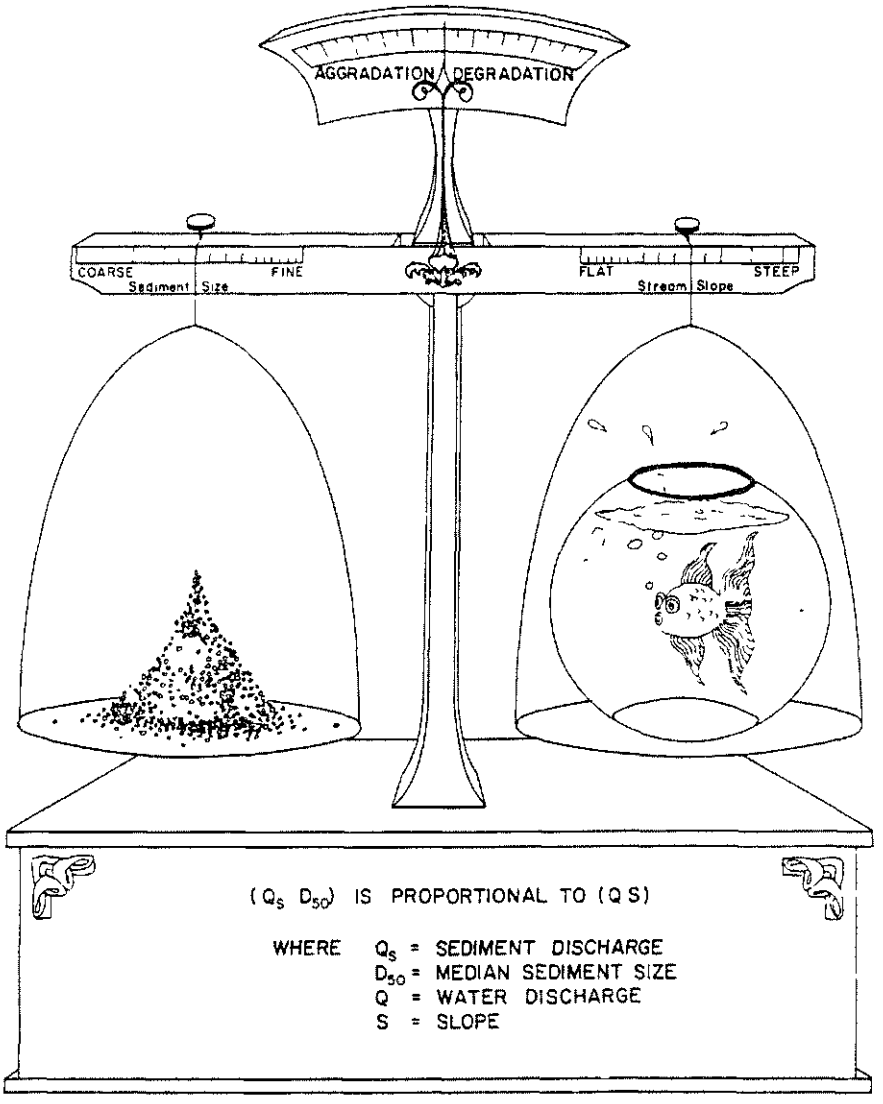


Figure 5.4. Schematic of the Lane relationship for qualitative analysis.

where $b_1$ is channel width, $d_1$ is depth, $\lambda$ is meander wave length, $S$ is channel slope and $P$ is sinuosity. Width/depth ratio, indicated to be directly related to sediment discharge, is implicitly included in Equation 5.2b because both depth and width appear separately.

Investigations have also focused on the relationship between channel characteristics, such as slope and sinuosity, and channel patterns (straight, meandering, braided). Results of Friedkin (1945), Leopold and Wolman (1957), and Lane (1957) suggest that for a given discharge there is a threshold slope separating braided and meandering channels. Figure 5.5 summarizes the various results, which in general can be fitted by equations of the form

$$S\ Q^{\alpha} = K \tag{5.3}$$

where $S$ is the channel slope, $Q$ is the discharge, $\alpha$ is a coefficient and $K$ is a constant. The data used to develop these relationships included both laboratory results and field measurements for predominantly sand-bed channels. Furthermore, the results were derived from perennial channels using either the mean annual discharge (dominant discharge) or the bankfull discharge for analysis. Consequently, a strict application of these relationships to the ephemeral streams typical of the Southwest is impossible; however, they can be used in a qualitative sense to develop an understanding of possible channel response.

Figure 5.6 illustrates a relationship between sinusoity, slope, and channel pattern (after Kahn, 1971). This figure also illustrates that any natural or artificial process which alters channel slope can result in modifications to the existing river pattern. Similar to the slope-discharge relations, strict application of Figure 5.6 is not feasible to ephemeral channels, since it was developed from limited laboratory results; however, application in a qualitative sense can be beneficial.

<u>Example</u> - A series of grade-control structures has been proposed that will reduce channel slope from 0.1 percent to 0.065 percent for an arroyo with a bankfull discharge of 2,500 cfs.

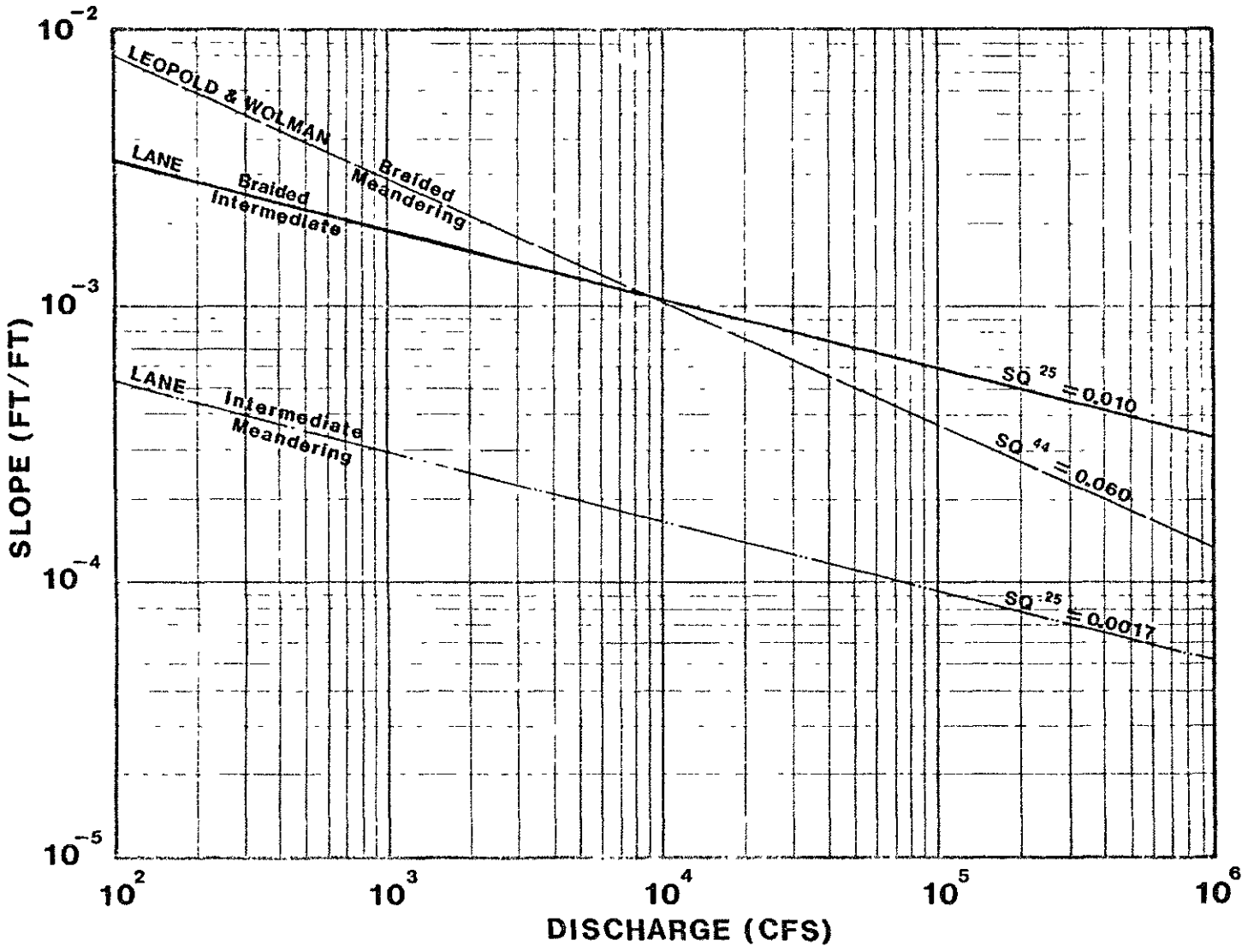


Figure 5.5. Slope-discharge relations.

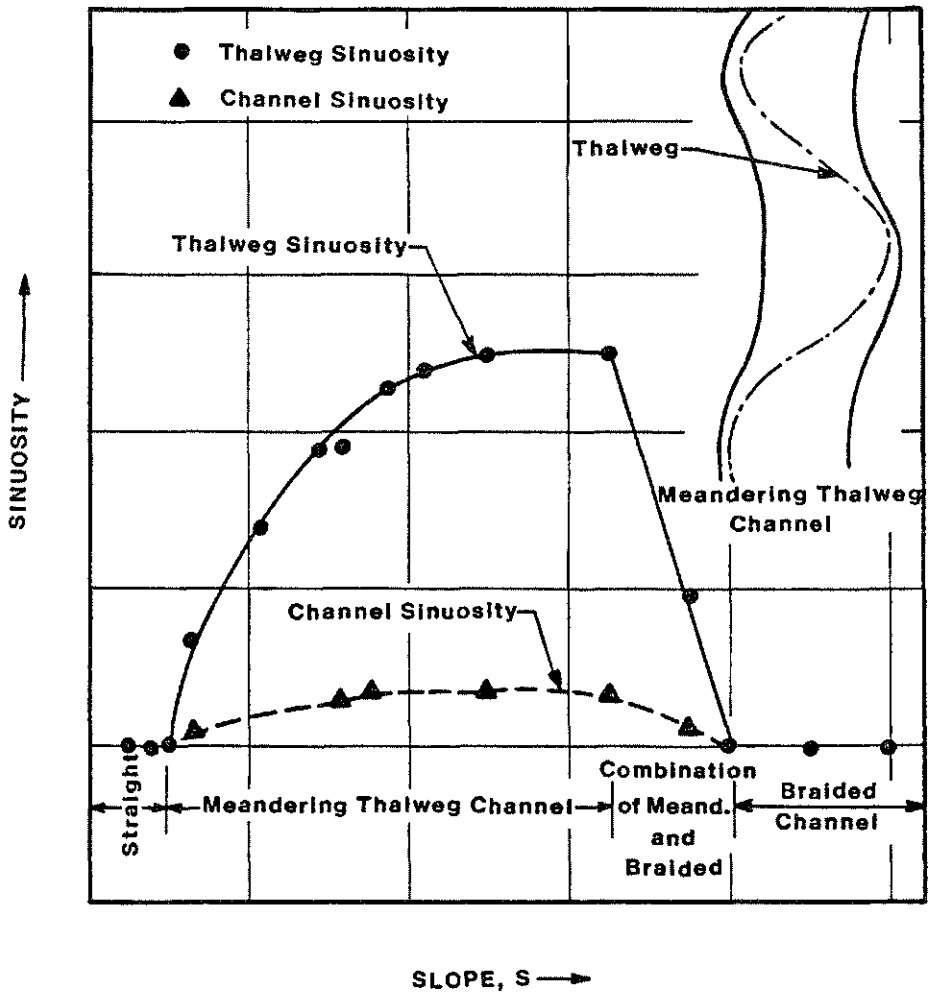


Figure 5.6. Channel pattern versus slope and simuosity (Kahn, 1971)

Assuming water discharge and $D_{50}$ sediment size remain constant, the Lane relation (Equation 5.1) indicates that the sediment discharge must decrease. That is,

$$Q^{\circ}S^{-} \propto Q_s^{-} \; D_{50}^{\circ}$$

(Note that if we had more than one dependent variable, for example, if the $D_{50}$ size was not assumed constant, it might not be possible to predict the direction of change in $Q_s$.) Application of the Schumm equilibrium equations (Equations 5.2a and 5.2b) provides a similar result.

According to the slope-discharge relation (Figure 5.5), a decrease in slope will produce a change in the direction towards a meandering channel. Using the bankfull discharge of 2,500 cfs suggests that the grade-control structures will not significantly change the channel pattern from an intermediate or mildly meandering characteristic; however, since we are applying ephemeral channel data to a relationship derived for perennial channels, it is impossible to be conclusive.

The Kahn relationship (Figure 5.6) suggests that even a small decrease in slope from an intermediate or mildly meandering channel will promote significant thalweg sinuosity. As with the slope-discharge relation, it is not possible to be conclusive; however, the application of these relationships together promotes the idea of a transition to a more stable, meandering channel after installation of grade-control structures.

### 5.2.3 Aerial Photograph Interpretation

Discussion - Maps and aerial photographs supplement each other and provide more information when used together than either does alone. For example, a topographic map provides quantitative information on land surface characteristics; however, due to the time since it was compiled, parts of the map may be obsolete. A recent aerial photograph will show changes that have occurred since the map was compiled and allows accurate assessment of present conditions.

There are two major types of aerial photography: vertical and oblique. A vertical photograph is taken with the optical axis of the camera held essentially vertically. Vertical photographs are used in most planimetric and topographic mapping, construction of mosaics, and orthophoto production.

Oblique photography is accomplished by purposely tilting the optical axis a sizeable angle from the vertical. A high oblique is a photograph taken with the camera inclined so that the apparent horizon appears. A low oblique is taken with the camera axis tilted but not to the degree that the horizon appears. Due to the greater ground coverage of obliques, high obliques are often used in the preparation of small-scale planimetric maps and charts. When taken as convergent photography, low obliques can be utilized in the compilation of accurate topographic maps.

Application - Aerial photographs provide information valuable to the qualitative and quantitative analysis of river hydraulics and channel geometry problems. Utilization of aerial photographs over a span of many years will provide a time-sequenced documentation of historical trends and changes in the river. Assessments made from aerial photographs are dependent largely on the quality and scale of the photos. Properly applied, photographic interpretation can provide an abundance of accurate and useful information.

Evidence of land-use changes, bank cutting, shifting of the thalweg, meander tendencies, lateral migration, vegetation changes, and sediment deposition can be documented by studying photographs for different years. If time-sequenced aerial photography is available for an area, it is a relatively simple procedure to trace or freehand a composite sketch showing morphologic evolution, or to document changes in channel width, sinuosity, etc. through direct measurements.

It should be noted that an aerial photograph is a perspective projection of the ground surface onto the focal plane of the camera. Thus, points in a plane closer to the camera at the time of exposure will have larger images than points located farther from the camera. For this reason, the scale can vary in different portions of a vertical photograph depending on topographic relief. Generally, the scale given for a set of aerial photographs is the average scale based on the difference between the average ground-surface elevation and flying height for all photographs taken during the flight. An average scale can be applied to a scaled distance to give a reasonable estimate of corresponding ground length so long as relief is not extremely variable. In areas of highly variable relief, scaling errors will result from use of an average scale and limit the accuracy and reliability of any quantitative measurements.

Time can be a limiting factor in acquisition of aerial photographs. Orders often require four to six weeks to be processed. Time delays are often increased by the fact that many agencies hesitate to select photos for you because of their uncertainty as to what is wanted. Therefore, unless you have access to indexes retained at the agencies, allow another four to six weeks to obtain copies of indexes from which you will designate preferred photos.

Photos are indexed by geographic coordinates, but are further referenced by codes representing the various flights making up the index mosaics. As flight paths tend to be straight, while rivers tend to meander, the necessity for careful identification of desired photos becomes more understandable.

Aerial photos come in a standard 9" x 9" size, usually costing $5.00 to $6.00 each. Often, however, these may be enlarged two, three, or even four times (two-times enlargements--18" x 18"--run $25.00 to $30.00). Note: flight elevations do vary, and thus scales will also vary. At a scale of 1:24,000, one inch on the photograph depicts 2,000 feet. This 1:24,000 scale photo then covers approximately 12 square miles. A 1:63,360 scale photo covers about 81 square miles. Be prepared to compensate accordingly.

The U.S. Geological Survey National Cartographic Information Center (NCIC) provides assistance in locating and acquiring maps, aerial photographs, satellite images, and other cartographic products. NCIC offers direct access to most of the nation's domestic aerial photographs (including some historical material) and satellite images available to the public. Important other sources also exist and NCIC will assist you in contacting them when appropriate. These sources include federal agencies and some private firms that retain the originals of photographs or that produce highly specialized products.

NCIC works in conjunction with the Earth Resources Observation Systems (EROS) Data Center in Sioux Falls, South Dakota. Both NCIC and the EROS Data Center research requests for information about photos and take orders for aerial and space photographs and space images. For photographs prior to 1941, the National Archives must be contacted. Addresses for these agencies are provided in Table 5.1.

Example - For an erosion-sedimentation analysis of Arroyo de las Calabacillas in New Mexico, three sets of aerial photographs covering a time period of 45 years were obtained. A 1935 soil conservation photograph was

Table 5.1. Agencies with Information on Aerial Photographs.

EROS Data Center
U.S. Geological Survey
EROS Data Center
User Services Section
Sioux Falls, South Dakota 57198
Telephone: 605/594-6151

NCIC Headquarters
National Cartographic Information Center
U.S. Geological Survey
507 National Center
Reston, Virginia 22092
Telephone: 703/860-6045

NCIC Offices
Eastern Mapping Center--NCIC
U.S. Geological Survey
536 National Center
Reston, Virginia 22092
Telephone: 703/860-6336

Mid-Continent Mapping Center--NCIC
U.S. Geological Survey
1400 Independence Road
Rolla, Missouri 65401
Telephone: 314/341-0851

National Cartographic Information Center
U.S. Geological Survey
National Space Technology Laboratories
NSTL Station, Mississippi 39529
Telephone: 601/688-3544

Rocky Mountain Mapping Center--NCIC
U.S. Geological Survey
Box 25046, Stop 504 Federal Center
Denver, Colorado 80225
Telephone: 303/234-2326

Western Mapping Center--NCIC
U.S. Geological Survey
345 Middlefield Road
Menlo Park, California 94025
Telephone: 415/323-8111, ext. 2427

National Archives Cartographic Division
Attn: Richard Spurr
841 South Pickett Street
Alexandria, Virginia 22304
Telephone: 703/756-6704

obtained from the National Archives with a four-times enlargement of its original 1:35,000 scale. A 3' x 3' mosaic was obtained based on 1967 photography available from NASA. The original photographs had a scale of 1:26,000 and those selected for the mosaic were enlarged four times. A 1980 set of 9" x 9" low-altitude photographs (scale 1:10,800) were obtained from a local aerial surveying firm. Part of the analysis of these photographs consisted of preparation of composite sketches illustrating plan form changes over the 45-year period (Figure 5.7). As can be seen from this figure, aerial photography indicates a history of meander development and cutoff in the area of the S bend and increased sinuosity at the horseshoe bend. From 1935 to 1967 several channel shifts occurred; however, from 1967 to 1980 the channel was unchanged. When combined with available information on historical flood occurrences or land-use changes, such qualitative aerial photograph interpretation can provide much valuable information on system response and evolution.

### 5.2.4 Bed- and Bank-Material Analysis

Discussion - Knowledge of the characteristics of bed and bank material is important to any fluvial systems analysis. Bed and bank material analysis in a qualitative Level I evaluation primarily involves visual observations made during site reconnaissance as well as evaluation of existing data pertaining to soils and geology of the study area. Soils and geologic information are interrelated to the extent that surficial geology influences soil type and development. Additionally, rock outcrops may comprise the channel bed and/or banks in certain reaches, limiting the extent to which degradation or lateral migration can progress. Thus, accurate delineation of geologic control is an integral part of a qualitative assessment of bed and bank materials in a fluvial system.

Application - Visual inspection of bed and bank materials can serve to identify physical conditions or features of significance in a system. For example, the relative cohesiveness of bank materials and their ability to resist erosion by water can readily be assessed by observing the height and steepness of the channel banks. During site reconnaissance observable bank failure areas should be noted. For example, block failure from development of tension cracks can be a significant point source of sediment in a given reach. Although block failures are most common to stratified banks, similar localized

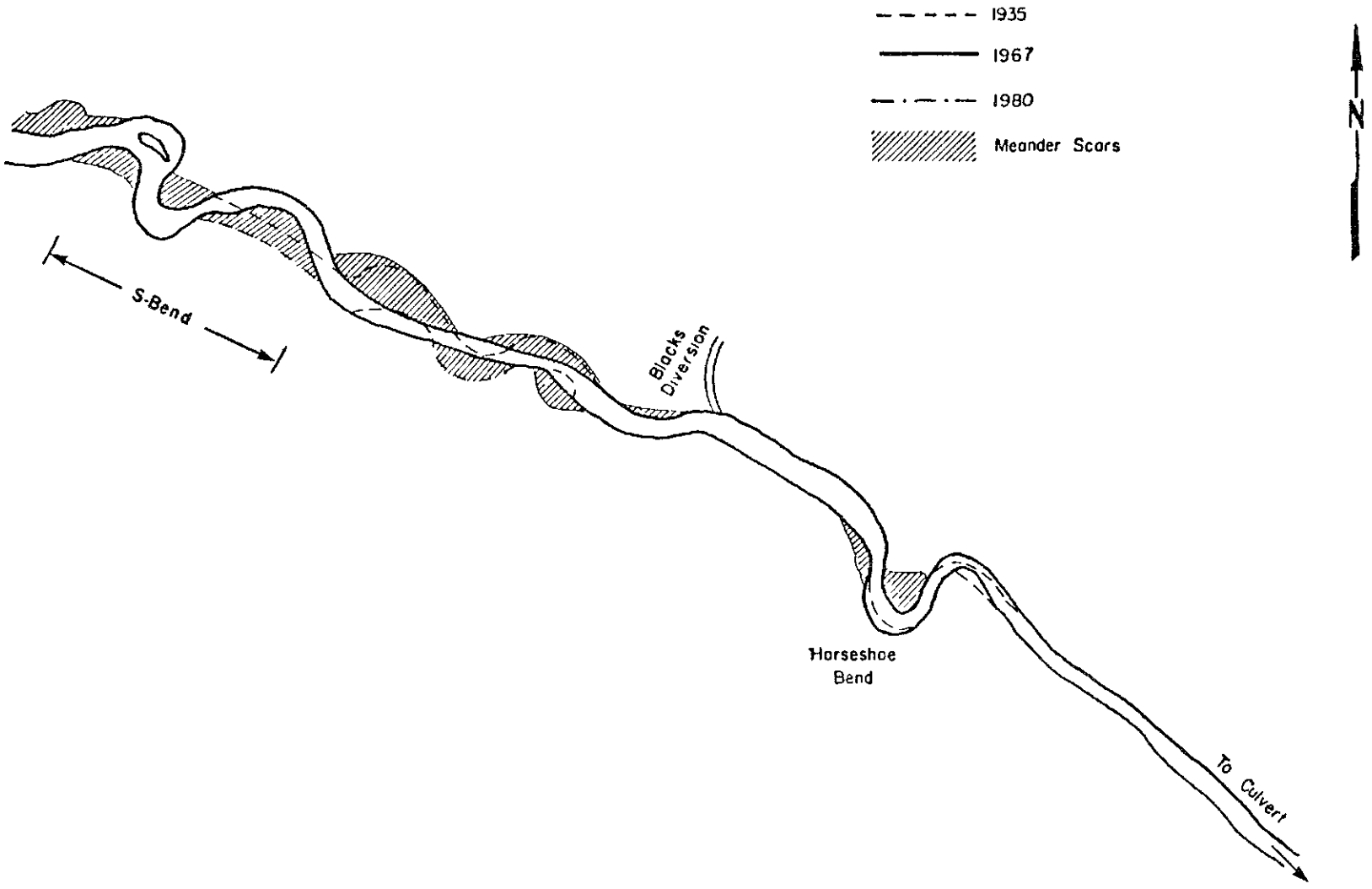


Figure 5.7. Example illustrating qualitative information derived from time sequence analysis of aerial photographs.

mass wasting phenomena occur in noncohesive and cohesive banks from the processes of sloughing and sliding, respectively. In addition to visual observation of bank material and conditions, observation of bed material and bar deposits can tell the observer much about the type of sediments being transported in the system.

Visual techniques can also be employed to assess the textural composition and predominant material sizes (i.e., sand, clay, silt) in the bed and banks. Incised banks should be investigated to determine the level of stratification, presence of clay lenses, and layer thicknesses.

In addition to field observations, information in the literature may be useful in a qualitative assessment of bed and bank material. Possible sources include Soil Conservation Service (SCS) soil survey reports and land-use surveys, and environmental statements.

Example - During a preliminary site visit for an erosion/sedimentation analysis of a sand-bed channel, a 20- to 30-foot high bluff was observed protruding into the channel. Closer inspection found it to be round-stone conglomerate, a relatively stable sedimentary rock outcrop. Results of HEC-2 water-surface profile computation during the quantitative analysis indicated this outcrop was a significant control point influencing channel hydraulics. As a result of field observations, it was known to be a stable formation that would continue to be a significant control, not one expected to erode away quickly.

### 5.2.5 Land-Use Changes

Discussion - Water and sediment yield from a watershed is a function of land-use practices. Thus, knowledge of the land use and historical changes in land use is essential to understanding the water and sediment sources in a watershed. Relative percentages of forest, agricultural and urban land can provide insight to the quantity and type of water and sediment load produced in a watershed.

The presence or absence of vegetative growth can have a significant influence on the runoff and erosional response of a fluvial system. The root structure of plants, bushes and trees helps to develop and maintain a stable soil structure and serves as an erosion-retarding force. Large-scale changes in vegetation resulting from fire, logging practices, land conversion and

urbanization can either increase or decrease the total water and sediment yield from a watershed. For example, fire and logging practices tend to increase water sediment yield, while urbanization promotes increased water yield and decreased sediment yield. In addition to greater runoff volumes, urbanization causes peak flows to occur sooner. Potential damages from floods also increase as the property value subject to damage increases.

Application - Information on land-use history and trends can be found in Federal, state and local government documents and reports (i.e., census information, zoning maps, future development plans, etc.). Additionally, analysis of historical aerial photographs can provide significant insight on land-use changes. For example, the changes in vegetative cover over a given time can be classified into groups, such as "no change," "vegetation increasing," "vegetation damaged," and "vegetation destroyed." Estimates can also be made of bank stability and riparian conditions from aerial photographs.

Example - An analysis of land-use changes along the Salt River was conducted during a hydraulic analysis of the Seventh Street bridge in Phoenix. The main changes that have occurred since 1960 have been induced by man. Photographs of the river in 1960 show a wide braided channel with scattered vegetation. The braided portion of the channel extends laterally nearly 3,000 feet at some points. Since this time, gravel mining activities, construction of roads and bridges, and development along the river have eliminated the vegetation and in many places channelized and contained the river so that it is no longer braided. This development has caused an increase in flow velocities accompanied by an increase in sediment transport rate and potential degradation in the channel bed. The effects of the increased sediment transport rate and degradation have been curtailed by the river's ability to form an armor layer of large cobbles and boulders. This layer exists through most of the study reach. When the armor layer is ruptured, the sediment transport will increase, degrading the channel until enough large material accumulates on the surface of the channel bed to re-form an effective armor layer. In recent years the increase in construction and gravel mining has disturbed the armor layer, and the bed profile of the channel has changed due to degradation, mining, and the reworking of the channel bed.

### 5.2.6 Flood History and Rainfall-Runoff Relations

Discussion - Consideration of flood history is an integral step in attempting to characterize watershed system response and morphologic evolution. Analysis of flood history is of particular importance to an understanding of dryland stream characteristics. Many dryland streams flow only during the spring and immediately after major storms. For example, Leopold, et al. (1966) found that arroyos near Santa Fe, New Mexico, flow only about three times a year. As a consequence, dryland stream response can be considered to be more hydrologically dependent than streams located in a humid environment. Whereas the simple passage of time may be sufficient to cause change in a stream located in a humid environment, time alone, at least in the short term, may not necessarily cause change in a dryland system due to the infrequency of hydrologically significant events. Thus, the absence of significant morphological changes in a dryland stream or river, even over a period of years, should not necessarily be construed as indicative of system stability.

Although the occurrence of single large storms can often be directly related to system change, this is not always the case. In particular, the succession of morphologic change in arid to semiarid regions may be linked to the concept of geomorphic thresholds as proposed by Schumm (1977). Under this concept, although a single major storm may trigger an erosional event in a system, the occurrence of such an event may be the result of a cumulative process leading to an incipiently unstable geomorphic condition.

Application - Where available, the study of flood records and corresponding system responses, as indicated by time-sequenced aerial photography or other physical information, may help the investigator determine the relationship between morphological change and flood magnitude and frequency. Evaluation of wet-dry cycles can also be beneficial to an understanding of historical system response. Observable historical change may be found to be better correlated with the occurrence of a sequence of events during a period of above-average rainfall and runoff than with the single large event. The study of historical wet-dry trends may explain certain aspects of system response. For example, a large storm preceded by a period of above-average precipitation may result in less erosion (due to better vegetative stabilization of the channel banks and watershed) than a comparable storm occurring under dry antecedent conditions; however, runoff volumes might be greater due

to saturated soil conditions. A good method to evaluate wet-dry cycles is to plot annual rainfall amounts, runoff volumes and maximum annual mean daily discharge for the period of record. A comparison of these graphs will provide insight to wet-dry cycles and flood occurrences. Additionally, a plot of the ratio of rainfall to runoff is a good indicator of watershed characteristics and historical changes in watershed condition.

Example - Analysis of the rainfall and runoff records for the Santa Margarita watershed in southern California has been completed. Figure 5.8 provides the precipitation record since 1877, and Figure 5.9 the maximum annual mean daily discharge. From Figure 5.9 it is apparent that 1938, 1943, 1969, 1978 and 1980 were years of significant flooding. Additionally, analysis of historical documents indicates that 1884 was also a significant flood year. From Figure 5.8, total precipitation in the 1884 flood year was second only to that of 1978. Both of these years were preceded by very dry years. In comparison, the flooding of 1916 resulted from significantly less rainfall, but was preceded by a wet year in 1915. Other years with rainfall totals similar to 1916 but preceded by dry years did not produce floods of record. The 1938 flooding occurred after a significantly wetter year in 1937. It can be concluded that antecedent soil moisture is a significant factor in the extent of flooding resulting from a given precipitation event in the Santa Margarita watershed.

The runoff-rainfall ratio for the period 1924 to 1982 is plotted in Figure 5.10. Rough estimation of average values for 10-year periods have been superimposed on the data. These estimates indicate periods of high runoff production from 1935 to 1945 and from 1975 to 1982, and extremely low production for the period in between (i.e., 1945 to 1975).

## 5.3 Level II Analysis

### 5.3.1 Watershed Sediment Yield

Discussion - The determination of erosion from natural and disturbed lands has great significance to water-resources planning and development. Erosion of the land surface affects not only the nature of the land itself, but also the erosion and sedimentation process in the receiving river system. Sediment eroded from the land surface can cause silting problems in reservoirs and channels, resulting in increased flood stages and damage. Conversely,

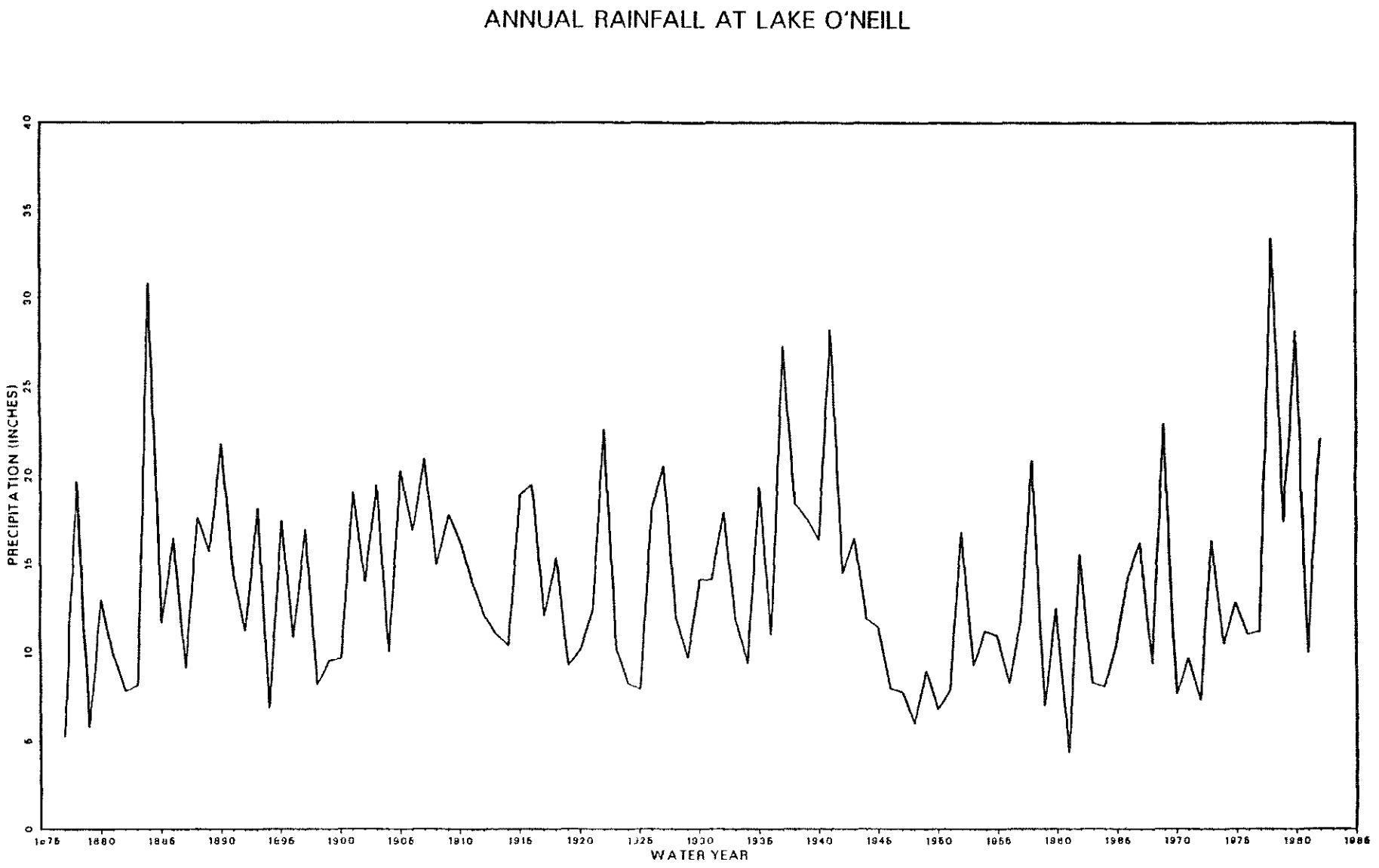


Figure 5.8. Annual rainfall for Santa Margarita Watershed.

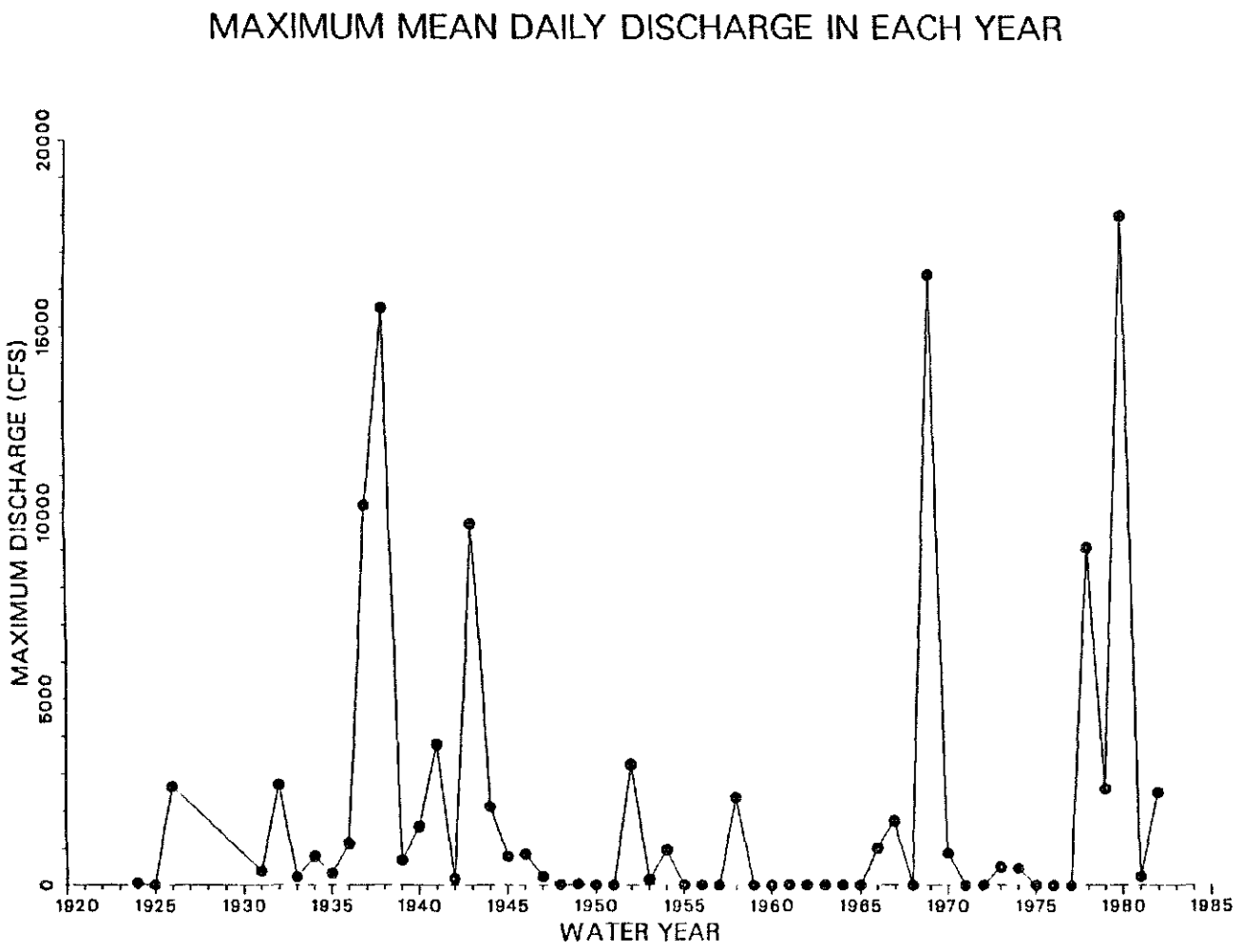


Figure 5.9. Maximum annual mean daily discharge for Santa Margarita River.

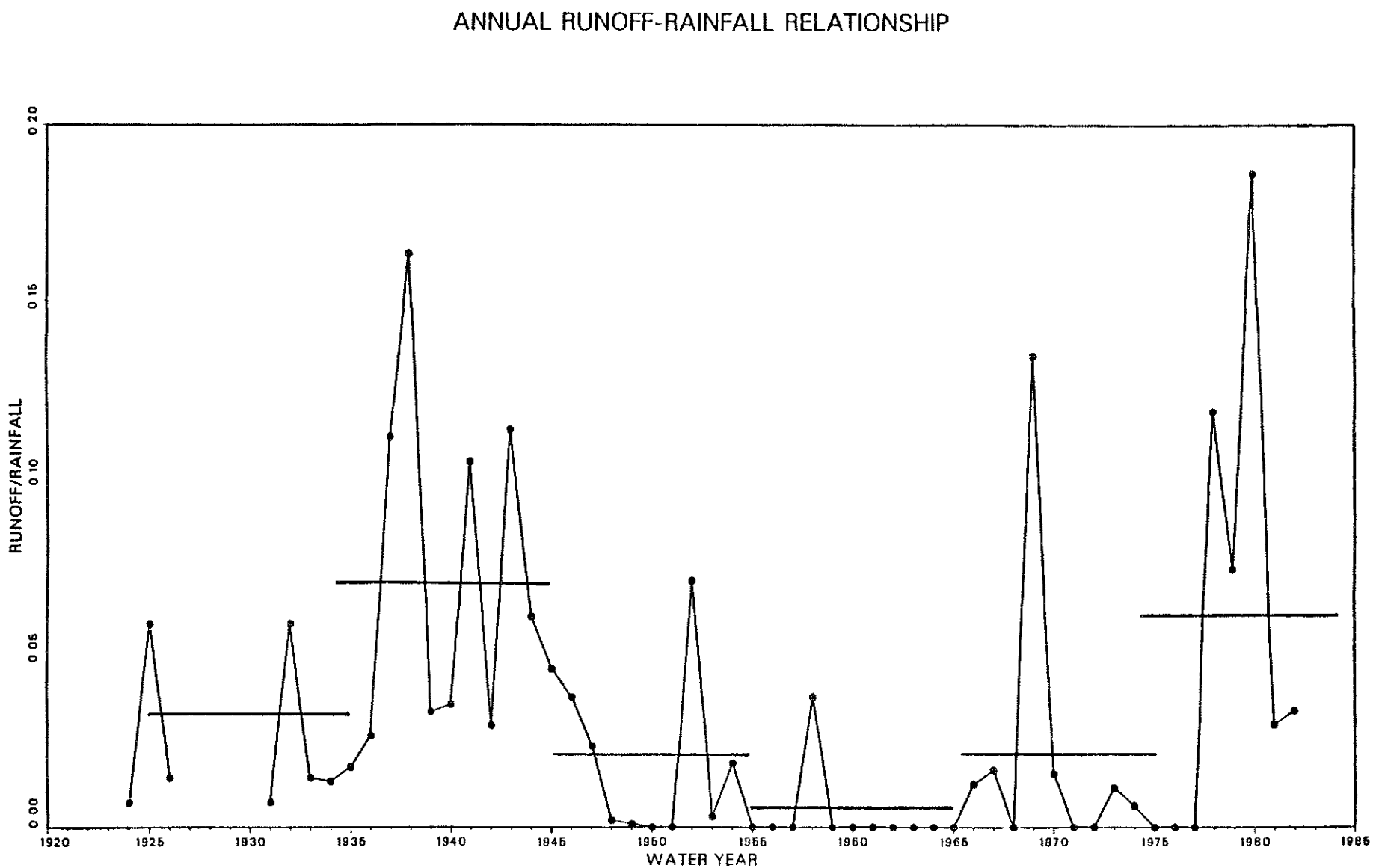


Figure 5.10. Annual runoff-rainfall ratio for Santa Margarita watershed.

reduction in erosion can also cause adverse impacts to river systems by reducing the supply of incoming sediment, thus promoting channel degradation and headcutting.

The wash load of the total sediment load in an alluvial channel is determined by the supply available in the watershed. Limited quantities of fine material moving as wash load usually will not pose direct problems for development in the riverine environment. It is usually assumed, unless there are detention structures that could effectively trap wash load, that such material does not come out of suspension and will pass through the system. A reduction in wash load can prevent the natural sealing of river banks induced by deposition of fine sediment, causing increased water loss and bank instability. Large concentrations of wash load, however, can influence the capacity of a stream to transport bed material through its influence on fluid viscosity and density, bank stability, growth of aquatic plants, and the biomass of the channel.

Formation of wash load is largely a function of raindrop detachment and transport by overland flow, which in turn, is inversely related to the level of surface cover and stabilization by vegetation. Precipitation generating erosion in dryland landscapes of the western states usually results from small storm cells that may be limited in areal extent, but can produce high-intensity and rainfall energy. This type of storm produces "flashy" runoff with a pronounced capacity for sediment removal and transportation. Thus, streams in the western states often carry large suspended sediment loads reflecting the sparsity (paucity) of vegetal cover and high transport capacity of rainfall runoff. This condition contrasts the low suspended sediment loads normally carried by streams in a humid environment due to well-developed soils and vegetative stabilization.

Application - Assessment of watershed sediment yield first requires a qualitative evaluation of sediment sources in the watershed and the types of erosion that are most prevalent. The physical processes causing erosion can be classified as sheet wash, rilling, gullying, and fluvial processes causing erosion of the stream bed and banks. Other types of erosional processes are classified under the category of mass movement, e.g., soil creep, earthflows, and landslides. Data from Soil Conservation Service (SCS) publications and maps, water-well log reports, reservoir records, climate records, and other

site-specific information can be utilized along with field observations to evaluate the area of interest.

One approach providing an approximate rating of sediment yield from a watershed was developed by the Pacific Southwest Interagency Committee (PSIAC, 1968). This method designed as an aid for broad planning purposes only, consists of a numerical rating of nine factors affecting sediment production in a watershed. This rating, in turn, is correlated with ranges of annual sediment yield in acre-feet per square mile. The nine factors are surficial geology, soil, climate, runoff, topography, ground cover, land use, upland erosion, and channel erosion and transport.

A strong correlation between PSIAC estimated annual sediment yield and actual annual sediment yield has been demonstrated by Shown (1970) and Renard (1980). Both workers tested the PSIAC method against actual annual sediment yield measured in ponds and dams in the Southwest. The comparisons were done on watersheds less than about 20 square miles in area, and PSIAC results agreed with or were slightly lower than actual measurements. Appendix A briefly describes application of the PSIAC methodology.

Another approach to determine sediment yield from natural or disturbed land surfaces is based on regression equations as typified by the Universal Soil Loss Equation (USLE). The USLE, an empirical formula for predicting soil loss due to sheet and rill erosion, is probably the most widely used method for predicting soil erosion. The equation was developed from over 10,000 plot-years of runoff and soil-loss data, collected on experimental plots of agricultural land in 23 states by the U.S. Department of Agriculture. The USLE approach relates annual soil loss due to sheet and rill erosion to the product of six major factors describing rainfall energy, soil erodibility, cropping and management, supplemental erosion-control practices such as contouring or terracing, and slope steepness and length, which are usually combined to form a topographic factor. Wischmeier and Smith (1978) provide detailed descriptions of this equation and its terms.

Although widely used, the USLE approach has some important limitations, particularly in the arid regions of the West. The data base used in developing the USLE was collected east of the Rocky Mountains. Extrapolation to western areas can introduce significant error. Many arid regions of the West get a large percentage of rainfall in the form of high-intensity, short-duration thunderstorms. As this is not the case in the central and eastern

United States, the effect of this type of rainfall cannot be totally incorporated. In addition, the weathering process caused by the wind and sun on the soil between rainstorms is much more severe in arid areas. Weathering creates an additional supply of easily eroded material that can increase the erodibility factor significantly.

Williams and Berndt (1972) recognized that application of the USLE is limited to soil loss, and developed another procedure, the Modified Universal Soil Loss Equation (MUSLE), for computing sediment yields from watersheds. This method determines sediment yield based on single storms. They introduced a runoff factor instead of rainfall energy into the USLE to estimate soil loss. This make the MUSLE more applicable to the arid regions of the West, since the effect of short-duration, high-intensity events can be more adequately represented. Appendix B briefly reviews application of the MUSLE methodology.

If the sediment yield from the land surface on an annual basis rather than from a single storm is desired, the MUSLE can also be used. This application is accomplished by determining the soil loss for events of varying return periods. Recommended return period are 2, 10, 25, 50, and 100 years. The sediment yields are then weighted according to their incremental probability, resulting in a weighted storm average.

The USLE, MUSLE, and PSIAC methods are generally applicable as predictors of wash load. Total sediment load in a fluvial system is estimated as the sum of wash load (computed from the USLE, MUSLE, or another comparable method) and bed-material load (computed according to Section 5.3.6). The substitution of the MUSLE for the USLE provides a methodology that is more applicable to western conditions, especially in arid regions.

Example - Examples illustrating application of the PSIAC and MUSLE methodologies are given in Appendices A and B.

### 5.3.2 Detailed Analysis of Bed and Bank Material

Discussion - Bed material is the sediment mixture of which the streambed is composed. Bed material ranges in size from huge boulders many feet in diameter to fine clay particles. The erodibility or stability of a channel largely depends on the size of the particles in the bed. It is often insufficient to know only the median bed-material size ($D_{50}$) in determining the

potential for degradation; knowledge of the bed-material size distribution is also important. Furthermore, the potential for or existence of an armor layer also needs to be addressed (see Section 5.3.7). Armoring potential differentiates a gravel- or cobble-bed stream or river from a sand-bed river. "Whereas the bed surface of a sand-bed stream typically appears to represent a random cut through the sandy bed material, gravel beds commonly consist of two separate populations, the surface layer and the underlying deposit" (Kellerhalls and Bray, 1971). As water flows over the bed of a gravel-bed stream, smaller particles that are more easily transported are carried away, while larger particles remain, armoring the surface layer of the bed. This armor layer can serve as a control unless a flow of sufficiently large magnitude occurs.

Bank material usually consists of particles of the same size as, or smaller than, bed particles. Thus, banks are often more easily eroded than the bed unless protected by vegetation, cohesion, or some type of man-made protection. River banks can be classified according to stability by vegetation, soil cohesion, amount of protection, lateral migration tendencies of the stream, etc.

Sediments are broadly classified as cohesive and noncohesive. With cohesive sediment the resistance to erosion depends on the strength of the cohesive bond binding the particles. Cohesion may far outweigh the influences of the physical characteristics of the individual particles. However, once erosion has taken place, cohesive material may become noncohesive with respect to transport.

Of the various sediment properties, size has the greatest significance to the hydraulic engineer, not only because size is important and the most readily measured property, but also because other properties, such as shape and specific gravity, tend to vary with particle size. In fact, size has been found to sufficiently describe the sediment particle for many practical purposes.

Size may be measured by calipers, optical methods, photographic methods, sieving, or sedimentation methods. The size of an individual particle is not of primary importance in stream mechanics or sedimentation studies, but the size distribution of the sediment that forms the bed and banks of a stream or reservoir is of great importance.

Application - The most commonly used method to determine size frequency is a volumetric sample that is laboratory-analyzed by mechanical or sieve analysis, supplemented by analysis with a hydrometer, pipette or bottom withdrawal (BW) tube when significant fine sediments are present. The VA tube technique is also utilized, particularly for samples that consist primarily of sands. Table 5.2 provides guidelines for application of the different techniques for particle size analysis. Detailed discussion of specific laboratory procedures is provided in several governmental publications (i.e., COE, 1970; USGS, 1969; ARS, 1979). In general, the results are presented as cumulative size-frequency curves. The fraction or percentage by weight of a sediment that is smaller or larger than a given size is plotted against particle size. A useful parameter describing the shape of a gradation curve is the gradation coefficient:

$$G = \frac{1}{2}\left(\frac{D_{84.1}}{D_{50}} + \frac{D_{50}}{D_{15.9}}\right) \qquad (5.4)$$

where $D_{84.1}$, $D_{50}$ and $D_{15.9}$ are based on a percent finer (by dry weight) analysis. This equation is only applicable to S-shaped, particle size-distribution curves.

The size of the bed or bank material sample required for sieve analysis will depend on the maximum particle size in the sample and the requirement that the sample be representative of the material to be tested. Within the constraints of obtaining a representative sample, bed and bank material samples should be limited in weight to facilitate handling. Corps of Engineers guidelines for obtaining a minimum weight sample for sieve analysis are presented in Table 5.3. As Table 5.3 indicates, for bed and bank materials that have maximum particle sizes in the coarse gravel to cobble range, the sample size required to ensure accurate representation becomes fairly weighty (i.e., 13 pounds for 3-inch maximum particle sizes). For a sample collection program that entails gathering numerous bed and bank material samples, the collective sample weights can become burdensome.

Another consideration pertaining to bed material sample collection on gravel-or cobble-bed streams is the potential existence of a two-layer system consisting of (1) a thin surface layer of coarser materials created by hydraulic sorting, and (2) undisturbed subsurface material. Samples containing materials from both layers would contain materials from two popula-

Table 5.2. Recommended Size Range, Analysis Concentration, and Quantity of Sediment for Commonly Used Methods of Particle Size Analysis (after ARS, 1979).

| Method of Particle Size Analysis | Analysis Recommended for Particles in This Size Range | Quantity of Sediment Required for Analysis | Desirable Range in Analysis Concentration |
|---|---|---|---|
| | mm | g | Mg/l |
| Sieves | 0.062 - 32 | see Table 5.3 | ----- |
| VA tube | 0.062 - 2.0 | 0.05 - 15.0 | ----- |
| Pipette | 0.002 - 0.062 | 1.0 - 5.0 | 2,000 - 5,000 |
| BW tube[1] | 0.002 - 0.062 | 0.5 - 1.8 | 1,000 - 3,500 |
| Hydrometer[2] | 0.002 - 0.062 | 20 - 200 | 25,000 - 50,000 |

[1]If necessary, may be expanded to include sands up to 0.35 mm, the accuracy decreasing with increasing size--the concentration and size increased accordingly

[2]Quantity depends on size of settling container--a 1,000 ml cylinder has about the minimum diameter for most hydrometers

Table 5.3. Minimum Recommended Sample Weights for Sieve Analysis (COE, 1970).

| Maximum Particle Size | Minimum Weight of Sample | |
|---|---|---|
| | g | lb |
| 3-in. | 6,000 | 13 |
| 2-in. | 4,000 | 9 |
| 1-in. | 2,000 | 4 |
| 1/2-in. | 1,000 | 2 |
| Finer than No. 4 sieve | 200 | 0.5 |
| Finer than No. 10 sieve | 100 | 0.25 |

tions in unknown proportions. Alternatively, the thin surface layer could be removed and subsurface materials sampled by normal volumetric methods. The importance of sampling surface and/or subsurface materials in a gravel-cobble bed system is dependent largely on the objectives of the study. If study objectives focus on hydraulic friction or initiation of bed movement, then the surface layer is of interest. Conversely, for analysis of bed-material transport, sampling efforts should focus on the underlying bed materials. Quite often it may be appropriate to consider both bed layers in a sample collection program, since the disruption of an armor layer during a flood and subsequent transport of underlying bed material may be of interest.

Kellerhalls and Bray (1971) note that standard volumetric sampling methods are not appropriate for evaluating material composition of thin surface layers in river beds composed of coarse fluvial sediments. Weight limitations presented in Table 5.3 also discourage use of volumetric methods to sample coarse bed and bank material. Kellerhalls and Bray discuss the advantages and disadvantages of various methodologies for sampling coarse fluvial sediments. In addition to volulmetric sampling, other methodologies are (1) grid sampling, (2) areal sampling, and (3) transect sampling. A principal concern with use of alternative methods is the equivalence of results to standard sieve-by-weight results so that all material compositions will be referenced to a common datum. Kellerhalls and Bray present a discussion of the various bed-material sampling methodologies and the weighting factors for conversion of sampling procedures to standard sieve-by-weight methods.

A sampling and analysis procedure not considered by Kellerhalls and Bray is the area-by-area approach. Following the methodology presented by Kellerhalls and Bray, it can be shown that this approach is equivalent to standard sieve-by-weight procedures. A common way of utilizing this approach entails superposing a 2' x 2' grid subdivided into 0.1' x 0.1' squares over a randomly selected area. In this application the grid is not used to identify discrete sampling points, as in standard grid sampling procedures, but rather to provide a convenient method of determining particle surface area. A slide photograph of the grid is taken with a 35 mm camera from above (vertical to the grid). A sample identification number or location can be included in the photograph by placing a placard at one edge of the grid.

Particle size analysis of the sample defined by the grid is accomplished by projecting developed slides onto a screen and determining the area (as a

percentage of total area) occupied by particles in specific size ranges. Since the grid is broken into 0.1-foot-square blocks, it is not possible to accurately differentiate particle sizes less than about 0.05 foot in diameter using this method.

Constructing a grid is relatively simple and consists of no more than some type of framework (aluminum angle, plastic pipe, etc.) with a grid pattern made of nylon twine. Grids can also be fabricated from flexible, clean plastic sheets with the grid pattern inked on; however, some grid squares may be distorted in photographs due to flexibility of the plastic. Another option, especially helpful when a grid is not immediately available, or perhaps not practical, involves taking a picture of the area of interest with a ruler placed in the center. Using this method, the photographic image can be projected onto a grid and the image size adjusted by moving the projector.

Important factors to consider in determining where and how many bed and bank material samples to collect include (1) size and complexity of the study area, (2) number, lengths and drainage areas of tributaries, (3) evidence of or potential for armoring, (4) structural features that can impact or be significantly impacted by sediment transport, (5) bank failure areas, (6) high bank areas, and (7) areas exhibiting significant sediment movement or deposition (i.e., bars in channels). For a large-scale study (i.e., five or more river miles) it is recommended as a minimum that sampling be conducted once every mile. At each sampling location a bed, bank and flood-plain sample would typically be taken. Occasional sampling at more frequent intervals may be required to characterize unique situations. It is especially important to adequately address tributary sediment characteristics, since a single major tributary and tributary source area could be the prominent supplier of sediment to a system. Samples might typically be taken 500 feet above and below the tributary on the main channel and at some location near the mouth of the tributary to completely characterize conditions.

The depth of bed material sampling depends on the homogeneity of surface and subsurface materials. When possible, it is desirable to dig down some distance to establish bed-material characteristics. If stratification of bed material is found, it is important to sample the material and note the depth at which it occurred. In homogeneous bed material, samples are typically taken near the surface, i.e., in the upper 12 inches of sand. Bank samples may be taken anywhere, if bank composition is homogeneous. For stratified banks, several samples may be required.

For purposes of Level II erosion and sedimentation analysis, it is usually desirable to define a single representative bed-material size distribution that can be utilized in evaluating sediment transport. For a more complex system, such as a system where an appreciable change in bed-material characteristics occurs, it may be necessary to use different representative gradation curves for different channel reaches. The criteria for selection of a bed-material gradation is that it adequately represents the range and distribution of bed material in the majority of the study area and should provide somewhat conservative estimates of sediment transport capacity.

Example - During a site reconnaissance 50 sediment samples were collected consisting of 16 bed samples (taken at depths of 0 to 12 inches), 12 bank samples, 6 tributary samples, 13 watershed samples and 3 flood-plain samples. Laboratory evaluation of these samples consisted of dry sieve analysis supplemented with hydrometer analysis where appreciable silt-clay percentages were encountered. Particle gradation curves were developed for the samples based on this analysis and plotted by reach.

Considering bed particle size gradation curves representative of sediment characteristics in the surface layer, a noticeable shift towards finer material occurred downstream of a small drainage entering from the right bank. A sample of alluvial fan material deposited by the small drainage documented this channel as the source of the fine material. Figure 5.11a illustrates particle size gradation curves of four samples collected upstream of the tributary, while Figure 5.11b depicts the representative gradation curve for this reach, as determined by overlaying and eye fitting (the representative curve could also be determined mathematically).

### 5.3.3 Profile Analysis

Discussion - Comparison of thalweg profiles over time can provide valuable insight to and understanding of aggradation/degradation patterns in a channel. This information is useful both by itself and as verification of mathematical modeling results. The amount and quality of information derived from this analysis is largely dependent on the number of years of data and the total record length. Changes in profile generally occur over many years; furthermore, in arid and semiarid regions these changes are hydrologically

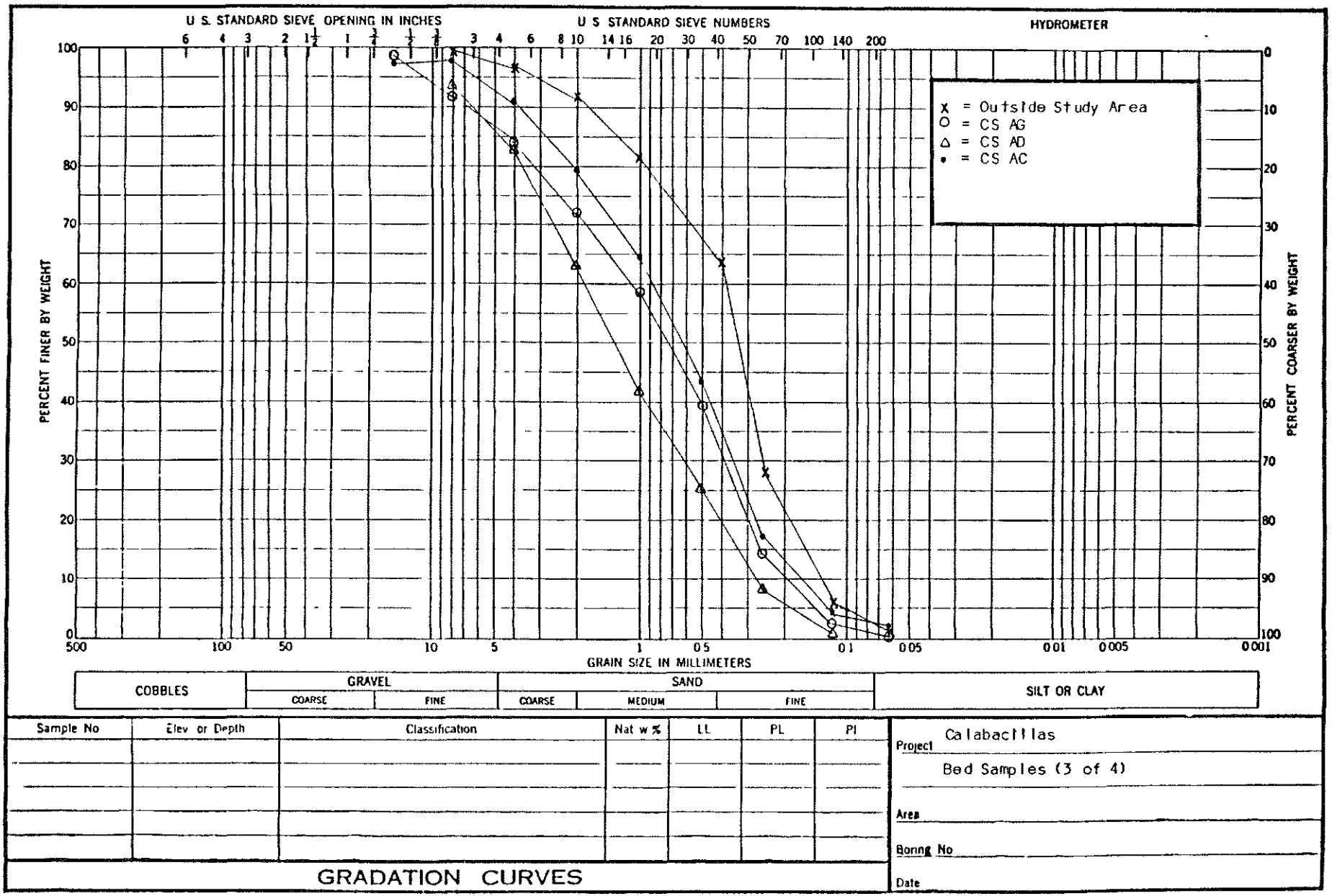


| Sample No | Elev or Depth | Classification | Nat w % | LL | PL | PI |
|---|---|---|---|---|---|---|
| | | | | | | |

GRADATION CURVES

Project: Calabacillas
Bed Samples (3 of 4)
Area
Boring No
Date

Figure 5.11a. Selected particle size gradations.

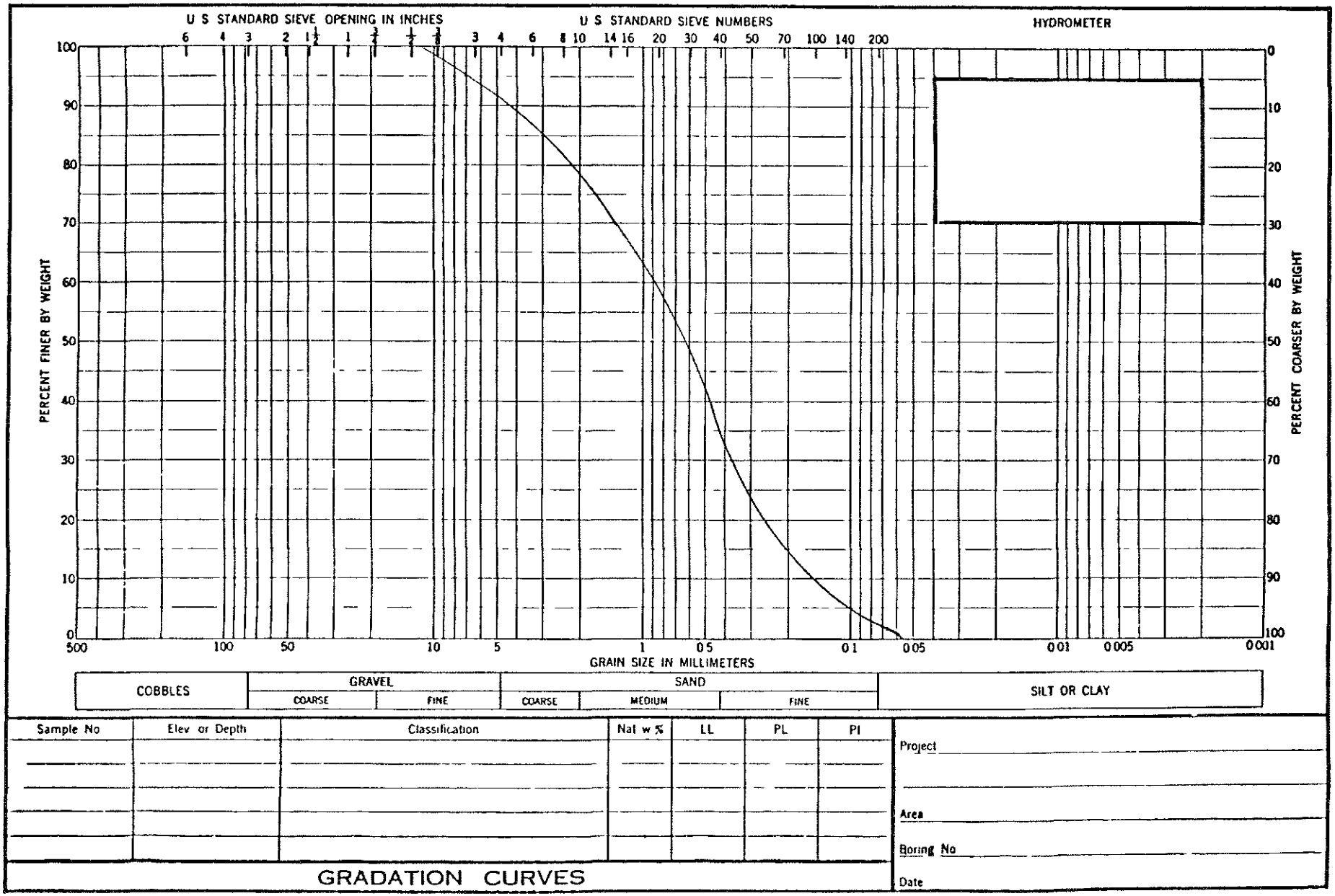


Figure 5.11b. Representative gradation curve.

dependent. If there have been no significant floods in the period of record, then little change would be expected in the channel profile.

Application - Channel profile data can be developed from a variety of sources. Topographic mapping, for example, USGS 7.5-minute quadrangle sheets, is a readily available source, particularly for analyses involving a relatively long study reach (for short study reaches, the scale and contour interval of a 7.5-minute map may not provide sufficiently accurate information). Other sources of topographic mapping include county and city agencies and private parties who prepare mapping for development purposes, as well as for flood-plain mapping. Similarly, HEC-2 input data prepared for flood insurance studies can be a valuable source of data.

Less detailed data, both temporally and spatially, are often available from elevation data of pipeline crossings, railroad and highway bridges, diversion structures, and grade-control structures. With knowledge of the elevations of these structures, it is relatively simple to make field measurements of present bed elevations. Additionally, when available, the construction plans for these structures can provide valuable historical insight. The invert elevations at the time of construction are usually provided on the plans or can be deduced from the given information.

Finally, a field survey of the thalweg is valuable when time and/or budget constraints permit this level of effort. Surveying just the thalweg profile is relatively quick, compared to cross-section surveying, and is a good way to see the study reach in detail.

Example - During a relatively small flood (2-year flood) a bridge failure occurred, causing loss of life. Litigation resulted, and in support of the defense, a comprehensive engineering investigation of the failure was conducted. A profile analysis was part of the investigation and provided a substantial amount of information. Extensive data of the channel profile were first published in a Soil Conservation Service (SCS) flood-plain information report, based on a 1967 survey. Cross-section data collected by the Corps of Engineers (COE) were used to establish a 1972 profile. A previous analysis by an engineering firm provided a 1976 profile, based primarily on soundings from bridges. A COE General Design Memorandum (GDM) provided a 1978 profile. An additional data point for 1958 was derived from county bridge construction plans. The recorded top of pile elevation, pile length of 40 feet, and

reported pile penetration of 23 feet into the existing creek bed placed the elevation of the bed at approximately 246 feet NGVD. While similar "as-built" data on other bridges in the study reach would have extended the profile for 1958, such data could not be obtained.

When the data for all these years were plotted, they provided a time-sequenced picture of profile changes. The comparison of these profiles established a strong system-wide degradation trend in the study reach. Combined with results from qualitative analysis, it was determined that the degradational trend had resulted from land-use changes (urbanization) that produced higher runoff volumes, and from extensive channelization beginning in the 1930's to straighten the system. From these and other results, it was concluded that the bridge failure at this location was imminent and could have occurred during any reasonable flow condition. Inspection of other bridges in the study reach by county maintenance crews led to extensive revetment and grade stabilization structures at all bridge crossings.

### 5.3.4 Incipient Motion Analysis

Discussion - An evaluation of relative channel stability can be made by evaluating incipient motion parameters. The definition of incipient motion is based on the critical or threshold condition where hydrodynamic forces acting on a grain of sediment have reached a value that, if increased even slightly, will move the grain. Under critical conditions, or at the point of incipient motion, the hydrodynamic forces acting on the grain are just balanced by the resisting forces of the particle. For given hydrodynamic forces, or equivalently for a given discharge, incipient motion conditions will exist for a single particle size. Particles smaller than this will be transported downstream and particles equal to or larger than this will remain in place.

Application - The Shields diagram (Figure 5.12) may be used to evaluate the particle size at incipient motion for a given discharge. The Shields diagram was developed through measurements of bed-load transport for various values of $\tau/(\gamma_s-\gamma)D$ at least twice as large as the critical value, and then extrapolated to the point of vanishing bed load. In the turbulent range, where most flows of practical engineering interest occur, Figure 5.12 suggests the parameter $\tau/(\gamma_s-\gamma)D$ is independent of flow conditions and the following relationship is established:

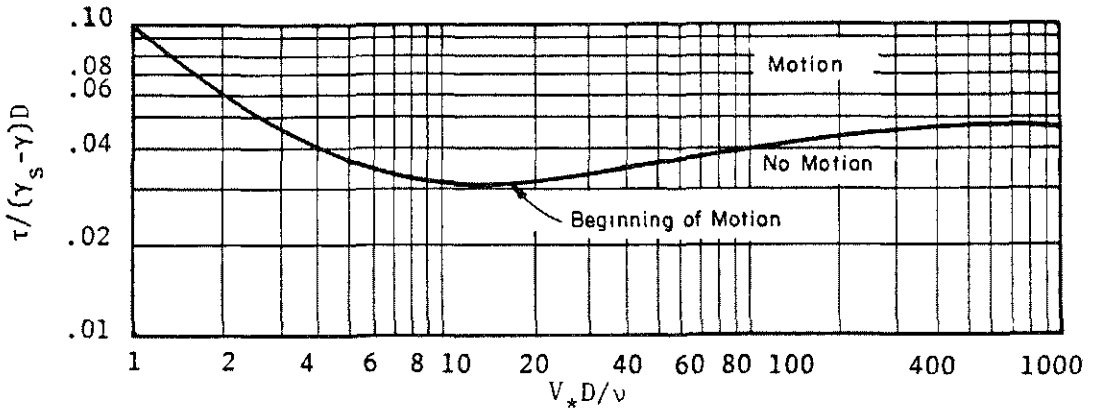


Figure 5.12. Shields' relation for beginning of motion (adapted from Gessler, 1971).

$$D_c = \frac{\tau}{0.047\,(\gamma_s - \gamma)} \tag{5.5}$$

where $D_c$ is the diameter of the sediment particle for conditions of incipient motion, $\tau$ is boundary shear stress, $\gamma_s$ and $\gamma$ are the specific weights of sediment and water, respectively, and 0.047 is a dimensionless coefficient referred to as the Shields parameter. [As originally proposed by Shields (1936), 0.060 was the parameter value in the turbulent range. The value of 0.047 was suggested by Meyer-Peter and Muller (1948), and further supported by Gessler (1971).] Any consistent set of units may be used with this equation.

The concept of incipient motion is of fundamental importance to sediment transport. Additionally, direct application of incipient motion concepts through Equation 5.5 are used in armor analysis and can provide useful insight for other Level II analyses. For example, given a discharge, hydraulic calculations can be used to determine information necessary to evaluate the boundary shear stress (Equation 4.7a or b) at various locations in a study reach. Using either computed or assumed standard values for water and sediment specific weights, the incipient motion particle size can then be evaluated for this discharge. This calculation may be repeated for other discharges characteristic of a given flood to determine what particle sizes would be in motion at various times during the flood. Results from this evaluation of incipient motion also indicate the total time during which various particle sizes would be in motion, as well as the percentage of time, relative to the total storm duration, that incipient motion conditions would be equaled or exceeded for each particle size.

Long-term incipient motion characteristics can be assessed in a similar fashion based on the annual hydrograph (i.e., annual record of mean daily or mean monthly discharge), instead of a single flood hydrograph. Such assessments are semi-quantitative since it must be assumed that the hydraulic properties at a point of interest have not changed appreciably over the long term. Additionally, results of any incipient motion analysis are generally more useful for analysis of gravel- or cobble-bed systems than for sand-bed systems. When applied to a sand-bed system, incipient motion results usually indicate that all particles in the bed material are capable of being moved (exceeding incipient motion conditions) for even very small discharges.

Example - Using results of a multiple-profile HEC-2 analysis, the hydraulic properties of an arroyo were known for a series of discharges characteristic of a 1980 flood. For each discharge the boundary shear stress was computed from Equation 4.7b and the incipient motion particle size from Equation 5.5. Results of this calculation are summarized on Figure 5.13.

Table 5.4 indicates the total time during which the various particle sizes of Figure 5.13 would be in motion. Also indicated in Table 5.4 is the percentage of time, relative to the total storm duration, that incipient motion conditions would be equaled or exceeded for each of these sizes. This type of information is useful in developing a Level II understanding of sediment transport characteristics, particularly in establishing the duration of significant transport during a flood.

### 5.3.5 Armoring Potential

Discussion - The armoring process begins as the non-moving coarser particles segregate from the finer material in transport. The coarser particles are gradually worked down into the bed, where they accumulate in a sublayer. Fine bed material is leached up through this coarse sublayer to augment the material in transport. As movement continues and degradation progresses, an increasing number of non-moving particles accumulate in the sublayer. This accumulation interferes with the leaching of fine material so that the rate of transport over the sublayer is not maintained at its former intensity. Eventually, enough coarse particles accumulate to shield, or "armor," the entire bed surface (Figure 5.14). When fines can no longer be leached from the underlying bed, degradation is arrested.

Examination of typical armor layers reveals several important characteristics:

- Less than a single complete covering layer of larger gravel particles seems to suffice for a total armoring effect for a particular discharge.

- A natural "filter" apparently develops between the larger surface particles and the subsurface material to prevent leaching of the underlying fines.

- The shingled arrangement of surface particles is not restricted to the larger material, but seems evident throughout the gravel gradation.

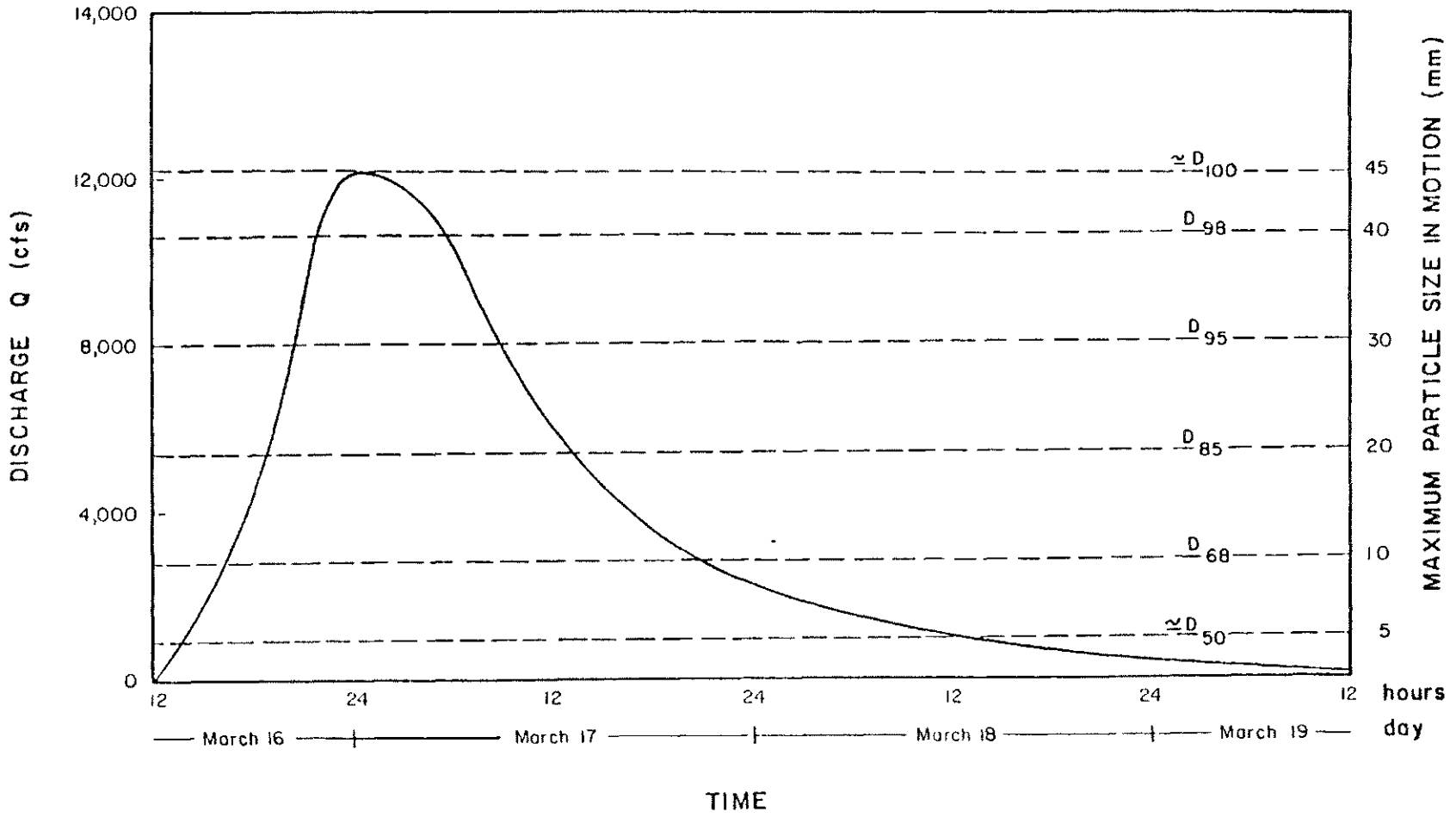


Figure 5.13. Frequency of motion for various particle sizes.

Table 5.4. Incipient Motion Characteristics.

| Particle Size (mm) | Time in Motion (hrs) | Percentage of Total Storm Duration in Motion |
|---|---|---|
| 5 | 56 | 78 |
| 10 | 34 | 47 |
| 20 | 22 | 30 |
| 30 | 15 | 20 |
| 40 | 9 | 13 |

Armored bed of Salt River upstream of Gilbert Road near Mesa, Arizona

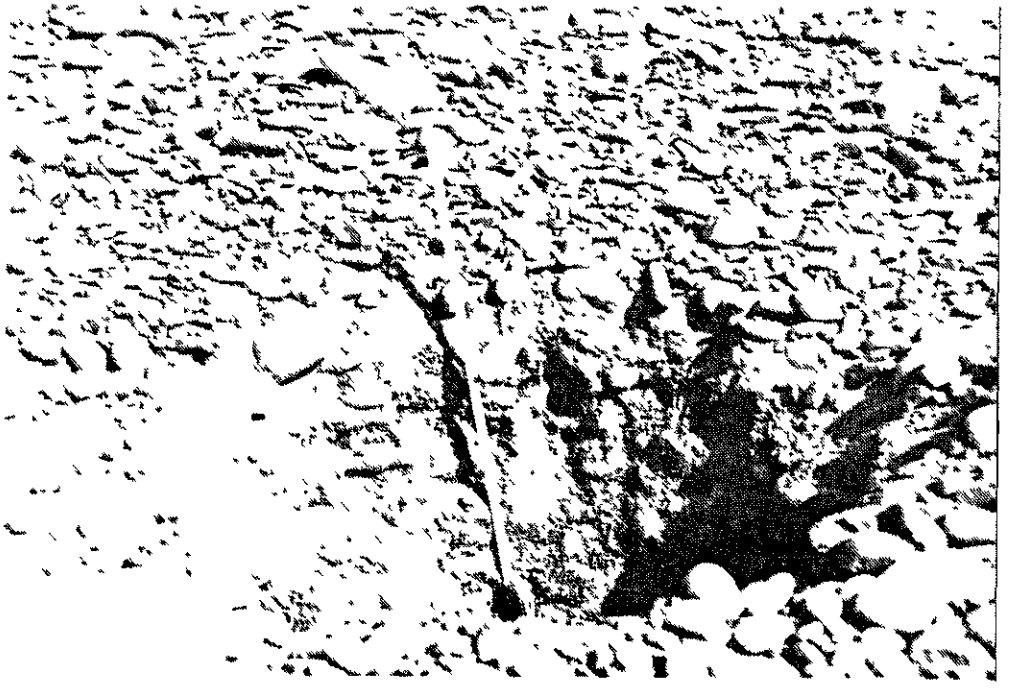

Excavation through armor layer of the Salt River near Mesa, Arizona. Tape length shown in photograph is 24 inches.

Figure 5.14

An armor layer sufficient to protect the bed against moderate discharges can be disrupted during high flow, but may be restored as flows diminish. However, in a cobble-bed system the armoring condition is usually stable enough that the channel bed can be considered rigid, i.e., bed form conditions will not develop (see Figure 4.2). It is evident that an armor layer will tend to accumulate in areas of natural scour in the river, such as on the upstream ends of islands and bars. However, caution should be used in eliminating scour protection along the toe of levee or channel embankments under the assumption that an armor layer will be created uniformly along the toe. If a uniform armor layer is not present, or if one fails to develop at a predicted depth during a design flow, the levee toe could be undermined by scouring action, thus leading to failure.

Application - Potential for development of an armor layer can be assessed using Shields' criteria for incipient motion (see Section 5.3.4) and a representative bed-material composition. In this case a representative bed-material composition is that which is typical of the depth of anticipated degradation. Using Equation 5.5 the incipient-motion particle size can be computed for a given set of hydraulic conditions. If no sediment of the computed size or larger is present in significant quantities in the bed, armoring will not occur. The $D_{90}$ to $D_{95}$ size of the representative bed material is frequently found to be the size "paving the channels" when scouring is arrested. Within practical limits of planning and design, the $D_{95}$ size is considered to be about the maximum size for pavement formation (SCS, 1977). Therefore, armoring is probable when the particle size computed from Equation 5.5 is equal to or smaller than the $D_{95}$ size.

By observing the percentage of the bed material equal to or larger than the armor particle size $(D_a)$ the depth of scour necessary to establish an armor layer $(\Delta Z_a)$ can be calculated from (USBR, 1984):

$$\Delta Z_a = y_a \left(\frac{1}{P_c} - 1\right) \tag{5.6}$$

where $y_a$ is the thickness of the armoring layer and $P_c$ is the decimal fraction of material coarser than the armoring size. The thickness of the armoring layer $(y_a)$ ranges from one to three times the armor particle size $(D_a)$, depending on the value of $D_a$. Field observations suggest that a rela-

tively stable armoring condition requires a minimum of two layers of armoring particles.

Example - As an example, consider the case where Equation 5.5 indicates that the critical particle size equals 1.5 inches and a representative bed-material gradation curve shows that this is the $D_{90}$ size. Thus, the depth to formation of an armor layer would equal

$$\Delta Z_a = y_a \left(\frac{1}{P_c} - 1\right) = 2\ (1.5)\ \left(\frac{1}{0.1} - 1\right) = 27 \text{ inches}$$

It should be recognized that development of an armor layer does not occur uniformly across a channel bed, but rather tends to begin along the thalweg and at other points of natural scour in the channel.

### 5.3.6 Sediment Transport Capacity

Discussion - Sediment transport equations are used to determine the sediment transport capacity for a specific set of flow conditions. Knowledge of sediment transport capacity is required for many fluvial systems analyses, including evaluation of aggradation/degradation, general scour/deposition, and lateral migration. The first step in evaluating sediment transport capacity is to select one or more of the available equations for use in solving the given problem. Selection of an appropriate sediment transport relation is predicated on an understanding of the system being studied. For example, some formulas were developed from data collected in sand-bed streams where most of the sediment was transported as suspended load. Conversely, other equations pertain to conditions where bed-load transport is dominant. Study objectives also determine what portion of the sediment transport needs to be estimated and the level of accuracy required in such an estimate. If it is desirable to know the relative contributions of bed load and suspended load to the bed-material discharge, then formulas for each are available. Other formulas provide direct determination of bed-material discharge. A common feature of bed-material discharge sediment transport equations is that wash load is not included; however, there are methodologies that incorporate sediment sampling data, such as the modified Einstein procedure, that can be used to estimate total sediment transport rate (including wash load).

Available sediment transport equations range from theoretical or empirical methods to methods that require measured suspended sediment loads

and/or other normal stream flow measurements. Table 5.5 summarizes some of the most commonly used sediment transport relations and their applications. As a result of the complexity of the Einstein bed load and suspended load methodologies, they will not be presented; however, it is important to note that the power relationships presented in this section were developed from a joint application of the MPM bed load and the Einstein suspended load equations. Similarly, the modified Einstein procedure, presented by Colby and Hembree (1955), will not be presented; however, the application of this procedure should be considered for evaluation of total sediment load when measured water and suspended sediment discharge data are available.

In using any sediment transport methodology, consideration should be given to solution by size fraction. Different transport capacities can be expected for different sediment sizes and some loss in accuracy may result from a calculation based on a single representative grain size (i.e., $D_{50}$ size). Solution of the total bed-material discharge by size fraction analysis is based on a weighted average of the sediment transport for the geometric mean particle size representing various intervals of the sediment gradation curve. The number of intervals required depends on the accuracy desired and the characteristics of the gradation curve; however, adequate results are usually obtained using four to six intervals. As a final note, with any methodology it is desirable to verify results against measured data whenever possible and adjust equation parameters accordingly to obtain suitable results.

Application - Meyer-Peter, Muller Equation. Based on experiments with sand particles of uniform sizes, sand particles of mixed sizes, natural gravel, lignite, and baryta, Meyer-Peter and Muller (1948) developed a formula for estimating total bed-load transport. Most of the data used in developing the Meyer-Peter, Muller (MPM) equation were obtained in flows with little or no suspended sediment load. A common form of the MPM equation derived for a wide channel with plane-bed conditions is:

$$q_b = \frac{12.85}{\sqrt{\rho}\ \gamma_s} (\tau_o - \tau_c)^{1.5} \qquad (5.7a)$$

Table 5.5. Sediment Transport Calculation Procedures.

| Procedure | Calculation | | | | Application | |
|---|---|---|---|---|---|---|
| | Bed Load | Suspended Bed-Material Load | Bed-Material Load | Total[1/] Sediment Load | Sand Bed | Cobble Bed |
| Meyer-Peter, Muller Equation (MPM) | X | | | | X[2/] | X |
| Einstein Bed Load Equation | X | | | | X | X |
| Einstein Suspended Load Methodology | | X | | | X | X |
| Power Relationships | | | X | | X | |
| Colby Methodology | | | X | | X | |
| Modified Einstein | | | | X | X | X |

[1/] Includes wash load

[2/] Must be supplemented with Einstein suspended load methodology to get suspended bed-material load component

where $q_b$ is the bed-load transport rate in cubic feet per second (cfs) per unit width for a specific size of sediment, $\tau_o$ is the tractive force (boundary shear stress), $\tau_c$ is the critical tractive force, $\rho$ is the density of water and $\gamma_s$ is the specific weight of dry sediment. The critical tractive force is defined by the Shields parameter (see Section 5.3.4). The tractive force or boundary shear stress acting under the given flow conditions is most often defined by Equation 4.7b. The use of Equation 5.7a is not recommended if dunes or antidunes are expected due to the plane bed assumption in its derivation. Other more complex forms of the equation are available for use under these circumstances (see USBR, 1960). Any application of the MPM relationships provides an estimate of bed-load transport only and should be supplemented by other methods if appreciable suspended bed-material transport is suspected.

A general form of the MPM equation was presented by Shen (1971) as

$$q_b = a_4 \, (\tau_o - \tau_c)^{b_4} \tag{5.7b}$$

in which $a_4$ and $b_4$ are constants. When the constants in this equation are calibrated with field data, good results are usually obtained.

A complete discussion of Meyer-Peter's formulas for beginning of motion and sediment transport is provided by Meyer-Peter and Muller (1948).

Empirical Power Relationships. Using a computer-generated solution of the Meyer-Peter, Muller bed-load transport equation combined with Einstein's integration of the suspended bed-material discharge, a procedure has been developed for estimating total bed-material discharge in sand-bed channels from power relationships of the form (Simons, Li and Fullerton, 1981)

$$q_s = a \; Y_h^b \; V^c \tag{5.8a}$$

where $q_s$ is the bed-material discharge in cfs per unit width, $Y_h$ is hydraulic depth, $V$ is the average velocity and $a$, $b$, and $c$ are regression coefficients. Using a computer-generated data base, representative values for coefficients $a$, $b$, and $c$ were determined for various sediment sizes, gradations and bed slopes. Results of this analysis are presented in Tables 5.6a and 5.6b. For evaluation of transport capacity at a sediment size or gradient coefficient not tabulated, interpolation between $q_s$ values for

sediment sizes and gradation coefficients bracketing the given size is required. The curves resulting from a plot of $D_{50}$ or G versus a, b, or c are not linear relationships. Therefore, prior to attempting a linear mathematical interpolation between these coefficients and exponents, the user may want to plot $D_{50}$ or G versus the tabulated values for a, b, and c and use the resulting curves for a visual interpolation of these values.

As Table 5.6 indicates, sediment transport rates are highly dependent on velocity, and to a lesser degree on depth. Sediment transport for some sediment sizes is directly proportional to depth, whereas transport of other sizes is inversely proportional to depth. Transport of smaller sediment sizes is generally proportionally dependent on depth since the smaller material is more easily suspended and the resulting sediment concentrations are more uniform. Thus, the larger the depth, the greater the amount of sediment that will be suspended for a given velocity. Larger sediment particles, on the other hand, are more difficult to suspend and keep in suspension. For a given velocity, as depth increases the intensity of turbulent transfer properties for these larger sizes decreases. The increase in area available for suspended sediment associated with the increased depth does not totally counterbalance the reduced turbulent transfer characteristics, resulting in an inverse relationship between transport and depth for larger particles. Sediment sizes exhibiting little dependence on depth fall between these extremes.

As an alternative to Equation 5.8a and Tables 5.6a and 5.6b, a single relationship was later developed (Zeller and Fullerton, 1983):

$$q_s = 0.0064 \frac{n^{1.77} V^{4.32} G^{0.45}}{Y_h^{0.30} D_{50}^{0.61}} \qquad (5.8b)$$

where n is Manning's roughness coefficient (based on bed forms and grain size roughness), V is the mean velocity, G is the gradation coefficient, $Y_h$ is the hydraulic depth, and $D_{50}$ is the median diameter. In this equation all units are in the ft-lb-sec system, except $D_{50}$, which is in millimeters.

Table 5.7 lists the range of parameters considered in the development of the sediment transport relations given in Tables 5.6a and 5.6b and in development of Equation 5.8b. The applicability of either methodology to any specific set of conditions should be checked in Table 5.7. It should be noted

Table 5.6a. Results of Regression Analysis.

($0.001 \leq S_o \leq 0.01$; $q_s = a\ Y_h^b\ V^c$)

| $D_{50}$ = | 0.1 mm | 0.25 mm | 0.5 mm | 1.0 mm | 2.0 mm | 3.0 mm | 4.0 mm | 5.0 mm |
|---|---|---|---|---|---|---|---|---|
| | | | | G = 1.0 | | | | |
| a | $2.90\times10^{-4}$ | $1.81\times10^{-5}$ | $3.19\times10^{-6}$ | $2.06\times10^{-6}$ | $3.45\times10^{-6}$ | $5.05\times10^{-6}$ | $6.15\times10^{-6}$ | $6.35\times10^{-6}$ |
| b | 0.505 | 0.0446 | -0.363 | -0.628 | -0.693 | -0.672 | -0.652 | -0.639 |
| c | 3.43 | 4.43 | 5.01 | 5.03 | 4.60 | 4.30 | 4.13 | 4.06 |
| | | | | G = 2.0 | | | | |
| a | | $6.80\times10^{-5}$ | $1.48\times10^{-5}$ | $3.54\times10^{-6}$ | $2.46\times10^{-6}$ | $2.81\times10^{-6}$ | $3.14\times10^{-6}$ | |
| b | | 0.315 | 0.0501 | -0.324 | -0.587 | -0.649 | -0.644 | |
| c | | 3.83 | 4.31 | 4.78 | 4.79 | 4.62 | 4.49 | |
| | | | | G = 3.0 | | | | |
| a | | | $5.25\times10^{-5}$ | $1.61\times10^{-5}$ | $3.71\times10^{-6}$ | | | |
| b | | | 0.317 | 0.112 | -0.260 | | | |
| c | | | 3.76 | 4.11 | 4.61 | | | |
| | | | | G = 4.0 | | | | |
| a | | | | $4.31\times10^{-5}$ | | | | |
| b | | | | 0.324 | | | | |
| c | | | | 3.70 | | | | |

$S_o$ = bed slope

$q_s$ = sediment transport rate in cfs (unbulked)

$Y_h$ = hydraulic depth in feet (area/top width)

V = average velocity in fps

G = gradation coefficient

Table 5.6b. Results of Regression Analysis.

($0.01 < S_o \leq 0.04$; $q_s = a\ Y_h^b\ V^c$)

| $D_{50}$ = | 0.1 mm | 0.25 mm | 0.5 mm | 1.0 mm | 2.0 mm | 3.0 mm | 4.0 mm | 5.0 mm |
|---|---|---|---|---|---|---|---|---|
| | | | | G = 1.0 | | | | |
| a | $4.74\times10^{-4}$ | $7.45\times10^{-5}$ | $1.66\times10^{-5}$ | $5.80\times10^{-6}$ | $3.58\times10^{-6}$ | $3.62\times10^{-6}$ | $4.03\times10^{-6}$ | $4.50\times10^{-6}$ |
| b | 0.557 | 0.305 | 0.0530 | -0.198 | -0.427 | -0.532 | -0.587 | -0.615 |
| c | 3.22 | 3.76 | 4.17 | 4.42 | 4.45 | 4.37 | 4.27 | 4.18 |
| | | | | G = 2.0 | | | | |
| a | | $1.27\times10^{-4}$ | $3.81\times10^{-5}$ | $1.16\times10^{-5}$ | $5.25\times10^{-6}$ | $4.20\times10^{-6}$ | $3.89\times10^{-6}$ | |
| b | | 0.383 | 0.199 | -0.0318 | -0.264 | -0.385 | -0.459 | |
| c | | 3.56 | 3.88 | 4.18 | 4.33 | 4.34 | 4.31 | |
| | | | | G = 3.0 | | | | |
| a | | | $7.40\times10^{-5}$ | $3.02\times10^{-5}$ | $1.08\times10^{-5}$ | | | |
| b | | | 0.310 | 0.161 | -0.0502 | | | |
| c | | | 3.65 | 3.86 | 4.10 | | | |
| | | | | G = 4.0 | | | | |
| a | | | | $5.30\times10^{-5}$ | | | | |
| b | | | | 0.264 | | | | |
| c | | | | 3.67 | | | | |

$S_o$ = bed slope

$q_s$ = sediment transport rate in cfs (unbulked)

$Y_h$ = hydraulic depth in feet (area/top width)

V = average velocity in fps

G = gradation coefficient

Table 5.7. Range of Parameters Examined for Power Relationships.

| Parameter | Value Range: Equation 5.8a when used with Tables 5.6a and 5.6b | Value Range: Equation 5.8b |
|---|---|---|
| Froude No. | <4 | unlimited |
| Velocity | 5-26 (ft/sec) | 3-30 (ft/sec) |
| Manning's n | 0.025 | 0.018-0.035 |
| Bed Slope | 0.001-0.040 (ft/ft) | 0.001-0.040 (ft/ft) |
| Unit Discharge | 5-200 (cfs/ft) | 10-200 (cfs/ft) |
| Particle Size | $D_5 \geq 0.062$ mm<br>$D_{90} \leq 15$ mm | $0.5 \text{ mm} \leq D_{50} \leq 10$ mm |
| Depth | Unlimited | 1-20 ft |
| Gradation Coefficient | 1-4 | 2-5 |

that these equations are based on the assumption that all sediment sizes present in the bed are transportable by the flow. If armoring is a possibility (see Section 5.3.5), the regression relations are not valid. Since the equations were developed for sand-bed channels, they do not apply to conditions where the bank material has cohesive properties. Transport rates would be overpredicted for a cohesive channel condition. For conditions meeting the criteria of Table 5.7, as well as other criteria mentioned, either equation should provide results within ten percent of the theoretical values computed with the Meyer-Peter, Muller bed load and Einstein suspended bed-material load methodologies that were used to develop the regression equations.

Colby's Approach. Colby (1964) developed the graphical procedure shown in Figures 5.15 and 5.16 for determining bed-material discharge (tons/day of dry sediment) in sand-bed channels. In developing his computational curves Colby was guided by Einstein's bed-load function (Einstein, 1950) and an immense amount of data from streams and flumes (Simons and Richardson, 1966). However, it should be understood that all curves for the 100-foot depth, most curves of the ten-foot depth, and some of the curves of 1.0-foot and 0.1-foot depths (Figure 5.15) are not based entirely on data but are developed from limited data and theory.

In utilizing Figures 5.15 and 5.16 to compute the bed-material discharge, the following procedure is required: (1) the required data are mean velocity $V$, depth (typically hydraulic depth), $Y_h$, median size of bed material $D_{50}$, water temperature, and fine-sediment concentration; (2) then the uncorrected sediment discharge $q_{s_i}$ for the given $V$, $Y_h$ and $D_{50}$ can be found from Figure 5.15 for the two depths that bracket the desired depth. A logarithmic scale of depth versus $q_{s_i}$ is used to interpolate in order to determine the bed-material discharge per unit width for the actual $Y_h$, $V$ and $D_{50}$; (3) two correction factors, $k_1$ and $k_2$, shown in Figures 5.16a and 5.16b, respectively, account for the effect of water temperature and fine suspended sediment on the bed-material discharge. If the bed-material size falls outside the 0.2- to 0.3-mm range, factor $k_3$ from Figure 5.16c is applied to correct for sediment size effect. True sediment discharge $q_s$ corrected for water temperature effect, presence of fine suspended sediment, and sediment size is given by

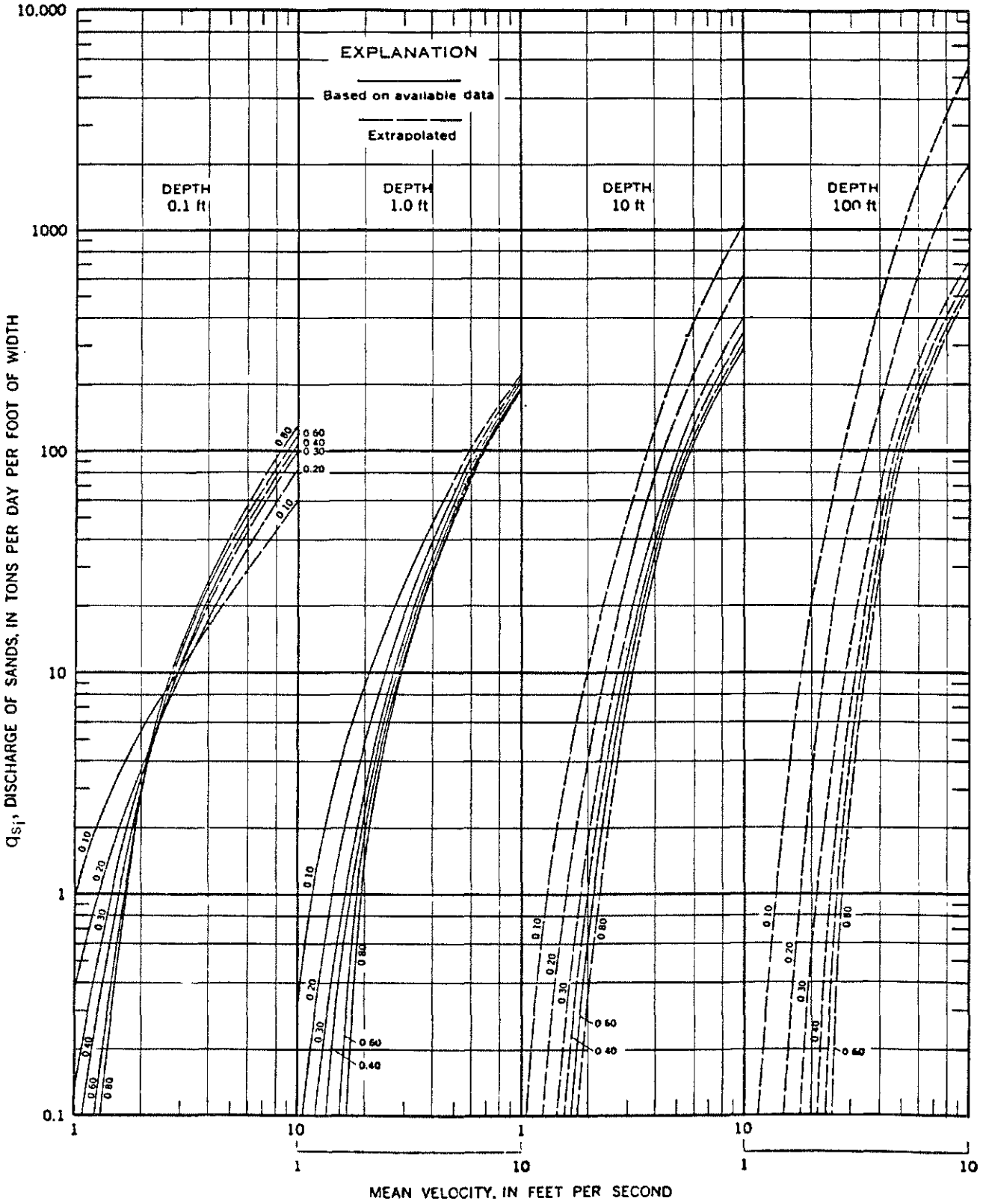


Note: The curves on this chart represent particle size in mm.

Figure 5.15. Relationship of discharge of sands to mean velocity for six median sizes of bed sands, four depths of flow, and a water temperature of 60°F (Colby, 1964).

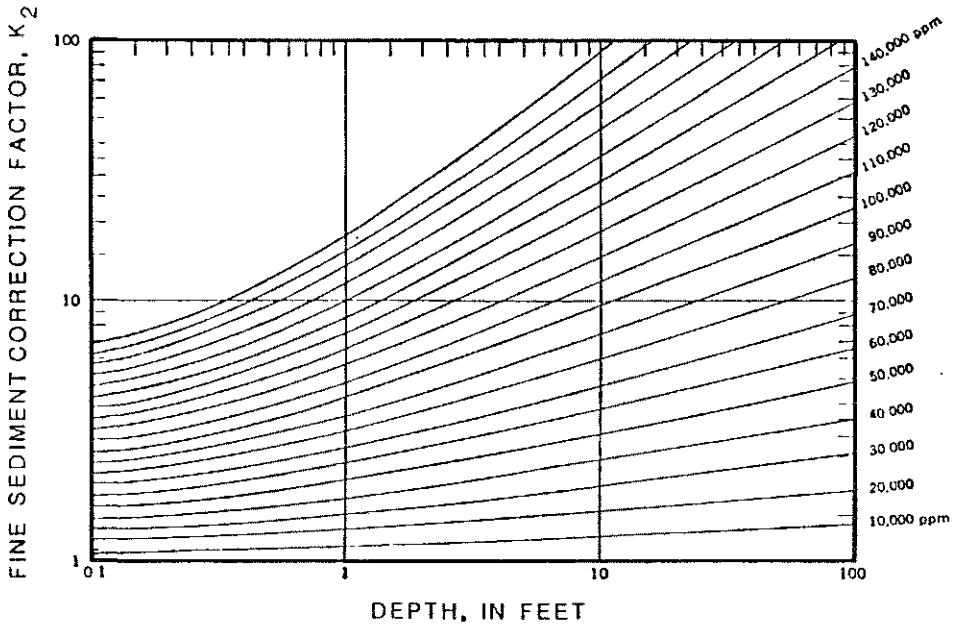


FIGURE 5.16b

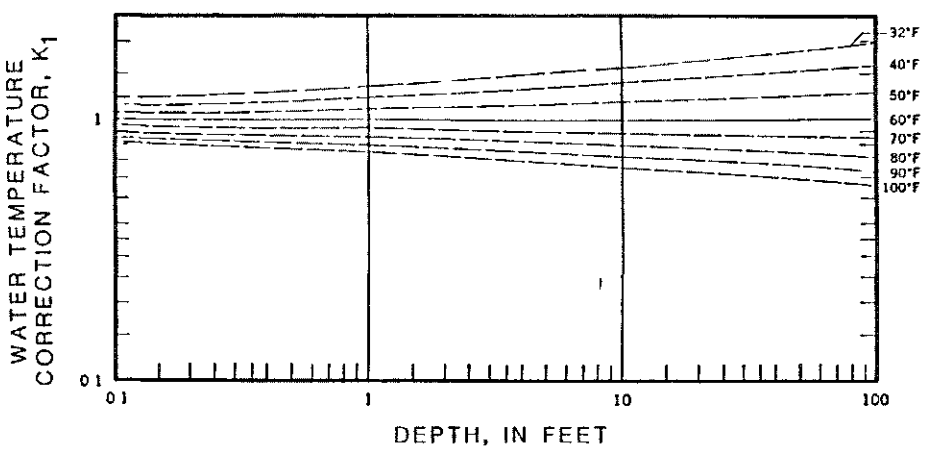


FIGURE 5.16a

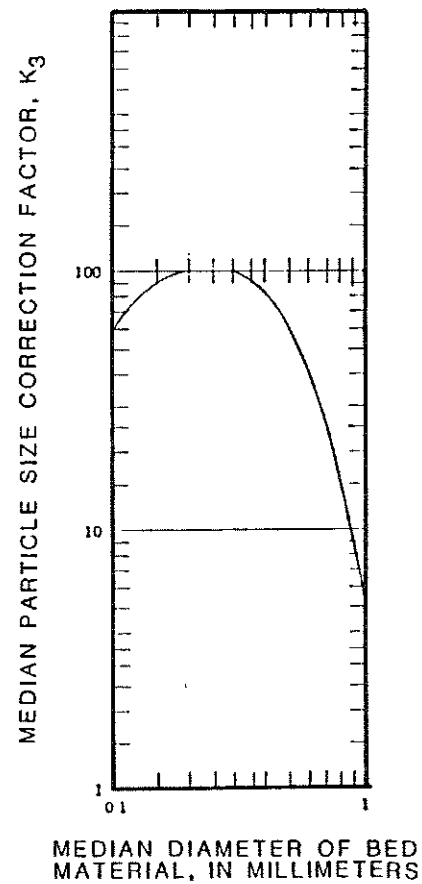


FIGURE 5.16c

Figure 5.16. Colby's correction curves for temperature and fine sediment (Colby, 1964).

$$q_s = [1 + (k_1 k_2 - 1)\ 0.01\ k_3]\ q_{s_i} \qquad (5.9)$$

As Figure 5.16 shows, $k_1 = 1$ when the temperature is 60° F, $k_2 = 1$ when the concentration of fine sediment is negligible, and $k_3 = 100$ when $D_{50}$ lies between 0.2 mm and 0.3 mm.

In spite of many inaccuracies in the available data and uncertainties in the graphs, Colby found

> "...about 75 percent of the sand discharges that were used to define the relationships were less than twice or more than half of the discharges that were computed from the graphs of average relationship. The agreement of computed and observed discharges of sands for sediment stations whose records were not used to define the graphs seemed to be about as good as that for stations whose records were used."

Example - Calculation of Sediment-Transport Rates Using:

A. Meyer-Peter, Muller (MPM) Bed-load Function

B. Colby Method

Before beginning the examples, the reader should remember that all sediment transport equations do not compute the same component of total sediment load. Table 5.5 was developed as an easy reference to make this distinction. In the following examples the Meyer-Peter, Muller equation is used to compute the bed-load transport rate. Since this equation was derived from flume experiments using flows with little or no suspended sediment load, it is not recommended for applications where suspended bed-material load is estimated to be a major component of the total sediment load. In contrast, the power relationships and the Colby Method were developed on the basis of predicting total bed-material transport rate.

Because of this difference between transport equations, the following examples will employ the MPM equation to evaluate the bed-load discharge for a gravel-cobble bed stream which would be expected to have very little suspended bed-material load, while the Colby Method will be applied to a sand-bed channel having both suspended bed-material load and bed load components.

Due to the simplicity of the power relationships (Equations 5.8a and 5.8b), no numerical examples will be presented.

Part A, Meyer-Peter, Muller Equation: The gradation curve for the bed material from a gravel-cobble bed stream was divided into three size frac-

tions. The geometric mean particle size and weight of each fraction is listed below:

Fraction #1 (33 1/3% of total sample weight): $D_G = D_{25} = 0.05$ ft

Fraction #2 (33 1/3% of total sample weight): $D_G = D_{50} = 0.10$ ft

Fraction #3 (33 1/3% of total sample weight): $D_G = D_{75} = 0.15$ ft

This reach of the stream is further defined by the following parameters:

For $Q = 5{,}000$ cfs, mean channel velocity, $\overline{V} = 8$ fps.

Darcy-Weisbach friction factor, $f = 0.06$

Specific weight of sediment, $\gamma_s = 165.4$ lb/ft$^3$

Density of water, $\rho = 1.9$ lb-sec$^2$/ft$^4$

Using the MPM Equation (Equation 5.7a), the following steps are required to compute bed-load discharge:

1. The boundary shear stress, $\tau_o$, is computed as follows:

$$\tau_o = \frac{1}{8} \rho f V^2$$

$$\tau_o = \frac{1}{8} (1.9)(0.06)(8)^2$$

$$\tau_o = 0.91 \text{ lb/ft}^2$$

2. The critical shear stress, $\tau_c$, is found using Shields' relation:

$$\tau_c = 0.047 D_c (\gamma_s - \gamma)$$

for $D_c = D_{25}$, $\tau_c = (0.047)(0.05)(165.4 - 62.4) = 0.24$ lb/ft$^2$

for $D_c = D_{50}$, $\tau_c = (0.047)(0.10)(165.4 - 62.4) = 0.48$ lb/ft$^2$

for $D_c = D_{75}$, $\tau_c = (0.047)(0.15)(165.4 - 62.4) = 0.73$ lb/ft$^2$

3. The MPM equation can now be used to compute the bed-load transport rate for each of the three sediment size fractions.

for $D_{25}$, $$q_{b_{25}} = \frac{12.85}{\gamma_s \sqrt{\rho}} (\tau_o - \tau_c)^{1.5} = \frac{12.85}{(165.4)\sqrt{1.9}} (0.91 - 0.24)^{1.5}$$

$$q_{b_{25}} = 0.031 \text{ cfs/ft}$$

for $D_{50}$, $q_{b_{50}} = \frac{12.85}{(165.4)\sqrt{1.9}} (0.91 - 0.48)^{1.5}$

$q_{b_{50}} = 0.016$ cfs/ft

for $D_{75}$, $q_{b_{75}} = \frac{12.85}{(165.4)\sqrt{1.9}} (0.91 - 0.73)^{1.5}$

$q_{b_{75}} = 0.004$ cfs/ft

4. The total unit bed-load transport rate can now be computed as the weighted average of the transport rates for each of the selected sediment size fractions. This procedure is accomplished as follows:

$$\text{total } q_b = \frac{\Sigma\,(q_{b_i} \times \%\text{ total weight})}{\Sigma\,(\%\text{ total weight})}$$

$$q_b = \frac{(0.031)(33\ 1/3\%) + (0.016)(33\ 1/3\%) + (0.004)(33\ 1/3\%)}{33\ 1/3\% + 33\ 1/3\% + 33\ 1/3\%}$$

$q_b = 0.017$ cfs/ft

Part B, Colby Method: Colby calculations will be made using the single median bed particle size as well as the sediment size fraction approach. Water temperature and fine sediment concentration are assumed equal to 70°F and 10,000 ppm, respectively, for the example calculations.

a. Calculations Using Single Bed Particle Size. The calculation will be made for a dicharge of 410 cfs, for which $Y_h$ = 1.36 ft, V = 2.93 fps, and b = 103 ft. From Figure 5.17, the median bed particle size $D_{50}$ is 0.225 mm. The solution involves the following steps:

1. Enter Figure 5.15 with a velocity of 2.93 fps for a depth of 1.0 ft and 10.0 ft and read the following values of $q_{s_i}$ for $D_{50}$ = 0.225 mm:

   Depth = 1.0 ft; $q_{s_i}$ = 15.5 tons/day/ft of width

   Depth = 10.0 ft; $q_{s_i}$ = 21.5 tons/day/ft of width

2. The depth and $q_{s_i}$ values determined in Step 1 are plotted on log-log paper in order to interpolate a value of $q_{s_i}$ for the given depth of 1.36 ft. This plot, which is shown in Figure 5.18, yields the following result:

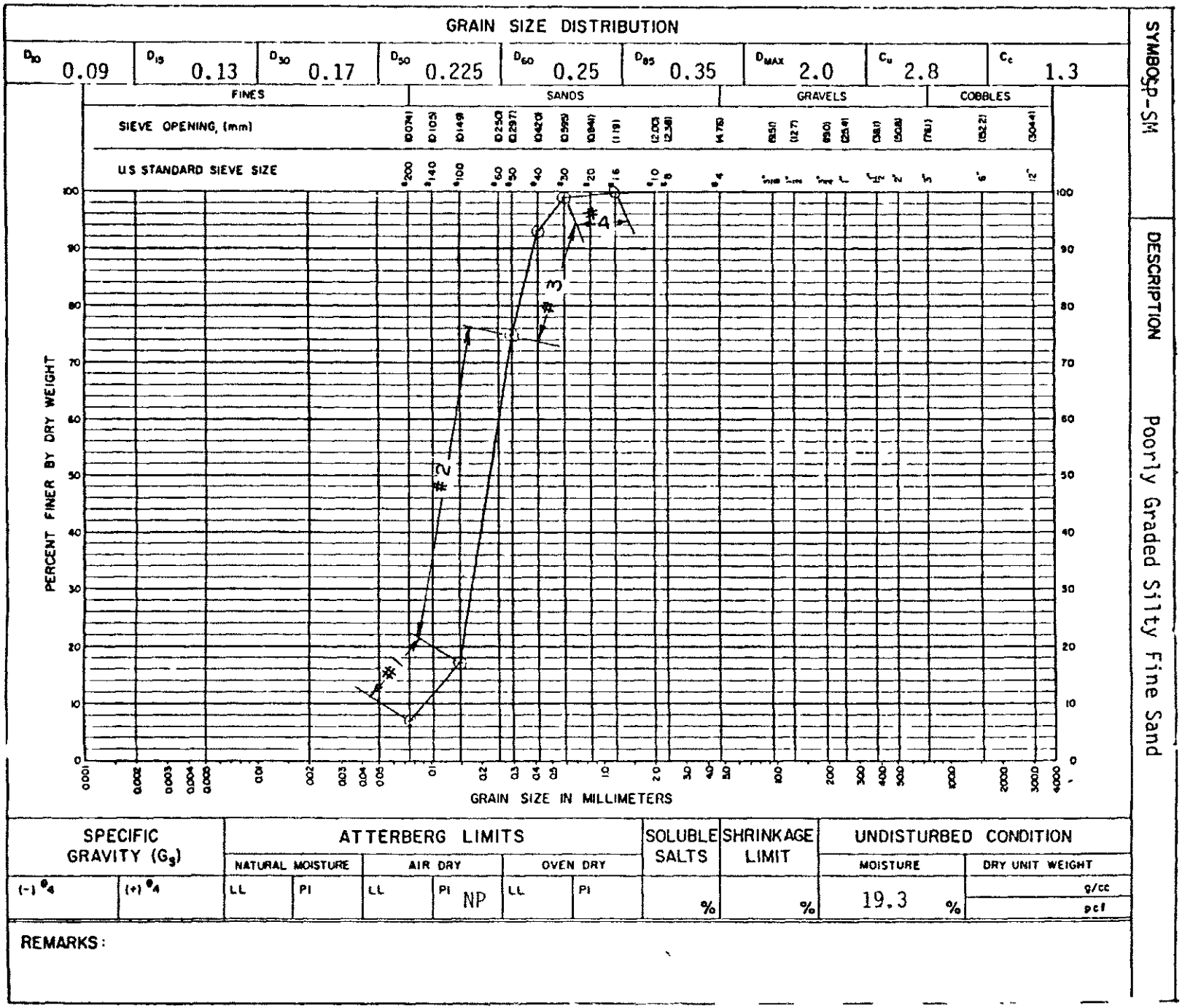


Figure 5.17. Bed material gradation curve.

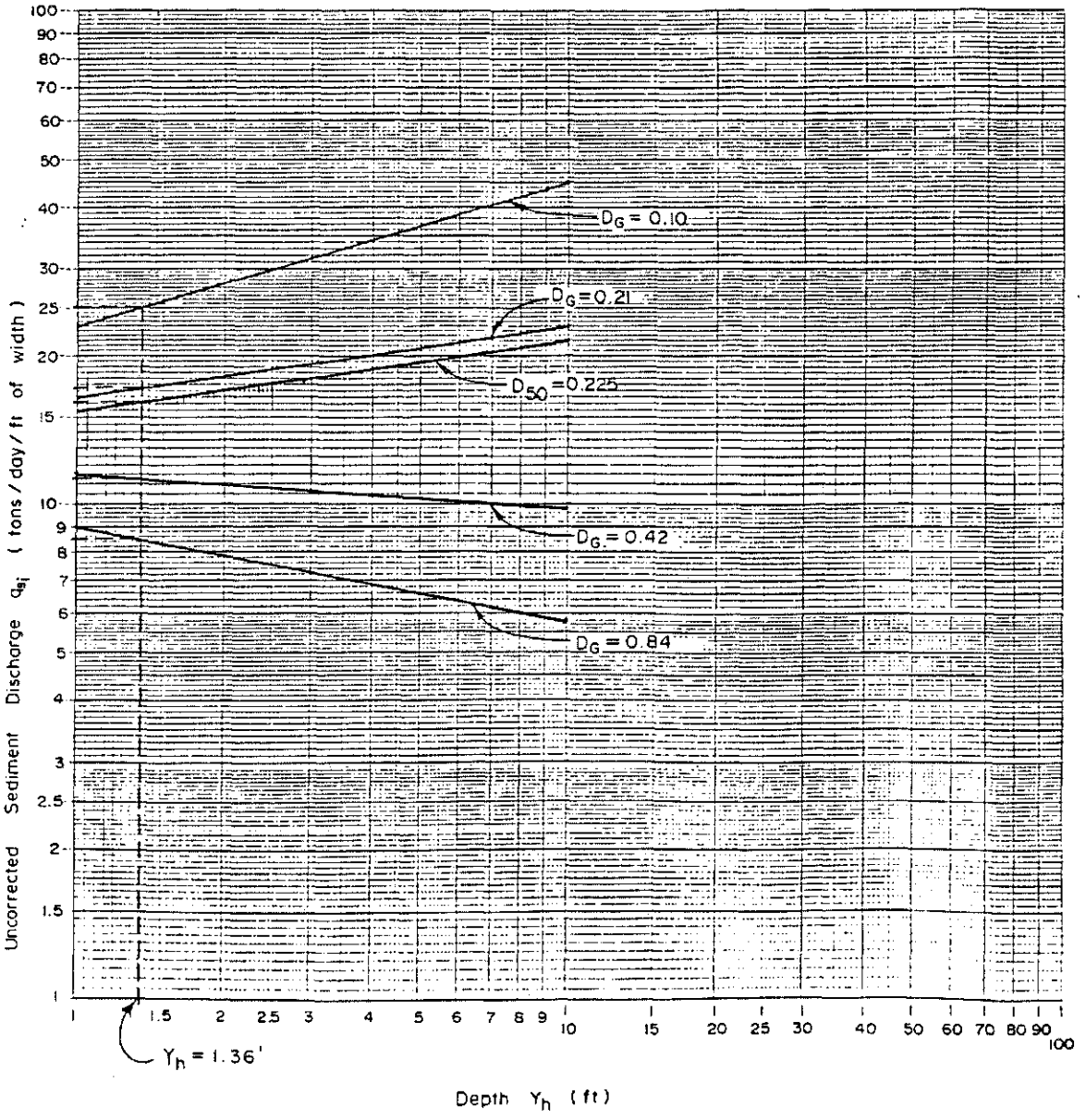


Figure 5.18. Log - log plot for uncorrected sediment discharge ($q_{s_i}$) versus hydraulic depth ($Y_h$).

Depth = 1.36 ft; $q_{s_i}$ = 16.2 tons/day/ft of width

3. Water temperature correction: Since the information in Figure 5.15 is based on a water temperature of 60°F and the given water temperature is 70°F, an adjustment must be made to compensate for the difference. This correction is made by entering Figure 5.16a with a depth of 1.36 ft and proceeding to the line for 70°F. A correction value, $K_1$, is then read as 0.92.

4. Figure 5.16b is now used to determine the correction factor for the fine sediment concentration of 10,000 ppm. Enter this curve with a depth of 1.36 ft and proceed to the curve for 10,000. A correction value, $K_2$, is then read as 1.2.

5. Sediment size adjustment. Since the $D_{50}$ bed particle size (0.225 mm) falls within the 0.2 to 0.3 mm range, a correction for sediment size is not necessary. For this condition, the $K_3$ correction factor = 100. This can be verified by entering Figure 5.16c with a median sediment size of 0.225 mm.

6. The true sediment transport, $q_s$, corrected for water temperature effect, presence of fine suspended sediment, and sediment size, is now computed as:

$$q_s = [1 + (K_1K_2 - 1)\ 0.01\ K_3]\ q_{s_i}$$

$$q_s = [1 + (0.92 \times 1.2 - 1)(0.01)(100)]\ 16.2$$

$$q_s = 14.52 \text{ tons/day/ft of width}$$

7. For the given channel width of 103 ft, the total bed-material transport rate, $Q_s$, for the cross section is $Q_s = q_s \times b = (14.52)(103) = 1{,}495.6$ tons/day.

8. The sediment concentration by weight, c, is computed as follows:

$$c = \frac{Q_s\ \gamma_s}{Q\gamma + Q_s\ \gamma_s} = \frac{Q_s\ (G_s)}{Q + Q_s\ (G_s)}$$

where $G_s$ = specific gravity of sediment $(\gamma_s/\gamma)$.

Since the Colby Method gives sediment transport in tons/day, a conversion to cfs must be made before the above formula can be used. This conversion is made as follows:

$$Q_s = \frac{1{,}495.6 \text{ tons}}{\text{day}} \times \frac{1 \text{ day}}{86{,}400 \text{ sec}} \times \frac{1 \text{ ft}^3}{165 \text{ lb of sediment}} \times \frac{2{,}000 \text{ lb}}{1 \text{ ton}}$$

$$Q_s = 0.21 \text{ cfs}$$

Therefore, $c = \frac{(0.21)(2.65)}{410 + (0.21)(2.65)} = 0.0013555$, or 1,355 ppm by weight

b. Calculations Using Sediment Size Fractions. The bed material that was used in the previous example had a mean particle size $D_{50}$ of 0.225 mm. To make the sediment transport calculations more representative of changes in the bed-material gradation curve, solution by size fraction is employed. Using this method, the gradation curve is divided into increments of similar size characteristics. The curve could be broken into soil fractions, e.g., coarse gravel, fine gravel, coarse sand, medium sand, etc., or it could be divided into even increments such as 20 percent by weight intervals. Other methods or criteria could be used as long as the individual size fractions are associated with particle sizes of similar characteristics. The gradation curve for this example (Figure 5.17) was divided into four size fractions, primarily on the basis of noticeable changes in the slope of the curve.

Once the gradation curve has been subdivided, the geometric mean particle size is determined for each grain size interval. The following steps illustrate the Colby Method calculations by size fraction for the same discharge and hydraulic conditions used previously.

1. The bed-material gradation curve (Figure 5.17) is subdivided into four increments and the geometric mean particle size for each increment calculated as given in Table 5.8. The adjustment to the fractional sample weight percentages in Table 5.8 is required to account for the seven percent of the total sample weight that was finer than the #200 sieve. Rather than resort to a hydrometer or similar analysis to grade the seven percent of fine material, this percentage was prorated among the four size fractions. If fine material constituted a significant portion of the total sample weight, a hydrometer analysis might be warranted.

2. Using the hydraulic parameters listed in part (a) of this example, enter Figure 5.15 with a velocity of 2.93 fps for depths of 1.0 ft and 10.0 ft and read values of $q_{s_i}$ for each of the four size fractions (see Table 5.9). It should be noted that an estimate had to be made for the $q_{s_i}$ value for the 0.84 mm size fraction since this value lies slightly outside the range of particle sizes shown in Figure 5.15. This procedure should be used with caution. If the mean size fractions are significantly outside the range of values shown in Figure 5.15, the Colby Method should not be used. In this case, the single non-conforming size frac-

Table 5.8. Geometric Mean Calculations for Colby Example.

| Grain Size Interval (mm) $D_i$ to $D_j$ | Geometric Mean $D_G = \sqrt{D_i \times D_j}$ (mm) | Percent of Total Sample Weight | Adjusted % of Total Sample Weight |
|---|---|---|---|
| 1.2 - 0.59 | $\sqrt{(1.2)(0.59)} = 0.84$ | 1.0 | 1.1 |
| 0.59 - 0.30 | $\sqrt{(0.59)(0.30)} = 0.42$ | 24.0 | 25.8 |
| 0.30 - 0.145 | $\sqrt{(0.30)(0.145)} = 0.21$ | 58.0 | 62.4 |
| 0.145 - 0.075 | $\sqrt{(0.145)(0.075)} = 0.10$ | 10.0 | 10.7 |
| | Total: | 93.0 | 100.0 |

Table 5.9. Uncorrected Sediment Transport Rate, $q_{s_i}$ (tons/day/ft) for Colby Example.

| | $D_G$ (mm) | | | |
|---|---|---|---|---|
| Depth (feet) | 0.84 | 0.42 | 0.21 | 0.10 |
| 1.0 | 9.0 | 11.5 | 16.5 | 23.0 |
| 10.0 | 5.8 | 9.8 | 23.0 | 45.0 |

tion constitutes only 1.1 percent of the total sample weight. Accordingly, any error induced by this procedure should be minimal.

3. The depth and $q_{s_i}$ values determined in Step 2 are plotted on log-log paper in order to interpolate a value of $q_{s_i}$ for the given depth of 1.36 ft. This plot, which is shown in Figure 5.18, yields the following results:

| $D_G$ (mm) | 0.84 | 0.42 | 0.21 | 0.10 |
|---|---|---|---|---|
| $q_{s_i}$ (tons/day/ft of width) | 8.5 | 11.3 | 17.2 | 25.1 |

4. The water temperature correction, $K_1$, and fine sediment concentration correction, $K_2$, are the same as computed in part (a) of this example, since these factors are not a function of the bed particle gradation curve.

$K_1 = 0.92$

$K_2 = 1.20$

5. A sediment size adjustment factor, $K_3$, will be required for three of the four size fractions since they lie outside the 0.2 to 0.3 mm range. The correction factors from Figure 5.16c are summarized below.

| $D_G$ (mm) | 0.84 | 0.42 | 0.21 | 0.10 |
|---|---|---|---|---|
| $K_3$ | 12 | 80 | 100 | 60 |

6. The true sediment transport rate, $q_s$, corrected for water temperature effect, presence of fine suspended sediment, and sediment size, is now computed for each size fraction using:

$$q_s = [1 + (K_1 K_2 - 1)\ 0.01\ K_3]\ q_{s_i}$$

The results are summarized in the following table.

| $D_G$ (mm) | 0.84 | 0.42 | 0.21 | 0.10 |
|---|---|---|---|---|
| $q_s$ (tons/day/ft of width) | 8.61 | 12.19 | 19.04 | 26.73 |

7. Once the unit transport rate is computed for each size fraction in Step 6, the actual transport amount of each size fraction within the total bed sample is determined by multiplying the computed transport rates times the percentage of each size fraction in the bed sample (see Table 5.10).

8. Knowing the total unit bed-material discharge from Step 7, the total bed-material discharge from the entire channel cross section can now be calculated by multiplying the sediment discharge rate from Step 7 by the effective channel width.

$$Q_s = b \times q_{s_T}$$

$$= (103)(17.98) = 1{,}851.9 \text{ tons/day}$$

Converting to cubic feet per second yields:

$$Q_s = (1{,}851.9)(1.403 \times 10^{-4})$$

$$Q_s = 0.26 \text{ cfs}$$

9. The sediment concentration is now computed.

$$C = \frac{Q_s\ (G_s)}{Q + Q_s\ (G_s)}$$

$$C = \frac{(0.26)(2.65)}{410 + (0.26)(2.65)}$$

$$C = 0.0016776 \quad \text{or} \quad 1{,}678 \text{ ppm by weight}$$

10. The results of the size fraction technique can be compared to the single bed particle size analysis presented in part (a) of this example for a discharge of 410 cfs. The single size technique produced a bed-material discharge of 0.21 cfs and a concentration of 1,355 ppm, while the size fraction analysis gave a discharge of 0.26 cfs and a concentration of 1,678 ppm. The calculation by size fraction is summarized in Table 5.11. Additionally, calculations for two other discharges are given and illustrate the relationships between $Q_s$ and C as discharge increases, particularly the leveling off of concentration.

Table 5.10. Total Sediment Transport Rate for Colby Example.

| Size Fraction | Percent of Total Sample | Unit Transport Rate | Actual Bed Material Discharge |
|---|---|---|---|
| 0.84 mm | $1.1 \times \frac{1}{100} \times$ | 8.61 | = 0.09 tons/day/ft. |
| 0.42 | $25.8 \times \frac{1}{100} \times$ | 11.48 | = 3.15 |
| 0.21 | $62.4 \times \frac{1}{100} \times$ | 19.04 | = 11.88 |
| 0.10 | $10.7 \times \frac{1}{100} \times$ | 26.73 | = 2.86 |
| | $q_{s_t}$ | Total Unit Discharge For Q = 410 cfs | 17.98 tons/day/ft. |

Table 5.11. Bed-Material Discharge Calculations for Colby Method Example Using Sediment Size Fractions.

| Q (cfs) | $D_g$ (mm) | $l_b$ (% of Total Sample Weight | $Y_h$ (ft) | V (fps) | b (ft) | $q_{s_i}$ tons/day/ft | $K_1$ | $K_2$ | $K_3$ | $q_s$ | $\frac{l_b q_s}{100}$ tons/day/ft | $q_{s_t}$ | $Q_s$ tons/day | $Q_s$ (cfs) | C (ppm) |
|---|---|---|---|---|---|---|---|---|---|---|---|---|---|---|---|
| 410 | 0.84 | 1.1 | 1.36 | 2.93 | 103 | 8.5 | 0.92 | 1.20 | 12 | 8.61 | 0.09 | 17.98 | 1,851.9 | 0.26 | 1,678 |
| | 0.42 | 25.8 | | | | 11.3 | | | 80 | 12.19 | 3.15 | | | | |
| | 0.21 | 62.4 | | | | 17.2 | | | 100 | 19.04 | 11.88 | | | | |
| | 0.10 | 10.7 | | | | 25.1 | | | 60 | 26.73 | 2.86 | | | | |
| 2,820 | 0.84 | 1.1 | 2.50 | 6.63 | 170 | 99.6 | 0.91 | 1.22 | 12 | 100.88 | 1.11 | 161.82 | 27,509.4 | 3.86 | 3,614 |
| | 0.42 | 25.8 | | | | 115.4 | | | 80 | 125.61 | 32.41 | | | | |
| | 0.21 | 62.4 | | | | 152.0 | | | 100 | 168.77 | 105.3 | | | | |
| | 0.10 | 10.7 | | | | 201.4 | | | 60 | 214.69 | 23.0 | | | | |
| 9,620 | 0.84 | 1.1 | 4.14 | 9.92 | 234 | 238.9 | 0.90 | 1.25 | 12 | 242.49 | 2.67 | 425.59 | 99,588.1 | 13.97 | 3,834 |
| | 0.42 | 25.8 | | | | 263.5 | | | 80 | 289.89 | 74.79 | | | | |
| | 0.21 | 62.4 | | | | 401.4 | | | 100 | 451.52 | 281.75 | | | | |
| | 0.10 | 10.7 | | | | 577.1 | | | 60 | 620.34 | 66.38 | | | | |

### 5.3.7 Equilibrium Slope

Discussion - The equilibrium slope is defined as the slope at which the channel sediment transporting capacity is equal to the incoming sediment supply. Mathematically, this concept is expressed as

$$Q_{s_{in}} = Q_{s_{out}} \tag{5.10}$$

where $Q_{s_{in}}$ is the supply rate of sediment into the channel and $Q_{s_{out}}$ is the sediment transport rate out of the channel. When this relationship is satisfied, the channel neither aggrades or degrades, i.e., it is in equilibrium. If the sediment transport rate in a given reach is less than sediment supply, the slope of that reach will have to increase to achieve equilibrium conditions. Conversely, if the transport rate is greater than supply, the slope will need to decrease.

Application - The equilibrium slope methodology is utilized to evaluate long-term channel response (aggradation/degradation), specifically, the slope the channel ultimately wants to achieve. Short-term response during a single flood (general scour/deposition) must be evaluated by other methods (see Section 5.3.8). An equilibrium slope analysis should begin with a study of historic bed profiles through the project area. If trends towards aggradation or degradation can be detected, they should be traced to a cause. Cases may arise in a relatively undisturbed watershed that show no significant change in bed profiles over long periods of time. The length of time necessary to establish stability in bed profiles is hydrologically dependent (i.e., a function of historical climatology and hydrology). However, in any case, the longer the record of available data, generally the more confident one can be in determining the stability of the bed. Watersheds that are considered in equilibrium may not require equilibrium slope analysis unless the proposed flood plain improvements alter the sediment supply or transport capacity.

If historic bed profiles or field inspections indicate the system is attempting to adjust to an equilibrium condition, an analysis should be completed to determine what equilibrium condition is being sought and how any proposed flood plain improvements might cause an alteration in the equilibrium adjustment. The results of this analysis can then be incorporated into the project design.

Since the analysis is utilized to evaluate long-term conditions, the appropriate discharge for calculation purposes is the dominant discharge, which is that discharge predominantly responsible for channel characteristics. The dominant discharge is typically between a two- and a five-year event for perennial channels, and a five- and a ten-year event for ephemeral channels. Often the dominant discharge is equal to the bankfull discharge. Since equilibrium slope calculations do not have much physical significance or importance in the overbank area, bankfull discharge can be considered an upper limit for equilibrium slope calculations.

The first and perhaps most critical step in an equilibrium slope analysis is to determine the sediment supply from the upstream reach for the dominant discharge. In the absence of actual sediment supply data (i.e. measured data or analytically calculated watershed sediment yield), the sediment supply is most often evaluated from computation of the transport capacity (see Section 5.3.6) of the upstream reach, under the assumption that it is in equilibrium. For natural, undisturbed channels and/or watersheds, this is a reasonable assumption that can often be verified through examination of historical data (such as profile analysis or aerial photographs). However, for disturbed channels, e.g. in an urbanizing area, calculation of sediment supply is more complicated. After urbanization, the transport capacity of the selected supply reach does not necessarily reflect sediment supply. Since urbanization generally reduces sediment supply, the calculated transport capacity will typically be larger than the actual sediment supply. Additionally, if channelization has occurred, the transport capacity of the existing channel may not be similar to that for the channel that existed in the natural, undisturbed watershed. Therefore, to properly establish the sediment supply to which the channel is adjusting, it may be necessary to look at historical conditions to estimate the natural channel characteristics. The calculated transport capacity of this channel is then reduced to reflect the effects of urbanization. The calculation is obviously subjective and relies on extensive engineering judgment and experience.

After establishing the upstream sediment supply rate, the transport capacity of the study reach is evaluated. The sediment transport capacity of the study reach (or each subreach therein) is computed on the basis of the same water discharge (i.e., dominant discharge) that was used for the assumed equilibrium sediment supply reach. If the calculated transport capacity does

not equal the supply, the slope of the study reach is adjusted and the transport capacity re-evaluated. This procedure is continued until the resulting sediment transport capacity equals the incoming supply, at which point the equilibrium slope will have been found. The equilibrium slope can be calculated for any number of reaches below the supply reach, not just the reach immediately below. When conducting this calculation, it is important to realize that the appropriate sediment supply, or inflow, to any subsequent reach is always the value computed from the supply reach.

An expedient way of determining hydraulic conditions necessary for evaluation of sediment transport capacity is to assume that uniform flow prevails. Manning's equation can then be used to calculate velocity, depth and top width for a given channel slope. This can be done for any channel shape by trial and error and can be adapted easily to hand-held programmable calculators. However, if significant backwater effects exist from a bridge or reservoir, the hydraulic conditions should be computed assuming gradually varied flow.

The selection of the proper channel geometry is important in equilibrium slope analysis. The sediment transport is proportional to some power of velocity (usually between 3.5 and 4.5 for sand bed channels) and is directly proportional to the flow width. This makes the equilibrium slope very sensitive to these parameters. The accurate determination of area, wetted perimeter, and top width as a function of depth are easy to develop and are usually sufficiently accurate below the bankfull level. Using power relationships, normal depth can be determined directly. Developed channel sections are usually trapezoidal and hydraulic conditions can be determined using hand-held programmable calculators.

When assumption of a wide channel is reasonable (i.e., width-to-depth ratio greater than 10), calculation of the equilibrium slope is simplified to a simple function of unit discharge. The equation is

$$S = \left(\frac{a}{q_s}\right)^{\frac{10}{3(b-c)}} q^{\frac{2(2c+3b)}{3(b-c)}} \left(\frac{n}{1.49}\right)^2 \qquad (5.11)$$

where a, b and c are the coefficients of the power relationship describing sediment transport (i.e., $q_s = a\, Y_h^b\, V^c$, see Tables 5.6a and 5.6b), n is the Manning n, S is the slope in ft/ft, q is the unit water discharge for the reach under consideration, and $q_s$ is the unit sediment discharge for the supply reach. The derivation of this equation is provided by Simons, Li & Associates, Inc. (1982); however, the form of this equation is slightly different due to the definition of the exponents in the power relationship describing sediment transport. Furthermore, Equation 5.11 should only be used if the restrictions listed in Table 5.7 for Equation 5.8a (as used with Tables 5.6a and 5.6b) are met. Otherwise, a set of regression coefficients specific to the site under investigation should be developed.

For calculation of equilibrium slope in several reaches below the supply reach, the calculation simplifies even further if Manning's n, channel geometry and total discharge (Q) are the same in each reach. For this case, the only variable is bed slope, $S_{ex}$. This condition typically exists for channelized conditions where channel geometry is constant and there is no tributary inflow. The equation is

$$S = S_{ex} \left(\frac{Q_s \text{ supply}}{Q_s \text{ capacity}}\right)^{\left(\frac{2}{c-x}\right)} \tag{5.12}$$

where $x = (3/5)\ (2/3\ c + b)$ and $S_{ex}$ is the existing channel slope (ft/ft) in a given reach. From this equation it can be qualitatively established that the equilibrium slope will be less than the existing slope when sediment supply is less than transport capacity, i.e., an equilibrium slope less than the existing slope indicates a degradational condition.

Results of equilibrium slope calculations are used to predict long-term changes to the bed profile of a river system. These changes normally will not occur as the result of a single flood. Usually, equilibrium slope conditions will evolve in response to the occurrence of many floods over a period of time. There is no accurate way to predict how long it will take such slope adjustments to occur. Large-scale, man-made changes to a river system may induce a complete equilibrium response within 10 to 100 years or even less, while natural changes on an undisturbed river may require a much longer time frame, perhaps on the order of 100 to 1,000 years.

A further complicating factor in the application of equilibrium slope calculations focuses on the location of a point from which the computed

equilibrium slope can pivot. If natural geologic controls such as rock outcroppings or man-made grade control structures are present, these features can serve as pivot points. For a given river reach with such controls, the slope adjustment will always pivot about the downstream control point, such that if the equilibrium slope is less than the existing slope, degradation will occur, while if the inverse is true, aggradation will occur. Figure 5.19 illustrates how this will occur for the two cases of equilibrium slope being both greater than and less than the existing bed slope.

Identification of pivot points is critical to equilibrium slope analysis and relies heavily on engineering judgment and interpretation. For example, at large horizontal distances from a pivot point, the vertical distance between the existing bed slope and the equilibrium slope may become unrealistic. In these cases the engineer must re-evaluate the selection of pivot points to insure that no potential control points have been missed. If no control points can be located, the amount of long-term degradation may be controlled by the channel bank height. Unless a channel is formed through rock or strongly cemented materials, there is usually a maximum vertical height at which a channel bank will no longer be stable. When this limit is reached, bank sloughing will begin to occur which causes the channel to adjust horizontally rather than through continued vertical cutting. As the channel widens, the velocity of flow will decrease, resulting in a decrease in sediment transport capacity. This type of channel widening will continue until the transport capacity is brought into equilibrium with the sediment supply to the reach.

In addition to stable bank heights being a potential control for the equilibrium slope, a check should also be made to determine if channel armoring will be a factor in limiting the amount of degradation to a value less than that predicted by the equilibrium slope analysis. This may reveal that armoring will arrest the vertical channel movement before the predicted equilibrium slope can be attained.

Due to the complex interaction of variables that determine long-term aggradation/degradation and the simplifying assumptions that must be made in analyzing such long-term changes, the numerical results from an equilibrium slope analysis must be carefully evaluated to ensure they are reasonable. Overall, the results of this type of analysis can be very subjective and in many cases may only be useful in a qualitative sense rather than quantitative.

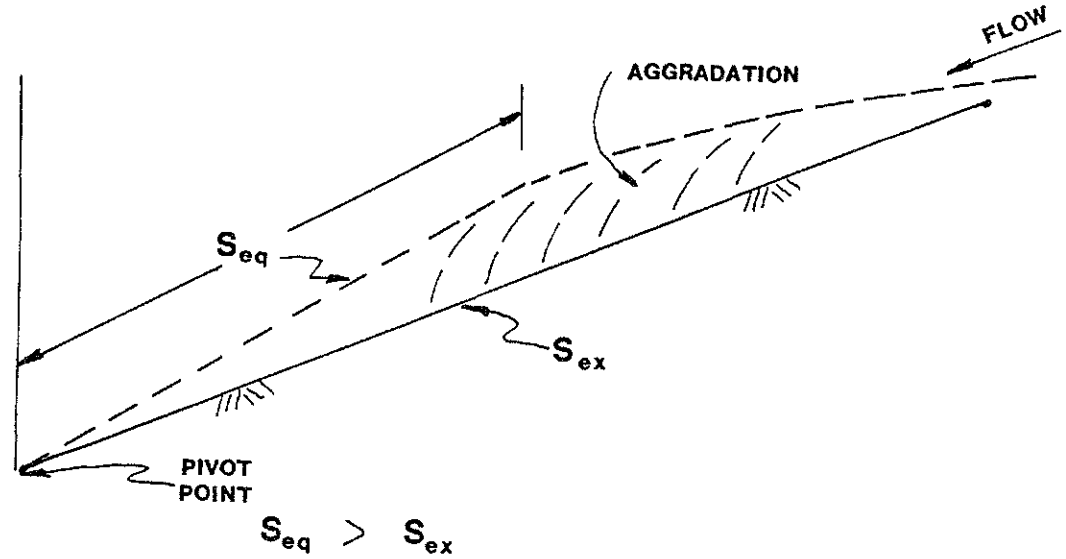


In this case, the sediment supply exceeds the sediment transport capacity of the reach. Under this condition, the bed slope must increase in order to increase the transport rate to match the supply rate. The initial excess of sediment supply will cause aggradation at the upstream end of the reach until the downstream portion of the bed slope is steep enough to transport all the incoming sediment.

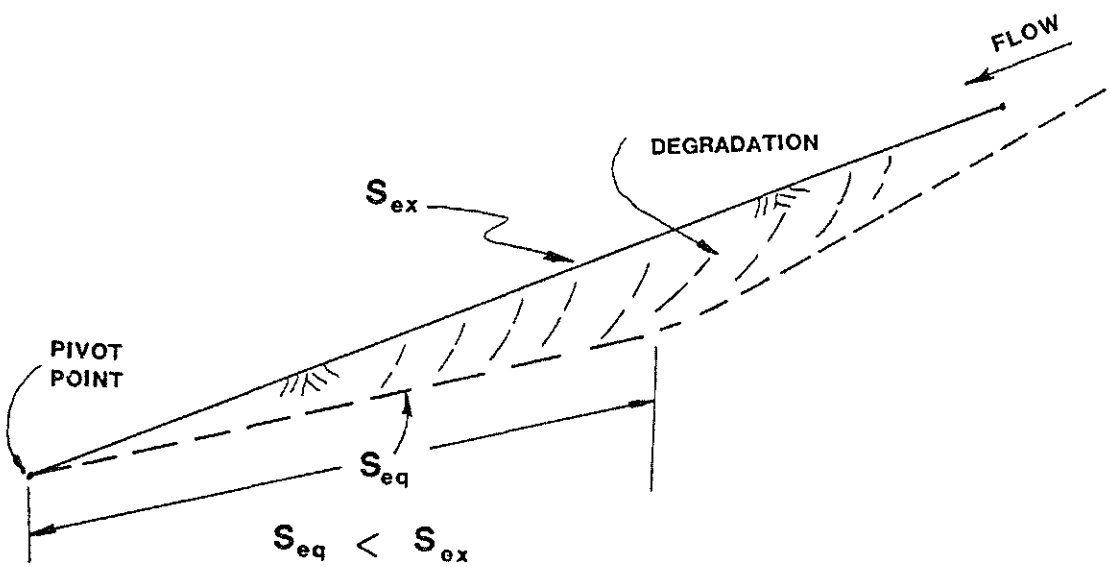


In this case, the incoming sediment supply is less than the sediment transport capacity of the reach. This sediment deficit will be satisfied by a removal of bed material through the reach until the bed slope is flattened enough to reduce the transport capacity to the point that it matches the incoming sediment supply.

Figure 5.19 Relationship between equilibrium slope and channel bed controls.

A summary of the equilibrium slope procedure is presented as follows:

1. Select upstream equilibrium supply reach and obtain the following data:

   a. channel geometry
   b. channel slope
   c. sediment size distribution
   d. channel resistance (Manning's n)

2. Determine dominant discharge.

3. Divide the segment of the river system under analysis into separate reaches of similar hydraulic characteristics and identify control points.

4. Obtain the same information as in Step 1 for each downstream reach that is to be analyzed.

5. Select an appropriate sediment transport equation (i.e., from Table 5.5 if applicable).

6. Establish the sediment supply provided by the upstream supply reach. This rate will be the sediment supply for all downstream reaches unless significant tributary flow is encountered downstream of the supply reach. If equilibrium conditions can be assumed in the supply reach, the sediment supply will equal the transport capacity of the supply reach.

7. Compute the sediment transport rate for each of the downstream reaches by varying the slope through each reach until a transport rate is found which matches the sediment supply. This establishes an equilibrium slope for each reach.

8. Pivot equilibrium slopes about control points (if any were identified) to determine long-term bed adjustment.

9. Check any degradation dimensions determined from Step 8 to see if the maximum stable bank height or armoring will control the amount of bed adjustment possible.

Example: Prior to the establishment of a strict flood plain management program, residential development was allowed to encroach into the flood plain of a desert wash located in a rural area of Arizona.

In order to resolve the flooding problem for this community, a levee/channelization project has been proposed. The channel improvements will consist of clearing vegetation from the exiting channel in order to lower the n value to 0.025 as well as widening the channel to 200 ft.

An equilibrium slope analysis is to be performed to determine the long-term aggradation/degradation that may be induced by these channel improvements. The results of this analysis will be incorporated into the design of the bank stabilization system for the proposed levee.

1. A field inspection of the site indicated the wash had very uniform characteristics both up and downstream of the reach for proposed channel improvements. Accordingly, the following channel parameters were considered representative of both the upstream sediment supply reach and the existing downstream reach which is to undergo channelization.

   a. Existing channel bottom width is approximately 150 ft.
   b. Existing bed slope = 0.007 ft/ft.
   c. $D_{50}$ (bed material) = 0.5 mm.
   c. G (gradation coefficient) = 2.0.
   e. Average channel depth is about 4 ft.
   f. Existing channel n value was estimated at 0.04.

2. A hydrologic analysis of the upstream drainage area indicated the 10-year event has a peak discharge of 3,000 cfs. When Manning's Equation was applied to the supply section channel geometry with a discharge of 3,000 cfs, the depth of flow was found to be about 3 ft. Since this is within a foot of being bankfull, 3,000 cfs was chosen as the dominant discharge.

3. The proposed channelization only extends along a 1,500-foot reach of the wash so the equilibrium slope analysis will be confined to this length. Since the existing channel conditions and proposed channel improvements are uniform throughout this length, only one downstream reach will be used for the analysis.

   An "at-grade" soil cement road crossing was discovered near the downstream end of the study reach. It was assumed this crossing would withstand the 100-year design flood, therefore it was to be a stable control point for the equilibrium slope analysis.

4. The existing channel conditions through the study reach are listed in Step 1.

5. Referring to Tables 5.5 and 5.6a, it was determined that a power relationship of the form $q_s = a\ Y_h^b\ V^c$ would be the most efficient way to analyze the sediment supply and transport capacities through the reach.

   From Table 5.6a, the following coefficients and exponents were obtained using the data from Step 1:

   $a = 1.48 \times 10^{-5}$

   $b = 0.0501$

   $c = 4.31$

   Accordingly, the sediment transport equation is:

   $$q_s = 1.48 \times 10^{-5}\ Y_h^{0.0501}\ V^{4.31}$$

6. Manning's Equation was used to compute the velocity and hydraulic depth for the upstream sediment supply section. The following parameters from Step 1 were used:

   $n = 0.04$

   $b = 150$ ft

   side slopes = 1:1

   bed slope = 0.007

   $Q = 3{,}000$ cfs

   The calculation yields $V = 6.40$ fps
   $y_h = 3.00$ ft

   The sediment supply is now calculated as the transport capacity of the upstream supply section:

   $$q_s = 1.48 \times 10^{-5} (3.00)^{0.0501} (6.40)^{4.31}$$

   $$q_s = 0.047 \text{ cfs/ft}$$

   Total sediment supply = $q_s$ x average flow width

   $$Q_{s_{in}} = (0.047)(153)$$

   $$Q_{s_{in}} = 7.19 \text{ cfs}$$

7. The transport capacity of the improved channel reach will now be computed with different bed slopes until one is found which will yield a transport capacity equal to the incoming supply rate. The proposed channel parameters are as follows:

   $n = 0.025$

   $b = 200$ ft

   side slopes = 1:1

   Using the dominant discharge of 3,000 cfs, Manning's Equation is first used to calculate the velocity and hydraulic depth for substitution into the sediment transport equation. The calculations, which employ a trial-and-error sequence, are summarized in the following table:

| Slope (ft/ft) | $Y_h$ (ft) | V (fps) | $q_s$ (cfs/ft) | Flow Width (ft) | $Q_s$ (cfs) |
|---|---|---|---|---|---|
| 0.007 | 1.92 | 7.65 | 0.098 | 204 | 19.99 |
| 0.0025 | 2.61 | 5.60 | 0.026 | 205 | 5.33 |
| 0.003 | 2.47 | 5.91 | 0.033 | 205 | 6.77 |
| 0.00315 | 2.44 | 6.00 | 0.035 | 205 | 7.18 |

A slope of 0.00315 yields a transport rate of 7.18 cfs which is approximately equal to the incoming supply rate of 7.19 cfs. Accordingly, this can be taken as the equilibrium slope.

8. By pivoting the equilibrium slope around the downstream control point (soil cement road crossing), it is determined that up to 5.8 feet of degradation is possible at the upstream end of the channelized reach (see Figure 5.20).

   This long-term degradation should be added to any other anticipated erosion or scour to get a total toedown depth necessary to protect the levee from undermining. Additionally, this long-term degradation may initiate a headcut upstream of the channelized reach. For this reason, consideration should be given to placing a grade-control/drop structure at the upstream end of the channel.

9. Backhoe pits were excavated to a depth of 8 feet at two locations in the existing channel. No bed material was encountered of a size large enough to form an armor layer. Accordingly, armoring will not limit the predicted amount of long-term degradation.

### 5.3.8 Sediment Continuity Analysis

Discussion - The sediment continuity principle applied to a given channel reach states that the sediment inflow minus the sediment outflow equals the time rate of change in sediment storage. Mathematically, this can be presented as

$$Q_{s_{in}} - Q_{s_{out}} = \frac{dVol}{dt} \qquad (5.13)$$

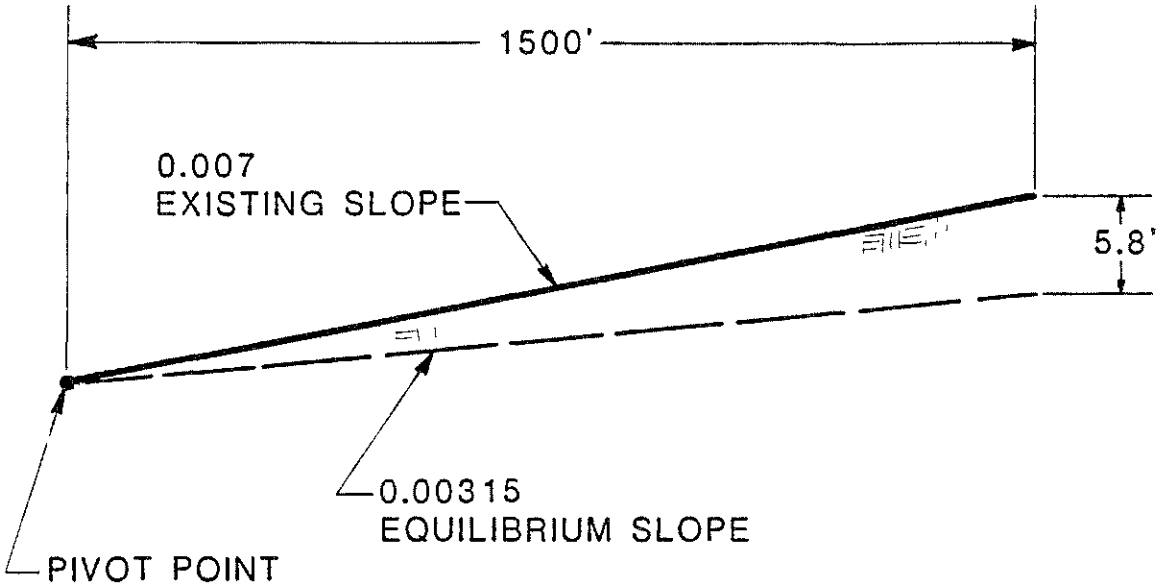


NOT TO SCALE

Figure 5.20. Existing and Equilibrium Slope Profiles for Example Problem.

For a given discharge acting for a given time, the volume of sediment deposited or eroded in a channel reach is simply the difference between the upstream sediment supply rate ($Q_{s_{in}}$) and the channel sediment transport rate ($Q_{s_{out}}$). If the supply rate is greater than the transport rate, the reach is depositional, while if transport is greater than supply, general scour will occur. (The basic principle of the equilibrium slope analysis is no change in volume, i.e., $dVol/dt = 0$ in Equation 5.10.)

The sediment continuity principle can be applied to analyze conditions during a single discharge (e.g. peak discharge of a 100-year flood) or during the hydrograph of a single flood. Either of these applications provides information on the short-term erosion/sedimentation occurring on a reach-by-reach basis.

Application - The first step in sediment continuity analysis is delineation of the study reach into a number of subreaches. Delineation of subreaches is based on (1) physical characteristics of the channel, such as top width and slope, (2) hydraulic parameters, such as depth and, particularly, velocity, (3) bed-material sediment characteristics, (4) areas of particular interest to study objectives, such as bridges or locations of proposed channel improvements, and (5) the desire to maintain reach lengths as uniform as possible throughout the system. Items 1, 2 and 3 are generally selected to provide consistency within the subreach, so that representative average conditions may be determined. For example, consistency in top width and channel length influence the utilization of sediment continuity results in evaluation of vertical channel response. As discussed in Section 5.3.9, erosion/sedimentation volumes from sediment continuity are often linearly distributed through the reach to determine vertical channel adjustments. Therefore, if an upstream reach length is 2,500 feet and the downstream reach is only 1,500 feet, the vertical adjustment of the channel bed responding to the imbalance in sediment supply and transport capacity between reaches will be much different from that had the downstream reach been dimensioned as 2,500 feet.

Furthermore, uniform channel lengths are important in maintaining the integrity of sediment continuity analysis. Sediment continuity analysis does not address the time or channel length that it takes for the difference between sediment supply and transport rate to achieve a balance. It is assumed that a balance will be achieved within the reach regardless of its length.

This is not necessarily correct. For example, in a very short depositional reach, particle settling times may not permit the calculated sedimentation to occur. For this reason it is recommended that reach lengths be kept as uniform as possible to avoid the introduction of an additional variable to the analysis that could bias or otherwise create unrealistic results.

After subreach delineation, characteristic geometric and hydraulic information must be developed for each subreach for the discharge(s) under consideration. This information may be computed manually through uniform flow or gradually varied flow calculations, or through computer programs such as HEC-2. For example, if HEC-2 output data are available, the required velocity, depth and top width data at various cross sections within the study reach will be provided. Within a given subreach these data can be averaged to define values representative of conditions in that reach for the given discharge.

After establishing representative hydraulic characteristics in each subreach for the given discharge(s), the sediment transport capacity of each subreach is calculated using an appropriate method (see Section 5.3.6). The sediment continuity principle is then applied by comparing transport capacity on a reach-by-reach basis, under the assumption that the sediment supply to any given subreach is equal to the transport capacity of the adjacent upstream reach. The comparison begins at the upstream end of the study reach by designating the first subreach as a supply reach, which initiates the calculation in Subreach 2.

Application of sediment continuity analysis to a flood hydrograph requires discretizing the hydrograph into a series of discrete discharges, as described in Section 3.5. The reach-by-reach comparison is then completed for each discharge and the total volume of erosion or deposition occurring in any given reach during the flood is computed as $VOL_i = \Sigma (Q_s \Delta T)$ where $VOL_i$ is the net volume change during the flood for subreach $i$, $Q_s$ is the excess transport capacity or supply in subreach $i$ for the given discharge (i.e. supply minus transport capacity), and $\Delta T$ is the time interval corresponding to that discharge from the discretized hydrograph. It is important to note that this procedure yields a net volume of erosion or deposition that occurs in response to passage of the complete flood hydrograph, i.e., we are looking at the <u>net change</u> in volume at the <u>end</u> of the hydrograph. There may be time intervals <u>within</u> the hydrograph where the volume change for that specific

interval would exceed the net volume change for the entire hydrograph. This is important to remember when using the sediment continuity procedure to compute general scour, since an analysis of net changes at the end of a hydrograph may under-estimate a transitory scour condition that might occur during a critical time interval within the hydrograph.

To expedite the calculation procedure when evaluating several hydrographs, the following analysis procedure is suggested. First, identify five to ten discharges adequate to span the discharge range of all hydrographs. After computing the average hydraulic characteristics in each subreach for each discharge, compute the corresponding sediment transport capacities. Then, for each subreach, develop a relationship of the form $Q_s = a\,Q^b$ where $Q_s$ is the sediment transport capacity in cfs, $Q$ is the water discharge in cfs, and $a$ and $b$ are regression coefficients. The analysis of the discretized hydrographs then proceeds as outlined above, with the sediment transport capacity for any given discharge in any given reach obtained by using the appropriate regression relationship.

It is important to note that the sediment continuity analysis described herein is based on the assumption of rigid-boundary conditions. For example, during evaluation of a flood hydrograph, the channel geometry is assumed to remain unchanged throughout the flood. A more accurate analysis technique is to update the channel cross sections for each discharge level of the flood to account for the computed erosion/sedimentation changes. This concept is referred to as quasi-dynamic routing, and is the basis of Level III analysis where computer models such as HEC-2SR are applied. However, for many practical engineering analysis and design problems the application of the sediment continuity procedure is adequate and more cost efficient.

Example - As part of a channel stability study of the Agua Fria River near Phoenix, Arizona, a sediment continuity analysis was conducted for the peak discharge of the 10- and 100-year floods. This application of the sediment continuity procedure provided insight to the short-term response of the channel. The approximate 30-mile study reach was divided into 10 reaches. Average hydraulic and geometric characteristics for the 10 reaches were established from HEC-2 analysis. For the 10-year flood peak the main channel velocities ranged from 5 to 7 feet per second (fps) and for the 100-year, 7 to 10 fps. Sediment transport capacity was estimated by the Meyer-Peter, Muller

bed-load equation in combination with the Einstein suspended load procedure. Reach 1 was utilized as the supply reach from which the sediment continuity calculation began. Table 5.12 gives the results from the analysis and indicates the general scour/deposition condition of each reach.

### 5.3.9 Quantification of Vertical and Horizontal Channel Response

Discussion - Sediment continuity results provide the rate and/or volume of erosion/sedimentation expected in each subreach. More meaningful results are obtained when these values are converted to represent vertical and/or horizontal changes in each subreach. Using the definitions established in Section 5.1.2, sediment continuity results from a single flood would be useful in quantifying general scour/deposition or short-term lateral migration.

Application - In the absence of significant controls the erosion/sedimentation amounts can be assumed uniformly distributed in the streamwise direction for any given subreach. If the cross-streamwise distribution is also assumed uniform, then with knowledge of the reach length and by assuming a representative channel width, typically top width, the uniform depth of vertical adjustment can be evaluated. As an alternative, the cross-streamwise distribution can be done according to flow conveyance; however, this can become a tedious calculation by hand calculator.

In making the distribution, the computed sediment volumes must be corrected for porosity. The sediment transport equations used in the sediment continuity analysis give answers in unbulked volumes per unit time. A porosity factor must be applied to these values to accurately represent the volume changes that will occur in the channel bed. For sand-bed channels, a typical porosity of $n = 0.4$ can be assumed. The unbulked sediment volumes computed by the transport equations are then corrected as follows:

$$V_t = \frac{V_s}{1-n} \tag{5.14}$$

where $V_t$ is the bulked sediment volume, $V_s$ is the sediment volume computed by transport equations, and $n$ is the porosity.

Evaluation of lateral migration amounts is more difficult and not as subjective to a rigorous analysis procedure as are vertical adjustments. The two basic mechanisms of lateral migration can be related to erosion/sedimentation

Table 5.12. Short-Term General Scour/Deposition Response.

| Reach | 10-Year | | | 100-Year | | |
|---|---|---|---|---|---|---|
| | $Q_s$ (cfs) | $\Delta Q_s$ (cfs) | Response | $Q_s$ (cfs) | $\Delta Q_s$ (cfs) | Response |
| 1 | 105 | | | 379 | | |
| 2 | 112 | -7 | Near Equilibrium | 254 | +125 | Deposition |
| 3 | 187 | -75 | Scour | 446 | -192 | Scour |
| 4 | 122 | +65 | Deposition | 541 | -95 | Scour |
| 5 | 158 | -36 | Scour | 581 | -40 | Scour |
| 6 | 131 | +27 | Deposition | 538 | +43 | Deposition |
| 7 | 168 | -37 | Scour | 676 | -138 | Scour |
| 8 | 81 | +87 | Deposition | 465 | +211 | Deposition |
| 9 | 80 | +1 | Equilibrium | 446 | +19 | Near Equilibrium |
| 10 | 106 | -26 | Scour | 492 | -46 | Scour |

$Q_s$ is sediment transport rate, $\Delta Q_s$ is general scour (-)/deposition (+) rates of the flood peak.

trends in the channel. The first mechanism, associated with channel reaches of large w/d (width/depth) ratio where significant sedimentation is occurring, is that which promotes bank instability and lateral migration as a result of increased velocities and shear stresses along the banks as the local energy gradient increases. The second mechanism, associated with channel reaches of small w/d ratio, typically in an erosional mode, is that which causes increased bank instability from bank failures as a result of development of a narrow, deep channel with steep banks.

There are several variations of the first mechanism involving channels where significant sedimentation is occurring. If sedimentation occurs as isolated sand and gravel bars, the local energy gradient increases due to higher flow velocities that result from a reduction in effective channel area. Additionally, relatively stable sand and gravel bar deposits deflect the flow towards the more erodible banklines. Consequently, severe localized bank failures may occur. However, if deposition occurs more uniformly across the channel, the local energy gradient downstream of the deposition increases due to higher velocities resulting from an increase in channel slope. The absence of current deflection and the more gradual increase in velocities results in less severe bank erosion, but erosion takes place over longer distances. Under either situation, quantifying lateral migration amounts from sediment continuity calculations is difficult. Generally, in these types of reaches the assessment of lateral migration potential must be made from qualitative analysis such as historical evidence, meander scars, meander width, geomorphic relationships, etc.

There are also variations of the second mechanism involving a typically erosional reach of the channel. The mode of bank failure as the channel deepens depends on bank material composition. In a channel with predominately clay banks, failure may be by sloughing due to undercutting by low-flow discharges. In a stratified bank with lenses of erodible material, enough of this material may be removed that the block of bank material above tilts downward, opening a vertical tension crack. Ultimately the bank fails in large blocks. Piping can also promote bank failure in a stratified bank. Quantifying lateral migration amounts for erosional reaches is easier than for reaches where sedimentation is occurring. The volume of erosion computed from sediment continuity analysis can be assumed to come entirely from the channel banks or can be distributed between bed and banks. However, since it is dif-

ficult to establish the distribution, and since the direction of lateral migration is not known with certainty, it is sometimes appropriate to assume the required volume first comes entirely from one bank and then the other. The exception to this procedure is when controls inhibit movement in a given direction. Additionally, it may be possible that the entire volume could come from a single location on one bank, for example, a short-radius bend in relatively erodible material.

In both mechanisms of lateral migration, development of saturated banks above the water line can increase bank erosion through local mass wasting. Saturated banks may develop during the rising stage of a flood, during which flow moves into the bank from the river, promoting increased bank stability, particularly in the saturated condition. Flow may also occur from the bank to the river due to a groundwater table that is higher than the river stage. This condition could develop during a wet period as water draining from the watershed saturates the flood plain to a level higher than normal.

Example - A preliminary design for a sewer line in the City of Globe, Arizona, proposed an alignment that followed the Pinal Creek channel for approximately 3 miles. To evaluate the adequacy of the proposed 6-foot burial, an erosion/sedimentation study was conducted. The study included application of the sediment continuity concept to estimate erosion/sedimentation volumes, and then the conversion of these volumes to general scour/deposition estimates.

The analysis was conducted for the 100-year flood (peak discharge 19,500 cfs). For simplicity, the hydrograph was discretized into three discharge levels: one peak and two medium flows. The study reach was divided into eight subreaches and, from a HEC-2 analysis, the average hydraulic conditions for each reach were determined. Sediment transport rates for each of the reaches for all three discharges were then calculated, and the sediment continuity equation (Equation 5.13) applied between reaches to estimate the erosion/sedimentation for each reach. The depth of general scour/deposition was then determined by uniformly distributing the calculated volumes in each reach. Table 5.13 presents the results and indicates as much as 9 feet of general scour is possible; therefore, the 6-foot burial depth was not con-

Table 5.13. Sediment Continuity Results. (100-Year Flood)

| Reach | Average Potential Bed Level Change (feet) |
|---|---|
| 1 | + 4.8 |
| 2 | + 8.3 |
| 3 | - 9.4 |
| 4 | + 1.2 |
| 5 | - 5.9 |
| 6 | - 0.5 |
| 7 | - 4.3 |
| 8 | Supply Reach |

sidered adequate unless some type of channelization or grade control was to be implemented in Reach 3.

5.3.10 Local Scour Concepts

Discussion - Local scour is observed whenever an abrupt change in the direction of flow occurs, such as at bridge piers or embankments. For example, local scour at bridge piers is a result of vortex systems developed at the pier. Local scour occurs when the capacity of the flow to remove or transport the bed materials is greater than the rate at which replacement material is supplied.

During a flood, an equilibrium condition between sediment supply and transport capacity at a scour hole may never become established. During the rising limb of the hydrograph scour occurs and endangers the hydraulic structure. After the peak has passed (during the falling limb), the scour hole refills as sediments drop out with the lower flows. Therefore, the critical time for structural stability during the storm is near the peak flow (see Figure 5.21). Soundings made of scour holes after the storm do not indicate the potentially dangerous situation that might have existed during the storm.

The depth of scour also varies with time depending upon the presence or absence of bed forms. The time required for dune or antidune motion is much larger than the time required for local scour. Thus, even with steady-state conditions, the depth of scour is likely to fluctuate with time when there are dunes or antidunes traveling on the channel bed. The depth of the scour hole is more variable with larger bed forms. When the crest of the dune or antidune reaches the local scour area, the transport rate into the hole increases, the scour hole fills and the scour depth temporarily decreases. When a trough approaches, there is a smaller sediment supply and the scour depth increases to try to re-establish equilibrium in sediment transport rates. A mean scour depth between these oscillations is referred to as equilibrium scour depth.

Application - A number of formulas are available for predicting local scour around bridge piers. Review of these formulas indicates that each is based on those factors that seem most important in evaluating local scour at bridge piers; however, most of these formulas are based primarily on model study data in sand-bed laboratory flumes with little or no field verification. Therefore, it is generally advisable to utilize several formulas to insure a

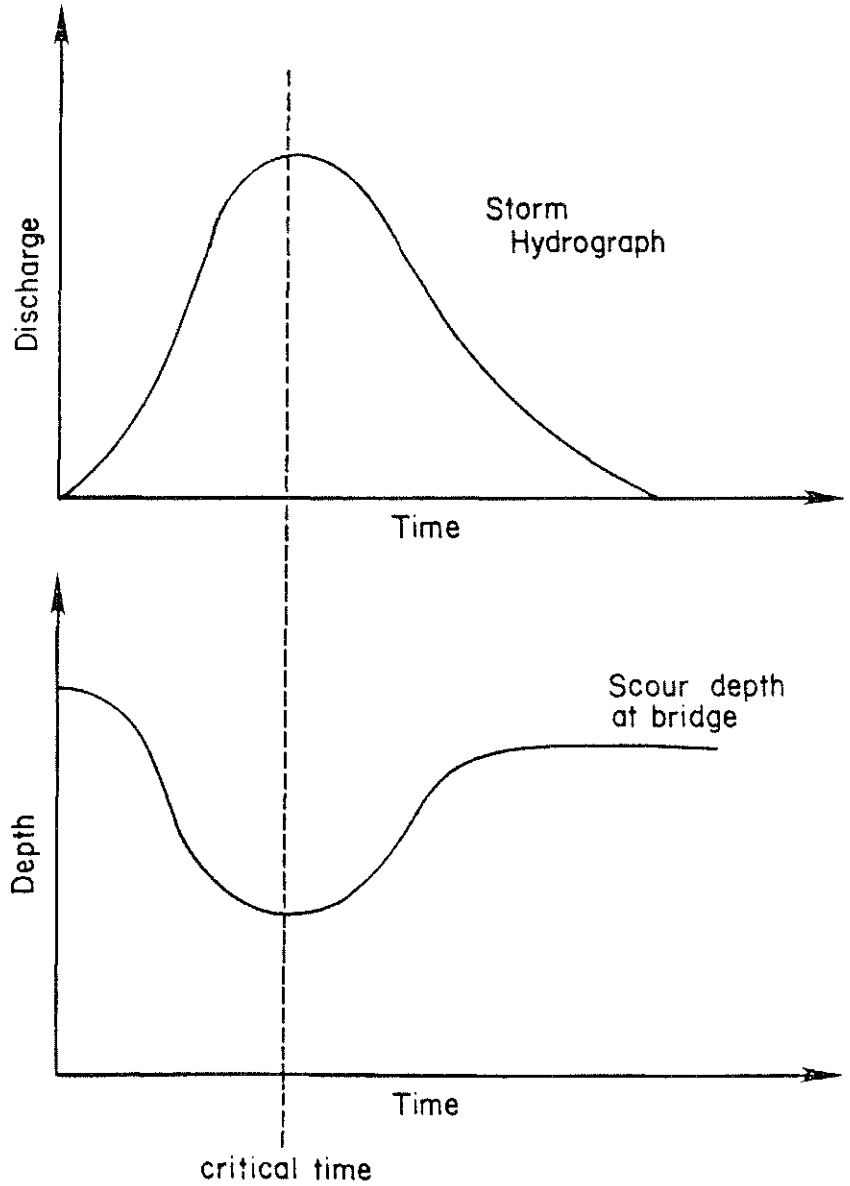


Figure 5.21. Temporal change of scour hole depth during a storm (typical).

reasonably accurate estimate. Several of these formulas have been found to be particularly successful based on previous experience. A relationship for square-nosed piers presented by Richardson, et al. (1975) is

$$\frac{\Delta Z_{\ell s}}{Y} = 2.2 \left(\frac{b_p}{Y}\right)^{0.65} Fr^{0.43} \tag{5.15a}$$

and for a group of circular cylinders

$$\frac{\Delta Z_{\ell s}}{Y} = 2.0 \left(\frac{b_p}{Y}\right)^{0.65} Fr^{0.43} \tag{5.15b}$$

where $\Delta Z_{\ell s}$ is the equilibrium depth of the scour hole, $b_p$ is the pier width (normal to the flow direction), $Y$ is the upstream depth of flow, and $Fr$ is the upstream Froude number ($Fr = V/\sqrt{gY}$ with $V$ the upstream velocity and $g$ the acceleration of gravity).

The equations by Shen et al. (1966, 1969) for circular piers are

$$\Delta Z_{\ell s} = 0.00073\ R_p^{0.619} \tag{5.16a}$$

and

$$\frac{\Delta Z_{\ell s}}{b_p} = 11.0\ Fr_p^2 \qquad \text{for} \quad Fr_p < 0.2 \tag{5.16b}$$

$$\frac{\Delta Z_{\ell s}}{b_p} = 3.4\ Fr_p^{0.67} \qquad \text{for} \quad Fr_p \geq 0.2 \tag{5.16c}$$

respectively, where $R_p$ is the pier Reynolds number ($V\ b_p/\nu$), $V$ is the mean velocity of the undisturbed flow, $b_p$ is the width of pier projected on a plane normal to the undisturbed flow, $\nu$ is the kinematic viscosity, and $Fr_p$ (pier Froude number) is $V/\sqrt{gb_p}$.

The shape of the pier is a very significant parameter with respect to scour depth because it reflects the strength of the horseshoe vortex at the base of the pier. A blunt-nose pier causes the deepest scour. Streamlining the front end of the pier reduces the strength of the horseshoe vortex, thus reducing the scour. Streamlining the downstream end of piers reduces the strength of wake vortices. Common shapes of piers are shown in Figure 5.22. The scour depth generally decreases as a consequence of streamlining, while

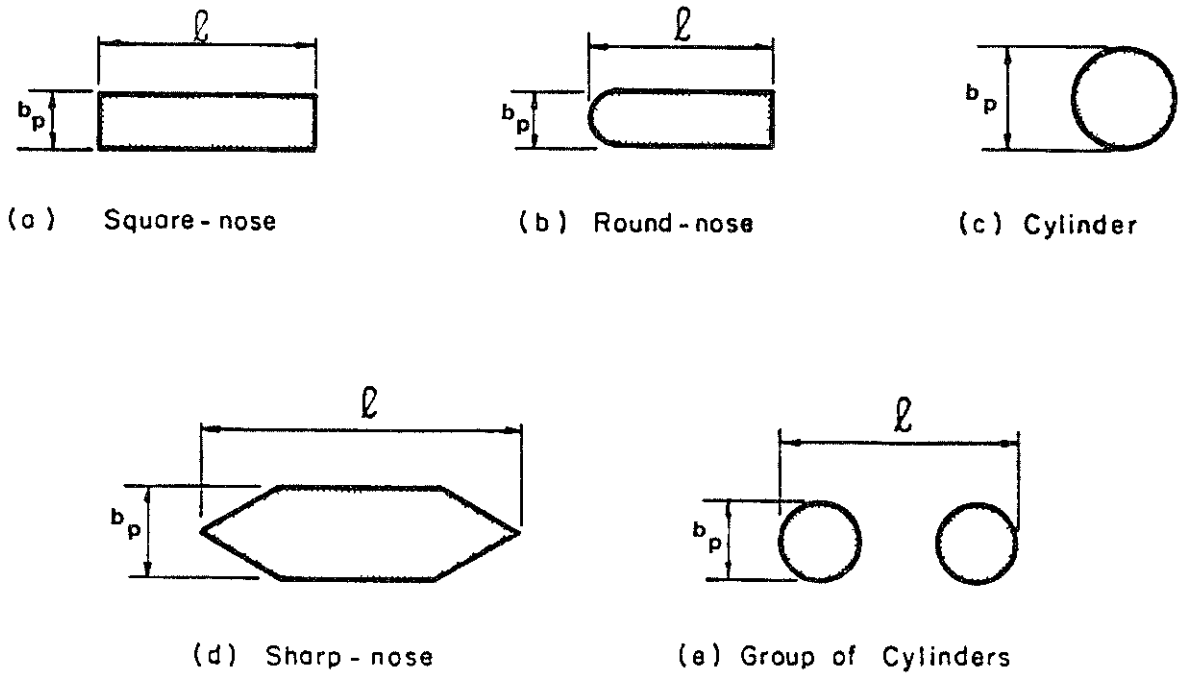


Figure 5.22. Common pier shapes.

skewed pier alignment (pier not parallel with flow direction) will create deeper scour holes. The reduction due to streamlining can be estimated from Table 5.14, while the increase due to skew can be determined from Figure 5.23 (Factor $K_{aL}$). As previously indicated, the maximum scour depth can be considerably greater than the equilibrium scour depth due to dune bed forms. Richardson, et al. (1975) suggest that scour depths can be up to 30 percent greater as a consequence of bed forms. Therefore, when dune or antidune bed forms are possible, a safety factor of 1.3 is recommended, unless the magnitude of the dune or antidune bed forms is calculated as a separate component.

Another important local scour zone at a bridge crossing occurs at the abutments. Detailed studies of scour around embankments have been made only in laboratories. For example, Liu, et al. (1961) investigated scour around vertical wall embankments for subcritical flow in a rectangular laboratory flume with sand-bed conditions and found

$$\frac{\Delta Z_{\ell s}}{Y} = 2.15 \left(\frac{a}{Y}\right)^{0.4} Fr^{0.33} \tag{5.17a}$$

where $Y$ is the upstream normal flow depth, $a$ is the embankment length (measured normal to the wall of the flume in the model studies), and $Fr$ is the upstream Froude number (using the upstream normal flow depth as length dimension). Liu, et al. also presented limited data for spill-through embankments, where a spill-through embankment has sloping sides (i.e. the more commonly constructed earthen embankment). Analysis of the data presented suggests the equation

$$\frac{\Delta Z_{\ell s}}{Y} = 1.1 \left(\frac{a}{Y}\right)^{0.4} Fr^{0.33} \tag{5.17b}$$

Richardson et al. (1975) suggest that Equation 5.17b be applied only for embankments where $a/y$ is less than 25. For embankments where $a/y$ is greater than 25, the equation

$$\frac{\Delta Z_{\ell s}}{Y} = 4\ Fr^{0.33} \tag{5.18}$$

is recommended. This equation was developed from field measurement of embankment scour at rock dikes on the Mississippi River. It is worthwhile to note that embankment scour equations are also useful for estimating local scour at bank protection, spur dikes and jetties.

Table 5.14. Reduction Factors When Applying Formulas for Square Nose Piers to Other Shapes (assuming equal projected widths of piers).

| Type of Pier | Reduction Factor |
|---|---|
| Square nose | 1.0 |
| Cylinder | 0.9 |
| Round nose | 0.9 |
| Sharp nose | 0.8 |
| Group of cylinders | 0.9 |

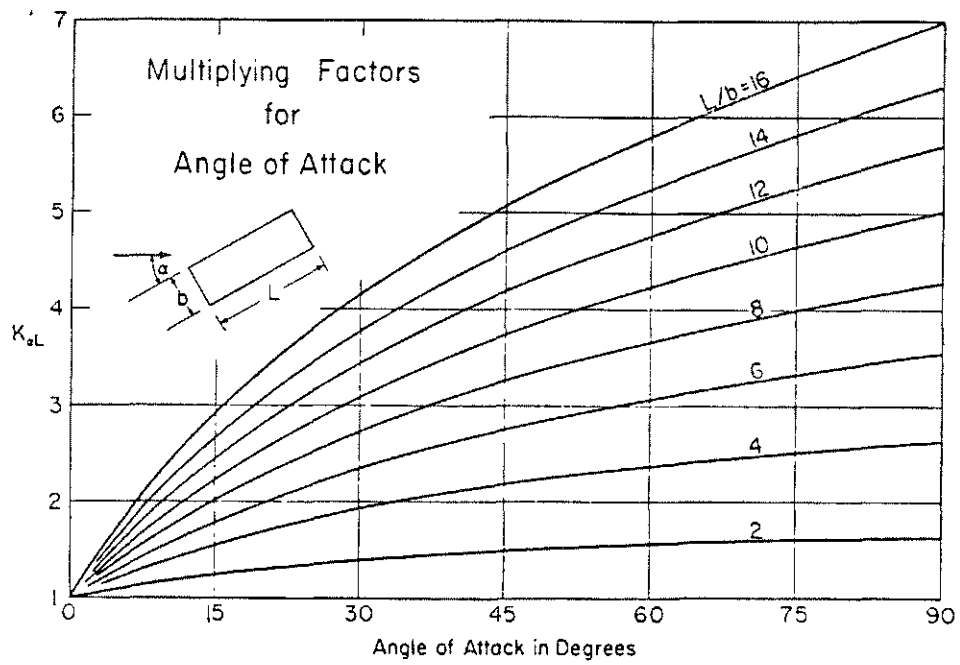


Figure 5.23. Scour increase factor, $K_{aL}$, with flow (from Lauren and Toch, 1956).

One of the difficulties in applying Equations 5.17b and 5.18 is definition of "embankment length." Model study investigations considered only short embankment lengths in smooth, rectangular flumes. In prototype situations, the embankments may span large distances across the overbank of a wide flood plain while stopping short of, or just slightly protruding into, the main channel. Due to the normally large difference in hydraulic characteristics between main channel and overbank flow, caution must be exercised in defining the embankment length for such cases. Figure 5.24 illustrates a recommended embankment length definition for different cases that may be encountered outside the realm of a rectangular laboratory flume. For Case 2 of Figure 5.24, the engineer should compute embankment scour using main channel hydraulics with the value of $a_1$, and compare this result to that obtained using overbank hydraulics with the value for $a_2$. The larger of these two scour depths would be the recommended design value. Due to the sensitivity of Equations 5.17a, 5.17b, and 5.18 to embankment length, engineering judgment should always be applied.

Another difficulty common to any scour calculation is the definition of the base level, and its relation to both flow depths and scour depths. In a nonprismatic natural channel, the upstream normal depth (Y) is generally defined by the hydraulic depth ($Y_h$) for purposes of scour calculations, while the computed scour amounts are referenced to the thalweg elevation. If dunes exist, the upstream normal depth would generally be referenced near the top of the dunes (in consideration of effective flow area), while the scour amounts should be referenced to the bottom of the dunes. In the presence of degradation and/or general scour, the ultimate bed invert elevation should first be established for these scour components, from which local scour depths are then referenced.

Once the scour depth is accurately established, the lateral extent of the scour hole is nearly always determinable from the depth of scour and the natural angle of repose of the bed material. A safety factor of 2 should be applied to the lateral scour hole dimension to account for nonuniform flow conditions. This can be accomplished by dividing the angle of repose by 2 and using the resulting angle to define the sides of the scour hole.

Example - The design of two bridge crossings on the Canada del Oro Wash near Tucson, Arizona, required the evaluation of local scour around the bridge

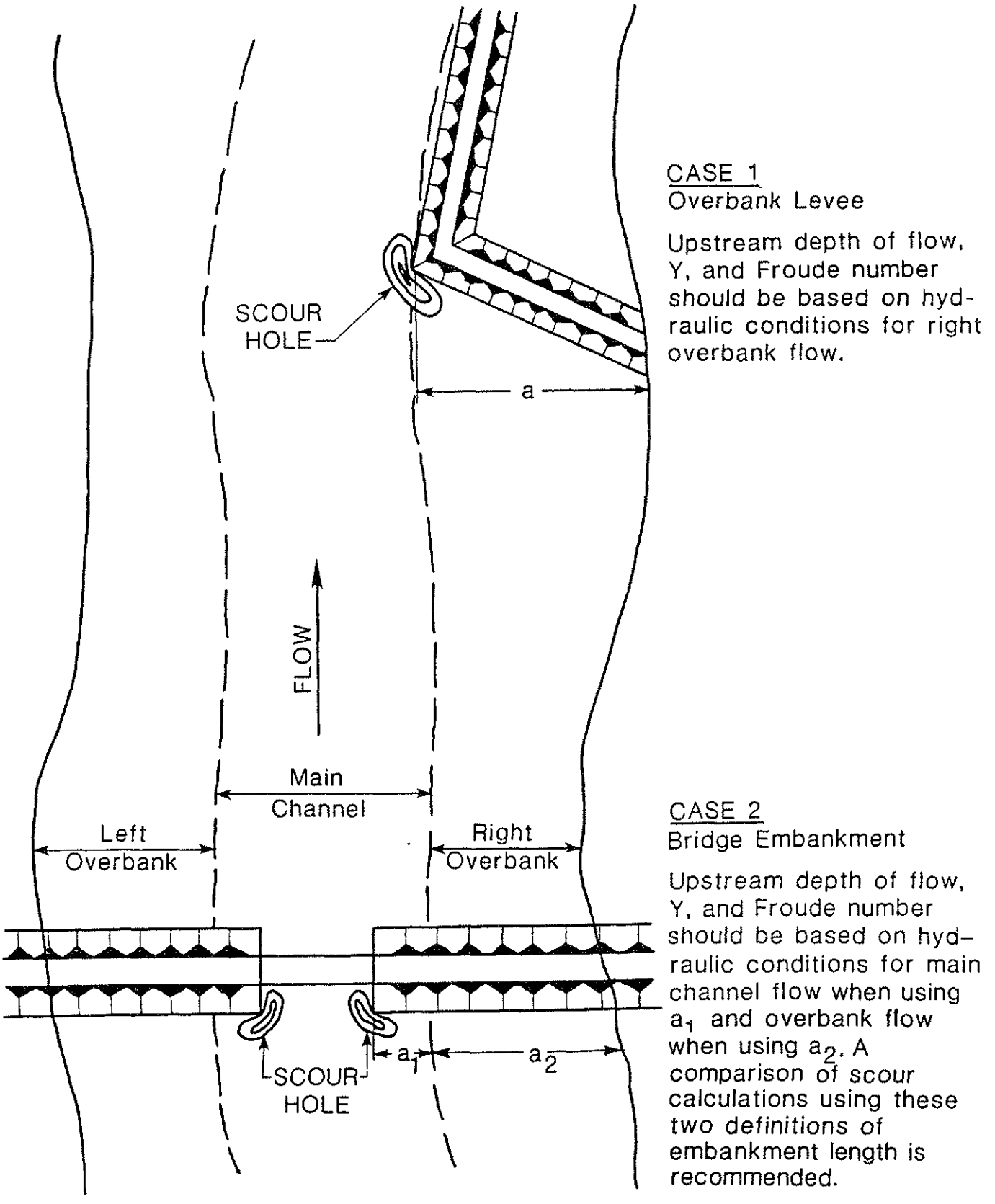


Figure 5.24. Definition sketch of embankment length "a".

piers. Each bent consists of four piers, aligned parallel to the flow (i.e., no skew), and each pier was a concrete cylinder three feet in diameter. The design conditions are stated as follows:

$Q_{100}$ = 33,000 cfs

Y (average depth of flow) = 6.0 feet

V (average velocity) = 18.2 fps

A review of historical photos taken during flood stage at other bridge locations on the Canada del Oro indicates that two additional feet of debris buildup beyond the normal pier width could be expected during a 100-year event. Accordingly, the effective pier width was set as follows:

$b_p$ = pier diameter + 2 = 3 + 2 = 5

Local scour was computed with Equations 5.15b, 5.16a and 5.16b. The computations are shown as follows:

<u>Equation 5.15b</u>: $\Delta Z_{\ell s} = 2.0\ Y\ (\frac{b_p}{Y})^{0.65}\ Fr^{0.43}$

Y and $b_p$ are given above.

$$Fr = \frac{V}{\sqrt{gY}} = \frac{18.2}{\sqrt{32.2 \times 6.0}} = 1.31$$

Substituting in Equation 5.15b:

$$\Delta Z_{\ell s} = 2.0\ (6.0)\ (\frac{5}{6.0})^{0.65}\ (1.31)^{0.43} = 12.0 \text{ feet}$$

<u>Equation 5.16a</u>: $\Delta Z_{\ell s} = 0.00073\ R_p^{0.619}$

where $R_p = \frac{Vb_p}{\nu}$

with an assumed water temperature of 70°F, $\nu = 1.059 \times 10^{-5}$ ft$^2$/sec,

therefore, $R_p = \frac{(18.2)(5)}{1.059 \times 10^{-5}} = 8.5 \times 10^6$

Substituting in Equation 5.16a,

$$\Delta Z_{\ell s} = 0.00073\ (8.5 \times 10^6)^{0.619} = 14.2 \text{ feet}$$

Equation 5.16b: The pier Froude number, $Fr_p$, must first be calculated to determine which form of Equation 5.16b should be used:

$$Fr_p = \frac{V}{\sqrt{gb_p}} = \frac{18.2}{\sqrt{32.2 \times 5}} = 1.43$$

Since $Fr_p > 0.2$, the following equation is used:

$$\Delta Z_{\ell s} = 3.4\ b_p\ Fr_p^{0.67}$$

$$= (3.4)(5)(1.43)^{0.67} = 21.6 \text{ feet}$$

A summary of the calculation is presented as follows:

| | Eq. 5.15b | Eq. 5.16a | Eq. 5.16b |
|---|---|---|---|
| Local equilibrium scour depth | 12.0 ft | 14.2 ft | 21.6 ft |
| | Average = 15.9 ft | | |

Considering the average of the three calculations, 16 feet of local scour could be expected during the design flow. However, because of the similarity of two of the three estimates, it is reasonable to assume that the equilibrium scour depth will probably be less than 16 feet.

5.3.11 Contraction Scour

Dicussion - Contraction scour was defined in Section 5.1.2 as a special case of general scour. Scour at a contraction occurs because the flow area becomes smaller than the normal channel and the average velocity and bed shear stress increase, hence there is an increase in stream power ($\tau V$) at the contraction and more bed material is transported through the contracted section than is transported into the section. As the bed level is lowered, velocity decreases, shear stress decreases and equilibrium is restored when the transport rate of sediment through the contracted section is equal to the incoming rate.

Application - Evaluation of contraction scour is by application of the sediment continuity principle for conditions after equilibrium has been achieved. That is,

$$Q_{s_1} = Q_{s_2} \tag{5.19}$$

where $Q_{s_1}$ is the sediment transport capacity at the upstream section and $Q_{s_2}$ is the value at the contraction. When the sediment transport capacity is expressed in the form of power functions (e.g. as given in Tables 5.6a, 5.6b and 5.7), the relationship is

$$a\ Y_1^b\ V_1^c\ W_1 = a\ Y_2^b\ V_2^c\ W_2 \tag{5.20}$$

Through manipulation and simplification of this equation, a relationship for the flow depth $Y_2$ (after equilibrium is established) can be derived as

$$Y_2 = \left(\frac{q_{s_2}}{a\ q_2^c}\right)^{\frac{1}{b-c}} \tag{5.21}$$

where

$$q_{s_2} = \frac{W_1}{W_2}\ q_{s_1} \qquad \text{(where} \qquad q_{s_1} = a\ Y_1^b\ V_1^c) \tag{5.22}$$

and

$$q_2 = \frac{W_1}{W_2}\ q_1 \tag{5.23}$$

The amount of general scour is then the difference between the pre-scour flow depth and that value from Equation 5.21 after equilibrium had been achieved, i.e.,

$$\Delta Z_{gs} = Y_2 - Y'_2 \tag{5.24}$$

where $\Delta Z_{gs}$ is the general scour depth and $Y'_2$ is the original flow depth at the contraction.

If the site under investigation has hydraulic and sediment properties that fall outside of the limits listed in Tables 5.6a, 5.6b and 5.7, a set of regression coefficients (a, b and c) should be developed for the specific

conditions at that site. For example, this regression analysis can be performed by using the Meyer-Peter, Mueller bed-load equation in combination with the Einstein suspended-load methodology to compute the unit width bed-material load transport rate for a range of discharges at the site under investigation. Each unit transport rate is then regressed against the corresponding velocity and depth parameters for the given water discharges (e.g. as established from HEC-2 results). The results of this regression analysis yield values for a, b and c (describing the equation $q_s = a\ Y_h^b\ V^c$) which can then be used in the above contractual scour analysis. As a less time consuming and less site-specific alternative to the regression analysis approach, the engineer may opt to utilize the scour equations presented on pages 58 through 62 of Sedimentation Engineering, ASCE Manuals and Reports on Engineering Practice No. 54 (1975).

Example - Construction of a bridge will result in a reduction in channel width from 320 to 240 feet. Water-surface profile analysis with the bridge in place established velocity and depth in the reach upstream of the proposed bridge as 8.6 fps and 10 feet, respectively, for a peak discharge of 27,500 cfs. Similarily, at the bridge site the velocity and depth were computed as 10.2 fps and 11.2 feet, respectively.

Considering the bed-material characteristics, the appropriate empirical power relationship for sediment transport (Table 5.6a) is

$$q_s = 3.45 \times 10^{-6}\ Y_h^{-0.693}\ V^{4.60}$$

Therefore, the unit sediment discharge upstream of the bridge is

$$q_{s_1} = 3.45 \times 10^{-6}\ (10)^{-0.693}\ (8.6)^{4.60}$$

$$= 0.014 \text{ cfs/ft}$$

and at the bridge site

$$q_{s_2} = \frac{320}{240}\ 0.014\ \frac{\text{cfs}}{\text{ft}}$$

$$= 0.019$$

The unit water discharge at the bridge site is

$$q_2 = \frac{320}{240}\left(\frac{27,500}{320}\right) = 114.6$$

The flow depth at the bridge site after equilibrium is

$$Y_2 = \left(\frac{0.019}{3.45\text{x}10^{-6}\ (114.6)^{4.60}}\right)^{\frac{1}{-0.693-4.60}}$$

$$= 12.1 \text{ ft}$$

The amount of scour is then

$$\Delta Z_{gs} = 12.1 - 11.2 = 0.9 \text{ ft}$$

5.3.12 Bend Scour

Discussion

The bends associated with meandering channels will induce transverse or "secondary" currents which will scour sediment from the ouside of a bend and cause it to be deposited along the inside of the bend. It is important to note that this scouring mecnanism is caused by the spiral pattern of secondary flow, and is not due to a shift of the maximum longitudinal velocity filament against the outer bank. Channel bends will cause a shift in this velocity filament, but through the bend the maximum longitudinal velocity is normally moved nearer to the inside bank, whereas the shift to the outer bank occurs downstream of the bend. It is at these downstream locations that the shift in longitudinal velocity patterns will most likely cause lateral erosion of a channel bank.

The discussion presented in this manual will address the vertical scour potential in a channel bend. A review of technical literature will reveal the existance of several theoretical relationships that have been developed to predict the amount of scour through a river bend. To date, there is no known procedure which consistently yields an accurate prediction of bend scour through a wide range of hydraulic and geometric conditions. Based on the assumption of constant stream power through the channel bend, Zeller (1981) developed the following relationship for estimating the maximum scour component resulting from channel curvature in sand-bed channels:

$$\Delta Z_{bs} = \frac{0.0685}{Y_h^{0.4}} \frac{YV^{0.8}}{S_e^{0.3}} \left[2.1 \left(\frac{\sin^2 \frac{\alpha}{2}}{\cos \alpha}\right)^{0.2} - 1\right] \tag{5.25}$$

where $\Delta Z_{bs}$ = bend scour component of total scour depth (feet)

$V$ = mean velocity of upstream flow (fps)

$Y$ = maximum depth of upstream flow (feet)

$Y_h$ = hydraulic depth of upstream flow (feet)

$S_e$ = upstream energy slope (bed slope for uniform flow conditions, feet/feet)

$\alpha$ = angle formed by the projection of the channel centerline from the point of curvature to a point which meets a line tangent to the outer bank of the channel (degrees, see Figure 5.25)

Mathematically, it can be shown that, for a simple circular curve, the following relationship exists between $\alpha$ and the ratio of radius of curvature to channel topwidth.

$$\frac{r_c}{W} = \frac{\cos \alpha}{4 \sin^2(\frac{\alpha}{2})} \tag{5.26}$$

where $r_c$ = radius of curvature to centerline of channel (feet)

$W$ = channel topwidth (feet)

If the bend under evaluation deviates significantly from a simple circular curve, the engineer should consider dividing the bend into a series of circular curves and analyzing the bend as a compound curve. Under this procedure, there would be a different value of $\alpha$ determined for each segment of the compund curve. A scour depth would then be computed for each segment of the curve using the $\alpha$ determined for that segment.

Application

Equation 5.25 can be applied to natural river bends to get an approximation of the scour depth that can be expected in the bend during a specific water discharge. The impact that other simultaneously occurring phenomena such as sand waves, local scour, long-term degradation, etc., might have on bend scour is not known for certain. In order that the maximum scour in a

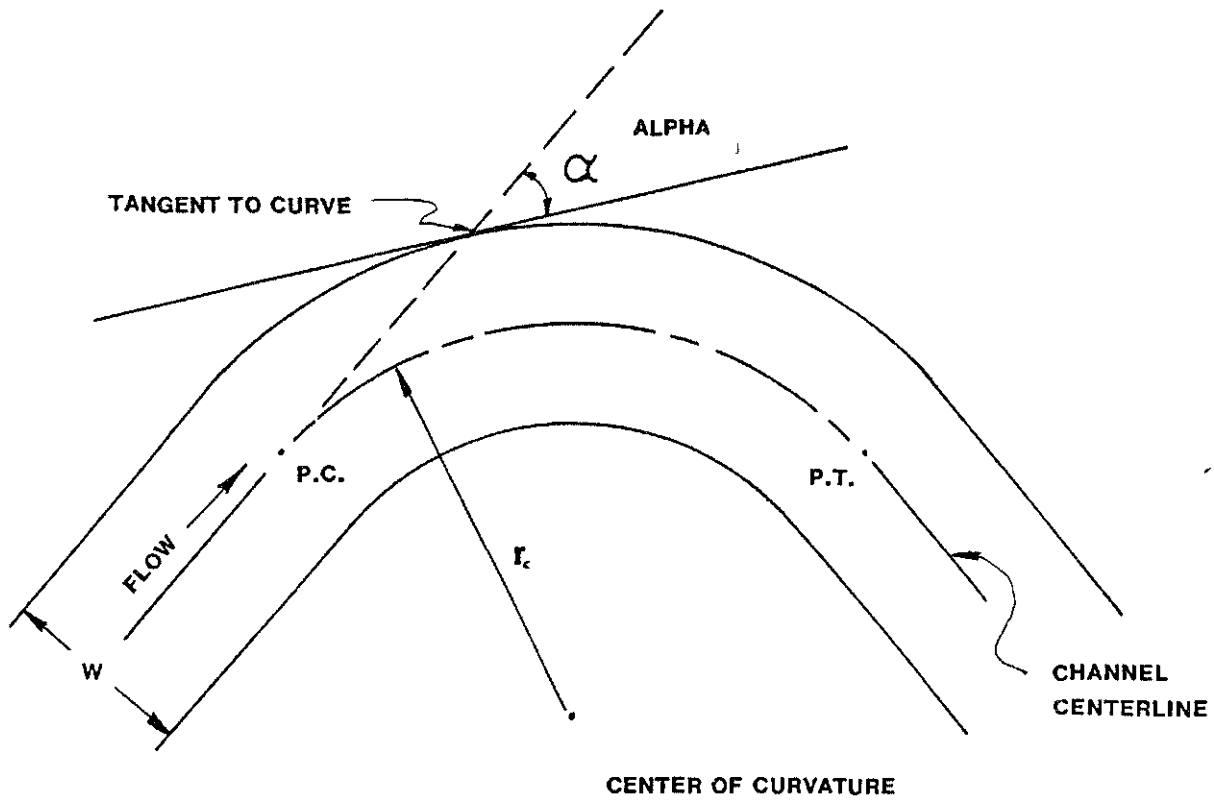


Figure 5.25 Illustration of terminology for bend scour calculations.

bend not be underestimated, it is recommended that bend scour be considered as an independent channel adjustment that should be added to those adjustments computed for long-term degradation, general scour, and sand wave troughs. Whether or not bend scour should be added on top of local scour would depend on the type of obstruction creating the local scour. For isolated structures, such as transmission towers, that would not appreciably disrupt the secondary flow pattern responsible for bend scour, it would be recommended that bend scour and local scour be computed separately and added together. For the case of a series of armored spur dikes placed along the outside bank of a bend, the spiral flow pattern may be disrupted to the point that significant bend scour would not occur. Engineering judgement would have to be exercised in such cases when computing the total vertical scour that might occur in the channel bed.

The longitudinal extent of the bend scour component is as difficult to quantify as the vertical extent. Rozovskii (1961) developed an expression for predicting the distance from the end of a bend at which the secondary currents will have decayed to a negligible magnitude. This relationship is:

$$X = 2.3 \left(\frac{C}{\sqrt{g}}\right) Y \qquad (5.27)$$

where X = distance from the end of channel curvature (point of tangency, P.T.) to the downstream point at which secondary currents have dissipated (feet)

C = chezy coefficient

g = gravitational acceleration (32.2 feet/second$^2$)

Y = depth of flow (to be conservative, use maximum depth of flow, exclusive of scour, within the bend) (feet)

Equation 5.27 should only be used as a guide in determining the distance downstream of a curve that secondary currents will continue to be effective in producing bend scour. As a conservative estimate of the longitudinal extent of bend scour, both through and downstream of the curve, the engineer would be advised to consider bend scour commencing at the upstream point of curvature (P.C.) and extending a distance X (computed with Equation 5.27) downstream of the point of tangency (P.T.) Engineering judgement should be used in electing to deviate from this generalized recommendation.

Example

Proposed channel improvements on a river system include the installation of soil-cement on the channel banks to prevent bank erosion. The river reach where these improvements are to be installed includes a channel bend which has the following hydraulic data:

| | |
|---|---|
| $Y = 9.39'$ | $S_e = 0.0013$ ft/ft |
| $V = 12.62$ fps | $\alpha = 24°$ |
| $Y_h = 9.18'$ | $n = 0.025$ |

In order to prevent undermining of the soil cement bank protection, it is desired to extend the soil-cement a certain distance below the natural channel bed. This toe-down depth will include allowances for long-term degradation, general scour, sand wave troughs and bend scour. The maximum bend scour component of the toe-down depth is computed as follows:

$$\Delta Z_{bs} = \frac{0.0685\ YV^{0.8}}{Y_h^{0.4} S_e^{0.3}} \left[2.1 \left(\frac{\sin^2 \frac{\alpha}{2}}{\cos \alpha}\right)^{0.2} - 1\right]$$

$$\Delta Z_{bs} = \frac{0.0685\ (9.39)\ (12.62)^{0.8}}{(9.18)^{0.4}(0.0013)^{0.3}} \left[2.1 \left(\frac{\sin^2 12°}{\cos 24°}\right)^{0.2} - 1\right]$$

$$\Delta Z_{bs} = 2.09 \text{ feet (use 2.1 feet)}$$

This dimension (2.1 ft) will be added to any other computed vertical bed adjustments (general scour, sand wave troughs, etc.) for the curved portion of the channel. The distance downstream of the curve to which the bend scour component will be applied, is computed using Equation 5.27.

$$x = 2.3 \left(\frac{C}{\sqrt{g}}\right) Y$$

where $C = \frac{1.486}{n} R^{1/6}$

For the design flow, the hydraulic radius, R, was determined to be 9.03 feet. Accordingly, C is computed as follows:

$$C = \frac{1.486}{0.025} (9.03)^{1/6}$$

$$C = 85.77$$

Substituting into Equation 5.27:

$$X = 2.3 \left(\frac{85.77}{\sqrt{32.2}}\right) (9.18)$$

$$X = 319 \text{ feet}$$

Therefore, the bend scour component (2.1 feet) will be applied to the soil-cement toe-down depth through the entire curve and for 319 feet downstream of the point of tangency of the curve.

5.3.13 Evaluation of Low-Flow Channel Incisements

Discussion - When large width-depth ratios exist, consideration should be given to the development of low-flow channels. For example, a channel formed predominantly by a 5-year to 10-year flood will develop width and depth characteristics to carry this relatively large discharge in a hydraulically efficient manner; however, for smaller floods these channel dimensions may result in a flow pattern approaching sheet flow conditions. Rather than carrying the flow in this manner, the channel will develop a low-flow channel that provides more efficient conveyance of the low-flow discharges. The development of a low-flow channel will create entirely different hydraulic conditions than those occurring in the original channel geometry, and may create bank instability from incisement. Therefore, it is important for the engineer/designer to anticipate the potential for low-flow channel incisement.

Application - There are no rigorous methodologies for the prediction of low-flow channel incisement. A field inspection of the study area is probably the best method to determine the potential for low flow channel incisement. If the existing channel has developed a low-flow channel, then it is appropriate to use the observed incisement depth for design purposes. If the existing channel does not have low-flow incisement, but proposed channelization or other changes result in conditions favorable for low-flow channel development, then as a rule of thumb a reasonable incisement depth ($\Delta Z_i$) is one to two feet. The incisement depth should be added to any other vertical channel

adjustment that is used to determine the burial depth of piers, pipelines, bank stabilization, etc.

5.3.14 Evaluation of Gravel Mining Impacts

Discussion - Common gravel mining practices in arid areas include instream mining, flood-plain mining and terrace mining. Instream and flood-plain mining activities have potential impacts on the river response and require adequate hydraulic, erosion and sedimentation analyses to develop an acceptable mining plan. For example, sand and gravel mining may affect the sediment movement and supply in a channel system. Such operations can be beneficial or detrimental, depending on watershed and river characteristics and on the mining and management practices followed.

Excessive sand and gravel removal from a river channel (removal greater than supply in any given reach) can endanger the stability of the river system and bridges by inducing general scour and headcutting. For example, bridges over the Salt, Gila and Agua Fria Rivers have been endangered during floods due to significant bed erosion and/or lateral migration of channels. Sand and gravel mining in the river channel has been identified as a contributor to documented bridge instability and/or failure. Analysis of the effects of sand and gravel mining on the stability of a river system and bridges is important, and protection of the bridges may be required where the sand and gravel mining is of significant magnitude.

On the flood plain adjacent to the river channel many of the same processes are at work; however, impacts are generally restricted to overbank flooding conditions. Water and sediment transport rates over the flood plain are generally reduced by the influence on resistance to flow of such flood plain features as vegetation and structures. Just as headcutting above instream gravel pits can endanger upstream bridges, erosion of flood plain gravel pits could encroach on adjacent properties or threaten nearby structures. Of equal concern when flood flows spill over into a gravel pit is the potential erosion of a dike or buffer zone designed to separate the pit from the active river channel. A headcut and erosion through such a buffer zone could alter local river channel characteristics and transport rates, and impact both upstream and downstream reaches. If the channel reach adjacent to a flood plain gravel pit is geomorphically active, e.g., migrating laterally,

the same result might occur if protective measures or an adequate buffer zone are not provided during site development.

Application - The extent of damage to the system that can result from a headcut induced by sand and gravel mining is a function of volume and depth of the gravel pit, location of the pit, bed-material size, flood discharge, and sediment inflow rates and volume. The presence of an instream gravel pit can add energy to the system by increasing the water-surface slope, or energy slope, just upstream of the pit. The steeper slope has greater erosive power and can initiate bank erosion and headcutting. These processes can tip the balance of sediment transport and induce degradation just upstream of the pit and aggradation in the pit. When storm runoff impinges on the gravel pit the energy slope, flow velocity and sediment transport capacity increase at the upstream boundary of the gravel pit and then attenuate in the gravel pit. In response to the changes of sediment transport capacities at the pit boundary, the channel initiates bank sloughing and/or downcutting upstream of the pit. Furthermore, since the velocity of flow through the pit is negligible compared with both the flood-plain and main channel velocities, the pit will act as a sediment trap. Due to this lowered velocity, water leaving the pit does not have the capacity to carry sand- and gravel-sized material. This relatively sediment-free water will flow back into the main channel downstream, and thus the possibility of general scour due to the introduction of clearer water into the main channel must be considered.

The length of time during which conditions are favorable for bank erosion and headcutting depends on the volume of the pit and on the inflow hydrograph. For a low-flow event an instream pit will not fill or reach equilibrium as soon as it will during a high-flow event. During a high-flow event the rising limb of the hydrograph rapidly fills the pit with water and drowns out the effect of a steeper energy slope. This concept is illustrated in Figure 5.26 for representative low- and high-flow hydrographs. The crosshatching indicates the relative times required to fill a gravel pit to the level where channel hydraulics control the flow conditions.

For a gravel pit in the overbank, low flows are generally not of concern. Flood flows will not be of concern until overbank flows occur. While overbank flows are filling a flood plain gravel pit, the same potential exists for headcutting and erosion as with an instream pit; however, once the flood plain pit is filled, it will constitute only a pool or slack-water area on the flood

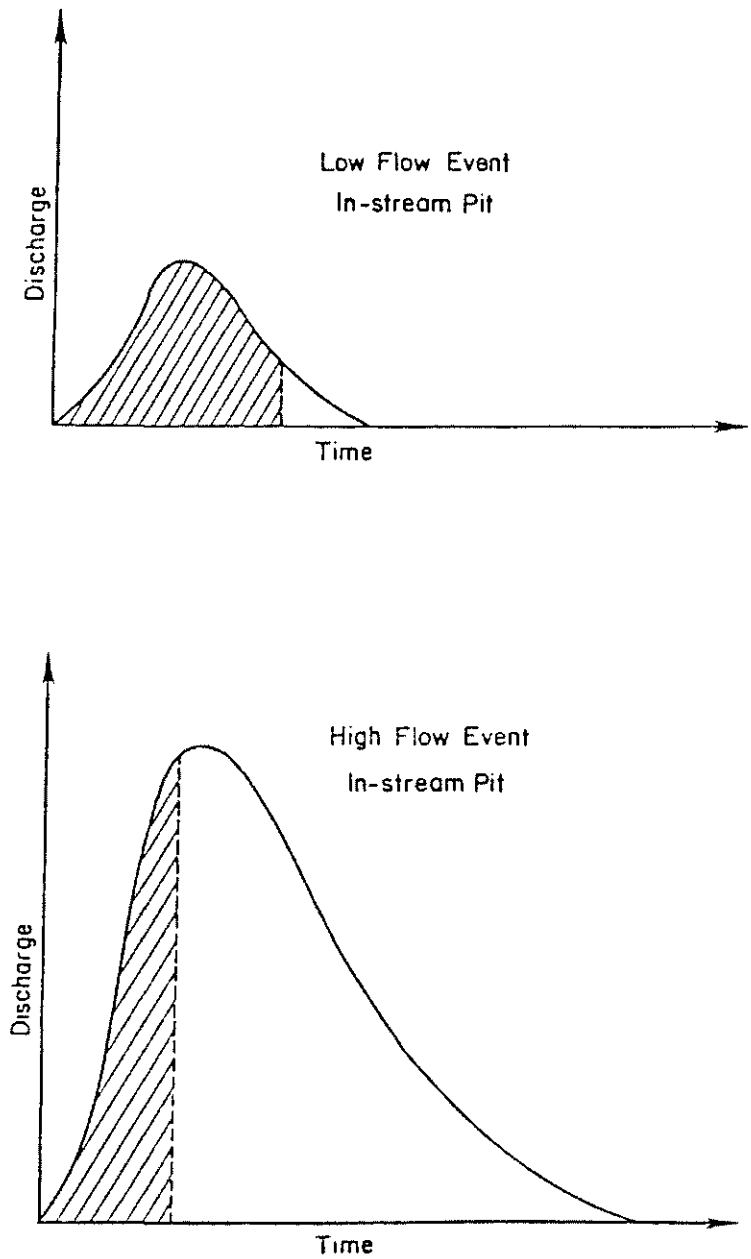


Figure 5.26. Relative time for filling a gravel pit and reaching equilibrium for a low and high flow event.

plain. The central segment of the hydrograph, then, is critical to the stability of a flood plain pit. This concept is illustrated in Figure 5.27, in which the crosshatched area represents the time between overbank spill into the pit and final filling of the pit.

The scour and deposition problems associated with sand and gravel mining are very complicated. Simplifying assumptions are needed to obtain a practical and economical solution. The dominant physical processes include water runoff, sediment transport, sediment routing by size fraction, degradation, aggradation, and breaking and forming of the armor layer. These processes are unsteady and complicated in nature. Furthermore, each situation is unique and requires independent analysis. No standard procedure can be adopted which is universally applicable to all gravel mining evaluations. However, some typical steps that might be required to analyze a headcut profile upstream of a gravel pit would include:

1. Selection of a design hydrograph. Several hydrographs may be evaluated to determine the sensitivity of the gravel pit to different size and shapes of hydrographs.

2. Determine gradation of bed material.

3. Compute hydraulic parameters (velocity and depth) for a range of slope values and the anticipated headcut geometry.

4. Determine unit discharge sediment transport relationship representative of the conditions identified in Steps 2 and 3.

5. Dimension pit geometry for beginning of flood conditions.

6. Select upstream sediment supply cross section and develop transport equation.

7. Route discretized hydrograph through sediment supply section and gravel pit. Adjust bed profile upstream and downstream of the pit entrance at the end of each time step to balance the volume of material eroded from the upstream edge of the pit with the volume of material deposited within the pit.

Example - An instream sand and gravel mining operation just downstream of the Oracle Highway Bridge over Rillito Creek in Tucson, Arizona, was analyzed. The reach length studied was approximately two miles (river mile 4.00 to 6.1), with the bridge located at river mile 5.05. The gravel pit extended from mile 4.65 to 5.03. Assumed dimensions of the pit for analysis purposes were 10 feet deep by 400 feet wide by approximately 2,000 feet long. Upstream of

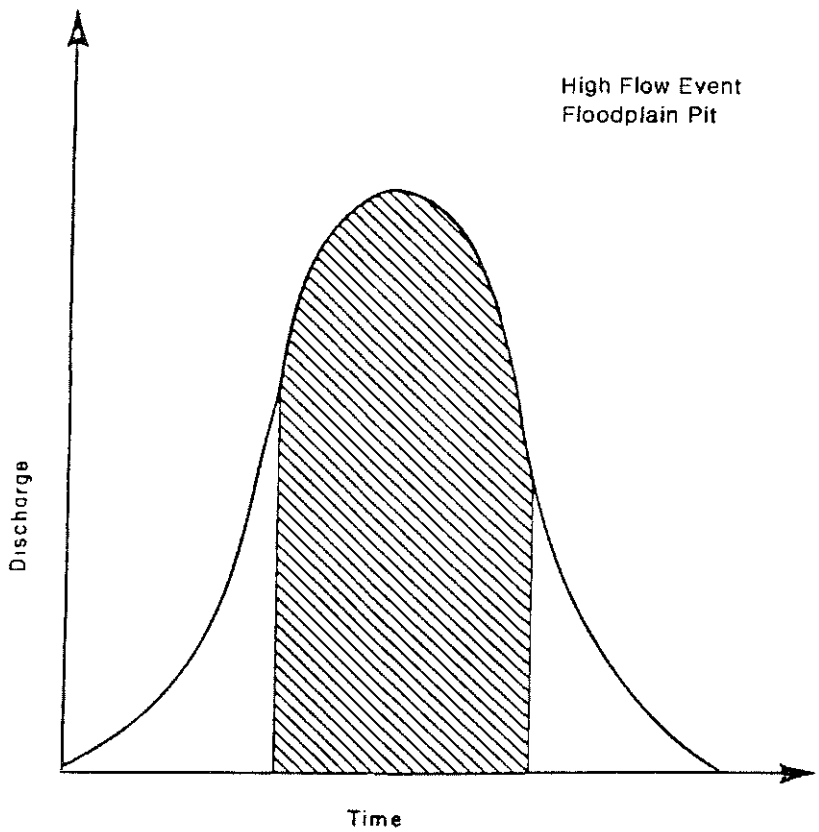


Figure 5.27. Critical time for erosion of a floodplain gravel pit.

the bridge the channel is 350 feet wide. Five cross sections were used within the pit to define the geometric conditions.

The hydrograph used for testing was the two-year flood event with a peak discharge of 7,000 cfs. The 18-hour duration was divided into six time steps of three hours each. The changes occurring in the geometry of the upstream edge of the pit were defined at each of these time increments.

The inital condition was a dry river bed and an empty gravel pit (i.e., no water). Prior to filling the pit with water and sediment, a normal depth approximation was used, rather than the HEC-2 analysis, to determine the hydraulic conditions and sediment transport rate needed for the headcut profile calculations. After the pit filled with water, HEC-2 analysis was used to define the hydraulic conditions. The inflow occurring during the first time step (three hours) initiates the headcut by eroding the corner off the upstream edge of the pit and depositing sediment in the bottom of the pit at the upstream end (Figure 5.28). The slope of the headcut and deposited material is 0.050; however, a discontinuity of 2.40 feet exists. At time 5.20 hours the discontinuity between the headcut and deposition slope disappears and a continuous slope of 0.050 exists. The changes occurring throughout the hydrograph are illustrated in Figure 5.28. The pivot point actually shifted upstream 18 feet, although the resolution on the figure does not illustrate this. The calculated scour occurring at the bridge as a result of the headcut was 4.7 feet at the end of the storm, which is consistent with actual soundings that indicated approximately five feet of general scour for this event.

### 5.3.15 Cumulative Channel Adjustment

Discussion - The potential vertical adjustment of the channel bed in any given reach is determined from consideration of all the possible incremental adjustments. For example, it is possible that a given reach will be simultaneously degradational while local scour and contractual scour are occurring at the bridge crossings. In this situation the three erosion components would have to be accounted for to establish the ultimate bed elevation.

Application - The cumulative channel adjustment at any given location is the summation of six possible components:

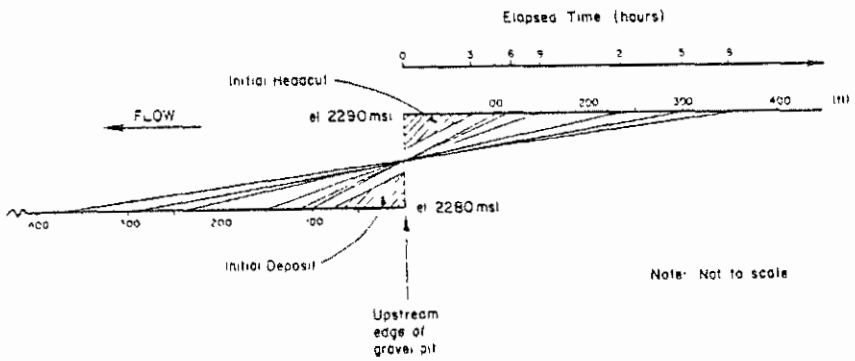


Figure 5.28. Definition sketch of the temporal changes at the upstream edge of a gravel pit.

$$\Delta Z_{tot} = \Delta Z_{deg} + \Delta Z_{ls} + \Delta Z_{gs} + \Delta Z_{bs} + \Delta Z_i + \frac{1}{2} h_a \qquad (5.28)$$

where $\Delta Z_{tot}$ is the total vertical adjustment in bed elevation, $\Delta Z_{deg}$ is the change from long-term degradation (Section 5.3.9), $\Delta Z_{ls}$ is the local scour depth (Section 5.3.10), $\Delta Z_{gs}$ is any relevant general scour depth (e.g. Section 5.3.11 or 5.3.14), $\Delta Z_{bs}$ is the bend scour depth (Section 5.3.12), $\Delta Z_i$ is the low-flow incisement depth (Section 5.3.13), and $h_a$ is the antidune wave height (Section 4.6.2). As a conservative practice, any long-term aggradation amount that might mitigate some elevation decrease is normally not considered.

Due to the complex interaction that will occur among these six phenomena, it is perhaps impossible to accurately predict the total cumulative bed adjustment that might occur at a given location. The hydraulic parameters (velocity, depth, top width, etc.) that are used to compute the dimension of each phenomenon will constantly change as this interaction proceeds; however, the parameters that are used in the calculations are normally based on rigid-bed conditions which give no consideration to channel geometry changes that may be initiated as a result of the simultaneous occurrence of all or part of the six phenomena. Accordingly, the application of a factor of safety to the total computed vertical adjustment ($\Delta Z_{tot}$) is very judgmental, i.e., no firm value can be recommended. In deciding to apply a factor of safety to the computed result, the engineer should consider the magnitude of damage that might accompany a design failure, the probability or risk that such an event might occur, the construction cost associated with applying a safety factor, and the reliability of the data that were used in the channel adjustment calculations. Depending upon the answer to such questions, typical safety factors will probably range from 1.0 to 1.5.

Example - In the example of Section 5.3.9, a potential degradation of 9 feet was calculated for Reach 3 of the Pinal Creek channel. For purposes of illustration, assume a bridge crossing in this reach produces local scour at the bridge piers of 12 feet and 0.5 feet of general scour through the contraction. The channel is straight through this reach of Pinal Creek, therefore bend scour is not applicable. Inadequate data exist to compute low-flow channel incisement, and therefore a value of one foot is assumed. The potential antidune height is calculated as 3.9 feet. Therefore, the total possible scour at the bridge piers, considering a safety factor of 1.0, is

$$\Delta Z_{tot} = 9 + 12 + 0.5 + 0 + 1.0 + \frac{1}{2}(3.9)$$

$$= 24.5 \text{ ft}$$

## 5.4 Level III Analysis

### 5.4.1 General

As discussed in Section 2.4.4, Level III analysis involves application of various physical-process mathematical models and provides the most accurate method of analysis. Physical-process models represent the system being modeled by dividing it into the relevant components, or physical processes. In comparison with regression-based models, where several controlling physical processes may be lumped into one parameter or equation, physical-process models uniquely consider the governing equations of each relevant physical process. For example, a physical-process model for water routing from a watershed would include equations describing interception losses, infiltration rates, overland flow routing, and channel flow routing. The sophistication of most physical-process models, particularly in terms of the number of physical processes considered and the iterations performed in solution of various equations, requires computer application for solution.

### 5.4.2 Application of Level III Analysis

The decision to conduct a Level III analysis is generally based on project objectives under the constraints of time and budget. For engineering analysis of fluvial systems, the most common Level III analysis applied is the evaluation of erosion/sedimentation using a moveable-bed model. Models developed for this purpose include HEC-6 (U.S. Army COE), HEC-2SR (Simons, Li & Associates, Inc.) and others. With a moveable-bed model the channel geometry is updated during a given flood simulation to reflect the erosion/sedimentation that has occurred. In contrast, the sediment continuity procedure (discussed in Section 5.3.6) is a simplification of this analysis where the channel boundary is not updated. Generally, results of sediment continuity tend to overpredict, providing conservative erosion/sedimentation volumes. Therefore, the decision to conduct a Level III analysis might be motivated by the desire or need for more accurate, refined results.

This need for more accurate results must be balanced by the time and money available. As the analysis becomes more complicated, accounting for

more factors, the level of effort necessary becomes proportionally larger. In the analysis of fluvial systems no computer model can be treated as a black box. Proper application of the model relies upon an understanding of how the model operates and upon careful evaluation and interpretation of results. As with any model, the computer is simply a tool to expedite tedious or multiple calculations, and conclusions will still rely on engineering judgment and interpretation.

This concern illustrates the value of the three-level analysis approach, where the results of Levels I and II provide insight and guidance to the Level III analysis. The Level III analysis is never a substitute for Levels I and II; rather, the results of all three levels complement each other and minimize the risk of erroneous conclusions. To initiate analysis of a complicated problem with a Level III approach prior to Levels I and II could not only provide incorrect solutions, but result in wasted time and effort.

As discussed in Section 5.3.6, for many practical engineering problems the sediment continuity analysis of Level II is adequate, without incurring the time or expense of a Level III analysis. In deciding if the Level II analysis is adequate, each case will need to be evaluated independently, weighing the objectives of the project against the available time and budget.

# VI. CHANNEL DESIGN CRITERIA

## 6.1 General

Information presented in Chapters I to V provides the basic tools to conduct a comprehensive engineering analysis of fluvial systems. Not all the techniques and methodologies presented will be applicable or necessary in every situation encountered. Project objectives and scope will determine the type of analysis and level of sophistication necessary. Through proper selection and application of the methodologies presented, the engineer or designer can complete a logical sequence of analyses that will provide a comprehensive understanding of the fluvial system and its response mechanisms.

Such knowledge of the fluvial system is useful in and of itself in order to explain various historical events and/or to predict possible future conditions. Furthermore, and of equal importance, such knowledge will establish the design criteria for channelization, bridge design, bank revetment and other structures located in the channel or flood plain. Information useful to both major and minor engineering design has been presented in Chapters I to V. Major design is one where if failure occurred, loss of life is possible and/or loss of property could be significant. For a minor design, lives are not in jeopardy and the potential loss of property is relatively insignificant. Major drainage design involves application of the more rigorous analysis procedures that provide reasonable quantitative results. Conversely, minor drainage design can often be completed using simplified concepts, rules of thumb, minimum criteria, etc. The following sections briefly discuss some of the specific applications of information in Chapters I to V to both major and minor engineering design work.

## 6.2 Bank/Levee Height

The total bank/levee height required will be the bank/levee height necessary to contain the design flood plus any freeboard. The minimum guidelines discussed in Section 4.6.5 (2.0 ft in rectangular, 2.5 ft in concrete trapezoidal, riprap or soil cement channels, and 3.0 for earthen levees) provide a means of checking the results of Equations 4.28a and 4.28b. These guidelines are often adequate for direct application to minor structure design. For major or minor designs with Froude numbers near one, an additional factor of safety may be appropriate due to the potential for standing waves and other flow instabilities, if such phenomena cannot be directly quantified.

## 6.3 Bank/Levee Toedown

Toedown is the distance bank revetment must be buried to prevent undermining as the bed elevation fluctuates. Equation 5.28 of Section 5.3.15 provides the total cumulative channel adjustment possible from six components (degradation, local scour, general scour, bend scour, low flow incisement and bed forms). Local conditions will establish which of these components must be accounted for.

Selection of a safety factor is dependent upon acceptable risk, construction costs, available data and sophistication of analysis, i.e. Level I, II or III. As stated in Section 5.3.15, safety factors will probably range from 1.0 to 1.5. Due to the nature of sediment transport calculations and the importance and expense of bank revetment, engineering judgment should always be applied.

## 6.4 Lateral Migration

One important application of lateral migration analysis (Section 5.3.9) in design work is for establishing a buffer zone for erosion and flooding in which development would not be considered prudent. In this context, the operational definition of the term "prudent" is related to the concepts of hydrologic uncertainty, that is, the acceptable degree of risk established by the return period (recurrence interval) of a hydrologic event. The National Flood Insurance Program establishes as a precedent that when considering hydrologic events in urban areas it is generally not considered an exercise of sound judgment to accept a degree of risk any greater than that associated with the 100-year event. With reference to the calculated risk diagram (Figure 6.1), using the 100-year event as a basis for the definition of "prudent" implies that there is a 90 percent certainty that the event will not occur in a 10-year period and about 78 percent certainty that it will not occur in 25 years. Conversely, this means acceptance of a calculated risk of 10 percent in a 10-year period and 22 percent in a 25-year period if boundaries of the buffer zone are based on the erosion and flooding potential of a 100-year flood. Asking a property owner to accept a greater risk than this would not appear to be prudent.

While damages due to flooding are generally associated with a single, short-term event, the impacts of erosion (lateral migration) can also be cumulative over the long term. Consequently, one must assess the erosion poten-

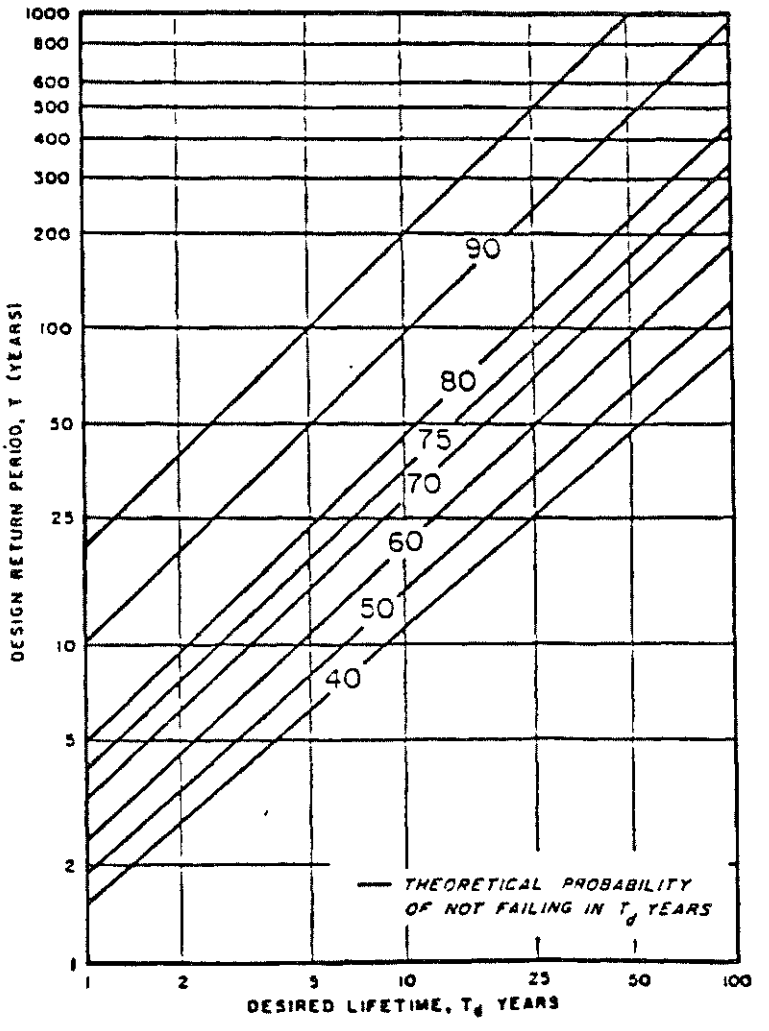


Figure 6.1. Calculated risk diagram.

tial not only of a single event, such as a 100-year flood, but also the cumulative impact of a series of smaller flows. One approach to evaluating long-term erosion impacts is to develop a "representative" annual storm and then to extrapolate in time the effect of this storm. This concept is similar to the practice in hydrology of adopting the two-year flood as being representative of the annual event; however, for purposes of long-term erosion analysis the representative annual event can be more accurately defined by a probability weighting of the erosion resulting from several single storms (see Section 3.4). With this approach the long-term analysis of erosion potential accounts for the probability of occurrence of various flood events during any one year.

After establishing the representative annual storm for evaluating long-term erosion (lateral migration) potential, the duration in years defining the "long term" must be determined. For example, based on both the limitations of the probability weighting approach and the single-event probability of occurrence of a 100-year flood in a 25-year period (22 percent), a reasonable definition of the "long term" for an urban area might be 25 years. Thus the boundaries of an erosion and flooding buffer zone could represent the envelope established by the reach-by-reach calculation of the erosion and flooding potential of either the 100-year flood (short term) or the cumulative erosion impact of a series of smaller events over a 25-year period (long term), whichever is greater.

The buffer zone is then plotted by consideration of the controlling factor (100-year flooding, 100-year erosion, or long-term erosion) for each cross section used in the analysis. The boundary of the buffer zone between cross sections can be drawn as a smooth curve or as a series of tangent lines that can be easily referenced to existing survey data and readily compared with existing survey plats. The buffer zone so defined goes one step further than the conventional 100-year flood plain boundary by considering potential changes in channel configuration from lateral migration. The selection of this definition of the buffer zone is supported by the legal and policy precedents of the National Flood Insurance Program, the short- and long-term degree of risk associated with the 100-year return period event, and the accuracy of the methodology used for estimating long-term erosion impacts [i.e. by limiting the extrapolation to reasonable length in time (e.g., 25 years)]. For detailed discussion of the methodology and its application the reader is referred to Lagasse, et al. (1984).

## 6.5 Grade-Control Structures

Grade-control structures are effective channel stabilization measures that may be used singly or as an integral part of a stabilization plan involving bed and bank revetment, etc. The primary function of a grade-control structure is to decrease the gradient of a channel to either create a condition of equilibrium (sediment inflow equal to sediment outflow), or to reduce the protection required from other stabilization measures. For example, a grade-control structure can be used to decrease the channel slope so that smaller riprap can be used for stabilization. If sufficient coarse material exists in the natural alluvium, it may be possible to use grade-control structures to assist in developing an armor layer and avoid the need for all or part of the bed or bank revetment.

Grade-control structures can range in complexity from simple rock riprap or soil-cement drop structures to large concrete structures with baffled aprons and stilling basins. For many applications in the Southwest a series of smaller soil-cement drop structures may be more effective and economical than a single concrete structure of larger dimensions.

The design of grade-control structures to create equilibrium conditions is based on the equilibrium slope (Section 5.3.7). The design of grade-control structures to be used in combination with riprap is based on the incipient motion slope, as defined by the Shields relation (Section 5.3.4). After establishing the required design slope, the number and spacing of the structures must be determined. The vertical height that must be controlled for a given reach to achieve the required slope can be evaluated from

$$\Delta H = (S_0 - S)\ \Delta X \qquad (6.1)$$

where $\Delta H$ is the total height requiring structural control within the reach, $S_0$ is the original channel slope, $S$ is the estimated design slope, and $\Delta X$ is the length of channel to be controlled. The number of drop structures required depends on the maximum allowable height of each structure ($H_{max}$), which is a function of the type of structure utilized. Rules of thumb for conservative design are three feet for riprap drop structures and five feet for soil cement. The number of structures required (N) to control the total vertical height within a reach is

$$N = \frac{\Delta H}{H_{max}} \tag{6.2}$$

and the spacing L of the drop structures is

$$L = \frac{\Delta X}{N} \tag{6.3}$$

## 6.6 Common Bank Protection Methods

Numerous types of bank protection are available, including vegetation, rock riprap (dumped, hand-placed, wire-enclosed and grouted), soil cement and concrete, mattresses (concrete, brick, willow and asphalt), jacks and jetties, dikes (rock-filled, earth-filled and timber), automobile bodies, and many others. Many publications on channel stabilization have been prepared by various government agencies and others detailing the design and application of different techniques. It is not intended that an exhaustive coverage of the various channel stabilization measures be made in this section, but rather to briefly review those methods that are most appropriate to, and have proven successful in, the Southwest. In particular the use of dumped rock riprap, wire-enclosed riprap and soil cement will be considered.

Rock riprap is usually the most economical material for bank protection when available in sufficient size and quantify within a reasonable haul distance. Rock riprap protection is flexible and local damage is easily repaired. Construction must be accomplished in a prescribed manner, but is not complicated. Although riprap must be placed to the proper level in the bed, there are no foundation problems. Appearance of rock riprap is natural and after a period of time vegetation will grow between the rocks. Wave runup on rock slopes is usually less than on other types of slopes. Finally, when the usefulness of the protection is finished, the rock is salvageable.

Important factors to be considered in designing rock riprap protection are:

1. Durability of the rock.
2. Density of the rock.
3. Velocity (both magnitude and direction) of the flow in the vicinity of the rock.
4. Slope of the bed or bank line being protected.

5. Angle of repose for the rock.

6. Size of the rock.

7. Shape and angularity of the rock.

A good discussion of many of these factors is provided by the Corps of Engineers (1970). In this COE publication the size of rock required is based on the tractive force approach, generally considered to be a more physically based and more accurate method than those based on the permissible velocity approach.

A tractive force approach that provides the entire channel design (geometry and riprap size), given the design discharge and slope, is detailed by Anderson, et al. (1970). A more involved tractive force approach that generally provides a more precise riprap size through detailed consideration of lift and drag forces is the safety factor approach, presented in Simons and Senturk (1977). Another tractive force approach that considers in detail the lift and drag forces is the probability methodology presented by Li and Simons (1979). This methodology defines the failure probability of riprap and provides a less subjective estimate of riprap stability than that provided by the safety factor approach. For example, Li and Simons demonstrate that for an assumed set of flow and geometry conditions (conditions that are in the range of many practical design situations) a riprap safety factor of 1.0 has a probability of failure of 0.5. Similarly, a safety factor of 1.5 has a probability of failure of about 0.1 and not until a safety factor of about 1.9 is the failure probability equal to zero.

In contrast to the relative complexity of factor of safety and failure probability designs, is a permissible velocity approach that has found acceptance due to its ease of application. The method is detailed by the Denver Urban Drainage and Flood Control District (1982) and is useful as a check on riprap designs developed from more complex procedures or as the primary design method, particularly for minor structure design. The method is limited to Froude numbers less than 0.8 and due to its simplicity is anticipated to provide conservative design, a consideration that may be of importance if larger rock sizes are not readily available or if budget constraints exist.

After evaluating the required median riprap size, the riprap gradation and filter requirements must be established. Riprap gradation should follow a smooth particle size distribution with a ratio of the maximum size and the

median size of about two and the ratio of the median size and the 20 percent size also about two. With a distributed size range, the interstices formed by larger stones are filled with smaller sizes in an interlocking fashion, preventing formation of open pockets. Riprap consisting of angular stones is more suitable than that consisting of rounded stones. Control of the gradation of the riprap is almost always made by visual inspection.

Filters underneath the riprap are recommended to protect the fine embankment or riverbank material from washing out through the riprap. Two types of filters are commonly used: gravel filters and plastic filter cloths. Detailed filter design is provided by the COE (1970), Anderson, et al. (1970), Simons, Li & Associates, Inc. (1981), and others.

When adequately sized riprap is not available, rocks of cobble sizes may be placed in wire mesh baskets and used for a variety of channel stabilization problems. The baskets are constructed into various geometric shapes depending on the application. For channel lining applications mattresses are commonly used, which as the name implies are relatively broad and flat (typically less than 12 inches thick). Rectangular baskets (gabions) of more symmetrical proportion are often used as building blocks for check dams, drop structures, bank protection, etc. Modern gabions and mattresses are made of a thick steel wire mesh, woven with a triple twist at the intersections. Heavy wire is sometimes added or woven into the mesh before or after filling to increase stability and durability. The wire mesh can be galvanized or coated with PVC if used under highly corrosive conditions.

The strength and flexibility of the steel wire mesh allows gabions and mattresses to change shape without failure if undermined. They are also permeable, which minimizes hydraulic lift forces, allows vegetation to grow and provides some trapping efficiency. It should be noted than when gabions or mattresses are used in streams transporting cobbles or rocks, the wire baskets can be damaged or broken, reducing or destroying the protection near the bed.

Gabions and mattresses are supplied to the job site as folded mesh and tied in pairs. They are unfolded, placed in position like brick, tied together and filled with durable rock. The mesh containers can also be filled first and placed by hand or by crane to areas difficult to access (e.g. under water).

After an extensive literature review, Simons, et al. (1983) concluded that there was little information on the design of mattresses for channel

lining; consequently, from model and prototype studies, design guidelines were formulated. The major findings of the model and prototype studies where (1) that hydraulic conditions in a mattress channel are the same as those in a gravel-cobble channel, (2) the roughness of the mattresses is mainly caused by the filling rocks, with an insignificant effect from the wire mesh, and (3) flow velocity and shear stress causing incipient motion of the filling rock within the mattress compartment are approximately twice as large as the same size of unbound rock. For steep slope cnannels of high velocity, rocks within mattress compartments were found to propagate downstream, causing a ripple deformation of the mattress surface. Additionally, because of relatively large velocities at the mattress-to-bed interface, filter requirements and design are critical to successful steep slope application. Following the design procedure suggested by Simons, et al. provides a mattress thickness that is 1.5 to 3.0 times less than the required thickness of dumped riprap. Consequently, significant economies of cost are often possible with mattress linings since less rock is required, the required size is smaller and excavation requirements are less.

In areas where any type of riprap is scarce, use of in-place soil combined with cement provides a practical alternative. The resulting mixture, soil cement, has been successfully used as bank protection in many areas of the Southwest. A stairstep construction is typically used, with each lift about 12 inches thick before compaction and about 6 to 8 inches after compaction. The lifts are usually about 8 feet wide to easily accommodate construction equipment. Unlike other types of bank revetment, where milder side slopes are desirable, soil cement in a stairstep construction can be used on steeper slopes (i.e. typically one to one), which reduces channel excavation costs. For many applications, soil cement is also more aesthetically pleasing than other types of revetment.

For use in soil cement, soils should be easily pulverized and contain at least 5 percent, but no more than 35 percent, silt and clay (material passing the No. 200 sieve). Finer textured soils usually are difficult to pulverize and require more cement, as do 100 percent granular soils, which have no material passing the No. 200 sieve. In construction, special care should be exercised to prevent raw soil seams between successive layers of soil cement. If uncompleted embankments are left at the end of the day, a sheepsfoot roller should be used on the last layer to provide an interlock for the next layer.

The completed soil cement installation must be protected from drying out for a seven-day hydration period. Procedures for constructing soil cement slope protection by the stairstep method can be found in "Suggested Specifications for Soil-Cement Slope Protection for Embankments (Central-Plant Mixing Method," Portland Cement Association Publication ISO52W).

When velocities exceed six to eight feet per second and the flow carries sufficient bed load to be abrasive, special precautions are advisable for soil cement design. The aggregates in this case should contain at least 30 percent gravel particles retained on a No. 4 (4.75 mm) sieve.

# VII. COMPREHENSIVE DESIGN EXAMPLE

## 7.1 Project Description

Sportsman's Haven is a small, resort-oriented community located along Pinto Creek in Gila County, Arizona. Due to its location within the 100-year flood plain, the community is subjected to flood damage when flows on Pinto Creek exceed the 10-year event of about 16,500 cfs. Attempts have been made locally to provide some degree of flood protection by constructing a levee embankment around the community. Due to the cohesionless nature of the embankment material, which was obtained from the bed of Pinto Creek, the levee is vulnerable to the erosive forces of the floodwaters. Additionally, the levee was not constructed to a sufficient height to prevent overtopping by the 100-year flood (46,785 cfs).

Under the authority of the Flood Control Planning Program, the Arizona Department of Water Resources undertook a reconnaissance level evaluation of this problem and prepared a preliminary levee system design which would provide the community with protection from the 100-year flood. This levee design project was selected to illustrate the application of several of the analytical tools presented in this manual. The following pages present a Level I and Level II analysis of the Pinto Creek levee system. Figure 7.1 presents a plan view of the study area and the proposed levee alignment.

## 7.2 Level I

General (qualitative) characteristics of Pinto Creek can be determined from a review of historical watershed data and an application of some empirical relationships involving slope, discharge, sinuosity ratio, etc. The amount of information to be derived from this type of analysis will vary from project to project since the amount of available data will vary from site to site.

The Level I analysis for the Pinto Creek Project will address the following items:

1. Sinuosity
2. Geomorphic relationships
   a. Lane
   b. Leopold and Wolman
3. Historical aerial photographs

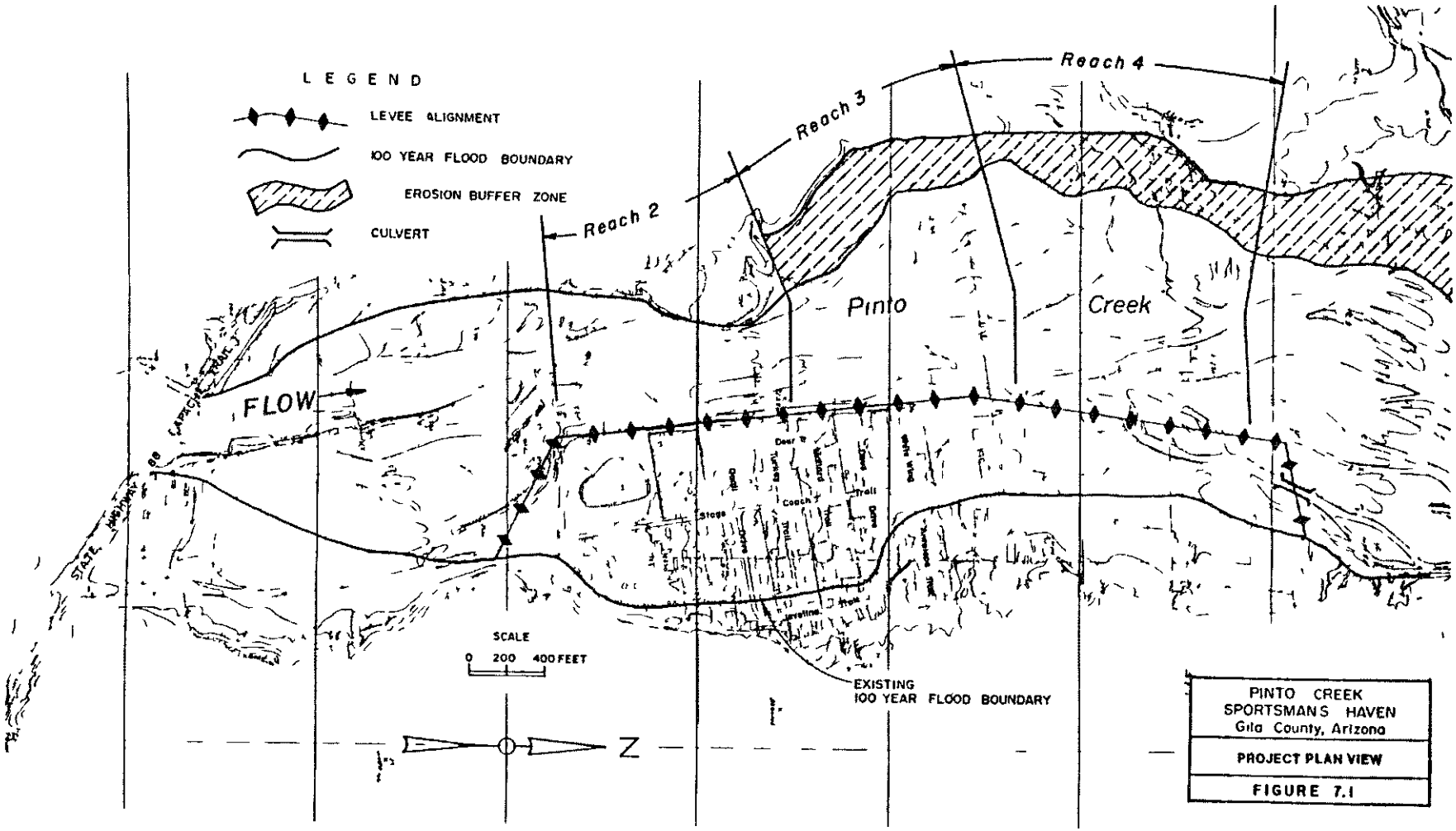


PINTO CREEK
SPORTSMAN'S HAVEN
Gila County, Arizona

PROJECT PLAN VIEW

FIGURE 7.1

4. Historical bed profile comparison
5. Visual geological investigation

A detailed discussion on each item follows.

1. Sinuosity - Leopold, Wolman and Miller adopted the sinuosity ratio, which is defined as the thalweg length divided by the valley length, as a criterion which could be used to classify river patterns. Through the observation of several natural river systems, they concluded that systems with a sinuosity ratio equal to or greater than 1.5 would be classified as meandering while those less than 1.5 would be braided or straight.
   The sinuosity of the study reach is computed as follows:

   $$\text{sinousity ratio} = \frac{\text{thalweg length}}{\text{down valley distance}}$$

   $$\text{sinuousity ratio} = \frac{8925}{8175} = 1.1$$

   This low value indicates that this reach of Pinto Creek is straight or braided. Additional analyses will next be conducted to confirm this fact. General conclusions will then be drawn regarding channel pattern classification.

2. Geomorphic Relationships - Figure 5.5 will be used to examine the relationship between slope, discharge and channel pattern. This analysis will be based on the premise that the dominant discharge will be most influential in determining the channel pattern. For the Pinto Creek Project, the average bed slope through the entire study reach is 0.0089 and the dominant discharge is 16,514 cfs. Applying these values to Figure 5.5 shows that the channel plots well into the braided region, using both Leopold and Wolman's criteria as well as Lane's. When using Figure 5.5 the engineer should remember that these relationships were derived from data on perennial channels, rather than ephemeral washes which are more common in Arizona. Accordingly, their strict application in the southwest United States should be with caution and knowledge of their derivation.

3. Historical Aerial Photographs - Three sets of historical photos were located for this reach of Pinto Creek. These photos were taken in 1947, 1967, and 1981. Examination of these pictures indicates a braided channel pattern has existed during the last 38 years (see Figure 7.2). Overall, the braided channel segments appear narrower in the 1947 and 1967 photos than in the 1981 photo. This may be in response to construction of the Pinto Creek bridge on Highway 88 in 1972. The approach embankments to this bridge partially obstruct the floodplain and cause the flow to be concentrated in a smaller width than existed prior to bridge construction. The widening of the main channel for about two miles downstream of the bridge may be the result of this local concentration of high velocity of flow which has cleared out a wider, cleaner channel section. This localized

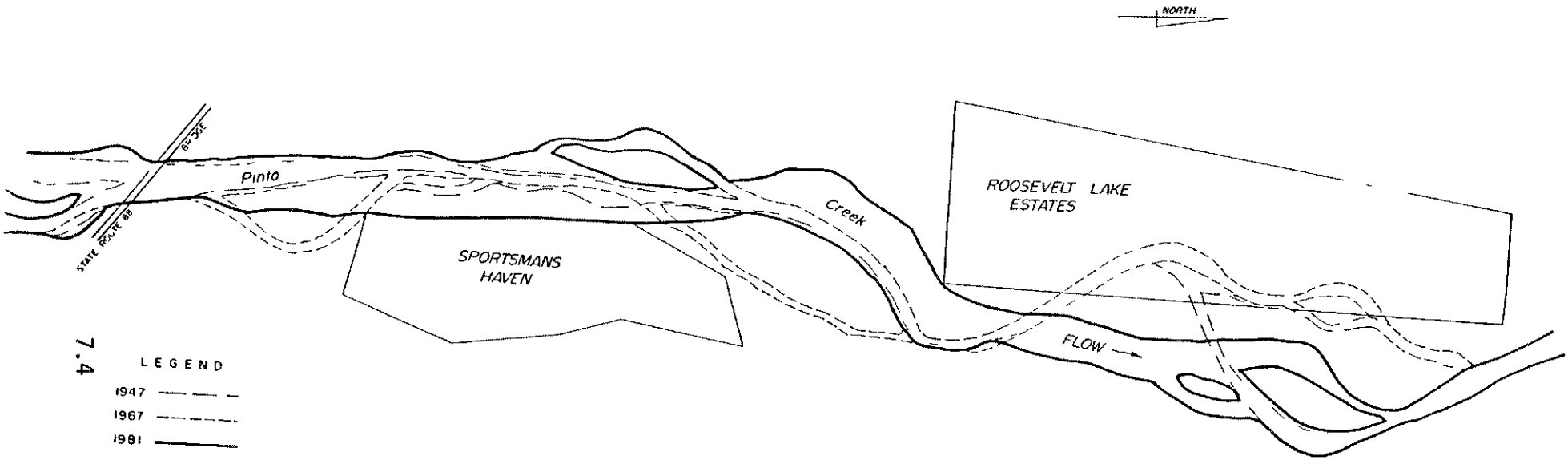


Figure 7.2 Time sequence analysis of historical aerial photographs.

response diminishes beyond the two-mile downstream limit where the channel assumes a more consistent pattern in all three photo sets.

4. Historical Bed Profile Comparison - USGS quadrangle maps were prepared for this area in both 1949 and 1964. Unfortunately, the 1949 map is a 15-minute quad while the 1964 edition is a 7.5-minute quad. This non-uniformity of scale presented a problem since this reach of Pinto Creek is on the edge of the maps and meanders back and forth between them, making it impossible to measure the entire study reach on either map. The third bed profile was taken from a 1981 topographic map (1" = 200, 2' C.I.) prepared especially for this project.

   Taking topographic measurements from these maps, superimposed bed profiles were plotted at a scale of 1" = 1,000' horizontal, 1" = 20' vertical (see Figure 7.3). Through the study reach, this plot shows a fairly consistent drop (about 3.0') in bed elevation from 1949 to 1964 and a varying amount of aggradation (about 0' to 1') from 1964 to 1981.

   There is no evidence of any significant manmade disturbance to the watershed that would readily explain the drop in bed elevation between 1949 and 1964, nor the aggradation that has occurred since 1964. Since Pinto Creek discharges into Roosevelt Lake, fluctuating lake levels could influence the bed profile to a certain degree but is doubtful that such influences would propagate this far (three miles) upstream from the lake. Further investigation into this possibility could be pursured by reviewing historical reservoir level data from the Salt River Project and correlating this information with historical hydrologic/hydraulic data for the watershed to see if significant flooding may have occurred during periods of low lake levels.

   Due to the scale discrepancies on the two quad maps and possible survey datum inconsistencies between the USGS maps and the 1981 base map, this bed profile comparison may not be totally accurate and, therefore, should be interpreted with caution. For these reasons, the historic bed profile evaluation for Pinto Creek will not be considered a reliable tool for the Level I analysis.

5. Visual Geological Investigation - A field visit was made to the project site in order to identify any geologic formations that might control either horizontal or vertical channel movement. This visit also provided an opportunity for a ground level inspection of the channel geometry, channel pattern, and bed material composition. No natural or artifical bed controls were located within the study reach which could be used for pivot points in an equilibrium slope analysis.

   The west bank through Reach 2 was found to consist of rock which will restrict lateral channel migration at this location. This is verified through a cross check with the historic photos which shows no westward bank movement through Reach 2 since 1947.

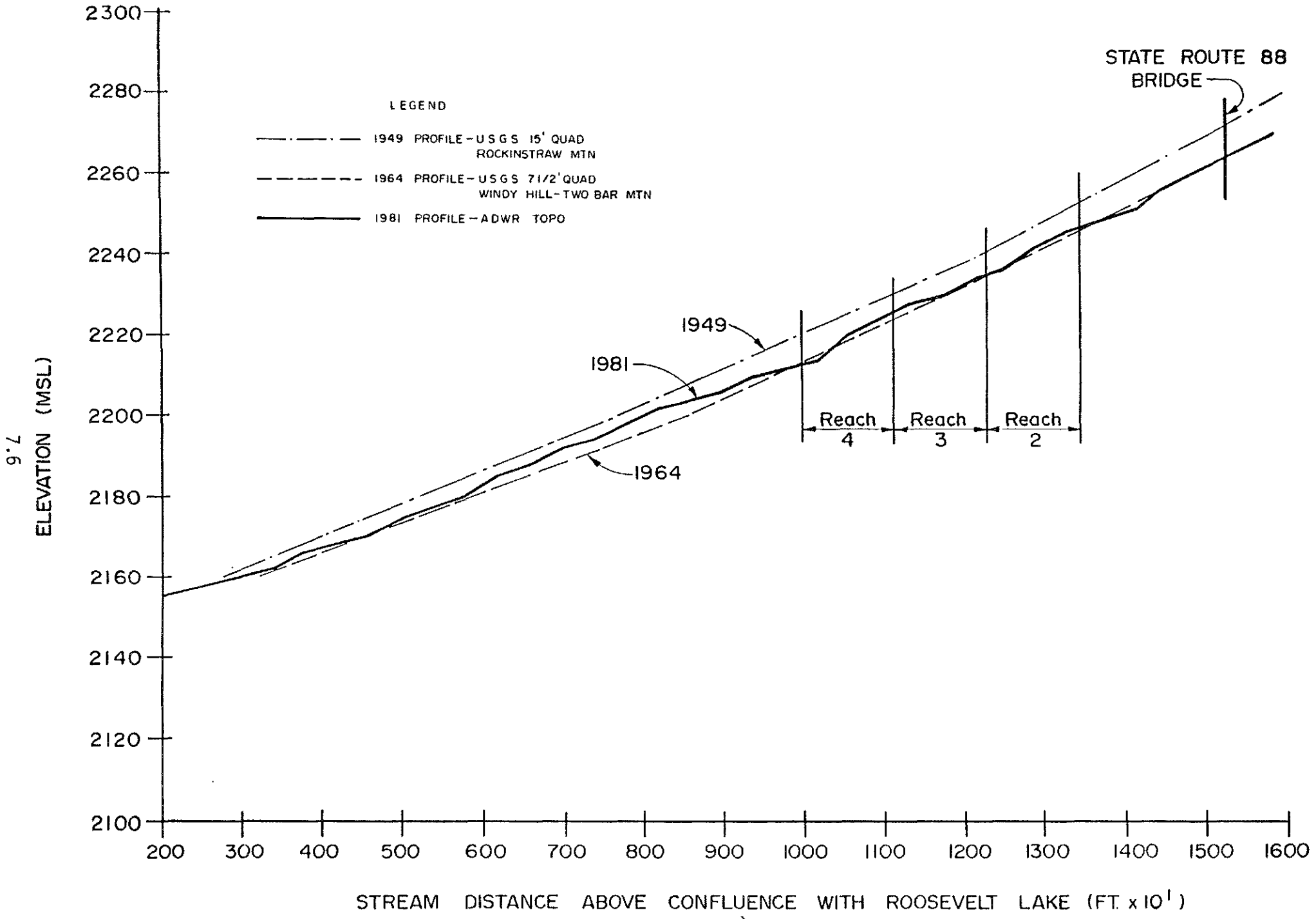


Figure 7.3 Comparison of historical bed profiles.

Visual inspection of the channel through all four reaches revealed a wide, braided pattern with poorly defined banks that were 2' to 3' in height. The channel bed was composed primarily of sand and sandy gravel with the intermittent presence of small cobbles. Island and bar formations were evident throughout the study reach. Except for the rock formation noted in Reach 2, all other portions of the channel banks consisted of erodible alluvium.

All aspects of this Level I analysis confirm the existence of a braided channel pattern. Braided channels are generally wide, have unstable, poorly defined banks and consist of two or more main channels that cross one another giving the riverbed a braided appearance at low flow. These channels have sinuosity ratios less than 1.5 and exhibit steeper slopes than meandering channels.

Braiding is believed to result primarily from random deposition of materials (sediment) transported during high flows in quantities or sizes too great for continued transport during low flows. Accordingly, as the stream discharge is reduced, larger sediment particles begin to drop to the bed as the stream "sorts" or leaves behind those sizes of the load which it is unable to transport. The accumulation of these particles on the channel bed initiates the formation of a bar which serves to trap even more sediment particles. Although the depth of flow over the growing bar is gradually decreased, velocity over the bar tends to remain undiminished or even to increase so that some particles moving along the bar are deposited beyond the downstream end where a significant decrease in velocity is associated with the marked increase in depth of flow. Thus, the bar grows by successive addition of sediment particles at its downstream end and some additional growth along its sides.

The growth of the bar will eventually reach a size that will significantly alter the channel capacity, at which time the channel will seek a new equilibrium condition by eroding and widening its banks. Additional bars will then be propagated through the same process described above until the channel obtains its characteristic braided pattern.

Because deposition is essential to the formation of the braided pattern, it is obvious that sediment transport is essential to braiding. Also, the channel banks must be sufficiently erodible so that they, rather than the newly formed bar, give way as the channel cross section is increased to provide the required flow capacity. Therefore, sediment transport and erodible

banks provide the essential conditions of braiding. However, rapidly fluctuating changes in stage contribute to the instability of the sediment transport regime as well as to erosion of the banks, so this factor should also be considered as a contributory cause of braiding. Studies by Leopold, Wolman and Miller also indicate that heterogeneity of the bed material may create irregularities in the movement of sediment, and thus, may also contribute to braiding.

## 7.3 Level II

The Level II analysis will provide the technical refinements necessary to establish dimensions and specifications for the actual levee design. The end product of this analysis will be:

1. levee crest profile
2. determine requirements for bank stabilization
3. maximum estimated depth of bed movement adjacent to all portions of the levee
4. estimated distance of lateral channel migration opposite the leveed reach of the stream

Figure 7.4 presents a block diagram showing the major components of the Level II analysis. A technical discussion and analysis of each of these components follows.

### 7.3.1 Levee Embankment Height

The Corps of Engineers HEC-2 program was used to establish the water surface profile for the 100-year design flood of 46,785 cfs. This program was initially run in the subcritical mode using channel "n" values shown in Table 4.2, "For Depth and Flood Control". Since it was anticipated that the large flow associated with the 100-year event would produce flow velocities sufficiently high to create antidunes, a channel "n" value of 0.030 was selected from Table 4.2. This "n" value, coupled with the subcritical assumption for HEC-2, should produce a design water-surface profile that reflects "worst case" type conditions. The reader should remember, however, that the "n" values selected for overbank areas should be based on the best estimate of actual roughness in these areas rather than Table 4.2. Overbank areas typi-

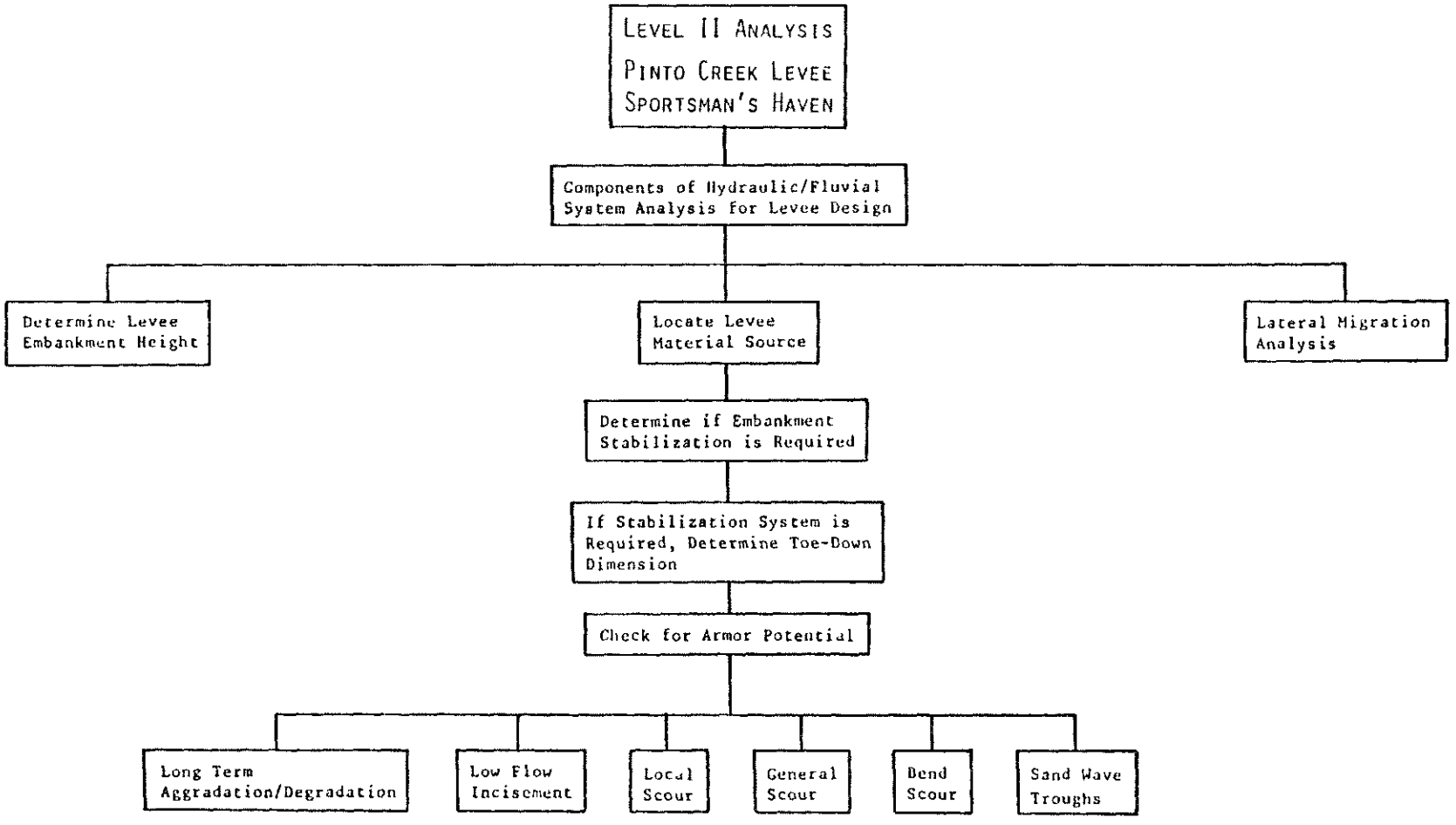


Figure 7.4 Block diagram of level II analysis.

cally exhibit dense vegetation or other obstructions to flow and thus have different hydraulic characteristics than the main channel. Overbank "n" values for the Pinto Creek analysis ranged from 0.045 to 0.085.

A review of the subcritical HEC-2 run using the "n" values listed above, indicated that critical depth was assumed at several cross sections. This leads one to suspect that the stream will probably be flowing at critical, or even supercritical at the peak of the design flood, which in turn lends credibility to the assumption of antidune formations in selecting a channel "n" value for the levee height analysis.

Once the design water surface profile is established under the criteria outlined above, the levee crest elevation is simply equal to the water surface elevation plus a freeboard dimension.

The freeboard dimension for this project is computed through application of only Equation 4.28b, since a soil-cement lining will be placed to the top of the levee embankment.

Freeboard for Earth Levee and Soil-Cement Lining

$$F.B._{TOT\ EMB/B.L.} = 1/2\ h_a + \Delta y_{se} + \Delta y_s + \Delta y_d + \Delta y_{agg}$$

Due to the absence of channel bends along the levee, $\Delta y_{se}$ and $\Delta y_s$ are both zero. Referring to Section 7.3.2.2.6, the reader will note that $h_a$ varies from reach to reach.

Of the two remaining terms, $\Delta y_d$ is zero due to the absence of a bridge pier along the levee, while $\Delta y_{agg}$ will have to be assumed since the lack of pivot points prevented a quantitative assessment of long-term aggradation (see Section 7.3.2.2.2). A value of two feet will be assigned to $\Delta y_{agg}$. The freeboard is now calculated as follows:

1. Reach 2: $F.B._{TOT\ EMB/B.L.} = 1/2\ (3.5) + 2.0 = 3.75$ feet
2. Reach 3: $F.B._{TOT\ EMB/B.L.} = 1/2\ (4.3) + 2.0 = 4.15$ feet
3. Reach 4: $F.B._{TOT\ EMB/B.L.} = 1/2\ (2.1) + 2.0 = 3.05$ feet

The freeboard dimension for both the levee and soil-cement lining is measured from the water-surface profile generated by the subcritical HEC-2 analysis, since that condition will give the maximum expected flood elevation for the design event.

The freeboard dimension for the upstream segment of levee that extends through the right overbank to high ground will be based on both velocity head and FEMA requirements. The freeboard for this segment of levee will initially be estimated as twice the velocity head for the overbank at cross section 1409. Accordingly, the freeboard is calculated to be:

$$F.B_{TOT\ EMB/B.L.} = 2\ (\frac{v^2}{2g}) = 2\ (\frac{3.97^2}{64.4}) = 0.49\ ft.$$

Due to the low value for velocity head and the potential for wave run-up in this area, the overbank levee (including bank lining) will be assigned a freeboard dimension equal to minimum FEMA standards of 3.0 feet.

### 7.3.2 Levee Embankment Stabilization

#### 7.3.2.1 Erosion of Embankment Material

The results of the subcritical HEC-2 analysis used to establish the levee height revealed channel velocities of 10 to 14 fps could be expected adjacent to the levee. If supercritical conditions were to occur as anticipated, the velocities would be even higher. Since the levee embankment should be designed to withstand the worst conditions expected during the design event, a supercritical HEC-2 run was made to establish an upper limit for a velocity profile through the project reach. Again, referring to Table 4.2, a channel "n" value of 0.025 was selected for the supercritical analysis used in the bank stability investigation. The end result of the lower "n" value and supercritical HEC-2 run was an average increase of about 1 fps in velocity at each cross section.

In this particular project, the supercritical analysis was somewhat academic in that the 10 to 14 fps velocities associated with the subcritical run already indicate that some form of bank protection will be needed to prevent erosion. This velocity range is well above that recommended for earth embankments in such publications as Hydraulic Design of Flood Control Channels, Corps of Engineers, 1970 and Open Channel Hydraulics, Chow, 1959. Cases may be encountered, however, where a subcritical water-surface profile may yield mean velocities that are low enough to be considered non-erosive. In these cases, the possibility of supercritical flow should be considered as a worst case condition for embankment erosion if there is a reasonable chance of it occurring. The ability of the levee or channel bank to withstand erosion

should then be based on the supercritical velocities. The erodibility of an earth embankment can be determined by using methods such as the "allowable velocity" approach presented in Design of Open Channels, Technical Release No. 25, October, 1977, U.S.D.A., SCS. The reader is referred to TR-25 for detailed examples of this procedure.

7.3.2.2 Toe-Down Requirements For Stabilization System

Since the water-surface profile analysis indicated erosive velocities would exist during the design event, provisions must be made to protect the levee embankment. Soil cement was selected as one of the most economical and durable alternatives.

One of the most important aspects in designing the soil cement system was to determine the depth below the channel invert that the soil cement must be extended in order to prevent undercutting by vertical adjustments to the channel bed. Phenomena that must be considered in this analysis include:

1. armor potential
2. long-term degradation
3. low flow incisement
4. local scour
5. general scour
6. bend scour
7. sand wave troughs

The analysis of each of these phenomena (excluding bend scour) is discussed in detail in the following sub-sections. Bend scour was omitted due to the absence of bends along the levee.

7.3.2.2.1 Armor Potential

The first step in analyzing the vertical adjustment of a channel bed should focus on the potential for armoring to occur during the design event. If armoring were to occur, it may act as a control for the majority of the channel bed and prevent further downward movement except at areas of localized disturbance such as bridge piers or along the nose of a spur dike. If it can be guaranteed that armoring will uniformally occur across the channel during the design flow, the toe-down depth for a bank stabilization system may be reduced from that which may be required for a non-armored channel. If this condition (armoring) were to occur, the embankment stabilization system should be keyed into the armor layer by extending the toe-down 2' to 3' below the top of the predicted armor layer elevation.

For purposes of this example, the armor calculations will be based on the hydraulic characteristics of Reach 2. Similiar procedures would be applied to Reaches 3 and 4 to see if channel armoring is probable at those locations.

1. The hydraulic parameters used in the armor analysis of Reach 2 are listed as follows:

$Q_{100}$ = 46,785 cfs (supercritical HEC-2 run)

Channel topwidth = 559 feet

Channel area = 2,859 feet$^2$

Energy slope = 0.0087 feet/feet

2. Using Shield's relationship (Sec. 5.3.4), compute the incipient motion particle size for the design event (100 year flood).

$$Dc = \frac{\tau}{0.047\ (\gamma_s - \gamma)}$$

Dc = sediment particle size (ft) at incipient motion

$\tau$ = shear stress on channel bottom (lb/ft$^2$)

$\gamma_s$ = specific weight of sediment (assume 165 lb/ft$^3$)

$\gamma$ = specific weight of water (62.4 lb/ft$^3$)

Shear stress will be computed using procedures in Section 4.3. Check width/depth ratio to see if $\gamma ds$ approaches $\gamma RS$:

$$\text{hydraulic depth} = \frac{A}{T} = \frac{2859}{559} = 5.11 \text{ feet}$$

$$\text{width/depth ratio} = \frac{b}{d} = \frac{559}{5.11} = 109 \ (b=T)$$

Since $\frac{b}{d} > 10$, $\gamma ds$ can be assumed equivalent to $\gamma RS$ and Figure 4.4 can be used to compute the maximum shear stress or tractive force on the channel bottom.

$$\text{From Figure 4.4b: } \frac{\tau_{max}}{\gamma ds} = 1.0$$

$$\tau_{max} = \gamma ds = (62.4)\ (5.11)\ (0.0087)$$

$$\tau_{max} = 2.77\ lb/ft^2$$

Substituting in Eq. 5.5: $Dc = \dfrac{2.77}{0.047\ (165 - 62.4)}$

$$Dc = 0.57\ ft\ or\ 175mm$$

3. Referring to Figure 7.5, which is an average gradation curve for the bed material in Pinto Creek, it can be seen there are no particle sizes in the bed as large as 175 mm. Therefore, it can be concluded that all bed particles will be moving during the peak of the 100-year event and that armoring will not occur.

7.3.2.2.2 Long-Term Aggradation/Degradation

A review of the Level I historical aerial photographs of Pinto Creek indicates the channel alignment through the study reach has not been stable. The observed lateral movement of the river has probably been accompanied by slope changes in the bed profile. An equilibrium slope analysis will be performed to estimate the long term response of the channel bed adjacent to the proposed levee.

For purposes of this example, an assumed stable sediment supply section was located approximately one mile upstream of the proposed levee. In locating a supply section, the engineer should look for a stable alignment on historical photos, a stable elevation on historical bed profiles, and field evidence of the river's impact on vegetation in the channel (exposed root systems, buried tree trunks, etc.).

It should be noted that the Highway 88 bridge lies between the selected equilibrium sediment supply section and the proposed levee alignment. If possible, it is preferable to not have any man-made obstructions within that reach of the channel between the equilibrium supply section and the reach of channel for which the equilibrium slope analysis is being performed. Such obstructions might create hydraulic conditions that could restrict the amount of sediment being supplied to the study reach from the upstream supply section. For this design example, the bridge was assumed to have no impact in controlling the sediment supply to the leveed reach of Pinto Creek. This

COMPOSITE CURVE OF REPRESENTATIVE BED MATERIAL THRU STUDY REACH

| | | | |
|---|---|---|---|
| PROJECT and STATE: Pinto Creek @ Sportsman's Haven, Arizona | | | SAMPLE LOCATION: various |
| FIELD SAMPLE NO | DEPTH: 0.5-2.0' | GEOLOGIC ORIGIN: River run- Channel bed material | |
| TYPE OF SAMPLE: Bulk | TESTED AT | APPROVED BY | DATE: 9/10/84 |
| SYMBOL: SW-SP | DESCRIPTION: Poorly graded sands, gravelly sands | | |

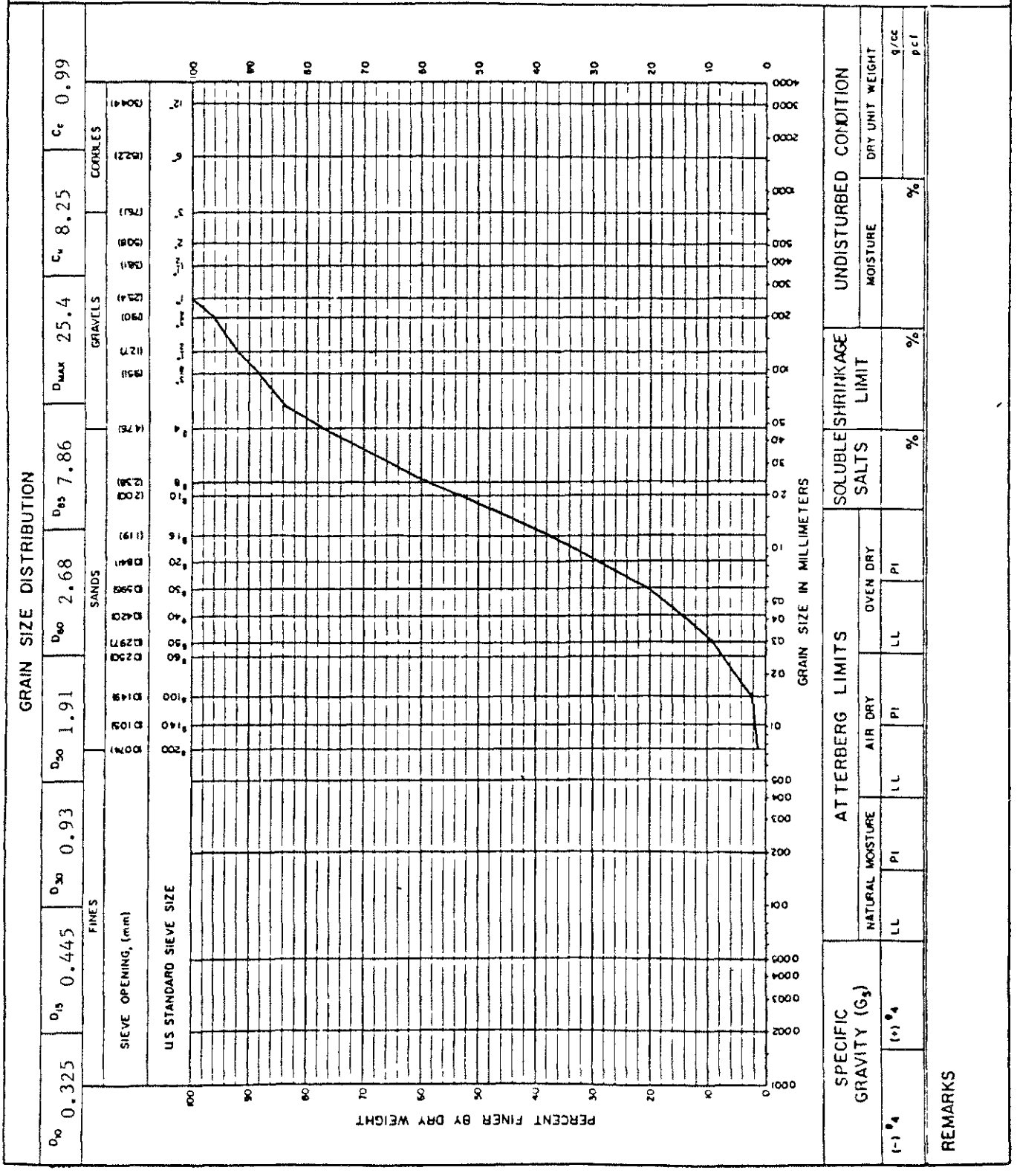




Figure 7.5

assumption was based on the fact that the bridge opening was greater than the effective channel width at the upstream supply section and the fact that the channel bed slopes and n values at both locations were about equal. Under these conditions, the bridge opening should be able to pass the incoming sediment supply from the 10-year event without causing any reduction in transport capacity.

Pinto Creek was divided into three reaches along the proposed levee alignment. The reach boundaries were selected to provide segments of similiar hydraulic characteristics. An equilibrium slope will be computed for each reach. A set of detailed calculations will only be shown for Reach 2, the same procedures would be applied to the other two reaches.

1. Dominant discharge = 16,514 cfs. This value was selected on the results of a HEC-2 analysis for Reach 2 which showed the bankfull discharge was about 16,620 cfs. Since the 10-year event had a discharge of 16,514 cfs, it was selected as the dominant discharge for use in the equilibrium slope analysis.

2. Compute sediment supply.

   a. Equation 5.8b will be used to compute the transport capacity for the upstream supply section. A gradation coefficient and $D_{50}$ particle size must be determined for use in this equation.

   b. A sieve analysis of bed material at the upstream supply section provided the following information:

      $D_{50}$ = 1.19mm

      $D_{15.9}$ = 0.37mm

      $D_{84.1}$ = 4.67mm

$$\text{Gradation coefficient} = G = \frac{1}{2}\left(\frac{D_{84.1}}{D_{50}} + \frac{D_{50}}{D_{15.9}}\right)$$

$$G = \frac{1}{2}\left(\frac{4.67}{1.19} + \frac{1.19}{0.37}\right)$$

$$G = 3.57$$

   c. A cross section plot of the upstream supply section is shown in Figure 7.6. Although this section was judged to have a constant "n" value of 0.025, it is recommended the section be analyzed as

having a main channel and an overbank. Even though the "n" value is constant, the hydraulic calculations for velocity and depth will differ if the entire section is considered to be "channel" versus analyzing the section as a channel with "overbank". The subdivision of the section into a channel and overbank should yield more accurate results since the velocity and hydraulic depth computations for each subdivision will be based on the calculated conveyance within each subdivision. This procedure eliminates the "weighted" velocity and hydraulic depth that would result from basing such calculations on the total conveyance for the entire cross section. In a 'benched' cross section, such as shown in Figure 7.6, this procedure allows computation of seperate sediment transport rates for the channel and overbank. When using a power relation such as Equation 5.8b, which is dependent upon velocity and hydraulic depth, it is prudent to consider this approach to insure that the velocity and depth parameters are truly representative of that portion of the cross section to which they are being applied.

Through a series of converging iterations with Manning's Equation, the following hydraulic parameters were determined for the supply section:

$Q$ = 16,514 cfs
$S$ = 0.0097
$n$ = 0.025 (channel and overbank)

Depth = 6.58 feet

| | |
|---|---|
| $Q_{CH}$ = 14,497 cfs | $Q_{OB}$ = 2,017 cfs |
| $V_{CH}$ = 19.50 fps | $V_{OB}$ = 9.71 fps |
| $A_{CH}$ = 743.3 ft.$^2$ | $A_{OB}$ = 207.6 ft.$^2$ |

d. Substitute data from b. and c. into Eq. 5.8b:

$$q_s = 0.0064 \frac{n^{1.77} V^{4.32} G^{0.45}}{Y_h^{0.30} D_{50}^{0.61}}$$

<u>For the "channel" section:</u>

average flow width = 117 feet

therefore; $Y_h = \frac{A}{W} = \frac{743.3}{117}$

$Y_h$ = 6.35 ft

$$q_{s_{CH}} = 0.0064 \left[ \frac{(0.025)^{1.77}(19.50)^{4.32}(3.57)^{0.45}}{(6.35)^{0.30}(1.19)^{0.61}} \right]$$

Figure 7.6. CROSS SECTION GEOMETRY FOR UPSTREAM SEDIMENT SUPPLY SECTION USED IN EQUILIBRIUM SLOPE ANALYSIS

SCALE : 1" = 30' HORIZONTAL
1" = 3' VERTICAL

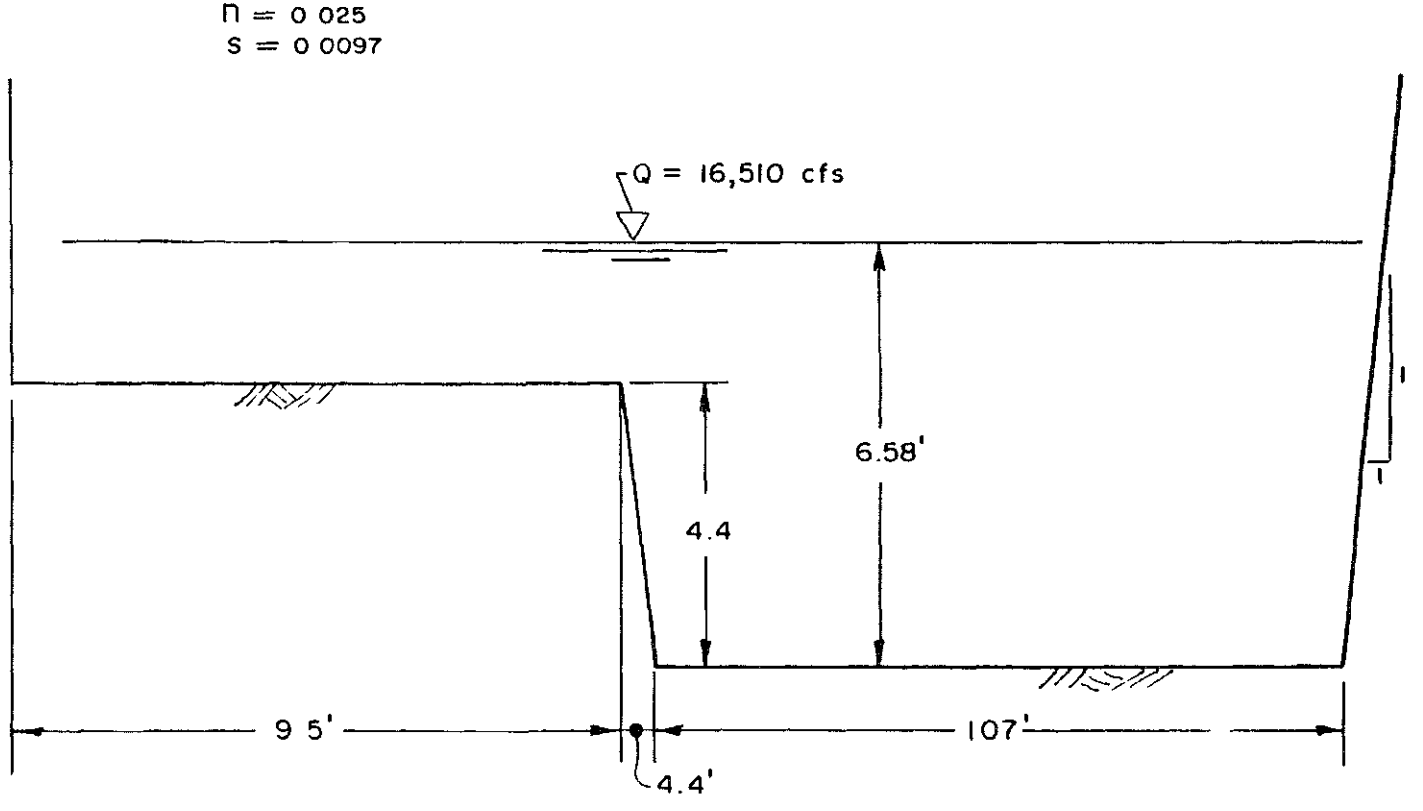

$$q_{s_{CH}} = 3.20 \text{ cfs/ft}$$

For a width of 117 ft; $Q_{s_{CH}} = q_{s_{CH}} \times W_{CH}$

$$Q_{s_{CH}} = (3.20)\ (117)$$

$$Q_{s_{CH}} = 374.5 \text{ cfs}$$

<u>For the overbank section:</u>

average flow width = 97 feet

therefore; $Y_h = \frac{207.6}{97}$

$$Y_h = 2.14 \text{ ft}$$

$$q_{s_{OB}} = 0.0064 \left[ \frac{(0.025)^{1.77}\ (9.71)^{4.32}\ (3.57)^{0.45}}{(2.14)^{0.30}\ (1.19)^{0.61}} \right]$$

$$q_{s_{OB}} = 0.218 \text{ cfs/ft}$$

For a width of 97 feet, $Q_{s_{OB}} = (0.218)\ (97)$

$$Q_{s_{OB}} = 21.2 \text{ cfs}$$

Total sediment transport = $Q_{s_{TOT}} = Q_{s_{CH}} + Q_{s_{OB}}$

$$Q_{s_{TOT}} = 374.5 + 21.2$$

$$Q_{s_{TOT}} = 395.7 \text{ cfs}$$

This value (395.7 cfs) will be used as the sediment supply for all downstream reaches for which the equilibrium slope analysis is performed.

3. Compute equilibrium slope. An iteration procedure is now employed to compute the sediment transport capacity for a cross section typical of Reach 2. Manning's Equation is used to compute V and $Y_h$, while Equation 5.8b is used to compute transport capacity. The bed slope value is adjusted between iterations until the transport rate equals the supply rate (395.7 cfs). All calculations are based on the

following data:

$Q$ = 16,514 cfs
$n$ = 0.025
$D_{50}$ = 1.91mm
$G$ = 3.74
$W$ = 552 feet
$q_s$ computed using Eq. 5.8b

A series of iterations resulting in an equilibrium slope of 0.0187 is presented in Table 7.1.

The same procedures outlined in Steps 1 through 3 are also applied to the equilibrium slope analysis for Reaches 3 and 4. A summary of the predicted equilibrium slopes for all three reaches adjacent to the proposed levee is shown below:

| Reach | Existing Slope | Equilibrium Slope |
|---|---|---|
| 2 | 0.0103 | 0.0187 |
| 3 | 0.0082 | 0.0195 |
| 4 | 0.0083 | 0.0310 |

The existing slope of Reach 2 is 0.0103 ft/ft. A review of the calculations in Table 7.1 indicates the existing sediment-transport rate for Reach 2 is considerably less than the incoming supply (395.7 cfs). The existing transport rates for Reaches 3 and 4, 112.9 cfs and 60.8 cfs, respectively, are also considerably less than the estimated sediment supply of 395.7 cfs. Due to this relatively large difference between the transport capacities of Reaches 2, 3, and 4 compared to the upstream supply reach, the engineer might suspect that the chosen equilibrium supply section is not really in equilibrium. Unless there have been significant man-made changes in the river system during recent years (refer to Level I historical data), it is unlikely that such large differences would exist between sediment transport rates for river cross sections that are within a mile of each other.

In consideration of the results obtained from the previous equilibrium slope calculations, the engineer should re-evaluate his selection of an equilibrium slope cross section to insure that it has truly been a long term, stable cross section. Additional field inspections might reveal the existance of a better supply section for the equilibrium slope analysis.

Table 7.1. Equilibrium Slope Calculations For Reach 2.

| Slope ft/ft | V (fps) | $Y_h$ (ft) | $q_s$ (cfs/ft) | W (ft) | $Q_s$ (cfs) |
|---|---|---|---|---|---|
| 0.0103 | 11.38 | 2.63 | 0.3115 | 552 | 171.9 |
| 0.0170 | 13.26 | 2.24 | 0.63 | 552 | 352.3 |
| 0.0190 | 13.69 | 2.18 | 0.732 | 552 | 404.2 |
| 0.0187 | 13.63 | 2.19 | 0.717 | 552 | 396.0 |

Since 396.0 cfs is approximately equal to the supply rate of 395.7 cfs, the calculations are terminated at this point and 0.0187 is accepted as the equilibrium slope.

For purposes of completing this example, it will be assumed that the original equilibrium slope calculations are valid. Accordingly, one could expect sediment deposits will begin to occur in the upstream portion of Reach 2 in an effort to steepen the bed slope to 0.0187 ft/ft for the remaining downstream portion of this reach.

Unfortunately, inspections of this area failed to reveal any natural or manmade controls which could be used as a pivot point for the computed equilibrium slopes. Under these circumstances, the equilibrium slope analysis can only be applied in a qualitative sense, i.e., Reaches 2, 3 and 4 should aggrade over the long term. Response to such aggradation might be lateral migration, channel braiding, channel widening, or a combination of these phenomena.

7.3.2.2.3 Low Flow Incisement

Field inspections of the study reach provided an opportunity to check the stream for low flow incisement. A low flow channel on the order of 2' to 2.5' was observed during this visit.

The proposed levee improvements do not include any modifications to the channel bed which would eliminate the existing low flow channel. In the absence of channel improvements, the invert of the existing low flow channel will be used as a base elevation from which all scour, degradation, etc. dimensions will be measured. This decision is justified on the probability that the existing low flow channel will migrate across the stream bed and ultimately be in contact with any point along the levee toe.

Had channelization been part of the proposed plan, it would have been prudent to add 2' to the toe-down depth for the soil cement since a new low flow channel would probably re-form through the channelized reach of the stream. This low flow depth can usually be based on the dimensions of low flow channels observed prior to construction of channel improvements. Any break in grade with the natural channel invert at the upstream and downstream end of the channelized reach should also be considered.

7.3.2.2.4 Local Scour

Potential for local scour occurs at the upstream end of the proposed levee where the alignment turns easterly to tie into high ground and becomes nearly perpendicular to the direction of flow. This will obstruct the right overbank flow and divert it westerly where it will merge into the main channel at the upstream corner of the levee. As the overbank flow passes the levee corner and re-enters the main channel, the velocity will increase and generate a scour pocket around the levee toe. The approximate dimensions of this scour hole must be considered in determining the soil cement toe down depth at this location.

Since the soil cement embankment will have sloping sides, either Equation 5.17b or 5.18 will be used, the final selection being determined by the ratio $\frac{a}{y}$. The analysis proceeds as follows:

1. Cross section 1409 (see Figure 7.7) will be used to determine the hydraulic data needed for this analysis. This cross section is chosen because it represents average right overbank flow conditions prior to being intercepted by the levee.

2. From the supercritical HEC-2 run for the 100-year event, the following data is obtained:

| XSEC | VROB (fps) | AROB ($ft^2$) | $Width_{ROB}$ (ft) | $Y_h$ (ft) |
|---|---|---|---|---|
| 1409 | 3.97 | 1232 | 560 | 2.20 |

3. Compute $\frac{a}{y}$. The embankment length, a, will be measured by taking the projected length of the right overbank levee perpendicular to flow (see Figure 7.7). In this particular case, "a" is equal to the width of the right overbank at cross section 1409. "Y" will be computed as the hydraulic depth of the right overbank at cross section 1409. Using the above definitions:

   a = 560 feet

   $Y_h$ = 2.20 feet

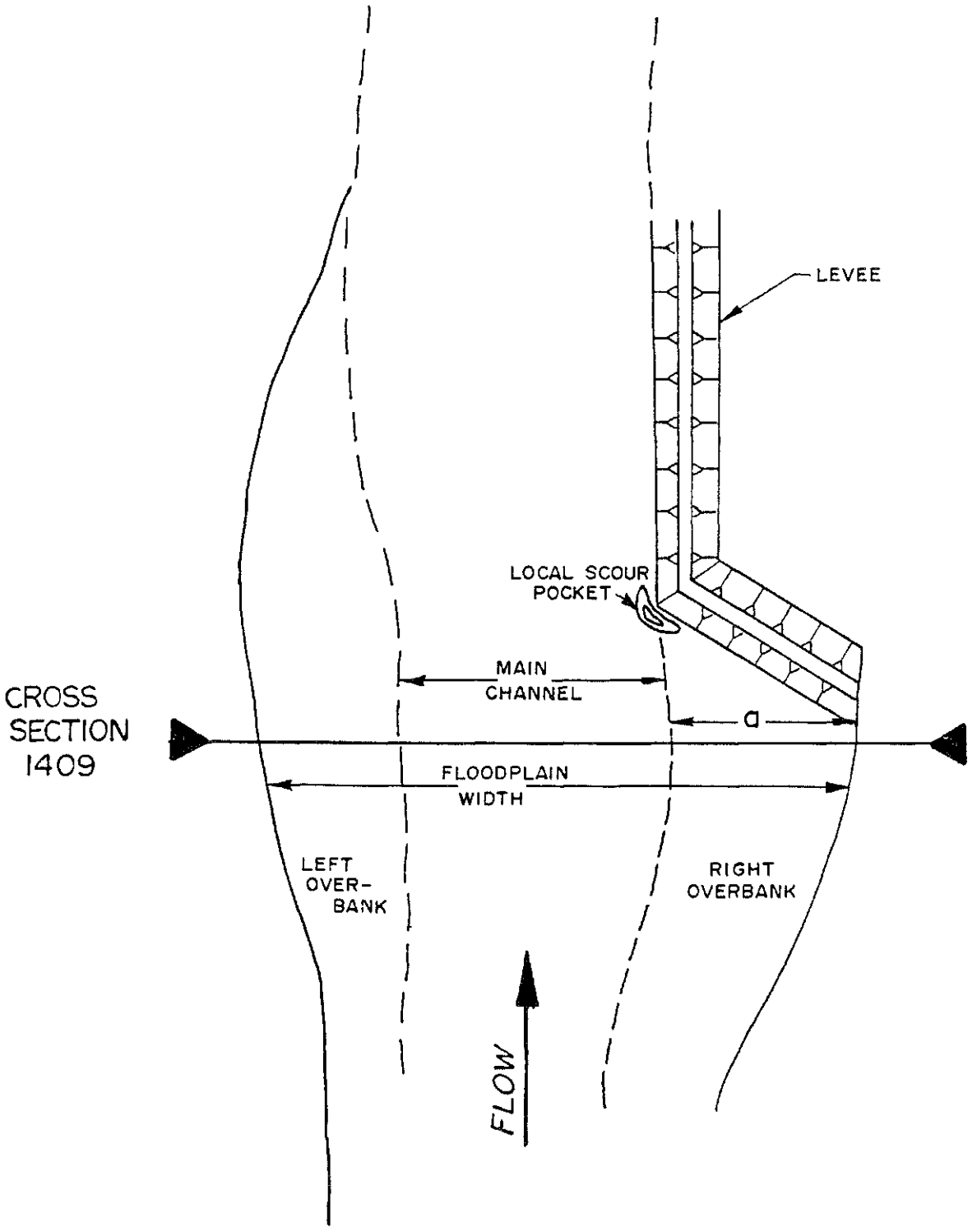


Figure 7.7 Plan view of levee alignment analyzed in local scour evaluation.

therefore; $\frac{a}{y} = \frac{560}{2.20} = 254$

Since $\frac{a}{y}$ is greater than 25, Equation 5.18 will be used.

4. Compute embankment scour.

$$\frac{\Delta Z_{ls}}{Y} = 4\ Fr^{0.33}$$

where $Fr = \frac{V}{\sqrt{g\ Y_h}} = \frac{3.97}{\sqrt{(32.2)\ (2.20)}}$

$$Fr = 0.47$$

therefore; $\Delta Z_{ls} = 4\ Fr^{0.33} Y$

$$\Delta Z_{ls} = (4)\ (0.47)^{0.33} (2.20)$$

$$\Delta Z_{ls} = 6.86\ ft$$

This vertical scour depth will be assumed to extend 50 feet on either side of the levee corner. Assuming the bed material at this location has an angle of repose of 30° (typical for sands and gravels), the sides of the scour hole will be assumed to slope along the levee toe at an angle of 15°. This procedure provides a safety factor of 2.0 as discussed in Section 5.3.10.

The remainder of the right overbank levee segment should also incorporate some toe down for the soil cement to prevent possible erosion that may occur as the overbank flow impinges on the levee and is diverted westerly. On the basis of engineering judgement, the remainder of this segment of the overbank levee will be toed down a distance slightly greater than the hydraulic depth (2.20 feet) at cross section 1409. A toe-down depth of 3.0 feet was chosen.

7.3.2.2.5 General Scour

Since the river cross section geometry is not constant through the three reaches along the proposed levee alignment, the sediment transport characteristics will vary from reach to reach. These variable transport characteristics will influence the amount of sediment being delivered from reach to reach for a given flood event. Any differences between sediment supply to a

reach and sediment transport capacity within that reach will cause either scour or deposition during the flow event being modeled. These short-term bed changes can be evaluated using the principle of sediment continuity. Any lowering of the bed that occurs as a result of this phenomenum is considered a type of general scour and needs to be considered in the design of the levee toe-down dimension.

General scour of this type is most accurately analyzed at Level III using a moveable bed computer model such as HEC-2SR. However, a Level II approximation can be achieved using rigid-bed hydraulic and sediment-transport calculations to estimate the imbalance between sediment-transport capacity and sediment supply between adjacent reaches. The net imbalance within a reach can be converted to a volume which in turn is converted to a channel bed depth adjustment.

Since the 100-year flood is the design standard for this levee project, this event was used in the following analysis. The data requirements and calculation sequence follows.

1. Discretize the 100-year flood hydrograph at 1 hour intervals (see Figure 7.8).

2. Develop sediment transport rating curves for each of the four reaches. The hydraulic data required for these calculations can be taken from the HEC-2 runs for the 2-, 5-, 10-, 25-, 50-, and 100-year peak discharge values. Since only one rating curve is developed for each reach, average hydraulic parameters which are characteristic of each reach must be used. For purposes of this example, the velocity, area, and topwidths from the HEC-2 analyses were averaged for all the cross sections in each reach. These average values were segregated by channel and overbank partitions in order that sediment transport calculations could be performed within each of these partitions. The total transport rate for each reach (for a given discharge) is the sum of the transport rate for the channel plus the transport rate for the overbank(s).

   The end product of this step is a curve representing a plot of $Q_S$ vs. $Q$ for the range of water discharge values being evaluated. Figure 7.9 illustrates the rating curve developed for Reach 2.

3. Route design hydrograph through the study reach. The purpose of this step is to determine the amount of sediment transported through each reach during the passage of a given hydrograph. This is accomplished in a tabular format as illustrated in Table 7.2. The sediment transport for each step of the hydrograph is read from the sediment transport rating curve for each reach. The transport rates for each time interval are then summed to get a total transport rate for each

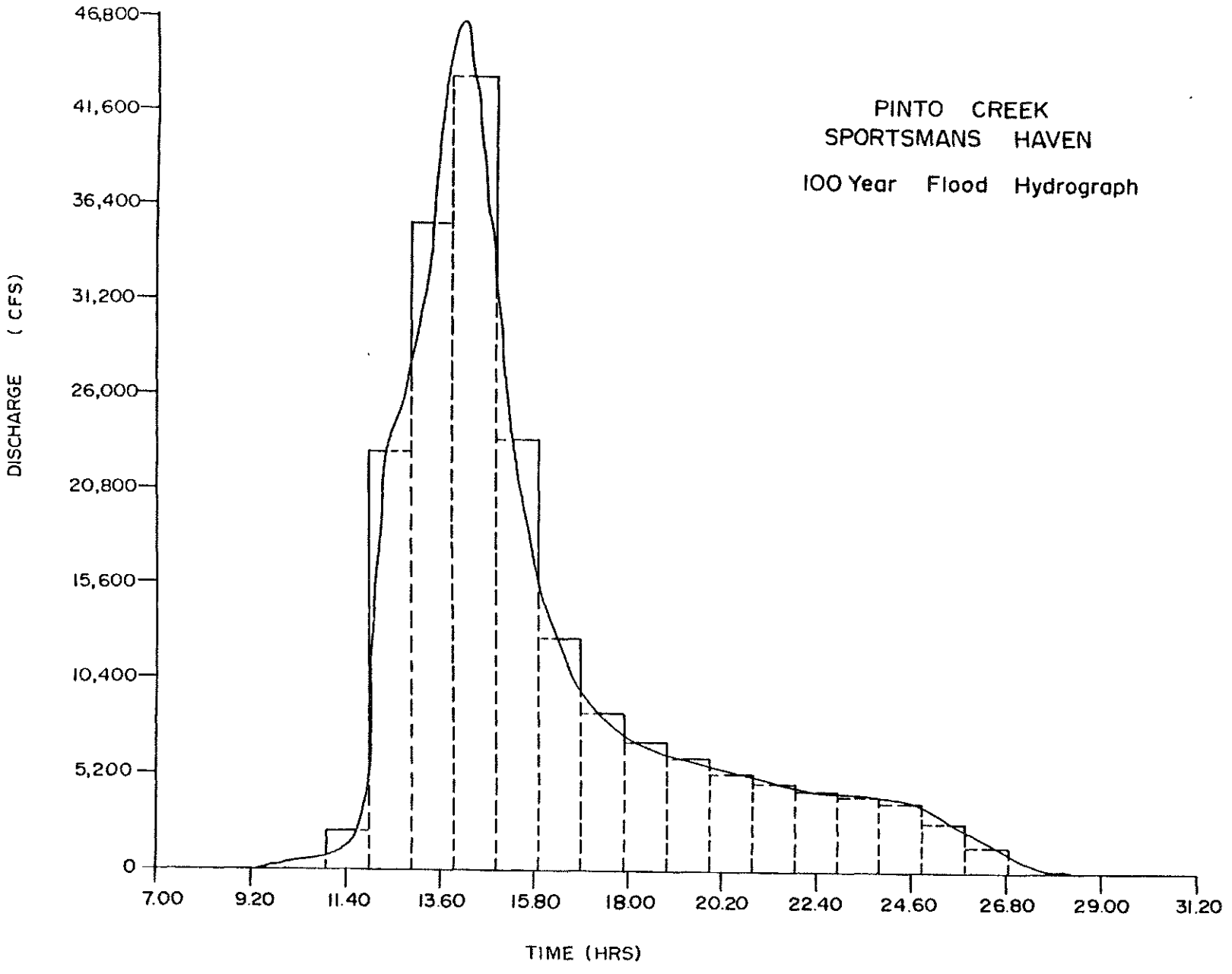


Figure 7.8 Discretized 100-year flood hydrograph.

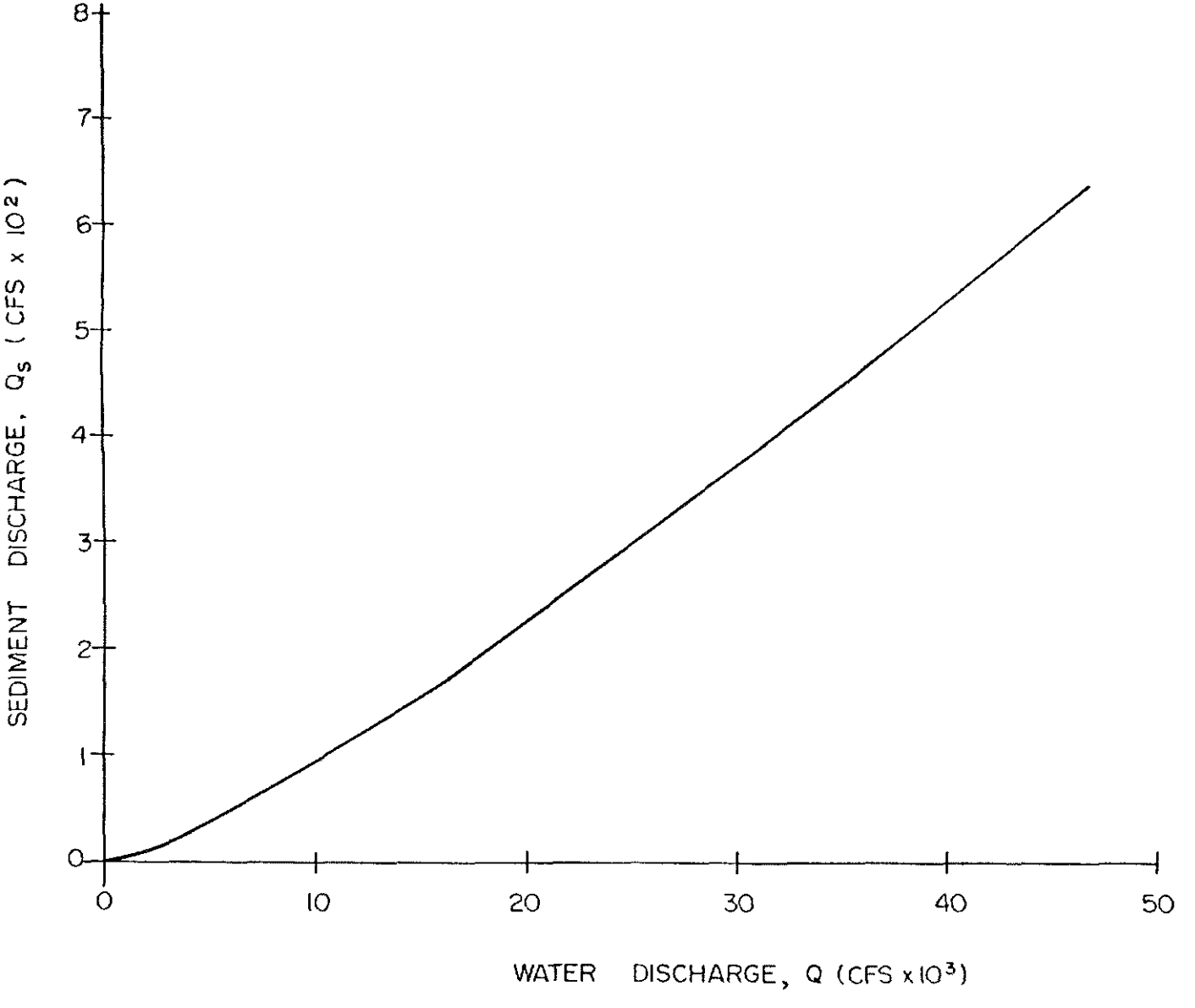


Figure 7.9 Sediment transport rating curve - Reach 2, Pinto Creek at Sportsman's Haven.

Table 7.2. General Scour Analysis Using Sediment Continuity, 100-year Event.

| Time (Hours) | Q (cfs) | $Q_s$ (cfs) Reach 1 | Reach 2 | Reach 3 | Reach 4 |
|---|---|---|---|---|---|
| 10.96 - 11.96 | 2,080 | 12 | 15 | 12 | 14 |
| 11.96 - 12.96 | 22,932 | 215 | 271 | 338 | 225 |
| 12.96 - 13.96 | 35,412 | 372 | 456 | 694 | 172 |
| 13.96 - 14.96 | 43,576 | 484 | 585 | 954 | 462 |
| 14.96 - 15.96 | 23,504 | 222 | 280 | 355 | 232 |
| 15.96 - 16.96 | 12,688 | 99 | 126 | 114 | 121 |
| 16.96 - 17.96 | 8,580 | 61 | 78 | 71 | 80 |
| 17.96 - 18.96 | 6,968 | 48 | 61 | 54 | 62 |
| 18.96 - 19.96 | 5,200 | 33 | 41 | 36 | 42 |
| 19.96 - 20.96 | 5,356 | 34 | 43 | 37 | 43 |
| 20.96 - 21.96 | 4,784 | 29 | 37 | 31 | 37 |
| 21.96 - 22.96 | 4,316 | 26 | 31 | 26 | 31 |
| 22.96 - 23.96 | 4,056 | 23 | 29 | 24 | 28 |
| 23.96 - 24.96 | 3,640 | 21 | 25 | 21 | 25 |
| 24.96 - 25.96 | 2,600 | 15 | 18 | 15 | 18 |
| 25.96 - 26.96 | 1,300 | 7 | 9 | 7 | 9 |
| | TOTAL: | 1,702 | 2,104 | 2,790 | 1,804 |
| | DIFFERENCE: | -402 | -686 | 986 | |

reach for the duration of the hydrograph. The difference in transport rates between adjacent reaches represents the sediment imbalance that must be satisfied through scour or deposition.

4. The transport rate imbalance between reaches must be converted to sediment volumes before channel bed adjustments can be computed. The volume conversion and sediment distribution through each reach is most easily accomplished in a tabular format. The following information is needed for this step:

   a. Difference in sediment transport rates ($\Delta Q_s$) between adjacent reaches.

   b. Time interval for the discretized hydrograph ($\Delta t$).

   c. Channel and overbank reach lengths.

   d. Channel and overbank widths.

   e. Channel and overbank conveyance values.

   f. Sediment porosity.

   The procedure consists of converting the $\Delta Q_s$ values to volumes by multiplying $\Delta Q_s$ (cfs) by the discretization interval, $\Delta t$ (hr) and a seconds to hours conversion factor (3,600). This calculation yields an unbulked sediment volume in cubic feet. This volume is then distributed through the channel and overbanks in proportion to the conveyance ratios for each of these partitions. The proportioned volume for each partition is then uniformally distributed by dividing the volume by the product of the partition length and width. The resultant answer will represent vertical bed movement in terms of unbulked sediment. To correct for sediment bulking, this answer must be divided by (1-n), where n is sediment porosity.

The general scour calculations, using the sediment continuity principle and rigid-bed hydraulics, are summarized in Table 7.3. This analysis predicts approximately 3 to 5 feet of general scour for Reaches 2 and 3 but nearly 6 feet of aggradation for Reach 4. This illustrates the dynamic changes that can occur in a riverbed during a major flood. The engineer must remember that these are net changes that would be expected at the <u>end</u> of the hydrograph. Transport imbalances may occur <u>during</u> the hydrograph that produce temporary scour that is more severe than the net change observed at the end of the flood. At Level II, this additional scour potential is accounted for by applying a factor of safety to the sum of all scour components.

Table 7.3. Pinto Creek 100-year Sediment Continuity Analysis.

| (1) | (2) | (3) | (4) | (5) | (6) | (7) | (8) | (9) | (10) Vertical Movement (feet) n = 0.4 | |
|---|---|---|---|---|---|---|---|---|---|---|
| Reach | $\Delta Q_s$ (cfs) | $\Delta t$ (hr) | Partition | Length (feet) | Width (feet) | $K_{PARTITION}$ | $K_{TOTAL}$ | $\frac{K_p}{K_T}$ | Unbulked | Bulked |
| | | | LOB | 1,190 | 54 | 12,759 | | 0.025 | -0.56 | -0.93 |
| 2 | -402 | 1.0 | CH | 1,190 | 547 | 505,858 | 518,613 | 0.975 | -2.17 | -3.62 |
| | | | ROB | N/A | 0 | 0 | | 0 | 0 | 0 |
| | | | LOB | 1,170 | 427 | 105,289 | | 0.256 | -1.27 | -2.12 |
| 3 | -686 | 1.0 | CH | 1,190 | 484 | 306,275 | 411,569 | 0.744 | -3.19 | -5.32 |
| | | | ROB | N/A | 0 | 0 | | 0 | 0 | 0 |
| | | | LOB | 1,320 | 672 | 206,149 | | 0.437 | 1.75 | 2.92 |
| 4 | 986 | 1.0 | CH | 1,190 | 487 | 266,009 | 472,158 | 0.563 | 3.45 | 5.75 |
| | | | ROB | N/A | 0 | 0 | | 0 | 0 | 0 |

$$\text{Vertical Movement} = \frac{\Delta Q_s \text{ ft}^3}{\text{sec.}} \times \frac{\Delta t \text{ hr.}}{1} \times \frac{3600 \text{ sec.}}{\text{hour}} \times \frac{1}{(\text{length}) \times (\text{width}) \text{ ft}^2} \frac{K_p}{K_T}$$

or/ col. 10 = col. 2 x col. 3 x 3600 ÷ [(col. 5) x (col. 6)] x col. 9

$\Delta t$ = time interval for discretized hydrograph

K = conveyance

7.3.2.2.6 Sand Wave Troughs

The results of the HEC-2 hydraulic analysis for this project indicate that supercritical flow will probably occur in Pinto Creek during the 100-year flood. This condition will lead to the formation of antidunes in a sand bed channel. Although the supercritical flow needed for the formation of antidunes dunes would normally be expected to occur near the center of the channel cross section, the formation of sand or gravel bars may create a meandering filament of high velocity flow. If this filament were to be diverted across the channel and begin flowing next to the levee, antidunes could form along the levee too. Under these conditions, the troughs created by these bed forms could undercut the soil-cement embankment and cause a levee failure. To protect against this type of failure, the soil cement should be extended a sufficient distance below the channel bed to prevent undercutting by antidunes.

The estimated depth of antidune troughs is computed by using Equation 4.25:

$$h_a = 0.027\ V^2$$

The computed value of $h_a$ represents the distance from the crest to the trough of an antidune (see Figure 4.7). Accordingly, $h_a$ must be divided by two to get the trough depth below the original bed elevation. When using this equation, the engineer must remember that, in reality, $h_a$ can never exceed the actual depth of flow ($Y_o$). Therefore, the trough depth calculations must be compared to the actual depths of flow expected in a channel. If the computed value of $h_a$ exceeds $Y_o$, $h_a$ should be assumed equal to $Y_o$.

The proper value to use for $V$ in Equation 4.25 is the maximum velocity expected within the channel cross section, rather than a weighted channel average of the velocity. This may entail subdividing a channel section into vertical strips and computing conveyance values for each, which can then be combined with known energy slopes from a HEC-2 analysis to derive a velocity for each strip.

If there is a wide variation in maximum velocity from one cross section to the next, the engineer should consider seperate antidune calculations for different reaches of the river. The squared velocity term in Equation 4.25 makes this calculation very sensitive to changes in this parameter.

For this project, average maximum velocities (based on the maximum velocity at each cross section within a reach) were determined for Reaches 2, 3, and 4 and trough depth calculations were performed for each reach. These calculations, which employed Equation 4.25, are summarized in Table 7.4.

### 7.3.3 Lateral Migration

Changes to the boundaries of river systems occur in the horizontal direction as well as the vertical. Quite often, horizontal movement is induced or aggravated by the construction of man-made improvements within a floodplain. In the case of the Pinto Creek project, the installation of an armored levee along the east bank of the river may accelerate erosion along the west bank. The soil cement embankment will eliminate a potential sediment source along the east bank that may have historically been required to help satisfy deficits between upstream supply and transport capacity within a given reach.

Analysis of lateral migration potential is perhaps most accurately determined through a Level I review of historical aerial photographs of the river system. The proposed installation of an armored levee, however, introduces a variable that is not reflected in the channel movement observed in historical photos.

As discussed in Section 5.3.9, quantification of lateral migration in a disturbed river system can be pursued through the application of the sediment continuity concept. If a sediment deficit is found to exist within a given reach as the result of routing the design hydrograph through the reach, a worst case condition can be established by assuming the sediment deficit is satsified by using one bank of the reach as the sole, local sediment supply. The sediment deficit could either be uniformly distributed along the entire bank line or be concentrated in a location where a bend might form or is already in existence. The following analysis for Pinto Creek will illustrate both cases.

1. Use sediment continuity and assume all sediment deficits will be satisfied by erosion of material from the west bank. The analysis will use data from the general scour analysis (Section 7.3.2.2.5) for the 100-year flood.

Table 7.4. Calculation of Antidune Trough Depths.

| Reach | Average Maximum Velocity (fps) | $h_a$ (feet)[1] | Trough Depth (feet) (1/2 x $h_a$) |
|---|---|---|---|
| 2 | 16.18 | 7.07 | 3.5 |
| 3 | 17.92 | 8.67 | 4.3 |
| 4 | 12.56 | 4.26 | 2.1 |

[1] $h_a = 0.027\ V^2$ (Equation 4.25).

2. Reach 2 - This reach will be armored along the east bank, as a result of the proposed soil-cement levee, and presently consists of natural rock along the west bank. As a result, no lateral channel movement is expected to occur in this reach.

3. Reach 3 - From the sediment continuity analysis, this reach has a total sediment supply deficit of 686 cfs (see Table 7.2). This value is converted to a volume as follows:

$$\text{Vol.} = \Delta Q_s \times \Delta t \times 3{,}600 \text{ sec./hr.}$$

$$\text{Vol.} = (686)\ (1 \text{ hour})\ (3{,}600)$$

$$\text{Vol.} = 2{,}469{,}600 \text{ feet}^3$$

Correct for bulking (assuming a porosity of n = 0.4),

$$\text{Vol.} = \frac{2{,}469{,}600}{0.6} = 4{,}116{,}000 \text{ feet}^3$$

The average west bank height (H) through Reach 3 is six feet, while the bank length is 1,170 feet. Assuming uniform erosion, the lateral bank movement is computed as follows:

$$\Delta W = \frac{\text{Volume Sed. Def}}{\text{HWB} \times \text{LWB}}$$

$$\Delta W = \frac{4{,}116{,}000}{(6)\ (1{,}170)}$$

$$\Delta W = 586 \text{ feet}$$

An alternative to the uniform erosion approach is to assume the erosion will occur as a semi-circular bend. The volume of erosion is computed as:

$$\text{Volume}_{\text{Bank}} = \frac{1}{2}\ \pi\ r^2\ H$$

Assuming the volume of bank erosion equals the volume of sediment deficit (i.e., bed and bank materials are similar); or

$$\text{Volume}_{\text{Bank}} = \text{Volume}_{\text{Sed. Def}}$$

we can solve for the radius of the semi-circle as follows:

$$r = \left(\frac{\text{Vol.}_{\text{Sed. Ded.}}}{1/2\ \pi\ H}\right)^{1/2}$$

$$r = \left[\frac{4,116,000}{(.5)(\pi)(H)}\right]^{1/2}$$

$$r = 661 \text{ feet}$$

The semi-circular erosion pattern gives a worst-case condition for this reach. Selection of the dimensions for an erosion buffer zone along the west bank is a matter of experience and engineering judgement, and should not be based solely on the results of a quantitative analysis such as that presented above. Cases may arise where it would be more economical to construct some type of structural measure to prevent erosion, rather than purchasing the right-of-way for an erosion buffer zone.

For this project, an erosion buffer zone was selected as the preferred alternative for the west bank. The west bank is undeveloped property and can be purchased at a low cost. Based on the results of the quantitative lateral migration analysis, a review of historical photos dating back to 1947, and the topography along the west bank, a variable width buffer zone was recommended for the west bank through Reach 3.

Due to the reconnaissance level nature of the Department of Water Resource study, subsurface geological data was not available for the stream bank opposite the proposed levee. However, a rock formation is visible along the west bank through the majority of Reach 2. The topography along the west bank suggests that this rock formation continues under the surface and probably constitutes the steep ridgeline along the west bank of Reach 3. On this assumption, the buffer zone for Reach 3 will be taken as that area from the west edge of the 100-year floodplain to the base of the steep ridge (see Figure 7.1). This width will vary from 200' to 300', and is within the limits derived from the quantitative analysis. Obviously, the geological assumptions used in this analysis would have to be verified prior to a final delineation and acquisition of the buffer zone.

4. Reach 4 - The sediment continuity analysis indicates this reach will receive more sediment than it is capable of transporting. As a result, bank erosion due to insufficient sediment supply should not occur. However, as the bed aggrades, the channel geometry could change and cause the main channel to shift westerly and possibly attack the western bank with high velocity flow. This is a very dynamic process which is difficult to quantify. Estimating the amount of lateral erosion in aggrading reaches is a matter of engineering judgement. Again, as for Reach 3, topographic features and historical photos were used in establishing a realistic buffer zone through Reach 4. This zone is an extension of the one through Reach 3 and essentially follows the base of another steep ridgeline which is suspected to be overlying rock along the northern half of the reach (see Figure 7.1 for buffer zone limits).

Although Figure 7.1 does not extend far enough downstream to show this feature, Pinto Creek makes about a 45° bend to the east after leaving Reach 4. In the absence of any visible topographic or geologic erosion resistant features in this downstream area, there is a good chance that some accelerated erosion could occur on the outside of this bend. This erosion process may be further accelerated as a result of the straightened alignment of the river from the Highway 88 bridge through Reach 4. The proposed levee tends to concentrate the flood water in a straight line that is directed into this bend. Prior to construction of the proposed levee, the water spread out through Sportsman's Haven and did not launch such a concentrated attack at the entrance to the bend.

As part of the final design phase of this project, it would be recommended that a detailed analysis be made of this problem in order that mitigation measures might be taken if the damage potential was found to be severe and directly related to construction of the upstream levee system.

The quantitative assessment of lateral migration presented in this section is based on a single flood event. Realizing that lateral migration is a continual process over a long period of time, some safety factor, say 2.0, could be applied to the quantitative calculations to establish a long-term limit. It must be emphasized, however, that quantitative calculations should only be used with considerable engineering judgement and an appreciation of historical events and physical constraints such as topography and geology.

## 7.4 Summary and Conclusions

Based on the preceding analyses, we are now prepared to establish the critical design dimensions for the proposed levee system.

1. Levee Crest Profile
   The crest of the levee will parallel the subcritical water-surface profile for the 100-year flood. As shown below, the top of the levee embankment and the soil-cement bank protection will be elevated an equal distance above this water-surface profile. These freeboard dimensions are minimum values and may be increased slightly during design to eliminate numerous grade breaks during actual levee construction.

| Reach | Freeboard Distance Above Design Water Surface Profile (feet) | |
|---|---|---|
| | Levee Crest | Soil-Cement Lining |
| Upstream | | |
| Right Overbank | 3.0 | 3.0 |
| 2 | 3.8 | 3.8 |
| 3 | 4.2 | 4.2 |
| 4 | 3.1 | 3.1 |

2. Requirements For Bank Stabilization
The need for bank stabilization to prevent erosion of the earth levee was discussed in Section 7.3.2.1. For this project, a soil-cement blanket is proposed along the stream-side face of the levee to prevent erosion.

3. Toe-Down Requirements For Soil-Cement Embankment
The soil cement must be extended far enough below existing ground elevation so as to prevent undermining by the multiple scouring processes that occur on both a short and long-term basis. This toe-down dimension is determined as the sum of all the vertical channel adjustments that were analyzed in Section 7.3.2.2. A summary of the recommended toe-down depths for specific reaches of the levee is presented in Table 7.5.

4. Lateral Channel Migration
Armoring of the proposed east bank levee through an application of soil cement may accelerate erosion along the opposite bank of the stream. As a precautionary measure, an erosion buffer zone is recommended along the west bank of Pinto Creek. The buffer zone dimensions are summarized as follows:

| Reach | Buffer Zone (feet) |
|---|---|
| 2 | 0 (natural rock) |
| 3 | 200 - 300 |
| 4 | 130 - 350 |

For this project, the buffer zone will be measured from the west edge of the 100-year flood plain. Unique circumstances on other projects might dictate that such buffer zones be measured from different reference points.

Table 7.5. Summary of Soil-Cement Toe-Down Dimensions.

| Reach | Long-Term Degradation (feet) | Low Flow Incisement (feet) | Local Scour (feet) | General Scour (feet) | Antidune Troughs (feet) | Safety Factor | Total[4] Calculated Toe-Down (feet) |
|---|---|---|---|---|---|---|---|
| Upstream Right Overbank | 0[1] | N/A[2] | 0 | 2.2[3] | 0 | 1.3 | 2.9 |
| Upstream Levee Corner | 0[1] | N/A[2] | 6.9 | 3.6 | 3.5 | 1.3 | 18.2 |
| 2 | 0[1] | N/A[2] | 0 | 3.6 | 3.5 | 1.3 | 9.2 |
| 3 | 0[1] | N/A[2] | 0 | 5.3 | 4.3 | 1.3 | 12.5 |
| 4 | 0[1] | N/A[2] | 0 | 0[1] | 2.1 | 1.3 | 2.7 |

[1]The equilibrium slope or general scour analysis predict aggradation or deposition, respectively, at these locations. As a conservative approach, aggradation or desposition is not algebraicly added into the toe-down depth, a zero bed adjustment is assumed for these cases.

[2]The invert of the existing low flow channel will be used as a base elevation from which all other bed profile adjustments will be measured.

[3]On the basis of engineering judgement, the hydraulic depth in the right overbank was selected as being representative of this type of scour.

[4]These are minimum values and may be increased slightly during design to eliminate numerous grade breaks during construction.

This concludes the design example. The intent of this section was to illustrate the application of analytical concepts presented in this manual to an actual project study. As can be seen from the above analysis, "real world" problems do not always conform to the ideal conditions often used to describe the theory of a technical procedure. For instance, in this problem we found no controls in the channel bed that could be used as pivot points for an equilibrium slope analysis. A problem was also suspected in the selection of a sediment supply section for the equilibrium slope analysis. The lateral migration analysis demonstrated the need for considerable engineering judgement in selecting an erosion buffer zone.

Very seldom will projects involving fluvial systems be encountered that lend themselves to an ideal or textbook solution. All the quantitative procedures outlined in this manual should only be used as guidelines. As emphasized throughout this design manual, the final solution to a specific problem must be based on engineering judgement and experience.

## VIII. REFERENCES


Agricultural Research Service, 1979, Field Manual for Research in Agricultural Hydrology, Agricultural Handbook 224, February.

Anderson, A. G., A. S. Paintal, and J. T. Davenport, 1970, Tentative Design Procedure for Riprap-Lined Channels; Project Report No. 96, St. Anthony Falls Hydraulics Laboratory, Minneapolis, Minnesota, NCHRP Report 108, Highway Research Board, Washington, D.C.

ASCE Task Force Committee, 1963, Friction Factors in Open Channels, Journal of the Hydraulics Division, Proc. ASCE, Vol. 89, No. HY2, March.

Bathurst, J. C., 1978, Flow Resistance of Large-Scale Roughness, Journal of the Hydraulics Division, ASCE, Vol. 104, No. HY12, Proc. Paper 14239, pp. 1587-1603.

Chow, V. T., 1959, Open-Channel Hydraulics, McGraw-Hill, New York, 680 pp.

Chow, V. T., 1962, Hydrologic Determination of Waterway Areas for the Design of Drainage Structures in Small Drainage Basins, University of Illinois Engineering Experiment Station Bulletin No. 462, 104 pp, Urbana, Illinois.

Colby, B. R., 1964, Practical Computations of Bed-Material Discharge, Journal of the Hydraulics Division, ASCE, Vol. 90, No. HY2.

Colby, B. R., and C. H. Hembree, 1955, Computation of Total Sediment Discharge, Niobrara River Near Cody, Nebraska, U.S. Geological Survey Water Supply Paper 1357.

Culvertson, D. M., L. E. Young, and J. C. Brice, 1967, Scour and Fill in Alluvial Channels: U.S. Geol. Surv. Open-File Report, 58 pp.

Denver Urban Drainage and Flood Control District, 1982, Urban Storm Drainage Criteria Manual, Volume 2, Section 5, Riprap (revised from 1969 version).

Einstein, H. A., 1950, The Bed Load Function for Sediment Transportation in Open Channel Flows, U.S. Department of Agriculture, Soil Conservation Service, Technical Bulletin No. 1026.

Friedkin, J. F., 1945, A Laboratory Study of the Meandering of Alluvial Channels, U.S. Army Corps of Engineers, Waterways Experiment Station.

Gessler, J., 1971, Beginning and Ceasing of Sediment Motion, River Mechanics, Chapter 7, edited by H. W. Shen, Fort Collins, Colorado, 22 pp.

Green, W. H., and C. A. Ampt, 1911, Studies on Soil Physics, I, Flow of Air and Water Through Soils, Journal of Agricultural Science, Vol. 4, pp. 1-24.

Haan, C. T., 1977, Statistical Methods in Hydrology, Iowa State University Press, Ames, Iowa.

Henderson, F. M., 1966, Open Channel Flow, The McMillan Company, New York.

Hershfield, D. M., 1961, Rainfall Frequency Atlas of the United States, for Durations from 30 Minutes to 24 Hours and Return Periods from 1 to 100 Years, Technical Paper No. 40, United States Weather Bureau.

Ippen, A. T., and P. A. Drinker, 1962, Boundary Shear Stress in Curved Trapezoidal Channels, Journal of the Hydraulics Division, ASCE, Vol. 88, No. HY5, September.

Kaan, H. R., 1971, Laboratory Study of River Morphology: unpublished Ph.D. Dissertation, Colorado State University, 189 pp.

Kellerhals, R., and D. I. Bray, 1971, Sampling Procedures for Coarse Fluvial Sediments, Journal of the Hydraulics Division, ASCE, Vol. 97, No. HY8, August.

Kennedy, J. F., 1963, The Mechanics of Dunes and Antidunes in Erodible-Bed Channels, Journal of Fluid Mechanics, Vol. 16, pt. 4, pp. 521-544.

Kite, G. W., 1977, Frequency and Risk Analyses in Hydrology, Water Resources Publications, Fort Collins, Colorado.

Lagasse, P. F., J. D. Schall, and M. R. Peterson, 1984, Erosion Risk Analysis for a Southwestern Arroyo, paper accepted for publication in the Journal of Urban Planning and Development, ASCE.

Lane, E. W., 1955, The Importance of Fluvial Morphology in Hydraulic Engineering: Am. Soc. Civil Eng. Proc., Vol. 81, No. 745, 17 pp.

Lane, E. W., 1957, A Study of the Shape of Channels Formed by Natural Streams Flowing in Erodible Material," Missouri River Division Sediment Series No. 9, U.S. Army Engineer Division, Missouri River, Corps of Engineers, Omaha, Nebraska.

Lane, E. W. and E. J. Carlson, 1953, Some Factors Affecting the Stability of Canals Constructed in Coarse Granular Materials, Proc. Minnesota International Hydraulics Convention, September.

Laursen, E. M., and A. Toch, 1956, Scour Around Bridge Piers and Abutments, Iowa Highway Research Board, Bulletin No. 4, May.

Leopold, L. B., W. W. Emmett, and R. M. Myrick, 1966, Channel and Hillslope Processes in a Semiarid Area, New Mexico, U.S. Geological Survey Professional Paper 352-G, U.S. Geological Survey, Washington, D.C.

Leopold, L. B., and M. G. Wolman, 1967, River Channel Patterns: Braided, Meandering, and Straight, USGS Prof. Paper 282-B, 85 pp.

Leopold, L. B., M. G. Wolman and J. P. Miller, 1964, Fluvial Processes in Geomorphology, San Francisco: W. Freeman.

Li, R. M., and D. B. Simons, 1979, Failure Probability of Riprap Structures, paper presented to the ASCE Conference and Exposition, Atlanta, Georgia, Oct. 23-25.

Li, R. M., M. A. Stevens and D. B. Simons, 1976, Solutions to the Green-Ampt Infiltration Equation, Journal of the Irrigation and Drainage Division, ASCE, Vol. 102, No. IR2, Proc. Paper 12196, June.

McCuen, R. J., W. J. Rawls, G. T. Fisher and R. L. Powell, 1977, Flood Frequency Estimation at Ungaged Locations: State of the Art, Water Supply and Management, Vol. 3, Pergamon Press, Ltd., Great Britain.

McPherson, M. B., 1969, Some Notes in the National Method of Storm Drainage Design, Technical Memorandum No. 6, ASCE Urban Water Resources Program, ASCE.

Meyer-Peter, E., and R. Muller, 1948, Formulas for Bed Load Transport, Proc., 3rd Meeting of IAHR, Stockholm, pp. 39-64.

National Weather Service, 1977, Five to 60 Minute Precipitation Frequency for the Eastern and Central United States (HYDRO-55).

Osterkamp, W. R., and E. R. Hedman, 1981, Perennial-Streamflow Characteristics Related to Channel Geometry and Sediment in the Missouri River Basin, in press, USGS Professional Paper.

Reich, B. M., 1960, Annotated Bibliography and Comments on the Estimation of Flood Peaks from Small Watersheds, Technical Report CER60M452, 66 pp., Civil Engineering Department, Colorado State University, Fort Collins.

Reich, B. M., 1971, Ruonff Estimates for Small Rural Watersheds, 136 pp., Civil Engineering Department, The Pennsylvania State University, University Park.

Renard, K. G., 1980, Estimating Erosion and Sediment Yield from Rangelands, Proceedings ASCE Symposium on Watershed Management, pp. 164-175.

Richardson, E. V., D. B. Simons, S. Karaki, K. Mahmood, and M. A. Stevens, 1975, Highways in the River Environment, Hydraulic and Environmental Design Considerations, Training and Design Manual prepared for U.S. Department of Transportation, Federal Highway Administration, May.

Roeske, R. H., 1978, Methods for Estimating the Magnitude and Frequency of Floods in Arizona, Arizona Department of Transportation, RS-15(121).

Rozovskii, I. L., 1961, Flow of Water in Bends of Open Channels, Israel Program for Scientific Translations, Jerusaleum, Israel.

Schumm, S. A., 1977, The Fluvial System, John Wiley and Sons, Inc., New York.

Schwab, G. O., R. K. Frevert, T. W. Edminster, and K. K. Barnes, 1966, Soil and Water Conservation Engineering, John Wiley and Sons, Inc., New York.

Shen, H. W., 1971, Wash Load and Bed Load, River Mechanics, H. W. Shen, ed., Water Resources Publications, Fort Collins, Colorado, 30 pp.

Shields, A., 1936, Anwendung der Ahnlichkeltschechanik und Turbulenz Forschung auf die Geschiebebewegung, Metteil. Preuss. Versuchsanst. Wasser, Erd. Schiffsbau, Berlin, No. 26.

Shown, L. M., 1970, Evaluation of a Method for Estimating Sediment Yield, U.S. Geological Survey Professional Paper 700-B, U.S. Geological Survey, Washington, D.C., pp. 245-249.

Simons, D. B., Y. H. Chen, and L. J. Swenson, 1983, Hydraulic Test to Develop Design Criteria for the Use of Reno Mattresses, report prepared for Maccaferri Steel Wire Products, Ltd., Ontario, Canada.

Simons, D. B., R. M. Li and W. T. Fullerton, 1981, Theoretically Derived Sediment Transport Equations for Pima County, Arizona, Simons, Li & Associates, Inc., Fort Collins, Colorado, prepared for Pima Coiunty DOT and Flood Control District, Tucson, Arizona.

Simons, D. B., and E. V. Richardson, 1960, Resistance to Flow in Alluvial Channels, Journal of the Hydraulics Division, ASCE, Vol. 86, No. HY5, May.

Simons, D. B., and E. V. Richardson, 1966, Resistance to Flow in Alluvial Channels, U.S. Geological Survey Professional Paper 422-J.

Simons, D. B., and F. Senturk, 1977, Sediment Transport Technology, Water Resources Publications, Fort Collins, Colorado.

Simons, Li & Associates, Inc., 1982, Engineering Analysis of Fluvial Systems, published by Simons, Li & Associates, printed and bound by BookCrafters, Inc., Chelsea, Michigan.

Soil Conservation Service, 1976 (TR55)

Soil Conservation Service, 1977, Design of Open Channels, Technical Release No. 25, October.

U.S. Army Corps of Engineers, 1970, Hydraulic Design of Flood Control Channels, Engineer Manual EM 1110-2-1601, July.

U.S. Army Corps of Engineers, 1970, Laboratory Soils Testing, EM 1110-2-1906, November.

U.S. Bureau of Reclamation, 1960, Investigation of Meyer-Peter, Muller Bedload Formulas: Sedimentation Section, Hydrology Branch, Division of Project Investigations, Denver, Colorado.

U.S. Bureau of Reclamation, 1977, Design of Small Dams.

U.S. Bureau of Reclamation, 1984, Computing Degradation and Local Scour, Technical Guideline for Bureau of Reclamation, prepared by E. L. Pemberton and J. M. Lara, January.

U.S. Geological Survey, 1969, Laboratory Theory and Methods for Sediment Analysis, TWRI, Book 5, Ch. C1.

Viessmann, W., T. E. Harbaugh and J. W. Knapp, 1972, Introduction to Hydrology, Intext Educational Publishers, New York.

Williams, J. R., and H. D. Berndt, 1972, Sediment Yield Computed with Universal Equation, Journal of the Hydraulics Division, ASCE, Vol. 98, No. HY12, Proc. Paper 9426, December, pp. 2087-2097.

Wischmeier, W. H., and D. D. Smith, 1978, Predicting Rainfall Erosion Losses, Agricultural Handbook 537, Science and Education Administration, USDA.

Yevjevich, V., 1972, Probability and Statistics in Hydrology, Water Resources Publications, Fort Collins, Colorado.

Zeller, M. E., and W. T. Fullerton, 1983, A Theoretically Derived Sediment Transport Equation for Sand-Bed Channels in Arid Regions, Proc. of the D. B. Simons Symposium on Erosion and Sedimentation, R. M. Li and P. F. Lagasse, eds.

Zeller, M. E., 1981, Scour Depth Formula for Estimation of Toe Protection Against General Scour, Pima County Department of Transportation and Flood Control District, Tucson, Arizona.

# APPENDIX A

## PACIFIC SOUTHWEST INTER-AGENCY COMMITTEE (PSIAC) METHOD FOR PREDICTING WATERSHED SOIL LOSS

Note: The information presented in APPENDIX A is from the following source: "Pacific Southwest Inter-Agency Committee, Report of the Water Management Subcommittee on Factors Affecting Sediment Yield in the Pacific Southwest Area and Selection and Evaluation of Measures for Reduction of Erosion and Sediment Yield," October, 1968.

### Introduction

The material that follows is suggested for use in the evaluation of sediment yield in the Pacific Southwest. It is intended as an aid to the estimation of sediment yield for the variety of conditions encountered in this area.

The classifications and companion guide material are intended for broad planning purposes only, rather than for specific projects where more intensive investigations of sediment yield would be required. For these purposes it is recommended that map delineations be for areas no smaller than 10 square miles.

It is suggested that actual measurements of sediment yield be used to the fullest extent possible. This descriptive material and the related numerical evaluation system would best serve its purpose as a means of delineating boundaries between sediment yield areas and in extrapolation of existing data to areas where none is available.

This may involve a plotting of known sediment yield data on work maps. Prepared materials such as geologic and soil maps, topographic, climatic, vegetative type and other references would be used as aids in delineation of boundaries separating yield classifications. A study of the general relationships between known sediment yield rates and the watershed conditions that produce them would be of substantial benefit in projecting data to areas without information.

## Sediment Yield Classification

It is recommended that sediment yields in the Pacific Southwest area be divided into five classes of average annual yield in acre-feet per square mile. These are as follows:

| | | | |
|---|---|---|---|
| Classification 1 | > 3.0 | acre-feet/square mile | |
| 2 | 1.0 - 3.0 | " | " |
| 3 | 0.5 - 1.0 | " | " |
| 4 | 0.2 - 0.5 | " | " |
| 5 | < 0.2 | " | " |

Nine factors are recommended for consideration in determining the sediment yield classification. These are geology, soils, climate, runoff, topography, ground cover, land use, upland erosion, and channel erosion and sediment transport.

Characteristics of each of the nine factors which give that factor high, moderate, or low sediment yield level are shown on Table A-1. The sediment yield characteristic of each factor is assigned a numerical value representing its relative significance in the yield rating. The yield rating is the sum of values for the appropriate characteristics for each of the nine factors. Conversion to yield classes should be as follows:

| Rating | Class |
|---|---|
| > 100 | 1 |
| 75 - 100 | 2 |
| 50 - 75 | 3 |
| 25 - 50 | 4 |
| 0 - 25 | 5 |

Guidelines which accompany the table are an integral part of the procedure. They describe the characteristics of factors which influence sediment yield and these are summarized in the space provided on the table.

The factors are generally described, for purposes of avoiding complexity, as independently influencing the amount of sediment yield. The variable impact of any one factor is the result of influence by the others. To account for this variable influence in any one area would require much more intensive investigational procedures than are available for broad planning purposes.

To briefly indicate the interdependence of the factors discussed separately, ground cover is used as an example. If there is no vegetation, litter or rock fragments protecting the surface, the rock, soil, and topography express their uniqueness on erosion and sediment yield. If the surface is very well protected by cover, the characteristics of the other factors are obscured by this circumstance. In similar vein, an arid region has a high potential for erosion and sediment yield because of little or no ground cover, sensitive soils and rugged topography. Given very low intensity rainfall and rare intervals of runoff, the sediment yield could be quite low.

Each of the 9 factors shown on Table A-1 are paired influences with the exception of topography. That is, geology and soils are directly related as are climate and runoff, ground cover and land use, and upland and channel erosion. Ground cover and land use have a negative influence under average or better conditions. Their impact on sediment yield is therefore indicated as a negative influence when affording better protection than this average.

It is recommended that the observer follow a feedback process whereby he checks the sum of the values on the table from A through G with the sum of and I. In most instances high values in the former should correspond to hig values in the latter. If they do not, either special erosion conditions exist or the A through G factors should be re-evaluated.

Although only the high, moderate and low sediment yield levels are shown on the attached table, interpolation between these levels may be made.

## Surface Geology

Over much of the southwest area, the effect of surface geology on erosion is readily apparent. The weaker and softer rocks are more easily eroded and generally yield more sediment than do the harder more resistant types. Sandstones and similar coarse-textured rocks that disintegrate to form permeable soils erode less than shales and related mudstones and siltstones under the same conditions of precipitation. On the other hand, because of the absence of cementing agents in some soils derived from sandstone, large storms may produce some of the highest sediment yields known.

The widely distributed marine shales, such as the Mancos and shale members of the Moenkopi Formation, constitute a group of highly erodible formations. The very large areal extent of the shales and their outwash deposits

gives them a rank of special importance in relation to erosion. Few of the shale areas are free from erosion. Occasionally, because of slope or cover conditions, metamorphic rocks and highly fractured and deeply weathered granites and granodiorites produce high sediment yield. Limestone and volcanic outcrop areas are among the most stable found within the western lands. The principal reason for this appears to be the excellent infiltration characteristics, which allow most precipitation to percolate into the underlying rocks.

In some areas, all geologic formations are covered with alluvial or colluvial material which may have no relation to the underlying geology. In such areas the geologic factor would have no influence and should be assigned a value of 0 in the rating.

## Soils

Soil formation in the Pacific Southwest generally has not had climatic conditions conducive to rapid development. Therefore, the soils are in an immature stage of development and consist essentially of physically weathered rock materials. The presence of sodium carbonate (black alkali) in a soil tends to cause the soil particles to disperse and renders such a soil susceptible to erosion.

There are essentially three inorganic properties--sand, silt, and clay--which may in any combination give soil its physical characteristics. Organic substances plus clay provide the binding material which tends to hold the soil separates together and form aggregates. Aggregate formation and stability of these aggregates are the resistant properties of soil against erosion. Unstable aggregates or single grain soil materials can be very erodible.

Climate and living organisms acting on parent material, as conditioned by relief or topography over a period of time, are the essential factors for soil development. Any one of these factors may overshadow or depress another in a given area and cause a difference in soil formation. For instance, climate determines what type of vegetation and animal population will be present in an area, and this will have a definite influence or determine the type of soil that evolves. As an example, soils developing under a forest canopy are much different from soils developing in a grassland community.

The raw, shaley type areas (marine shales) of the Pacific Southwest have very little, if any, solid development. Colluvial-alluvial fan type areas are

usually present at the lower extremities of the steeper sloping shale areas. Infiltration and percolation are usually minimal on these areas due to the fine textured nature of the soil material. This material is easily dispersed and probably has a high shrink-swell capacity. Vegetation is generally sparse, and consists of a salt desert shrub type.

There are areas that contain soils with definite profile development, and also, stony soils that contain few fines, which constitutes an improved physical condition for infiltration and plant growth over the fine textured shaley areas. These areas usually occur at higher and more moist elevations where bare, hard crystalline rocks provide the soil parent material. Vegetation and other ground cover, under these circumstances, provide adequate protection against the erosive forces and thus low sediment yield results.

In arid and semi-arid areas, an accumulation of rock fragments (desert pavement) or calcareous material (caliche) is not uncommon. These layers can offer substantial resistance to erosion processes.

The two extreme conditions of sediment yield areas have been described. Intermediate situations would contain some features of the two extremes. One such situation might be an area of predominately good soil development that contains small areas of badlands. This combination would possibly result in an intermediate classification.

## Climate and Runoff

Climatic factors are paramount in soil and vegetal development and determine the quantity and discharge rate of runoff. The same factors constitute the forces that cause erosion and the resultant sediment yield. Likewise, temperature, precipitation, and particularly the distribution of precipitation during the growing season, affect the quantity and quality of the ground cover as well as soil development. The quantity and intensity of precipitation determine the amount and discharge rates of runoff and resultant detachment of soil and the transport media for sediment yield. The intensity of prevailing and seasonal winds affects precipitation pattern, snow accumulation and evaporation rate.

Snow appears to have a minor effect on upland slope erosion since raindrop impact is absent and runoff associated with snow melt is generally in resistant mountain systems.

Frontal storms in which periods of moderate to high intensity precipitation occur can produce the highest sediment yields within the Southwest. In humid and subhumid areas the impact of frontal storms on sediment may be greatest on upland slopes and unstable geologic areas where slides and other downhill soil movement can readily occur.

Convective thunderstorm activity in the Southwest has its greatest influence on eroison and sedimentation in Arizona and New Mexico and portions of the adjoining states. High rainfall intensities on low density cover or easily dispersed soils produces high sediment yields. The average annual sediment yield is usually kept within moderate bounds by infrequent occurrence of thunderstorms in any one locality.

High runoff of rare frequency may cause an impact on average annual sediment yield for a long period of time in a watershed that is sensitive to erosion, or it may have little effect in an insensitive watershed. For example, sediment that has been collecting in the bottom of a canyon and on side slopes for many years of low and moderate flows may be swept out during the rare event, creating a large change in the indicated sediment yield rate for the period of record.

In some areas the action of freezing and thawing becomes important in the erosion process. Impermeable ice usually forms in areas of fine textured soils where a supply of moisture is available before the advent of cold weather. Under these conditions the ice often persists throughout the winter and is still present when the spring thaw occurs. In some instances water tends to run over the surface of the ice and not detach soil particles, but it is possible for the ice in a surface layer to thaw during a warm period and create a very erodible situation. Spring rains with ice at shallow depth may wash away the loose material on the surface.

In some areas of the Pacific Southwest, particularly those underlain by marine shale, freezing and thawing alters the texture of soil near the surface, and thus changes the infiltration characteristics. These areas generally do not receive enough snow or have cold enough temperatures to build a snow pack for spring melt. Later in the year soil in a loosened condition is able to absorb a large part of the early rainfall. As rains occur during the summer, the soil becomes compacted on the surface, thus allowing more water to run off and affording a greater chance for erosion.

## Topography

Watershed slopes, relief, floodplain development, drainage patterns, orientation and size are basic items to consider in connection with topography. However, their influence is closely associated with geology, soils, and cover.

Generally, steep slopes result in rapid runoff. The rimrock and badlands, common in portions of the Pacific Southwest, consist of steep slopes of soft shales usually maintained by the presence of overlying cap rock. As the soft material is eroded, the cap rock is undercut and falls, exposing more soft shales to be carried away in a continuing process. However, high sediment yields from these areas are often modified by the temporary deposition of sediment on the intermediate floodplains.

The high mountain ranges, although having steep slopes, produce varying quantities of sediment depending upon the type of parent materials, soil development, and cover which directly affect the erosion processes.

Southerly exposed slopes generally erode more rapidly than do the northerly exposed slopes due to greater fluctuation of air and soil temperatures, more frequent freezing and thawing cycles, and usually less ground cover.

The size of the watershed may or may not materially affect the sediment yield per unit area. Generally, the sediment yield is inversely related to the watershed size because the larger areas usually have less overall slope, smaller proportions of upland sediment sources, and more opportunity for the deposition of upstream derived sediments on floodplains and fans. In addition, large watersheds are less affected by small convective type storms. However, under other conditions, the sediment yield may not decrease as the watershed size increases. There is little change in mountainous areas of relatively uniform terrain. There may be an increase of sediment yield as the watershed size increases if downstream watersheds or channels are more susceptible to erosion than upstream areas.

## Ground Cover

Ground cover is described as anything on or above the surface of the ground which alters the effect of precipitation on the soil surface and profile. Included in this factor are vegetation, litter, and rock fragments. A

good ground cover dissipates the energy of rainfall before it strikes the soil surface, delivers water to the soil at a relatively uniform rate, impedes the flow of water, and promotes infiltration by the action of roots within the soil. Conversely, the absence of ground cover, whether through natural growth habits or the effect of overgrazing or fire, leave the land surface open to the worst effects of storms.

In certain areas, small rocks or rock fragments may be so numerous on the surface of the ground that they afford excellent protection for any underlying fine material. These rocks absorb the energy of falling rain and are resistant enough to prevent cutting by flowing water.

The Pacific Southwest is made up of land with all classes of ground cover. The high mountain areas generally have the most vegetation, while many areas in the desert regions have practically none. The abundance of vegetation is related in a large degree to precipitation. If vegetative ground cover is destroyed in areas where precipitation is high, abnormally high erosion rates may be experienced.

Differences in vegetative type have a variable effect on erosion and sediment yield, even though percentages of total ground cover may be the same. For instance, in areas of pinyon-juniper forest having the same percentage of ground cover as an area of grass, the absence of understory in some of the pinyon-juniper stands would allow a higher erosion rate than in the area of grass.

## Land Use

The use of land has a widely variable impact on sediment yield, depending largely on the susceptibility of the soil and rock to erosion, the amount of stress exerted by climatic factors and the type and intensity of use. Factors other than the latter have been discussed in appropriate places in this guide.

In almost all instances, use either removes or reduces the amount of natural vegetative cover which reflects the varied relationships within the environment. Activities which remove all vegetation for parts of each year for several years, or permanently, are cultivation, urban development, and road construction. Grazing, logging, mining, and fires artifically induce permanent or temporary reduction in cover density.

High erosion hazard sites, because of the geology, soils, climate, etc., are also of high hazard from the standpoint of type and intensity of use. For

example, any use which reduces cover density on a steep slope with erodible soils and severe climatic conditions will strongly affect sediment yield. The extent of this effect will depend on the area and intensity of use relative to the availability of sediment from other causes. Construction of road or urban development with numerous cut and fill slopes through a large area of widespread sheet or gully erosion will probably not cause a change in sediment yield classification. Similar contruction and continued disturbance in an area of good vegetative response to a favorable climate can raise yield by one or more classifications.

Use of the land has its greatest potential impact on sediment yield where a delicate balance exists under natural conditions. Alluvial valleys of fine, easily dispersed soils from shales and sandstones are highly vulnerable to erosion where intensive grazing and trailing by livestock have occurred. Valley trenching has developed in many of these valleys and provides a large part of the sediment in high yield classes from these areas.

A decline in vegetative density is not the only effect of livestock on erosion and sediment yield. Studies at Badger Wash, Colorado, which is underlain by Mancos shale, have indicated that sediment yield from ungrazed watersheds is appreciably less than from those that are grazed. This difference is attributed to the absence of soil trampling in the ungrazed areas, since the density of vegetation has not noticeably changed since exclusion began.

Areas in the arid and semi-arid portions of the Southwest that are surfaced by desert pavement are much less sensitive to grazing and other use, since the pavement affords a substitute for vegetative cover.

In certain instances the loss or deterioration of vegetative cover may have little noticeable on-site impact but may increase off-site erosion by acceleration of runoff. This could be particularly evident below urbanized areas where accelerated runoff from pavement and rooftops has increased the stress on downstream channels. Widespread destruction of cover by poor logging practices or by brush and timber fires frequently increases channel erosion as well as that on the directly affected watershed slopes. On the other hand, cover disturbances under favorable conditions, such as a cool, moist climate, frequently result in a healing of erosion sources within a few years.

## Upland Slope Erosion

This erosion form occurs on sloping watershed lands beyond the confines of valleys. Sheet erosion, which involves the removal of a thin layer of soil over an extensive area, is usually not visible to the eye. This erosion form is evidenced by the formation of rills. Experience indicates that soil loss from rill erosion can be seen if it amounts to about 5 tons or more per acre. This is equivalent in volume per square mile to aproximately 2 acre-feet.

Wind erosion from upland slopes and the deposition of the eroded material in stream channels may be a significant factor. The material so deposited in channels is readily moved by subsequent runoff.

Downslope soil movement due to creep can be an important factor in sediment yield on steep slopes underlain by unstable geologic formations.

Significant gully erosion as a sediment contributor is evidenced by the presence of numerous raw cuts along the hill slopes. Deep soils on moderately steep to steep slopes usually provide an environment for gully development.

Processes of slope erosion must be considered in the light of factors which contribute to its development. These have been discussed in previous sections.

## Channel Erosion and Sediment Transport

If a stream is ephemeral, runoff that traverses the dry alluvial bed may be drastically reduced by transmission losses (absorption by channel alluvium). This decrease in the volume of flow results in a decreased potential to move sediment. Sediment may be deposited in the streambed from one or a series of relatively small flows only to be picked up and moved on in a subsequent larger flow. Sediment concentrations, determined from field measurements at consecutive stations, have generally been shown to increase many fold for instances of no tributary inflow. Thus, although water yield per unit area will decrease with increasing drainage area, the sediment yield per unit area may remain nearly constant or may even increase with increasing drainage area.

In instances of convective precipitation in a watershed with perennial flow, the role of transmission losses is not as significant as in watersheds with ephemeral flow, but other channel factors, such as the shape of the channel, may be important.

For frontal storm runoff, the flow durations are generally much longer than for convective storms, and runoff is often generated from the entire basin. In such instances, sediment removed from the land surfaces is generally carried out of the area by the runoff. Stream channel degradation and/or aggradation must be considered in such cases, as well as bank scour. Because many of the stream beds in the Pacific Southwest are composed of fine-grained alluvium in well defined channels, the potential for sediment transport is limited only by the amount and duration of runoff. Large volumes of sediment may thus be moved by these frontal storms because of the longer flow durations.

The combination of frontal storms of long duration with high intensity and limited areal-extent convective activity will generally be in the highest class for sediment movement in the channels. Storms of this type generally produce both the high peak flows and the long durations necessary for maximum sediment transport.

Sediment yield may be substantially affected by the degree of channel development in a watershed. This development can be described by the channel cross sections, as well as by geomorphic parameters such as drainage density, channel gradients and width-depth ratio. The effect of these geomorphic parameters is difficult to evaluate, primarily because of the scarcity of sediment transport data in the Pacific Southwest.

If the cross section of a stream is such as to keep the flow within defined banks, then the sediment from an upstream point is generally transported to a downstream point without significant losses. Confinement of the flow within alluvial banks can result in a high erosional capability of a flood flow, especially the flows with long return periods. In most channels with wide floodplains, deposition on the floodplain during floods is often significant, and the transport is thus less than that for a within bank flow. The effect of this transport capability can be explained in terms of tractive force which signifies the hydraulic stress exerted by the flow on the bed of the stream. This average bed-shear stress is obtained as the product of the specific weight of the fluid, hydraulic radius, and energy gradient slope. Thus, greater depth results in a greater bed shear and a greater potential for moving sediment. By the same reasoning, steep slopes (the energy slope and bed slope are assumed to be equivalent) also result in high bed-shear stress.

The boundary between sediment yield classifications in much of the Pacific Southwest may be at the mountain front, with the highest yield

designation on the alluvial plain if there is extensive channel erosion. In contrast, many mountain streams emerge from canyon reaches and then spread over fans or valley flats. Here water depths can decrease from many feet to only a few inches in short distances with a resultant loss of the capacity to transport sediment. Sediment yield of the highest classification can thus drop to the lowest in such a transition from a confined channel to one that has no definition.

Channel bank and bed composition may greatly influence the sediment yield of a watershed. In many areas within the Pacific Southwest, the channels in valleys dissect unconsolidated material which may contribute significantly to the stream sediment load. Bank sloughing during periods of flow, as well as during dry periods, piping, and bank scour generally add greatly to the sediment load of the stream and often change upward the sediment yield classification of the watershed. Field examination for areas of head cutting, aggradation or degradation, and bank cutting are generally necessary prior to classification of the transport expectancy of a stream. Geology plays a significant role in such an evaluation. Geologic controls in channels can greatly affect the stream regimen by limiting degradation and headcuts. Thus, the transport capacity may be present, but the supply of sediment from this source is limited.

Man-made structures can also greatly affect the transport characteristics of the stream. For example, channel straightening can temporarily upset the channel equilibrium and cause an increase in channel gradient and an increase in the stream velocity and the shear stress. Thus, the sediment transport capacity of the stream may be temporarily increased. Structures such as debris dams, lined channels, drop spillways, and detention dams may drastically reduce the sediment transport.

AN EXPLANATION OF THE USE OF THE RATING CHART (TABLE A-1) FOR EVALUATING FACTORS AFFECTING SEDIMENT YIELD IN THE PACIFIC SOUTHWEST FOLLOWS

Table A.1. Factors Affecting Sediment Yield in the Pacific Southwest.

| Sediment Yield Levels | A SURFACE GEOLOGY (10)* | B SOILS (10) | C CLIMATE (10) | D RUNOFF (10) | E TOPOGRAPHY (20) | F GROUND COVER (10) | G LAND USE (10) | H UPLAND EROSION (25) | I CHANNEL EROSION & SEDIMENT TRANSPORT (25) |
|---|---|---|---|---|---|---|---|---|---|
| High | a. Marine shales and related mudstones and siltstones. | a. Fine textured, easily dispersed, saline-alkaline, high shrink-swell characteristics<br>b. Single grain silts and fine sands | a. Storms of several days' duration with short periods of intense rainfall.<br>b. Frequent intense convective storms<br>c. Freeze-thaw occurrence | a. High peak flows per unit area<br>b. Large volume of flow per unit area | a. Steep upland slopes (in excess of 30%) High relief, little or no floodplain development | Ground cover does not exceed 20%<br>a. Vegetation sparse, little or no litter<br>b. No rock in surface soil | a. More than 50% cultivated<br>b. Almost all of area intensively grazed<br>c. All of area recently burned | a. More than 50% of the area characterized by rill and gully or landslide erosion | a. Eroding banks continuously or at frequent intervals with large depths and long flow duration<br>b. Active headcuts and degradation in tributary channels |
| ** | | | | | | | | | |
| Moderate | (5)<br>a. Rocks of medium hardness<br>b. Moderately weathered<br>c. Moderately fractured | (5)<br>a. Medium textured soil<br>b. Occasional rock fragments<br>c. Caliche layers | (5)<br>a. Storms of moderate duration and intensity<br>b. Infrequent convective storms | (5)<br>a. Moderate peak flows<br>b. Moderate volume of flow per unit area | (10)<br>a. Moderate upland slopes (less than 20%)<br>b. Moderate fan or floodplain development | (10)<br>Cover not exceeding 40%<br>a. Noticeable litter<br>b. If trees present understory not well developed | (0)<br>a. Less than 25% cultivated<br>a. 50% or less recently logged<br>c. Less than 50% intensively grazed<br>d. Ordinary road and other construction | (10)<br>a. About 25% of the area characterized by rill and gully or landslide erosion<br>b. Wind erosion with deposition in stream channels | (10)<br>a. Moderate flow depths, medium flow duration with occasionally eroding banks or bed |
| ** | | | | | | | | | |
| Low | (0)<br>a. Massive, hard formations | (0)<br>a. High percentage of rock fragments<br>b. Aggregated clays<br>c. High in organic matter | (0)<br>a. Humid climate with rainfall of low intensity<br>b. Precipitation in form of snow<br>c. Arid climate, low intensity storms<br>d. Arid climate, rare convective storms | (0)<br>a. Low peak flows per unit area<br>b. Low volume of runoff per unit area<br>c. Rare runoff events | (0)<br>a. Gentle upland slopes (less than 5%)<br>b. Extensive alluvial plains | (-10)<br>a. Area completely protected by vegetation, rock fragments, litter. Little opportunity for rainfall to reach erodible material | (-10)<br>a. No cultivation<br>b. No recent logging<br>c. Low intensity grazing | (0)<br>a. No apparent signs of erosion | (0)<br>a. Wide shallow channels with flat gradients, short flow duration<br>b. Channels in massive rock, large boulders or well vegetated<br>c. Artificially controlled channels |

* THE NUMBERS IN SPECIFIC BOXES INDICATE VALUES TO BE ASSIGNED APPROPRIATE CHARACTERISTICS. THE SMALL LETTERS, a, b, c, REFER TO INDEPENDENT CHARACTERISTICS TO WHICH FULL VALUE MAY BE ASSIGNED.

** IF EXPERIENCE SO INDICATES, INTERPOLATION BETWEEN THE 3 SEDIMENT YIELD LEVELS MAY BE MADE.

## Use of the Rating Chart of Factors Affecting Sediment Yield in the Pacific Southwest

The following is a summary of the sediment yield classification presented for this methodology.

| Classification | Rating | Sediment Yield AF/sq. mi. |
|---|---|---|
| 1 | > 100 | 3.0 |
| 2 | 75 - 100 | 1.0 - 3.0 |
| 3 | 50 - 75 | 0.5 - 1.0 |
| 4 | 25 - 50 | 0.2 - 0.5 |
| 5 | 0 - 25 | < 0.2 |

In most instances, high values for the A through G factors should correspond to high values for the H and/or I factors.

An example of the use of the rating chart is as follows:

A watershed of 15 square miles in western Colorado has the following characteristics and sediment yield levels:

| | Factors | Sediment Yield Levels | Rating |
|---|---|---|---|
| A | Surface geology | Marine Shales | 10 |
| B | Soils | Easily dispersed, high shrink-swell characteristics | 10 |
| C | Climate | Infrequent convective storms, freeze-thaw occurrence | 7 |
| D | Runoff | High peak flows; low volumes | 5 |
| E | Topography | Moderate slopes | 10 |
| F | Ground cover | Sparse, little or no litter | 10 |
| G | Land use | Intensively grazed | 10 |
| H | Upland erosion | More than 50% rill and gully erosion | 25 |
| I | Channel erosion | Occasionally eroding banks and bed but short flow duration | 5 |
| | | TOTAL | 92 |

This total rating of 92 would indicate that the sediment yield is in Classification 2. This compares with a sediment yield of 1.96 acre-feet per square mile as the average of a number of measurements in this area.

# APPENDIX B
# MODIFIED UNIVERSAL SOIL LOSS EQUATION FOR PREDICTING WATERSHED SOIL LOSS

The Modified Universal Soil Loss Equation (MUSLE) described by Williams (1975) is an empirically derived methodology for predicting watershed sediment yield on a per-storm basis. The MUSLE is

$$Y_s = R_w \; K \; LS \; C \; P \qquad (B.1)$$

where $Y_s$ is sediment yield in tons for the storm event, $R_w$ is a storm runoff energy factor, $K$ is the soil erodibility factor, $LS$ is the topographic factor representing the combination of slope length and slope gradient, $C$ is th ecover and management factor and $P$ is the erosion control practice factor. Factors $K$, $LS$, $C$ and $P$ are as defined for the Universal Soil Loss Equation (USLE), as reviewed in later paragraphs (Smith and Wischmeier, 1975, Wischmeier, 1960, and Wischmeier and Smith, 1978, provide detailed descriptions of the USLE factors and their values).

The storm runoff energy factor $R_w$ in Equation B.1 represents the modification of the USLE where $R_w$ is given by

$$R_w = \alpha \, (Vq_p)^{\beta} \qquad (B.2)$$

In Equation B.2, $V$ is the storm event runoff volume in acre-feet, $q_p$ is the storm event peak flow rate in cfs, and $\alpha$ and $\beta$ are coefficients. Utilization of a storm runoff factor makes the MUSLE applicable to semiarid regions of the West where short-duration, high-intensity storms are cominant. For watersheds having measured sediment data, values for the coefficients $\alpha$ and $\beta$ can be derived through calibration. Williams and Berndt (1972) determined values for $\alpha$ and $\beta$ of 95 and 0.56, respectively, for experimental watersheds in Texas and Nebraska.

Soil erodibility factor $K$ was found by Wischmeier et al. (1971) to be a function of percent of silt, percent of coarse sand, soil structure, permeability of soil, and percent of organic matter. The soil erodibility nomograph is shown in Figure B.1.

Wischmeier (1972) presented a method including graphical aids for determining the cover and management factor (cropping-management factor $C$). The

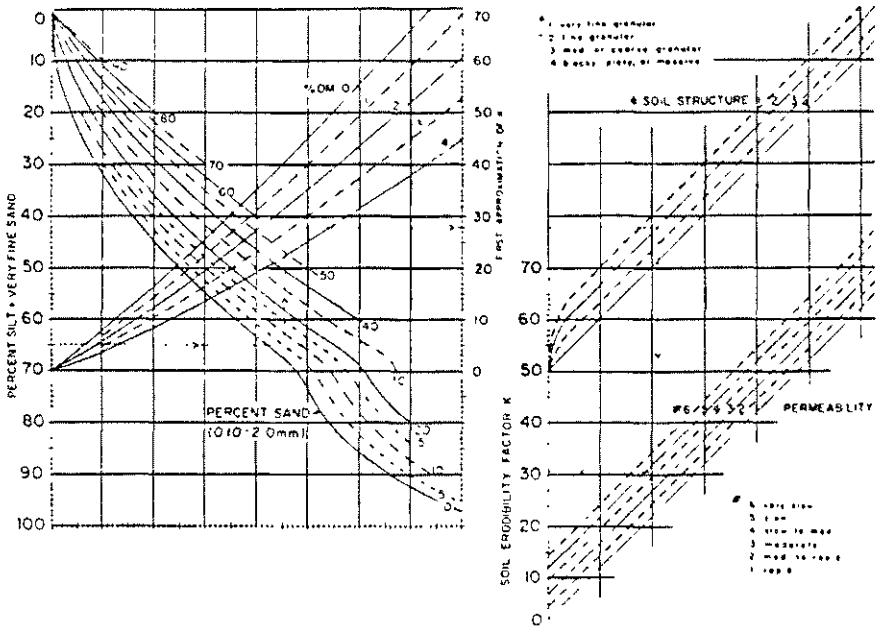


Figure B.1. Soil erodibility nomograph used to determine factor K for specific topsoils or subsoil horizons. Solutions are in tons/acre (from Wischmeier et al., 1971).

cropping-management factor can be divided into three distinct types of effects as follows: Type I -effects of canopy cover ($C_I$), Type II - effects of mulch or close-growing vegetation in direct contact with the soil surface ($C_{II}$), and Type III - tillage and residual effects of the land use ($C_{III}$). The cover and management factor is defined as the product of these factors:

$$C = C_I \, C_{II} \, C_{III} \tag{B.3}$$

Type I - Canopy Cover. Leaves and branches that do not directly contact the soil are effective only as canopy cover. A canopy can intercept falling raindrops, but waterdrops falling from the canopy may regain an appreciable velocity, although not the terminal velocities of free-falling raindrops. Therefore, canopy cover reduces rainfall erosivity by reducing impact energy at the soil surface. The amount of reduction depends on height and density of the canopy. Figure B.2 shows the canopy factor as a function of height and density of the canopy. Canopy factors for various percentages of cover at heights of 0.5, 1.0, 2.0 and 4.0 meters may be obtained directly from this graph.

Type II - Mulch and Close-Growing Vegetation. A mulch at the soil-atmosphere interface is much more effective than an equivalent percentage of canopy cover. Because intercepted raindrops have no remaining fall-height to the ground, their impact on the soil surface is eliminated. A mulch that makes a good contact with the ground also reduces runoff velocity, which greatly reduces the potential of runoff to detach and transport soil material.

Substantial rainfall simulator data are now available on erosion-reducing effectiveness of various amounts and types of mulches used on cropland and construction sites. Extrapolation of these data to other mulches and close covers such as those associated with range or woodland is facilitated by expressing them on the basis of percent surface cover rather than tons per acre. This conversion and a preliminary summarization of data are reflected in the relationship curve shown in Figure B.3.

Type III - Residual Effects of Land Use. This category includes residual effects of land use on soil structure, organic matter content and soil density, effects of tillage or lack of tillage on surface roughness and porosity, roots and subsurface stems, biological effects, and other factors. This factor can be evaluated from Figure B.4 by knowing the percent of root network in the topsoil relative to a good rotation meadow. This percent of root network

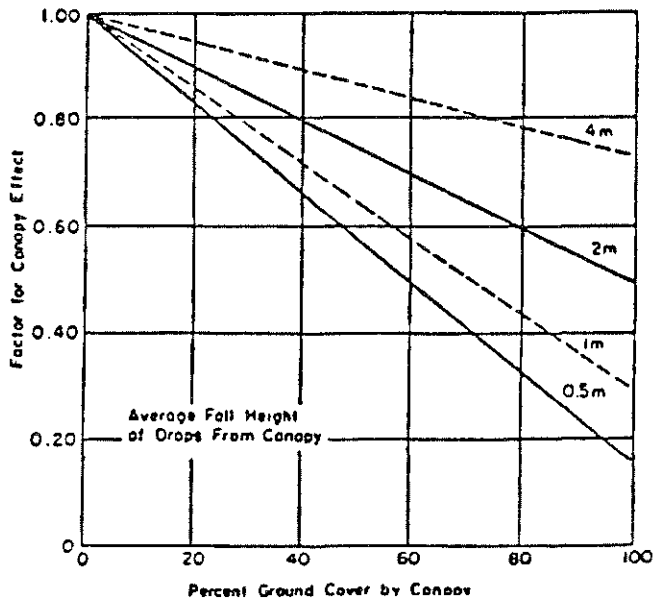


Figure B.2. Influence of vegetal canopy on effective-EI (after Wischmeier, 1972).

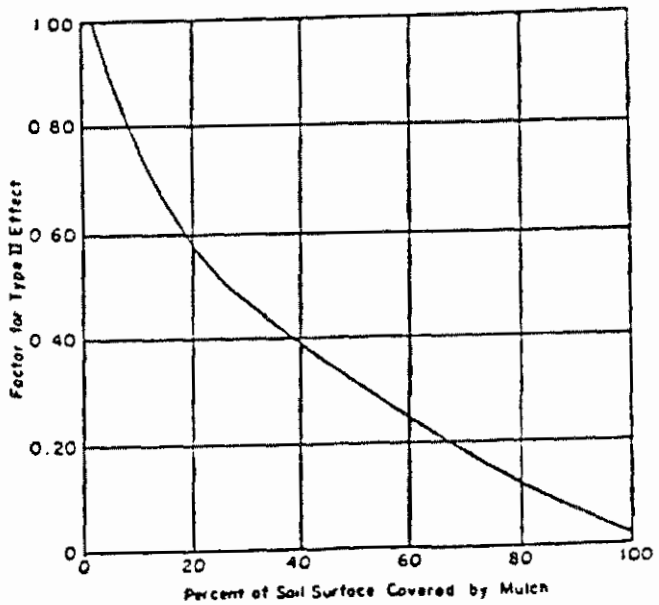


Figure B.3. Effect of plant residues or close-growing stems at the soil surface (after Wischmeier, 1972).

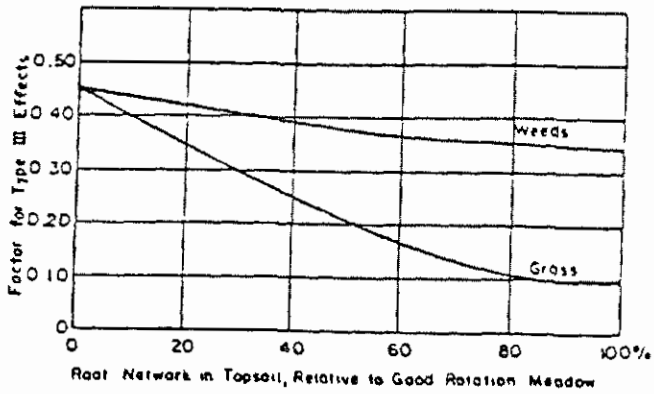


Figure B.4. Type III effects on undisturbed land areas (after Wischmeier, 1972).

is often a difficult value to estimate. The overall C factor can be evaluated by the product of three subfactors, i.e., Type I, II and III subfactors.

The topographic factor LS is defined as the ratio of soil loss from any slope and length to soil loss from a 72.6-foot plot length at a nine percent slope, with all other conditions the same. Slope length is defined as the distance from the point of overland flow origin to the point where either slope decreases to the extent that deposition begins or runoff water enters a well-defined channel (Smith and Wischmeier, 1957). Effect of slope length on soil loss is primarily a result of increased potential due to greater accumulation of runoff on the longer slopes. Based on data for slopes between three and 20 percent and with lengths up to 400 feet, Wischmeier and Smith (1965) proposed the topographic factor be computed as

$$LS = \left(\frac{\lambda}{72.6}\right)^n (0.065 + 0.0454\ S + 0.0065\ S^2 \qquad (B.4)$$

where $\lambda$ is slope length, $S$ is percent slope, and $n$ is an exponent depending upon slope. The exponent $n$ is given by

$n = 0.3$ for slope $<$ 3 percent

$n = 0.4$ for slope = 4 percent

$n = 0.5$ for slope $>$ 5 percent

Erosion-control practice factor P accounts for the effect of conservation practices such as contouring, strip cropping, and terracing on erosion. It is defined as the ratio of soil loss using one of these practices to the loss using straight row farming up and down the slope. Terracing is generally the most effective conservation practice for decreasing soil erosion. This factor has no significance for wildland areas and can be set at 1.0.

When estimating sediment yield using the MUSLE, a useful computation is to express sediment yield in terms of an average concentration (ppm) based on the total water and sediment yields. This value can be compared with measured stream data in the area, if available. Annual sediment yield from the land surface can be estimated using the MUSLE in combination with the probability-weighting procedure described in Section 3.4. Application of the MUSLE to estimate watershed soil loss is illustrated in the following example.

Example:

Watershed area = 25.3 $mi^2$

Annual rainfall = 10.0 in.

Average runoff = 1.5 percent of rainfall = 0.15 in.

Watershed soil: 43 percent silt and very fine sand
40 percent sand
1 percent organic matter
Fine granular structure
Moderate permeability

Average watershed slope = 14 percent

Average slope length = 280 ft

Canopy cover density = 10 percent

Average fall height = 1.5 ft

Close-growing vegetation density = 15 percent

Root network in topsoil (weeds) = 20 percent

For purposes of illustration, assume $\alpha = 95$ and $\beta = 0.56$.

Step 1: Determine Factor Values

$R_W$ Factor

See Table B.1.

K Factor

K factor nomograph (Figure B.1) $K = 0.26$

C Factor

From Figure B.2 for 10 percent canopy cover $C_I = 0.90$

From Figure B.3 for 15 percent ground cover $C_{II} = 0.67$

From Figure B.4 for 20 percent root network $C_{III} = 0.42$

$$C = C_I \, C_{II} \, C_{III} = 0.25$$

LS Factor

Applying Equation B.4,

$$LS = \left(\frac{280}{72.6}\right)^{0.5} [0.065 + 0.0454\,(14) + 0.0065\,(14^2)] = 3.9$$

P Factor

No supporting practices, therefore $P = 1.0$

Step 2: Apply Equation B.1

$$Y_s = R_W\,(0.26)\,(3.9)\,(0.25)\,(1.0)$$

$$= 0.25\,R_W$$

Results are given in Table B.2.

Table B.1. Factor $R_w$ Calculation.

| Return Period (years) | Runoff Volume (ac-ft) | Peak Runoff (cfs) | $R_w$ |
|---|---|---|---|
| 2 | 123 | 340 | 37,800 |
| 5 | 320 | 900 | 108,400 |
| 10 | 595 | 1,650 | 215,400 |
| 25 | 915 | 2,540 | 349,000 |
| 50 | 1,200 | 3,330 | 472,800 |
| 100 | 1,510 | 4,190 | 611,500 |

Table B.2. MUSLE Sediment Yield Estimate.

| Return Period (years) | $R_w$ | Washload (tons) |
|---|---|---|
| 2 | 37,800 | 9,000 |
| 5 | 108,400 | 27,000 |
| 10 | 215,400 | 54,000 |
| 25 | 349,000 | 87,000 |
| 50 | 472,800 | 118,000 |
| 100 | 611,500 | 153,000 |